Metal Transport near a Tailings Facility in the Alberta Oil Sands

by

Stephanie Roussel

A thesis submitted to the Faculty of Graduate and Postdoctoral Affairs
in partial fulfillment of the requirements for the degree of

Master of Science

in

Earth Sciences

Carleton University
Ottawa, Ontario

Abstract

The main concern that surrounding the large-scale, industrial oil sands operations in the Alberta Oil Sands is the potential for oil sands process-affected water to leak from tailings facilities into the surrounding environments. Many parameters control trace metal migration as OSPW enters wetland environments that comprise approximately 30% of Northern Alberta, including pH, redox potential, temperature, organic matter, inorganic water chemistry, and hydrology. This study aims to quantify the control organometallic complexes exert on the mobility of trace metal loads where tailings facilities are adjacent to wetland environments. Geochemical modeling indicated that humic substances are the primary sorption phase, and likely dominate the chemical behavior of many metals, however, organometallic complexes are not currently taken into account in environmental monitoring programs. A refined understanding of the environmental and geochemical processes operating within this system is required to determine the potential risk OSPW leakage represents to these ecosystems.

Acknowledgements

First and foremost, I would like to express my deepest gratitude to my supervisor, Dr. Richard Amos, for taking on an international student all the way from Texas and allowing me the opportunity to study at Carleton University. I would also like to thank my co-supervisor Paul Gammon for organizing the field study aspect associated with this thesis and for spending so much time reviewing and discussing the results with me. This thesis would not have been possible without the guidance, encouragement, and expert supervision of both Rich and Paul. Thanks to Sam Morton for his relentless efforts in perfecting the mini-piezometer and drive point modifications that made the groundwater sampling possible, and his contribution in the field work. Funding from NSERC and the SOURCES Project of Natural Resources Canada's Environmental Geoscience Project made this project possible.

I would also like to thank the hydro students at both Carleton University and The University Ottawa for their friendship and support; y'all made my time in Canada exponentially more enjoyable. Last but not least, I would like to thank my family for their endless love and support. I am grateful for parents who support and encourage my siblings and me to follow our dreams and pursue every opportunity that comes our way.

Preface

This thesis is presented as two proposed manuscripts, which will be submitted for publication. Consequently, redundancies of Chapter 1 may be seen in the two following chapters. Sample collection for Chapter 2 was conducted by Dr. Paul Gammon and Dr. Jason Ahad at the Geologic Survey of Canada, and section 2.2 was written by Paul Gammon as he collected the data, and section 2.3 was written by Jason Ahad, as he conducted the Orbitrap Spectra analysis. Figure 2-1 was produced by Paul Gammon. The remainder of Chapter 2 was written by the candidate. Sample collection for Chapter 3 was conducted by the candidate, under the supervision and guidance of Dr. Richard Amos and Dr. Paul Gammon. Figure 3-5 and 3-6 were produced by Paul Gammon. The candidate performed all modeling and analyses.

Table of Contents

List of Tables

List Figures

List of Appendices

Chapter 1: General Introduction

1 General Introduction

1.1 Alberta Oil Sands

The Alberta Oil Sands have the third largest reserves of crude oil in the world, behind Saudi Arabia and Venezuela. With the current economic conditions and extraction technology, over 170 billion barrels of crude oil are attainable. It is predicted that oil sands production will increase from 2.3 million barrels per day (in 2014) to 4 million barrels per day by 2024, following the ever increasing demand for fossil fuels (Government of Alberta, 2007a). The Alberta Oil Sands cover an area of approximately 142,200 square km, and are subdivided into three distinct oil sands regions: Athabasca (AOSR), Cold Lake (CLOSR), and Peace River Oil Sands Reserves (PROSR) (Government of Alberta, 2007b). The AOSR has the largest total surface area, and contains the only reserves that are shallow enough to be mined using conventional open-pit techniques (Canadian Association of Petroleum Producers, 2015).

1.2 Regional Geology/ Source Rock

The general geology of the AOSR is comprised of two main units, Devonian limestone bedrock and Cretaceous sedimentary deposits, that are overlain by muskeg, sandstone and shale overburden, and Quaternary deposits that originate from glacial till, fluvial, lacustrine, and aeolian environments (Fenton, 1994). The Sr- rich Devonian Limestone bedrock was deposited during a time of marine

regression, and is considered to be an aquitard, as it typically has very low hydraulic conductivity (Savard et al., 2012).

The limestone bedrock is overlain by three main Cretaceous deposits that are part of the Mannville Group of the Western Canada Sedimentary Basin: McMurray, Clearwater, and Grand Rapids formations (Flach, 1984; Savard et al., 2012). These formations contain the largest amount of coal, oil, and gas reserves in Alberta. The McMurray formation directly overlies the unconformity surface of the limestone bedrock, and is the primary bitumen source rock unit in the AOSR. The McMurray Formation is a poorly consolidated, bitumen impregnated sandstone unit that is composed primarily of water, mineral matter, and bitumen(Hein and Cotterill, 2006). At its maximum thickness, the McMurray Formation is approximately 150 meters (Flach, 1984). Deposition of the McMurray Formation occurred during a period of marine transgression in fluvial, estuarine, marginal marine, and tidal flat environments (Hein and Cotterill, 2006; Savard et al., 2012).

Overlying the McMurray Formation is the Clearwater Formation: a green, glauconitic sandstone that grades upward to a grey marine shale. The Clearwater Formation is overlain by the Grand Rapids Formation, which is a black and white, poorly consolidated sandstone, with particles of quartz, feldspar, glauconite, chert, muscovite, and biotite (Savard et al., 2012).

1.3 Bitumen Extraction Processes

Due to the viscous nature of bitumen, it must be diluted with hot water and/or chemical diluents such as naphthenic acids in order to extract the bitumen from the other constituents (Poveda and Lipsett, 2014). There are two primary

methods currently used to extract bitumen from oil sands, *in-situ* methods, which account for approximately 80% of the attainable reserves, and open-pit (surface) mining, which accounts for the remaining 20% (Government of Alberta, 2007a).

In-situ techniques, including steam-assisted gravity drainage (SAGD), cyclic steam simulation (CSS), and vapor recovery extraction (VAPEX) (Poveda and Lipsett, 2014), are used to liquefy the bitumen for extraction, by pumping steam underground, through horizontal wells (Canadian Association of Petroleum Producers, 2015). While no solid waste byproduct is created using *in-situ* methods, bitumen recovery is only approximately 35-60% (Government of Alberta, 2007a).

Surface mining techniques are used when deposits are situated less than 70 meters below ground surface (Government of Alberta, 2007b). The minable surface area in the AOSR is approximately 4,800 km^2 (Government of Alberta, 2007a). As of 2014, less than 2% of the minable surface area had been mined (895 km^2)(Government of Alberta, 2007b). Surface mining utilizes a modified version of the Clark Hot Water Process, and entails digging up hard oil sands, breaking it up with mechanical crushers, and mixing hot water and/or chemical diluents to separate the bitumen from the other components. Caustic soda (NaOH) and hot water are commonly added to the slurry mixture to further separate clay materials, dissolved metals, and other organic matter from the bitumen, which consequently increases the salinity of the waste byproducts (Allen, 2008; Small et al., 2015). The hot slurry (40-55 °C) is then transported to a plant where the bitumen is extracted (Masliyah et al., 2004). The extracted bitumen mixture (froth) is composed of approximately 60% bitumen, 30% water, and 10% solid minerallic material

(Masliyah et al., 2004). Diluents such as naphthenic acids and paraffinic solvents are added to the froth to further separate the remaining residual water and solids from the bitumen (Small et al., 2015). Once separated, the bitumen goes through an "upgrading" process that turns it into a fluid suitable for pipeline transport and further refinement (i.e. synthetic crude or fluidised bitumen).

Surface mining techniques are extremely effective for bitumen extraction (approximately 90% bitumen recovery). However, this process uses sediments that have more than 80% non-bituminous components, and requires approximately two tons of oil sands and 2-4 barrels of water to produce one barrel of synthetic crude oil (Poveda and Lipsett, 2014). Large-scale synthetic crude production (~2.5 mbbl/day at present) generates a tremendous amount of tailings waste and oil sands process-affected water (OSPW) that must be stored (Government of Alberta, 2007a). As of 2013, tailings facilities in Northern Alberta contained over 975 million cubic meters of waste (Government of Alberta, 2007b) from open-pit mining methods (Poveda and Lipsett, 2014).

1.4 Tailings Ponds

The Government of Alberta requires that oil sands operators abide by a "Zero Discharge Policy", meaning no waste byproducts may be released into the surrounding environment. Tailings impoundments consisting of engineered dam and dyke systems are designed to ideally hold 100% of the waste produced from surface mining activities. The primary function of a tailings pond is to act as a holding reservoir for solid constituents to settle out of recyclable water. As of 2013, tailings ponds and related structures occupied an area of approximately 220 square

kilometers (equivalent to 41,000 Canadian football fields) (Government of Alberta, 2007a). Tailings material generally consists of approximately 20-30% solid material, 3% residual bitumen, and alkaline water (Chen et al., 2013).

Solid tailings material separates into three distinct layers: 1) coarse grained tailings, 2) fine fluid tailings, and 3) froth-treatment tailings (Kasperski and Mikula, 2011). Course grained tailings are composed of sand sized grains, >44 μm, that usually settle out first. In some instances these are later recycled to build additional dam and dyke systems to hold fine tailings. Fine fluid tailings is composed of fines, <44μm, and usually remain in suspension much longer (Kasperski and Mikula, 2011). It takes approximately 3-5 years for fine tailings to settle to 30-40 weight percent, which are then termed mature fine tailings (MTF) (Kasperski and Mikula, 2011). MFT settle very slowly, with some estimates suggesting these could take 150 years to consolidate (Kasperski and Mikula, 2011). Froth treatment tailings is comprised of residual water, sand, fines, residual bitumen, and solvents left over from the extraction process (Kasperski and Mikula, 2011).

Due to the substantial amount of time it takes for fine fluid tailings to consolidate, two techniques are used by oil sand operators to hasten the dewatering and consolidation process: consolidated or composite tailings (CT) and paste technology (Masliyah et al., 2004). CT involves adding gypsum to the mature fine tailings, which consolidates the fines and the coarse sands to a uniform mixture, and paste technology involves the addition of thickeners (flocculants or polyelectrolytes) to fine tailings before it is pumped into the tailings pond (Masliyah et al., 2004). These techniques increase the efficiency with which water can be

extracted and recycled for additional bitumen extraction, however, they also decrease water quality which may compromise the effectiveness of future extraction (Allen, 2008; Kasperski and Mikula, 2011).

1.5 Oil Sands Process-Affected Water (OSPW)

As OSPW is repeatedly recycled and reused, it becomes increasingly enriched in numerous components of environmental concern such as process chemicals, solvents, naphthenic acids, organic material, dissolved inorganic salts, trace metals, and residual bitumen (Kasperski and Mikula, 2011; Poveda and Lipsett, 2014). The alkaline OSPW is distinguishable by elevated concentrations of dissolved metals, naphthenic acids (NAs), and major ions such as sodium, bicarbonate, chloride, sulfate, and ammonia (Allen, 2008; Chen et al., 2013). Trace metals commonly found in OSPW include Al, Fe, Pb, Mo, Ti, V, and Zn, in addition to As, Cd, Cr, Cu, Ni, Pb, and Zn which are considered priority pollutants (Allen, 2008; CCME, n.d.; US EPA, 2014). In two particular tailings ponds analyzed by Allan, total dissolved solids (TDS) ranged from 2000-2500 mg/L, and increased at a yearly rate of 75 mg/L per year between 1980 and 2001 (Allen, 2008). Allen summarized several reports and concluded that overall, OSPW water is typically hard water (12-25 mg/L Ca^{2+}, 5-10 mg/L Mg^{2+}), has a pH between 8.0 and 8.4, and an alkalinity of approximately 800-1000 mg/L HCO_3^- (Figure 1-1; Allen, 2008).

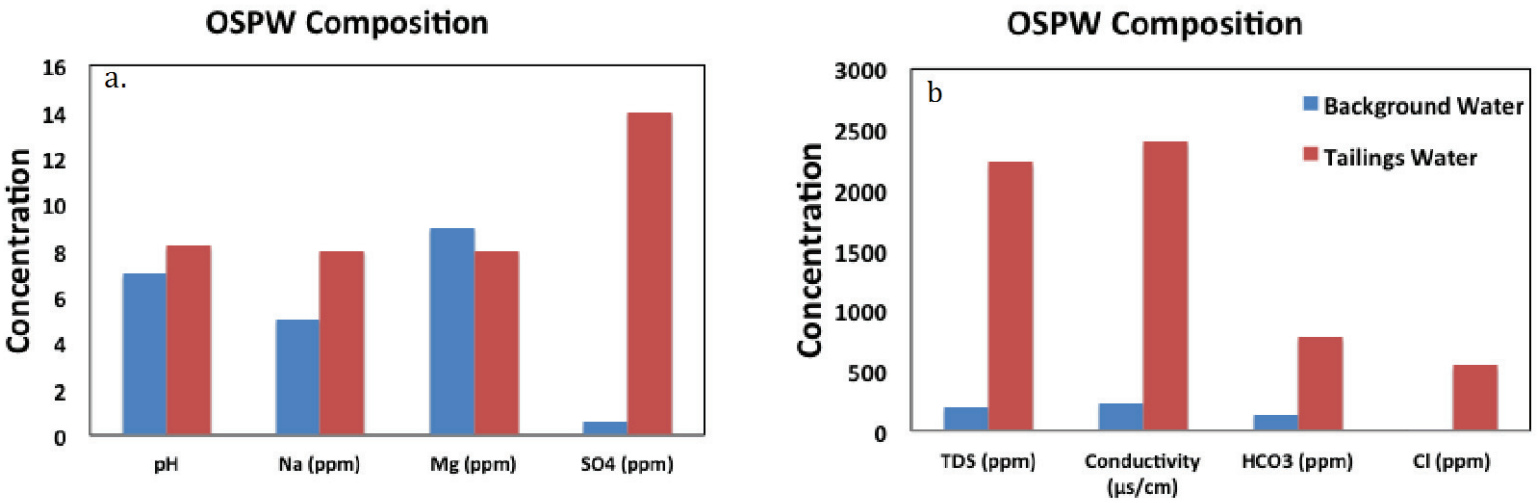

Figure 1- 1 : General OSPW chemistry (concentrations taken from Allen, 2008).

1.6 Acid Extractable Organics

Acid extractable organics (AEO) include all polar organics including naphthenic acids and humic substances. Naphthenic acids (NA) are water soluble, polar, complex suits of carboxylic acids (Allen, 2008; Kasperski and Mikula, 2011; Savard et al., 2012; Scott et al., 2005). NAs become soluble and concentrated (>100 mg/L) in OSPW during the hot-water processes used to extract bitumen from oil sands (Allen, 2008; Rogers et al., 2002; Savard et al., 2012). NAs are naturally present in bitumen, and are considered a primary toxin found in tailings ponds, however, aerobic biodegradation can reduce toxicity in isolated OSPW by 100% after approximately 10 years (Allen, 2008; Scott et al., 2005).

In the AOSR, humic substances account for a substantial portion of AEOs in both surface waters and groundwaters, (Bryan et al., 2002; Weng et al., 2002).

These humic substances are complex, naturally occurring, ever-present, macromolecules, that emanate from plant remnants and terrestrial sediments (Appelo and Postma, 1994; Wood, 1996). Humic substances can be further subdivided into humic acids (HA) and fulvic acids (FA). HAs typically contain less oxygen and have larger molecular weights compared to FAs. Previous research concluded that the majority of AEOs in wetland environments are primarily composed of FAs (Artinger et al., 2000; Christensen and Christensen, 1999; Weng et al., 2002; Wetzel, 2001). It is hypothesized that HA is not measurable in these organic-rich environments due to a "sorption sieve" process onto organic and mineral phases (Bryan et al., 2002; Weng et al., 2002). These humic substances do not pose a direct toxic threat to the surrounding environment; however, they heavily influence metal transport, speciation, and overall redox geochemistry within organic-rich systems (Aiken et al., 2011). Soluble humic substances typically have negatively charged surfaces that attract positively charged inorganic ions, creating organic-metal (organometallic) complexes. Organometallic complexes behave differently (i.e. fixation, release, and transportation) than their pure organic or inorganic components, which make them of particular interest in the AOSR.

1.7 Redox Potential

Redox reactions occur when an element changes oxidation state by either donating or accepting electrons. This tendency for donation or acceptance is known as the redox potential (pE) of an element. In an idealized system, redox buffering occurs in a stepwise ladder function that reflects the available chemical energy released by the reaction. In surface systems, this manifests as microbially-mediated

dissolved organic carbon (DOC) oxidation via reaction pathways that involve oxidants in the following order: firstly oxygen, then nitrate, then Mn oxyhydroxides, then Fe oxyhydroxides, then oxidized S, and lastly methane (Christensen et al., 2000). Conceptually the redox ladder represents chemical reactions of a redox couple (e.g. an organic matter-nitrate couple) until one of the reactants is exhausted, after which the pE will drop until the next redox couple becomes energetically favorable for microbial exploitation (Scott and Morgan 1990). However this idealized sequence rarely occurs in real world systems. Due to the relatively slow kinetics of redox reactions, most groundwater systems never reach thermodynamic equilibrium, which allows the aquifer to possess both reducing and oxidizing capacities simultaneously. "pE" is the measure of redox amplitude, and there is no systematic variable that measures redox-buffering capacity.

It is beneficial to characterize redox gradients as these define speciation and sorption reactions (Christensen et al., 2000). Redox processes within an aquifer largely control chemical speciation, bioavailability, toxicity, and mobility of metals (Borch et al., 2010). A leaking tailings pond could potentially create a plume composed of OSPW that contained trace metals and organic material. Plumes typically have strongly reduced conditions near the source, which lessen along the vertical and horizontal redox gradient as the plume migrates (Christensen et al., 2000). Reducing conditions are typically driven by the presence of organic matter that is being consumed through microbial activity, while oxidizing conditions are typically driven by the presence of oxygen and nitrate (Appelo and Postma, 1994).

1.8 Research Approach and Rationale

The potential impact that tailings facilities have on local and regional groundwater and surface water supplies is a fundamental concern in the Alberta Oils Sands. In some AOSR localities, ancient river sands underlie tailings ponds, which creates a preferential flow path connecting OSPW seepage from tailings impoundments to surrounding down gradient stream and river systems (Furguson et al., 2009; Holden et al., 2011; Holden, 2012). Thus there is potential for OSPW to leak from the large tailings impoundments into the surrounding environment. Complex biological and geochemical reactions alter the migration of OSPW through aquifers in the AOSR. Sorption processes and ion exchange reactions are heavily dependent on organic matter and redox properties present within a groundwater system, and largely control the mobility of trace metal-rich OSPW. However, little is understood of how metals behave in typical AOSR environments. The most comprehensive approach to date is the small, laboratory scale, reactive transport models generated by Holden et al (2011, 2012), and the small field-based reactive transport model of Savard et al. (2012); neither of which investigated either redox processes or organometallic complexes.

A two-phased research approach was taken to gain a more comprehensive understanding of how inorganics, organics, and redox properties affect the mobility of trace metals in the AOSR. Phase One includes a large-scale, comparative analysis of two datasets with monitoring wells adjacent to two different tailings ponds. To the best of our knowledge, a study has not been conducted in the Alberta Oil Sands

Region to determine the impact organic ligands have on metal complexation and transport. It is integral to understand these processes as they potentially alter the behavior and transport of metal ions within an aquifer (Appelo and Postma, 1994; Kim et al., 1990; Wood, 1996). A detailed analysis of the organic components was conducted and modeled in combination with inorganic data to determine the impact humic substances have on metal transport in the AOSR. Through this analysis, a potential OSPW plume was hypothesized adjacent to Tailings Pond 2, and was further investigated in Phase Two. Phase Two includes a high resolution, depth discrete field study located near a monitoring well that suggested OSPW leakage. A grid of vertically and horizontally discrete piezometer nests were installed, sampled, and analyzed. A detailed geochemical analysis was conducted to determine the effect that redox properties and organic material have on metal transport. A better understanding of these concepts will improve the accuracy with which plume evolution is modeled and estimated, the potential contamination risk and need for remediation.

2 References

Aiken, G.R., Hsu-Kim, H., Ryan, J.N., 2011. Influence of Dissolved Organic Matter on the Environmental Fate of Metals, Nanoparticles, and Colloids. Environ. Sci. Technol. 45, 3196–3201. https://doi.org/10.1021/es103992s

Allen, E.W., 2008. Process water treatment in Canada's oil sands industry: I. Target pollutants and treatment objectives. J. Environ. Eng. Sci. 7, 123–138. https://doi.org/10.1139/S07-038

Appelo, C.A.J., Postma, D., 1994. Geochemistry, Groundwater, And Pollution, Second. ed. Balkema, Great Britian.

Artinger, R., Buckau, G., Geyer, S., Fritz, P., Wolf, M., Kim, J.I., 2000. Characterization of groundwater humic substances: influence of sedimentary organic carbon. Appl. Geochem. 15, 97–116. https://doi.org/10.1016/S0883-2927(99)00021-9

Borch, T., Kretzschmar, R., Kappler, A., Cappellen, P.V., Ginder-Vogel, M., Voegelin, A., Campbell, K., 2010. Biogeochemical Redox Processes and their Impact on Contaminant Dynamics. Environ. Sci. Technol. 44, 15–23. https://doi.org/10.1021/es9026248

Bradl, H.B., 2004. Adsorption of heavy metal ions on soils and soils constituents. J. Colloid Interface Sci. 277, 1–18.

Bryan, S.E., Tipping, E., Hamilton-Taylor, J., 2002. Comparison of measured and modelled copper binding by natural organic matter in freshwaters. Comp. Biochem. Physiol. Part C Toxicol. Pharmacol. 133, 37–49. https://doi.org/10.1016/S1532-0456(02)00083-2

Canadian Association of Petroleum Producers, 2015. Oil Sands [WWW Document]. Can. Assoc. Pet. Prod. URL http://www.capp.ca/canadian oil and natural gas/oil sands (accessed 5.24.16).

Chen, M., Walshe, G., Chi Fru, E., Ciborowski, J.J.H., Weisener, C.G., 2013. Microcosm assessment of the biogeochemical development of sulfur and oxygen in oil sands fluid fine tailings. Appl. Geochem. 37, 1–11. https://doi.org/10.1016/j.apgeochem.2013.06.007

Christensen, J.B., Christensen, T.H., 1999. Complexation of Cd, Ni, and Zn by DOC in Polluted Groundwater: A Comparison of Approaches Using Resin Exchange, Aquifer Material Sorption, and Computer Speciation Models (WHAM and MINTEQA2). Environ. Sci. Technol. 33, 3857–3863. https://doi.org/10.1021/es981105t

Christensen, T.H., Bjerg, P.L., Banwart, S.A., Jakobsen, R., Heron, G., Albrechtsen, H.-J., 2000. Characterization of redox conditions in groundwater contaminant plumes. J. Contam. Hydrol. 45, 165–241. https://doi.org/10.1016/S0169-7722(00)00109-1

Fenton, M.., 1994. Chapter 26 - Quaternary Geology of the Western Plains [WWW Document]. URL http://ags.aer.ca/publications/chapter-26-quaternary-geology-of-the-western-plains#Introduction (accessed 5.25.16).

Flach, P.D., 1984. Oil Sands Geology - Athabasca Deposit North.

Furguson, G.P., Rudolph, D.L., Baker, J.F., 2009. Hydrodynamics of a large oil sand tailings impoundment and related environmental implications. Camadian Geotech. J. 46, 1446–1460.

Government of Alberta, 2007a. About Oil Sands [WWW Document]. Alta. Energy. URL http://www.energy.alberta.ca/OilSands/585.asp (accessed 5.24.16).

Government of Alberta, 2007b. Facts and Statistics [WWW Document]. URL http://www.energy.gov.ab.ca/OilSands/791.asp (accessed 5.24.16).

Hein, F.J., Cotterill, D.K., 2006. The Athabasca Oil Sands — A Regional Geological Perspective, Fort McMurray Area, Alberta, Canada. Nat. Resour. Res. 15, 85–102. https://doi.org/10.1007/s11053-006-9015-4

Holden, A.A., 2012. The Geochemical Evolution of Oil Sands Tailings Pond Seepage, Resulting from Diffusive Ingress Through Underlying Glacial Till Sediments (Ph.D.). University of Alberta (Canada), Canada.

Holden, A.A., Donahue, R.B., Ulrich, A.C., 2011. Geochemical interactions between process-affected water from oil sands tailings ponds and North Alberta surficial sediments. J. Contam. Hydrol. 119, 55–68. https://doi.org/10.1016/j.jconhyd.2010.09.008

Kasperski, K.L., Mikula, R.J., 2011. Waste Streams of Mined Oil Sands: Characteristics and Remediation. Elements 7, 387–392. https://doi.org/10.2113/gselements.7.6.387

Kim, J.I., Buckau, G., Li, G.H., Duschner, H., Psarros, N., 1990. Characterization of humic and fulvic acids from Gorleben groundwater. Fresenius J. Anal. Chem. 338, 245–252. https://doi.org/10.1007/BF00323017

Masliyah, J., Zhiang, Z. (Joe), Zhenghe, X., Czarnecki, J., Hassan, H., 2004. Understanding Water-Based Bitumen Extraction from Athabasca Oil Sands. Can. J. Chem. Eng. 82, 628–654.

Poveda, C.A., Lipsett, M.G., 2014. Surface Mining Operations in Oil Sands: Establishing Sustainable Development Indicators (SDIs). GBR: WIT Press.

Rogers, V.V., Liber, K., MacKinnon, M.D., 2002. Isolation and characterization of naphthenic acids from Athabasca oil sands tailings pond water. Chemosphere 48, 519–527. https://doi.org/10.1016/S0045-6535(02)00133-9

Savard, M.M., Ahad, J.M.E., Gammon, P., Calderhead, A.I., Rivera, A., Martel, R., Klebek, M., Lefebvre, R., Headley, J.V., Welsh, B., Smirnoff, A., Pakdel, H., Benoit, N., Liao, S., Jautzy, J., Gagnon, C., Vaive, J., Girard, I., Peru, K., 2012. A local test study distinguishes natural from anthropogenic groundwater contaminants near an Athabasca Oil Sands mining operation (No. 7195). Geological Survey of Canada.

Scott, A.C., Mackinnon, M.D., Fedorak, P.M., 2005. Naphthenic Acids in Athabasca Oil Sands Tailings Waters Are Less Biodegradable than Commercial Naphthenic Acids. Environ. Sci. Technol. 39, 8388–8394. https://doi.org/10.1021/es051003k

Small, C.C., Cho, S., Hashisho, Z., Ulrich, A.C., 2015. Emissions from oil sands tailings ponds: Review of tailings pond parameters and emission estimates. J. Pet. Sci. Eng. 127, 490–501. https://doi.org/10.1016/j.petrol.2014.11.020

US EPA, O., 2014. Toxic and Priority Pollutants Under the Clean Water Act [WWW Document]. URL https://www.epa.gov/eg/toxic-and-priority-pollutants-under-clean-water-act#priority (accessed 7.15.16).

Weng, L., Fest, E.P.M.J., Fillius, J., Temminghoff, E.J.M., Van Riemsdijk, W.H., 2002. Transport of Humic and Fulvic Acids in Relation to Metal Mobility in a Copper-Contaminated Acid Sandy Soil. Environ. Sci. Technol. 36, 1699–1704. https://doi.org/10.1021/es010283a

Wetzel, R.G., 2001. 23 - Dwtritus: Organic Carbon Cycling and Ecosystem Metabolis, ETRITUS: ORGANIC CARBON CYCLING AND ECOSYSTEM METABOLISM, in: Limnology (Third Edition). Academic Press, San Diego, pp. 731–783.

Wood, S.A., 1996. The role of humic substances in the transport and fixation of metals of economic interest (Au, Pt, Pd, U, V). Ore Geol. Rev., Organics and Ore Deposits 11, 1–31. https://doi.org/10.1016/0169-1368(95)00013-5

Chapter 2: The Sorption Sieve: Organometallic Complexes in the Alberta Oil Sands

Stephanie Roussel[1], Paul Gammon[2], Richard Amos[1], Jason Ahad[3], John Hedley[4], Kerry Peru[4], and Martine Savard[3]

[1] Department of Earth Sciences, Carleton University, 2115 Herzberg Laboratories 1125 Colonel By, Drive, Ottawa, Ontario, K1S 5B6, Canada
[2] Natural Resources Canada-Geologic Survey of Canada, 601 Booth Street, Ottawa, Ontario, K1A 0E8, Canada
[3] Natural Resources Canada-Geologic Survey of Canada, 490 Rue de la Couronne, Québec, G1K 9A9, Canada

Manuscript to be submitted for publication.

Abstract

Tailings facilities located within the large-scale, industrial oil sands operations in Northern Alberta, Canada have the potential to leak oil sands process-affected water (OSPW), containing trace metals, into the surrounding organic-rich, wetland environments. Many parameters influence the complexation and transportation of trace metals in groundwater, including pH, redox potential, temperature, organic matter, inorganic water chemistry, hydrology, and complexation state. This study quantifies the impact organometallic complexes exert on the mobility of mining-related, metal loads within this landscape, particularly where tailings ponds are adjacent to wetland environments. Numerical modeling (WHAM 7 and PHREEQC) suggested that most metals predominantly complex with organic matter when present, with the exception of Sr, Be, Ni, Co, Pb, and Y, which preferentially sorb to oxyhydroxides (80-100%, 100%, 10-40%, 10-50%, 100%, and 80-100% respectively). Attenuation is most significant for the chalchophile elements, Zn and Cu, that strongly partition to humic acids (15-40% and 70-100% respectively). In contrast, rare earth elements (REEs) predominantly partition to fulvic acids (nearly 100%) and have accentuated transport. While groundwaters have higher concentrations of total acid extractable organics (AEOs), they have a substantially reduced component of the higher molecular weight (>500 m/z) humic acids. This is due to the sorption of higher molecular weight humic acids to solid substrates, a “sieve-like” process that attenuates the transport of metals sorbed to those higher molecular weight compounds, and accentuates the transport of metals that preferentially sorb to lighter molecular weight (<500 m/z) fulvic

acids. This study indicates that organometallic complexes likely dominate much of the chemical behavior of metals in the wetland environments in the Athabasca Oil Sands Region (AOSR), yet are not considered in current environmental monitoring programs. An understanding of these processes is integral to determine the potential risk OSPW leakage represents to surrounding ecosystems.

1 Introduction

As the demand for fossil fuels steadily increases, so does the development of unconventional hydrocarbon extraction methods. In 2014, approximately 2.3 million barrels of oil were produced daily in the Albertan oil sands, and by 2024 this is expected to increase to four million barrels per day (Government of Alberta, 2007a). The Alberta oil sands are extracted through surface mining techniques when deposits are less than 70 meters below the surface, and in situ extraction methods, such-as Steam Assisted Gravity Drive (SAGD), for reserves below that (Government of Alberta, 2007b).

In the AOSR, the source rock McMurray Formation contains up to 20% bitumen by weight (Carrigy, 1962; Chalaturnyk et al., 2002). For surface mining, bitumen recovery is generally better than 90% (Masliyah et al., 2004), whereas *in-situ* production methods only recover approximately 35-60% of bitumen (Government of Alberta, 2007a). The byproducts of surface mining extraction include residual bitumen, waste rock, and oil sands process-affected water (OSPW), all of which must be deposited into large tailings pond facilities due to the Government of Alberta's Zero Discharge Policy (Government of Alberta, 2007b). Tailings facilities cover an area approximately 220 km^2 of Northern Alberta (Alberta, 2013). The tailing ponds and surrounding ecosystems are a primary focus for understanding the environmental footprint of this industry (Small et al., 2015). Of most concern is the potential for OSPW to leak from the dykes and tailings impoundments into the surrounding ecosystems. The large scale of tailings ponds means that inevitably some are situated above permeable deposits that could

potentially create a preferential groundwater flow path for OSPW leakage into the surrounding environments (Furguson et al., 2009; Holden et al., 2011).

Tailings pond OSPW is alkaline and distinguishable by elevated concentrations of dissolved metals (e.g. Al, As, B, Cd, Cr, Cu, Fe, Pb, Mo, Ni, Ti, V, and Zn), naphthenic acids (NAs) and major ions such as sodium, bicarbonate, chloride, sulfate, and ammonia (Allen, 2008; Chen et al., 2013). Leakage of such fluids would deliver priority pollutants to the surrounding environment (eg. Naphthenic acids, As, Cd, Cr, Cu, Ni, Pb, and Zn) (Allen, 2008; CCME, n.d.; US EPA, 2014).

The AOSR is located within the Boreal Plains Ecozone of Northern Canada (Devito et al., 2005). A flat topography and strong climatic seasonality means this ecozone is comprised of approximately 30% peatlands within wetland environments (Warner et al., 1997). The wetlands encountered in this study are comprised of marsh, swamp, and fen complexes that locally are termed "muskeg" (Johnson and Miyanishi, 2008; Warner et al., 1997). The large area of muskeg within the AOSR means that many oil sands tailings ponds are adjacent to wetlands and consequently any OSPW leakage will infringe on these environments. The AOSR wetland hydrology is controlled by the sub-humid local climate (~450 mm per year precipitation; ~75% rain, 25% snow), and an overall precipitation deficit of approximately 50 mm per year (Johnson and Miyanishi, 2008).

In wetland environments, geochemistry is dominated by the interactions of organic matter with wetland hydrology (Appelo and Postma, 1994; Wetzel, 2001). In wetland surface- and groundwaters, humic substances account for a substantial portion of dissolved organic matter (DOM)(Weng et al., 2002). Humic substances

are highly variable, complex, naturally occurring, ever-present macromolecules that originate from plant remnants and terrestrial sediments (Appelo and Postma, 1994; Wood, 1996). Humic substances are further divided into two main components, humic acids (HAs) and fulvic acids (FAs). For the purpose of this paper, the term "humic substances" will refer to humic plus fulvic acids, and "humic acids" will refer to just the single humic acid component. This distinction is based on the chemical treatment of humic substances, in which acidification of the alkaline extract precipitates HAs and leaves FAs in solution (Killops and Killops, 2005). Fulvic acids generally have lower molecular weights and contain more oxygen compared to humic acids (Wetzel, 2001).

Humic substances can impact numerous aspects of metal transport, in particular metal speciation and redox geochemistry through microbially mediated reactions (Aiken et al., 2011). The organic molecules themselves are not typically considered environmentally hazardous; however, humic substances commonly have negatively charged surfaces that attract positively charged cations to form stable organic-metal (organometallic) complexes with metal ions (Appelo and Postma, 1994; Wetzel, 2001). Organometallic complexes can change the chemical behavior (i.e. fixation, release, and transportation) of a metal from its inorganic dissolved aqueous form to resemble the overall chemical behavior of the organic humic ligand (Aiken et al., 2011; Appelo and Postma, 1994; Crabtree, 2005; Kim et al., 1990; Wood, 1996).

Previous studies on potential contaminant transport in the AOSR have focused on the toxicity and the transport of naphthenic acids, surface contaminants,

hazardous metals, small-scale field reconstructions, and laboratory based experiments (Abolfazlzadehdoshanbehbazari et al., 2013; Furguson et al., 2009; Holden et al., 2011; Oiffer, 2006; Savard et al., 2012).

Abolfazizadehdoshanbehbazari (2013) and Holden et al. (2011) both studied sorption and ion exchange interactions between inorganics and surficial sediments in the AOSR. Abolfazizadehdoshanbehbazari (2013) used a small-scale model to observe these reactions, and used the results to predict a flow model for OSPW seepage. Holden et al. (2011) used batch sorption experiments to model the effects of adsorption and ion exchange with inorganic metals in an AOSR clay till aquitard (Holden et al., 2011). Both studies concluded that inflow of OSPW acts as a catalyst for sulfate salt dissolution reactions and calcium-magnesium carbonate mineral precipitation. They also observed that sodium and chloride primarily remained in solution (Holden et al., 2011). Oiffer (2006) analyzed naphthenic acids, organic, and inorganic components, and focused on the transport properties that affect naphthenic acids in the subsurface. Both Savard et al. (2012) and Ferguson et al. (2009) assessed groundwater flow around tailings impoundments in order to establish a base for estimating the local environmental impacts. All of these important studies took an inorganic approach to metal behavior; however, to the best of our knowledge, no field scale research has actually been conducted to determine how measured humic substances affect trace metal transport within the AOSR. Consequently, the impact of organic-driven geochemical processes on the transportation, dissolution, precipitation, and complexation reactions of the organic and inorganic constituents of OSPW are largely unknown and unstudied.

This study investigates the chemical behavior of trace metals in organic-rich environments situated adjacent to large tailings facilities in the AOSR. A geochemical modeling approach was taken (WHAM7 and PHREEQC) to investigate the partitioning of trace metals between colloidal humic substances, clays, and oxyhydroxides. The analysis aims to determine the general principles of how organic complexation will impact inorganic metal behavior in these organic-rich environments.

2 Methods

2.1 Study Area

This study uses two datasets from different site localities, and contains both groundwater and surface water samples. For both sites, surface mining has occurred continuously over the last two decades, and all monitoring wells are located between a tailings pond and an adjacent surface water creek or river (i.e. wells are positioned down the hydraulic gradient from the tailings ponds) (Savard et al., 2012). The two sites are on the property of different mining companies, both of which provided well access and historical data. Confidentiality was an important component for obtaining access to these facilities; therefore, the tailings pond locations and operating companies are anonymous. Surface water samples were collected from the nearby Muskeg and Athabasca Rivers.

Dataset 1 is composed of nine groundwater samples and one surface water sample, collected in October 2014, near Tailings Pond 1(TP1). Most of TP1 monitoring wells are situated in an organic-rich muskeg complex that mostly

overlies a thin (<2 m) till veneer, or in a few instances bituminous McMurray Formation sandstone. In this area, the till is generally comprised of bituminous McMurray Formation (Andriashek, 2003).

Dataset 2 is composed of eight groundwater samples, five surface water samples, a background (BG) surface water sample, and a seep pipe (SP) sample, all of which were collected in October 2015, near Tailings Pond 2 (TP2). The BG surface water sample was taken from the Muskeg River located upstream (N57.324, W111.118), away from any potential waterborne transport pathways from mining operations. The seep pipe site is located at the base of a large tailings pond, at a topographic height and with drainage infrastructure that ensures it can only be sourced from tailings pond-derived waters that have travelled through the subsurface and then been captured by the dyke system before being pumped back into the tailings pond. TP2 monitoring wells differ from TP1 monitoring wells in that they are situated in a non-wetland environment with wells screened and sampling waters within river sediments (aquifer sands) that overlie McMurray Formation bituminous sandstone.

2.2 Field Sampling and Measurement

All the groundwater samples were collected from screened wells of 2" diameter. Before sampling, three well-volumes of water were initially purged and discarded. Groundwater was pumped from the wells using a stainless steel bladder pump lined with a Teflon covered LDPE bladder (Solinst Canada Ltd. model 407SS, Georgetown, ON, Canada). To minimize the chances of inducing turbidity during pumping, low flow rate (<0.5 L/min) procedures were used.

After triple-rinsing sample bottles with unfiltered well water, unfiltered samples for organic analyses were pumped into fluorinated HDPE bottles (Thermo Fisher Scientific, Waltham, MA, USA). To collect filtered samples for metals analyses, a 0.45-µm filter was fitted directly onto the sample line, which ensures no change in groundwater oxygenation prior to sampling. Both filter (Durapore Sterivex capsule, MilliporeSigma, MA, USA) and sample container (HPDE, Thermo Fisher Scientific, Waltham, MA, USA) were triple-rinsed with filtered well water prior to sample collection. Once collected, water samples were refrigerated at 4°C until analysis. As companies were reluctant to have our team use preserving HNO_3 on site without their training and certification, the samples for ICP analysis were acidified to 1% v/v ultrapure HNO_3 (Seastar Chemicals, BC, Canada) once back in the laboratory, and then left to sit for one month to redissolve any potential precipitates.

A YSI ProPlus multiparameter (YSI, Ohio, USA) meter was used to obtain temperature (T), specific conductivity (SC), pH, dissolved oxygen (DO), and oxidation-reduction potential (ORP). Calibration of the YSI meter was conducted every morning using standard solutions (Zobells for ORP; 4,7, and 10 for pH; 1413 µS/cm solution for SC; and 0 oxygen solution generated via the $NaSO_3$ method for DO (Pickering, 1979)). A field-portable, battery-powered HACH spectrophotometer (model DR2800, HACH, CO, USA) was used to determine Fe^{2+} (HACH method 8146) and S^{2-} (HACH method 8131) within 5 minutes of pumping (HACH, 2007). Calibration of the spectrophotometer was carried out via standard methods (HACH, 2007).

2.3 Analytical Methods

Inductively Coupled Plasma Optical Emission Spectroscopy (ICP-ES, ARCOS, Spectro, Kleve, Germany) and Quadrupole Mass Spectroscopy (Q-ICP-MS, Xseries 2, ThermoFisher Scientific, Bremen, Germany) element analysis were conducted at Natural Resources Canada- Geologic Survey of Canada in Ottawa, Ontario, via standard methods (Arbogast and Geological Survey (U. S.), 1996; Lamothe et al., 1999). The Fe^{3+} concentrations were calculated by taking the difference between the total Fe as determined by ICP analysis, and the field measured Fe^{2+} HACH results (HACH, 2007).

Characterization and quantification of total acid extractable organics (AEOs) containing humic substances and NAs were determined by high-resolution Orbitrap mass spectrometry in aliquots of unprocessed water samples shipped to Environment and Climate Change Canada (Saskatchewan, SK). Analyses were carried out by 5 μL loop injection (flow injection analysis) using a Surveyor MS pump (Thermo Fisher Scientific Inc.) and a mobile phase of 50:50 acetonitrile/water containing 0.1% NH_4OH. Mass spectrometry analysis was performed on a dual pressure linear ion trap-orbitrap mass spectrometer (LTQ Orbitrap Elite, Thermo Fisher Scientific, Bremen, Germany) equipped with an electrospray ionization (ESI) interface operated in negative ion mode. Data was acquired in full scan mode from m/z 100 to 600 at a setting of 240,000 resolution. The majority of ions were singly charged, and the average mass resolving power (m/Δm50%) was 242,000 at m/z 400. Mass accuracies of less than 1 ppm were obtained using a lock mass compound (n-butyl benzenesulfonamide) for scan-to-scan mass calibration correction.

2.3.1 PHREEQC

The numerical model, PHREEQC, was used to calculate the dominant valence state for various redox sensitive elements to ensure input compatibility with WHAM7. It was also used to determine the mineral saturation indices for various oxyhydroxides and clays likely present within the system. The databases used for these calculations were MINTEQV4 and LLNL (Allison, 1991; USGS, 2016). The input parameters included Ag, Al, Alkalinity, As, B, Ba, Be, Br, Ca, Cd, Cl, Co, Cr, Cu, F, Fe^{2+}, Fe^{3+}, K, Li, Mg, Mn, Mo, Na, Ni, NO_3, P, Pb, pe, pH, S, Se, Sn, SO_4, Sr, Temperature, Tl, U, V, and Zn.

2.3.2 WHAM7

Windermere Humic Aqueous Model VII (WHAM7) is a combination of an inorganic speciation model and Humic Ion-Binding Model VII (Tipping et al., 2011). It is used to simulate the equilibrium chemical reactions that occur when metals enter soil/groundwater systems. For this investigation, WHAM7 was used to calculate the "Fraction Bound to Colloidal Phases" in order to characterize the sorption preference of metal ions to humic substances, oxyhydroxides, and clays in the dissolved aqueous phase. The input parameters for WHAM7 include, temperature, pH, inorganic solute concentrations, colloidal FAs, Fe and Mn oxyhydroxides, and clay concentrations.

Some wells tested positive for S^{2-}, and thus might have been producing sulfide precipitates; however, WHAM7 does not model sulphide phases and hence the potential role of sulfide sorption remains unconstrained in this analysis.

2.3.2.1 WHAM7 Input Parameters

Concentrations of total AEOs, determined by high-resolution mass spectrometry, were used to estimate concentrations of colloidal FAs. As illustrated by several Orbitrap mass spectra (Figure 2-1), AEOs in groundwater samples contained negligible high molecular weight species (i.e., $m/z > 500$). A sensitivity model was run to estimate how partitioning would change if HAs were present within the system. For this test, HA and FA concentrations were both estimated at 50% of the total measured AEOs. Using PeakFit software (Systat Software Inc., California, USA) a smoothed spectrum was generated for each sample, from which the peak spectral amplitude was taken as the mode, which is identified by the arrows in Figure 2-1.

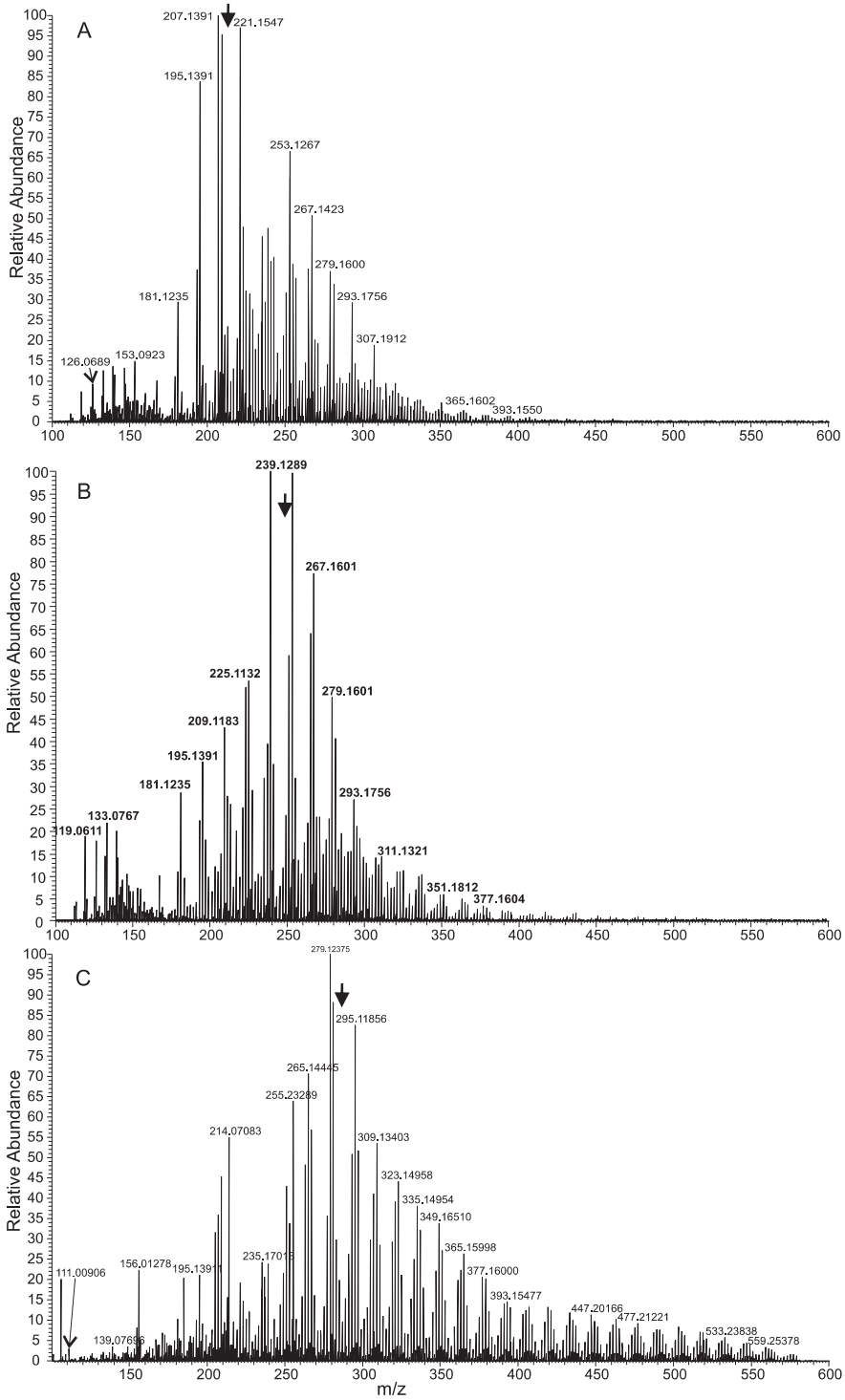

Figure 2- 1: Mass spectra from Orbitrap data. A) Reduced groundwater from a wetland Dataset 1 (mode of the distribution is depicted by the solid arrow). B) Reduced groundwater spectrum for a well from minerallic Dataset 2 (mode is at a higher m/z than for A). C.) Oxidized surface water sample from the Muskeg River mouth. Surface water samples all contained substantially more high m/z compounds than groundwaters, which is reflected in the spectra having the highest m/z modes.

The molar mineral concentrations for colloidal Fe and Mn oxyhydroxides were estimated by calculating Fe^{3+} as FeO(OH) (Goethite) and Mn as $Mn(OH)_2$, which are the assumed mineralogy in WHAM7. It was assumed that Fe^{3+} and Mn were contained within no other colloidal phases. As samples were filtered at 0.45 μm, all calculated oxyhydroxides within the water samples were colloidal in size. A model was run without Fe and Mn oxyhydroxides to ascertain the sensitivity these components have within the analysis. A similar model was run with Fe oxyhydroxide, but without Mn oxyhydroxide concentrations, to determine the relative impacts of these oxyhydroxides on the system.

The initial clay concentrations were calculated using the dissolved Al concentrations converted to clay mineral equivalencies of kaolinite ($Al_2Si_2O_5(OH)_4$). Clays are both colloidal and non-colloidal particulate substrate phases, and hence their real impact may be inaccurately under-represented by filtered water chemistry. Consequently a sensitivity model was run to determine how the system would be affected if clay concentrations were set artificially high at three times the FA concentration.

2.4 Ions and Metals Investigated

In addition to the major ions typically associated with OSPW (Al, Cl, Cr, Cu, Fe, Pb, Mg, Na, Ni, SO_4, and Zn) (Allen, 2008; Chen et al., 2013), Ba, Be, Ce, Co, Dy, Er, Eu, Gd, F, K, La, Nd, Pr, Sm, Sr, Tb, U, Y and Yb were also investigated. Although Al, Cd, and Tl are typically found in OSPW, the majority of samples in both of the datasets had concentrations below the detection limits; therefore, these elements were not included in this investigation. Similarly, Ni, Zn, Pb, and Co measured below the detection limit in Dataset 1, and were therefore not modeled for that dataset.

Arsenic (As), Mo, Ti, and V are not included in the WHAM7 database and were thus excluded from the analysis.

3 Results

3.1 Water Chemistry

The groundwater and surface water samples in this study are generally representative of the majority of the water types likely to be encountered in the AOSR: muskeg-derived, organic-rich waters (Dataset 1), minerallic-substrate waters (Dataset 2), river surface waters (Dataset 1 & 2), and production-impacted waters (seep pipe sample in Dataset 2). In particular, the BG and seep pipe samples represent the end members likely to be present in the AOSR. The seep pipe is representative of tailings pond water that have become iron-reducing during transport through the subsurface, and consequently is more consistent with the groundwaters than the tailings pond samples themselves. The BG water is considered to be unaffected by mining activities.

The overall major ion loads as indicated by Na, Cl, K, Br, and alkalinity show no real difference between Dataset 1 and 2. The groundwaters in Dataset 1 were primarily Na-rich bicarbonate waters, and the one surface water sample was a Ca-rich sulfate. The groundwaters and surface waters in Dataset 2 were all Ca-rich mixtures of bicarbonate and sulfate waters (Figure 2-2). The seep pipe sample was a Ca-rich, sulfate (Figure 2-2). The redox potential of most groundwater samples in both datasets was reducing, with the exception of three oxidized well samples from Dataset 2 which is likely due to low pumping rates. Dissolved oxygen (DO)

concentrations in the reducing groundwater wells ranged from 0.03-0.97 ppm, and in the three wells that had oxidizing conditions ranged from of 3.9-7.9 ppm. Fe^{2+} concentrations in most groundwater samples were well above the detection limit (Table 2-1). In contrast, the surface waters in both datasets were fully oxidized; DO concentrations ranged from 3.9-12.6 ppm and undetectable amounts of Fe^{2+}. The pH in Dataset 1 ranged from 7.6-8.3 in groundwater and 8.1 in the surface water sample. The pH in Dataset 2 ranged from 6.6-7.1 in groundwater and 7.4-8.4 in surface waters (Table 2-1). The seep pipe sample had a DO of 4.1 ppm and a pH of 6.9.

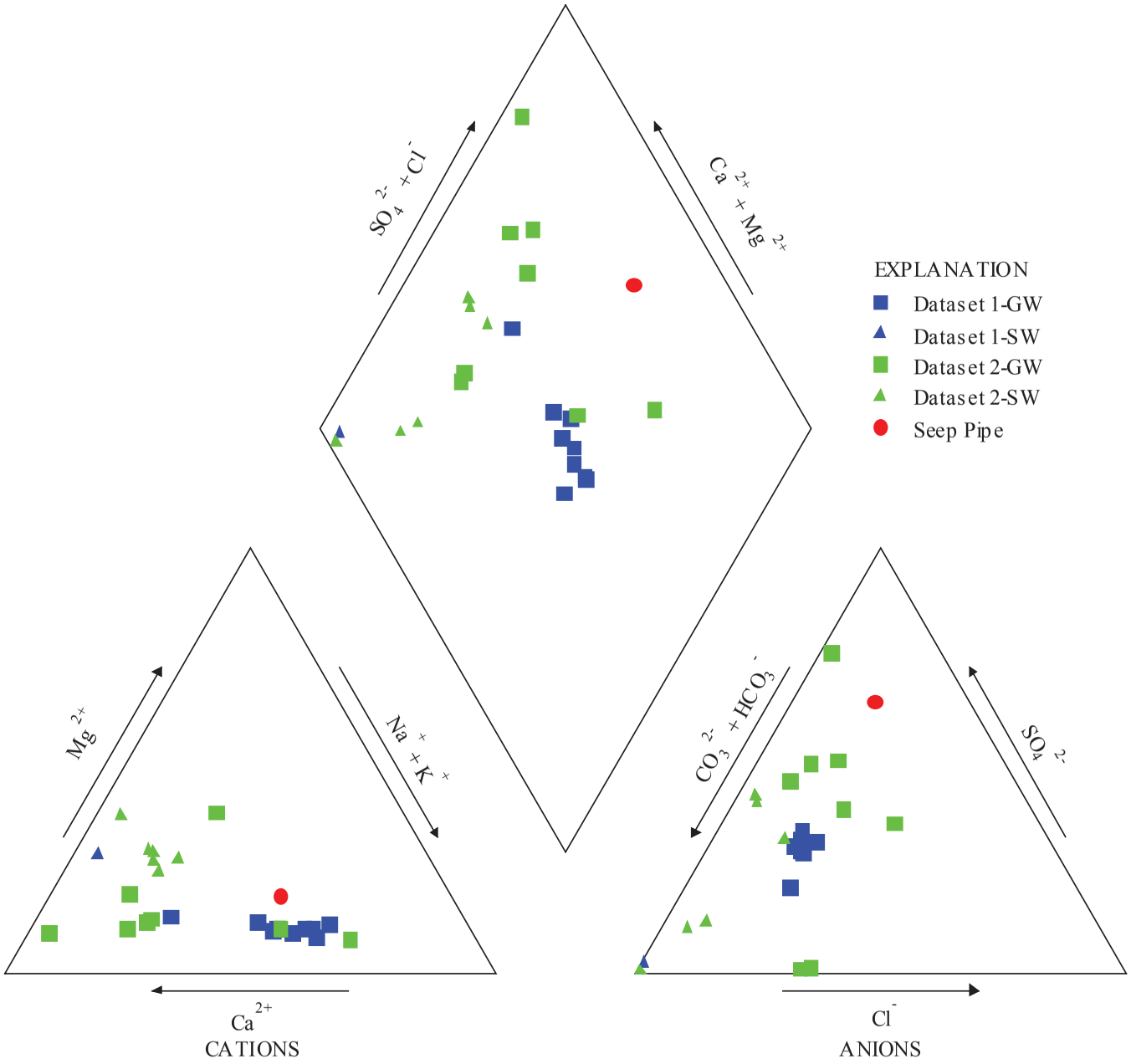

Figure 2-2: Piper diagram of dataset 1 and 2.

In Dataset 1, AEOs concentration ranged from 2.65- 8.53 ppm (averaged 5.74 ± 1.96) in groundwaters and was 1.78 ppm in the surface water sample. The AEOs concentrations in Dataset 1 were generally lower than those in Dataset 2, which ranged from 7.3-58.9 ppm in groundwater and 1.3-7.8 in surface waters (averaged 19.3 ± 19.93 ppm and 4.18 ±3.13 ppm respectively)(Table 2-1). The Orbitrap mass spectra for these water samples differed markedly and systematically through the different environments (Figure 2-1). In comparison to the broad m/z range of organic compounds in the surface water samples, all groundwaters contained lower relative abundances of high molecular weight m/z components. The wetland organic-substrate samples of Dataset 1 were slightly reduced in higher m/z components in comparison to the minerallic-substrate Dataset 2 samples, as reflected by the spectral mode for those wells (wetland spectral mode m/z = 217.5 ± 6.6; minerallic spectral mode m/z = 248.7 ± 8.2; two-tailed t-test $P < 0.001$).

Both datasets had inorganic element concentrations with notable differences (Table 2-1). Cobalt, Ni, Pb, and Zn concentrations were low, but measurable in Dataset 2, but below detection limits in Dataset 1 (Table 2-1). Concentrations of As in Dataset 1 were also low compared to those in Dataset 2. In contrast, concentrations of B, Cr, Li, Mn, Na, and V were elevated in Dataset 1 compared to Dataset 2 (Table 2-1). Sodium concentrations in Dataset 1 were more than two times greater than those in Dataset 2 (Table 2-1). Strontium concentrations in Dataset 2 were more than two times greater than those in Dataset 1 (Table 2-1).

In most groundwater wells, the following were elevated in comparison to BG and most surface water sites: Alkalinity, As, B, Ba, Br, Ca, Ce, Cl, Cr, F, Li, Mn, Mo, Na,

Ni, S, SO_4^{2-}, Sr, U, V, Y, and Zr (Table 2-1). This was also true for Ni and Zn in Dataset 2, but not so for these two elements in Dataset 1 (Table 2-1). Ni was elevated in the seep pipe in comparison to all surface and groundwaters (Table 2-1). Although Al and Cu are typically associated with OSPW (Allen, 2008), Al was low throughout all but one sample. Copper was elevated in surface waters in comparison to groundwaters, where many samples were near or below the detection limit. Cobalt, K, and Mg concentrations were elevated in the seep pipe sample; however, such high concentrations were not found in any groundwater wells (Table 2-1).

Table 2- 1: Range; Mean ± Standard Deviation for Dataset 1 & 2 split into groundwater (GW), Surface water (SW), and seep pipe (SP). Alk = alkalinity; DOC=dissolved organic carbon; AEOs = acid extractable organics; Te, Se, Eu, Ho, Lu, Tb, Tm, PO_4, Cs, Cd, Nd, Ta, W, Ga, In, Sn, Tl are below detection limits.

		Dataset 1		Dataset 2		
		GW (n=9)	SW (n=1)	GW (n=9)	SW (n=6)	SP (n=1)
OTHER PARAMETERS						
pH		8.0 ±0.22; 7.6-8.3	8.1	6.8 ±0.20; 6.6-7.1	8.1 ± 0.41; 7.4-8.4	6.9
pe		10.4 ±0.32; 9.9-10.9	11.9	10.8 ± 1.30; 8.7-12.5	13.17 ± 0.33; 12.6-13.5	10.6
DOC	**ppm**	12.1 ± 2.39; 9.8-17.2	4.8	28.3 ± 21.55; 12.1-75.1	11.45 ±7.83; 3.7-19.9	32.3
AEOs	**ppm**	5.74 ± 1.96; 2.7-8.5	1.8	18.34 ± 18.06; 7.3-58.9	4.18 ± 3.13; 1.3-7.8	50.4
T	**C**	7.2 ±1.4; 5-9	7.4	8.3 ±1.3; 5.4-9.7	6.2 ±0.7; 5.2-7.2	12.4
ALK	**ppm**	445 ±49.6; 246-516	167	486 ±152; 245-676	151 ± 31.5; 245-676	459.0
DO	**ppm**	0.42 ± 0.35; 0.4-1.0	6.6	2.5 ± 2.64; 0.4-7.1	10.2 ± 3.27; 3.9-12.6	4.1
NO^3	**ppm**	<0.02	<0.02	0.31 ±0.47; 0.31 ±0.47	<0.02	<0.02
SO^4	**ppm**	113-151; 127.3 ±23.1	1.9	113-151; 246 ±203	26.5 ±21.3; 0.25-50.4	763.3
ALKALI METALS						
K	**ppm**	1.98-3.53; 2.6 ±0.51	1.1	1.98-3.53; 2.1 ±10	1.00-1.32; 1.2 ±0.12	20.4
Li	**ppb**	28.44-53.29; 53.3 ±16.5	8.2	28.4-76.8; 29.9 ±28.8	4.93-12.6; 8.2 ±3.3	212
Na	**ppm**	90.17-209; 160 ±38.3	3.1	90.2-209; 77.3 ±31.8	3.62-17.9; 13.0 ±5.1	303
Rb	**ppb**	0.71-2.7; 1.4 ±0.46	0.64	0.71-2.38; 1.9 ±1.5	0.69-1.46; 1.0 ±0.33	17.7
ALKALINE EARTH METALS						
Ba	**ppb**	162-343; 230 ±61.4	57.4	55.2-317; 183 ±94	26.9-62.1; 45.2 ±14.1	76.0
Be	**ppb**	0.012-0.11; 0.03 ±0.03	<0.005	0.01-0.14; 0.03 ±0.05	<0.005	0.0
Ca	**ppm**	81.3-165; 104 ±25.9	46.2	63.2-332; 212 ±100	35.9-48.8; 43.0 ±4.2	203
Mg	**ppm**	13.1-22.1; 17.5 ±3.1	11.4	9.27-95.3; 34.9 ±30.6	11.1-17.3; 13.2 ±2.1	66.4
Sr	**ppb**	186-280; 219.4 ±30.4	93.9	320-747; 481 ±157	90.1-349; 220 ±116	2351
Co	**ppb**	<0.05	<0.05	0.03-8.53; 2.6 ±3.3	0.03-0.19; 0.10 ±0.07	49.5
Cr	**ppb**	0.25-1.42; 0.250.45 ±0.38	0.05	0.05-0.77; 0.36 ±0.29	<0.05	0.21
Cu	**ppb**	<0.1	2.0	<0.1	0.16-0.70; 0.44 ±0.20	<0.1
Fe	**ppm**	3.13-33.5; 9.6 ±9.1	0.2	0.12-4.90; 1.4 ±1.7	0.02-0.39; 0.19 ±0.18	32.4
Fe2+	**ppm**	2.11-3.67; 3.7 ±0.5	BDL	0-4.53; 1.3 ±1.6	0-0.06; 0.01 ±0.02	UNK
Fe3+	**ppm**	0.50-29.8; 6.9 ±8.7	0.2	0-0.37; 0.1 ±0.1	0.02-0.39; 0.2 ±0.2	UNK
Hf	**ppb**	0.01--.05; 0.02 ±0.01	<0.01	0.1-0.13; 0.04 ±0.04	<0.01	0.06
Mn	**ppb**	246-627; 419 ±142	75.4	114-786; 417 ±258	6.52-119; 29.5 ±44.2	5026
Mo	**ppb**	0.03-0.29; 0.16 ±0.09	<0.05	0.11-0.68; 0.33 ±0.23	0.06-0.84; 0.42 ±0.38	4.5
Ni	**ppb**	<0.2	<0.2	0.1-11.1; 4.5 ±4.1	0.37-0.65; 0.52 ±0.12	58.1
Re	**ppb**	<0.005	<0.005	0-0.3; 0.01 ±0.01	<0.005	0.04
Sc	**ppm**	<0.001	<0.001	<0.001	<0.001	0.002
Ti	**ppb**	1.39-5.54; 2.2 ±1.3	<0.5	0.59-1.43; 1.0 ±0.35	0.61-0.88; 0.72 ±0.14	1.2
Y	**ppb**	0.05-1.55; 0.38 ±0.48	<0.01	0.13-1.08; 0.33 ±0.34	0.02-0.06; 0.04 ±0.01	0.14
Zr	**ppb**	0.61-2.08; 0.98 ±0.47	<0.05	0.29-6.26; 2.0 ±2.1	0.03-0.21; 0.09 ±0.08	0.78

Table 2-1 cont.: Range; Mean ± Standard Deviation for Dataset 1 & 2 split into groundwater (GW), Surface water (SW), and seep pipe (SP). Alk = alkalinity; DOC=dissolved organic carbon; AEOs = acid extractable organics; Te, Se, Eu, Ho, Lu, Tb, Tm, PO_4, Cs, Cd, Nd, Ta, W, Ga, In, Sn, Tl are below detection limits.

		Dataset 1		Dataset 2		
		GW (n=9)	SW (n=1)	GW(n=9)	SW (n=6)	SP (n=1)
POST TRANSITION						
Al	**ppm**	0.008-0.01; 0.01 ±0.0002	0.01	<0.005	<0.005	<0.005
Pb	**ppb**	<0.01	<0.01	0.01-0.10; 0.03 ±0.03	0.01-0.03; 0.02 ±0.01	0.08
V	**ppb**	0.96-8.35; 2.3 ±2.4	<0.1	0.21-3.16; 0.91 ±1.1	0.11-0.22; 0.17 ±0.04	0.41
Zn	**ppb**	<0.5	0.94	0.25-54.4; 9.3 ±20	0.25-0.78; 0.39 ±0.23	9.0
METALLOIDS						
As	**ppb**	0.21-1.43; 0.62 ±0.46	<0.1	0.42-1.29; 0.77 ±0.30	0.23-0.33; 0.27 ±0.03	1.6
B	**ppb**	121-819; 408 ±210	24.6	29.9-619; 195 ±208	7.71-47.0; 27.6 ±14.7	1982
Si	**ppm**	5.63-11.4; 7.3 ±1.8	6.5	3.06-7.25; 4.8 ±1.4	0.81-5.90; 2.9 ±2.2	7.9
Sb	**ppb**	<0.01	<0.01	0.01-0.22; 0.05 ±0.07	0.02-0.05; 0.03 ±0.01	<0.01
Ge	**ppb**	0.06-0.16; 0.08 ±0.03	<0.02	<0.02	<0.02	0.07
NONMETALS						
Br	**ppm**	0.17-0.25; 0.19 ±0.03	<0.05	0.03-0.41; 0.23 ±0.14	<0.05	0.33
Cl	**ppm**	56.4-74.0; 61.1 ±5.8	0.62	21.1-147; 74.3 ±48.1	0.72-12.1; 5.3 ±4.0	151
P	**ppm**	0.03-0.35; 0.15 ±0.09	<0.05	<0.05	<0.05	<0.05
S	**ppm**	39.7-52.1; 45.0 ±7.9	0.77	2.20-173; 86.8 ±69.6	0.41-17.6; 9.5 ±7.2	264
LANTHANIDES						
Ce	**ppb**	0.03-1.0; 0.27 ±0.35	<0.01	0.13-3.96; 0.85 ±1.4	0.015-0.024; 0.02 ±0.004	0.04
Dy	**ppb**	0.01-0.22; 0.05 ±0.07	<0.005	0.01-0.15; 0.05 ±0.05	0.003-0.007; 0.01 ±0.00	0.02
Er	**ppb**	0.01-0.14; 0.03 ±0.04	<0.005	0.01-0.10; 0.03 ±0.03	<0.005	0.01
Gd	**ppb**	0.01-0.24; 0.05 ±0.07	<0.005	0.01-0.17; 0.05 ±0.06	<0.005	0.01
Nd	**ppb**	0.02-0.78; 0.19 ±0.25	<0.005	0.04-0.63; 0.17 ±0.22	0.013-0.022; 0.02 ±0.00	0.04
Pr	**ppb**	0.01-0.15; 0.04 ±0.05	<0.005	0.01-0.15; 0.04 ±0.05	<0.005	0.01
Sm	**ppb**	0.0-0.18; 0.04 ±0.06	<0.005	0.01-0.14; 0.04 ±0.05	<0.005	0.01
Yb	**ppb**	0.01=0.13; 0.03 ±0.04	<0.005	0.01-9.09; 0.03 ±0.03	<0.005	0.02
ACTINIDES						
U	**ppb**	0.01-0.13; 0.06 ±0.04	0.01	0.05-10.6; 2.9 ±4.04	0.04-0.53; 0.29 ±0.22	1.9

3.2 PHREEQC Modeling

PHREEQC was used to determine the valences of Co, Cr, Cu, Mn, and U to ensure speciation compatibility for WHAM7. WHAM7 assumes U^{4+} and Cr^{3+} and PHREEQC calculations indicate that U^{6+} and Cr^{6+} were the dominant valences;

therefore, these elements were omitted from the WHAM7 model. PHREEQC determined the valences of Co, Cu, and Mn as 2+, which were compatible with WHAM7's assumed elemental valences. PHREECQ verified Ce, Pr, Nd, Sm, Eu, Gd, Tb, Dy, Er, Tb, Yb, and La to have 3+ valences, which were compatible with WHAM7 speciation. PHREEQC indicated that goethite (FeO(OH)) and manganite (MnO(OH)) were likely the oxyhydroxide minerals within this system, with average saturation indices of 5.7 ±0.98 and 2.1 ±2.1 respectively, in all samples. However, it predicted that Mn carbonates such as rhodochrosite ($MnCO_3$) were more likely to form than Mn oxyhydroxides. Rhodochrosite was near saturation in both Dataset 1 and 2 (SI averaging -0.53 ±0.7).

3.3 WHAM 7 Modeling and Sensitivity Tests

WHAM7 represents components that are sorbed to humic substances, oxyhydroxides, and clays, but does not indicate where the remainder of non-sorbed ions reside. Some conservative ions such as Na, K, Mg, Ca, Ba, Cl, F and SO_4 were assumed to remain in solution (i.e., they were all 100% not sorbed to any component in the models and are therefore not graphically displayed). However, for some non-conservative elements, where results indicate less than 100% sorption to the above mentioned solid-phase substrates, it is unlikely that these ions exist in their free dissolved forms within this system (e.g., the model indicates 62 ± 20% of Ni is not sorbed to FA or oxyhydroxides). These ions could reside in aqueous ion complexes, other unconstrained substrates (e.g. sulfides or carbonates), or perhaps even clay species that are not properly considered in the WHAM7 model and underlying empirical database. Consequently, the non-sorbed component is termed "Remainder" herein.

Sensitivity tests were done to determine the impact each colloidal phase (humic substances, oxyhydroxides, and clays) had on sorption phase preference within the system. The estimated FA concentrations were consistent with other aquifers where AEOs fractions (i.e. the fraction containing humic substances) of dissolved organic carbon (DOC) were predominantly FAs, with undetectable amounts of HAs (Artinger et al., 2000; Christensen and Christensen, 1999; Weng et al., 2002; Wetzel, 2001). This is thought to be due to HAs tendency to readily sorb to particulate mineral and solid-phase organic substrates, and hence are either immobilized or extracted during filtration (Bryan et al., 2002; Weng et al., 2006). The AEOs concentrations measured in these samples was thus assumed to represent the FA concentrations, and used as input into WHAM7. However, a sensitivity test was done to determine the impact measurable concentrations of humic acid would have on the system. The addition of colloidal HAs to the solution phase did not affect the percentage of sorption to humic substances or oxyhydroxides, the metals that partitioned to FA were just split between HAs and FAs (Table 2-2). There were important differences in this split, with Cu preferring sorption to HA over FA whilst rare earth elements (REEs) strongly partitioned to FAs rather than HAs (Table 2-2). Note that sorption coefficients of REEs in WHAM have been questioned (Tosiani et al., 2004), but that fine detail is not considered relevant to this first-order estimation.

Sensitivity Test 1 removed clay minerals from the system, which in all simulations, including sensitivity tests with artificially high concentrations of clay minerals, did not predict clay to represent a significant sorption phase for metals.

Consequently, the role of clay in metal sorption at our study sites will not be discussed further.

Sensitivity Test 2 removed Mn oxyhydroxides from the model, and sorption percentages for all metals remained the same, except for Pb and Co (Table 2-2). The Pb that partitioned to Mn oxyhydroxides was added to the sorption percentage of Fe oxyhydroxides (100% in surface water and 97% in groundwater). Cobalt sorption to FA did not change; however, the portion of Co that sorbed to Mn oxyhydroxides transferred to "Remainder".

Sensitivity Test 3 removed Fe oxyhydroxides to determine the impact of a potential overestimation of Fe-oxyhydroxides (discussed further below; Table 2-2). Unsurprisingly, the test indicated that all REEs remained nearly 100% sorbed to FA in both groundwater and surface water. Beryllium's sorption switched from 100% sorbed to Fe oxyhydroxides to primarily sorbed to FA (approximately 70%) in groundwater and surface water. In contrast, Sr did not sorb to FA at all, but rather transferred to "Remainder". Lead, Cu, and Y in groundwater and surface water transferred nearly completely to FA (93%, 100%, and 100% respectively). For Pb, this was a switch from almost completely sorbed to oxyhydroxides to almost completely sorbed to FAs. Approximately 25% and 35% of Zn sorbed to FAs in surface water and groundwater, respectively, which was a minor increase over the sorption calculated with oxyhydroxide phases. Cobalt and Fe^{2+} minimally sorbed to FAs (approximately 5% each). Nickel in both groundwater and surface water sorbed partially to FAs (22 ±15%).

Table 2- 2: Results of sensitivity tests to determine the significance of each colloidal phase. Sensitivity test 1 included FA, FeOx, and MnOx. Sensitivity test 2 removed MnOx and only included FA and FeOx. Sensitivity test 3 removed FeOx and only included FA as 100% AEO. Sensitivity test 4 split the AEO (50:50) between FA and HA.

	Sensitivity Test 1			Sensitivity Test 2		Sensitivity Test 3	Sensitivity Test 4	
	FA	FeOx	MnOx	FA	FeOx	FA	HA (50%)	FA (50%)
TRANSITION METALS								
Co	4 ±3	20 ±21	12 ±13	5 ±3	21 ±21	6 ±4	3 ±3	3 ±2
Cu	87 ±20	13 ±20	0 ±0	87 ±20	13 ±20	100 ±0	56 ±8	44 ±8
Ni	19 ±12	18 ±20	1 ±1	19 ±12	18 ±20	22 ±15	12 ±11	11 ±7
Pb	1 ±2	77 ±28	22 ±27	1 ±3	98 ±3	93 ±5	44 ±4	48 ±4
Zn	28 ±20	21 ±26	1 ±1	28 ±20	21 ±26	32 ±17	16 ±11	15 ±7
Y	14 ±19	86 ±19	0 ±0	14 ±19	86 ±20	100 ±0	35 ±7	65 ±7
Al	0 ±0	1 ±1	0 ±0	0 ±0	1 ±1	0 ±0	0 ±0	0 ±0
Cr(III)	97 ±4	3 ±4	0 ±0	97 ±5	3 ±5	100 ±0	25 ±11	75 ±11
Fe(II)	5 ±4	11 ±6	1 ±1	5 ±3	12 ±6	5 ±3	4 ±3	2 ±1
Rare Earth Elements								
La	98 ±2	0 ±0	0 ±0	98 ±2	0 ±0	98 ±2	40 ±6	57 ±6
Ce	98 ±2	0 ±0	0 ±0	99 ±2	0 ±0	99 ±2	37 ±6	60 ±6
Pr	100 ±0	0 ±0	0 ±0	100 ±0	0 ±0	100 ±0	36 ±7	64 ±7
Nd	100 ±1	0 ±0	0 ±0	100 ±1	0 ±0	100 ±1	37 ±6	63 ±6
Sm	100 ±0	0 ±0	0 ±0	100 ±0	0 ±0	100 ±0	36 ±7	64 ±7
Eu	100 ±0	0 ±0	0 ±0	100 ±0	0 ±0	100 ±0	26 ±7	63 ±9
Gd	100 ±1	0 ±0	0 ±0	100 ±1	0 ±0	100 ±1	36 ±7	64 ±7
Tb	100 ±0	0 ±0	0 ±0	100 ±0	0 ±0	100 ±0	36 ±9	64 ±9
Dy	100 ±0	0 ±0	0 ±0	100 ±0	0 ±0	100 ±0	35 ±7	65 ±7
Er	100 ±0	0 ±0	0 ±0	100 ±0	0 ±0	100 ±0	33 ±7	67 ±7
Yb	100 ±0	0 ±0	0 ±0	100 ±0	0 ±0	100 ±0	35 ±7	65 ±7
ALKALINE EARTH METALS								
Sr	0 ±0	84 ±11	0 ±0	0 ±0	84 ±11	0 ±0	0 ±0	0 ±0

3.3.1 Rare Earth Elements (REE)

Ce, Pr, Nd, Sm, Eu, Gd, Tb, Dy, Er, Yb, and La are all lanthanide metals that almost completely partitioned to FAs in both groundwater and surface water (where concentrationsweare measurable; Figure 2-3). While La and Y are sometimes considered transition metals, they are typically treated as REEs (Greenwood and Earnshaw, 1997), and will be herein. In the presence of Fe oxyhydroxides, Y in both Dataset 1 and 2 predominantly sorbed to Fe oxyhydroxides (80-100%), with a small percentage (2-11%) sorbing to FAs. However, when oxyhydroxides were eliminated from the system, Y partitioned

almost completely to FAs. There were no substantial differences between Dataset 1 and 2 for any of these metals. REEs in Dataset 1 and 2 showed no differences in concentrations in groundwater, however, in surface waters in Dataset 1, all REEs were below the detection limits, and in Dataset 2, only Ce, Dy, La, and Nd were barely above the detection limits.

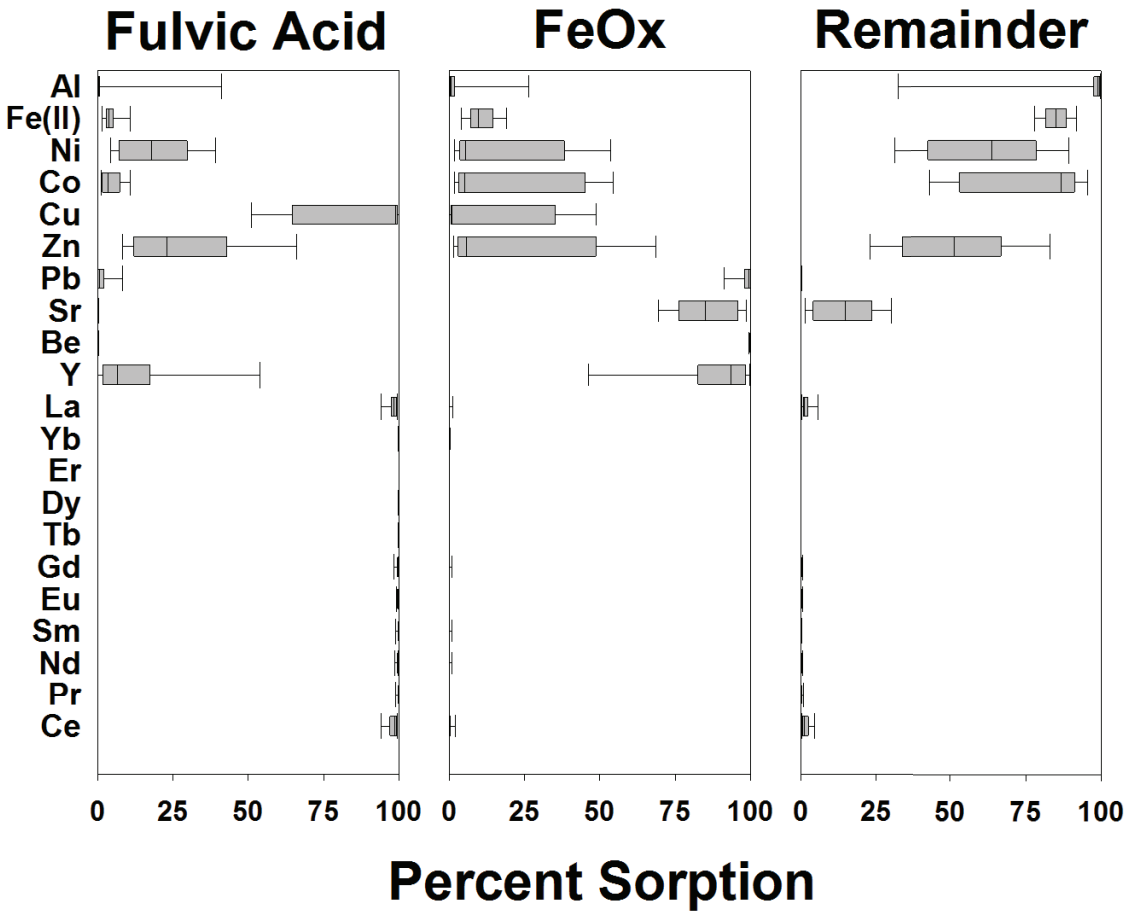

Figure 2- 3: Box and whisker plots show the percent sorption for each element on the two primary sorption phases.

3.3.2 Alkaline Earth Metals

Beryllium and Sr are both alkaline earth metals that primarily sorb to Fe oxyhydroxides. Beryllium concentrations in surface water were below the detection limit (0.005 ppb); however, in groundwater samples Be sorbed nearly 100% to Fe oxyhydroxides (Figure 2-3). Strontium in groundwater sorbed approximately 80% to Fe oxyhydroxides, while in surface water samples, it sorbed almost completely to Fe oxyhydroxides (on average 98%; Figure 3). For both metals, there were no differences in sorption between Dataset 1 and 2.

For the rest of the alkaline earth metals (Table 2-1), groundwater samples generally contained higher concentrations than surface waters. In addition, concentrations in Dataset 2 groundwaters were typically greater than those measured in Dataset 1.

3.3.3 Transition/ Post Transition Metals

In Dataset 1, all analyses for Pb, Cu, Co, Ni, and all except one for Zn and Al sample, were below detection limits. For those transition metals above detection limits for both datasets, there were no major differences in concentrations (Table 2-1; Figure 4). However, in Dataset 2, the sorption phases for chalcophile elements Pb, Zn, and, Cu differed within the model. In Dataset 2, Pb in both surface and groundwaters overwhelmingly partitioned to Fe oxyhydroxides (90-99%; Figure 2-3), with a minor portion sorbed onto FAs. When Mn oxyhydroxides were present within the system, Pb in surface waters primarily sorbed to Fe oxyhydroxides (90-

100%), while in groundwater, partitioning was split between Mn (0-40%) and Fe (60-100%) oxyhydroxides (Table 2-2).

Both Zn and Cu partially sorbed to FAs (15-40% and 70-100% respectively), with variable sorption to Fe oxyhydroxides (0-50% and 0-30% respectively; Figure 2-3 & 2-4). In Dataset 2, there were variations in Zn partitioning with respect to surface versus groundwater. In groundwaters, the Zn partitioned to Remainder and FAs (approximately 60% and 30% respectively) with a small percentage partitioning to Fe oxyhydroxides (approximately 10%; Figure 2-4). In contrast, Zn in surface waters primarily partitioned to Fe oxyhydroxides (approximately 60%) with minor sorption to FAs (approximately 10%; Figure 2-4). As the pH increased from 6.5-7.0 (groundwater) to 8.0-8.5 (surface water), so did total Zn sorption to Fe oxyhydroxides (from 0-10% to 40-70%; Figure 2-5a.) Additionally, as pH increased above 8 (surface water), Zn sorption preference changed from predominantly FAs to Fe oxyhydroxides (Figure 2-5).

In dataset 2, Cu in the surface water samples primarily sorbed to FA (50-100%) with a significant amount sorbing to Fe oxyhydroxides (35-50%; Figure 2-4). When oxyhydroxides were removed from the model, Cu completely partitioned to FA in both groundwater and surface water (Table 2-2).

Cu, Pb, and Zn commonly bond with sulfides. Unfortunately, the potential role of sulfide remains unconstrained since WHAM7 does not model these phases. No surface water samples contained significant concentrations of dissolved sulfide. Six of the groundwater samples in Dataset 1 measured above detection limit (10 ppb) concentrations of sulfide (26-73 ppb) and three samples in Dataset 2 (68-429

ppb). PHREEQC estimated that in both datasets, covellite (CuS), gelena (PbS), sphalerite (ZnS), and millerite (NiS) were under saturated (SIs = -5.0 ±1.3, -14.4 ±1.4, -14.6 ±1.4, and -18.2 ±1.6 respectively). The lack of substantial Cu, Pb, and Zn concentration differences between samples with and without measured S^{2-}, indicate this impact of sulfide is probably minor.

As their name suggests, "iron loving", siderophile elements, Co, Ni, and Fe^{2+} readily sorb to Fe minerals (Goldschmidt, 1937), although all behaved differently in the model. Co concentrations in Dataset 1 were below the detection limit. In Dataset 2, Co in surface water primarily partitioned to "Remainder" (40-80%) and Fe oxyhydroxides (10-50%), with increasing partitioning to Fe oxyhydroxides with pH (Figure 2-4 & 2-5b). Co in groundwater was not significantly sorbed to either FA or Fe oxyhydroxides (1-10% and <5%, respectively) and mostly resided in "Remainder" (Figure 2-4). When Mn oxyhydroxides were represented in the model, Co in groundwater and surface water sorbed to Mn oxyhydroxides at low percentages (10-20% and <5% respectively%). In Dataset 2, Ni in groundwaters primarily partitioned to "Remainder" (60-90%), with minor partitioning to FAs (10-40%). In surface water, partitioning was split between Fe oxyhydroxides and "Remainder" (15-60% and 30-75% respectively), with some partitioning to FA (5-40%; Figure 2-4). As pH increased (surface water), so did Ni sorption to both FAs and Fe oxyhydroxides (Figure 2-5c). There is generally no Fe^{2+} in oxidized surface waters. In groundwater, this ion primarily partitioned to "Remainder", with minor sorption to Fe oxyhydroxides (~10%), and FA (~5%; Figure 2-3). PHREEQC indicates that Cu, Pb and Zn have the strongest affinity for carbonates, malachite

($Cu_2CO_3(OH)_2$), cerussite ($PbCO_3$), and smithsonite ($ZnCO_3$)in this system, however, they are slightly undersaturated as indicated by the SI's of -8.3 ±0.8, -3.4 ±0.4, and -3.7 ±0.5, respectively.

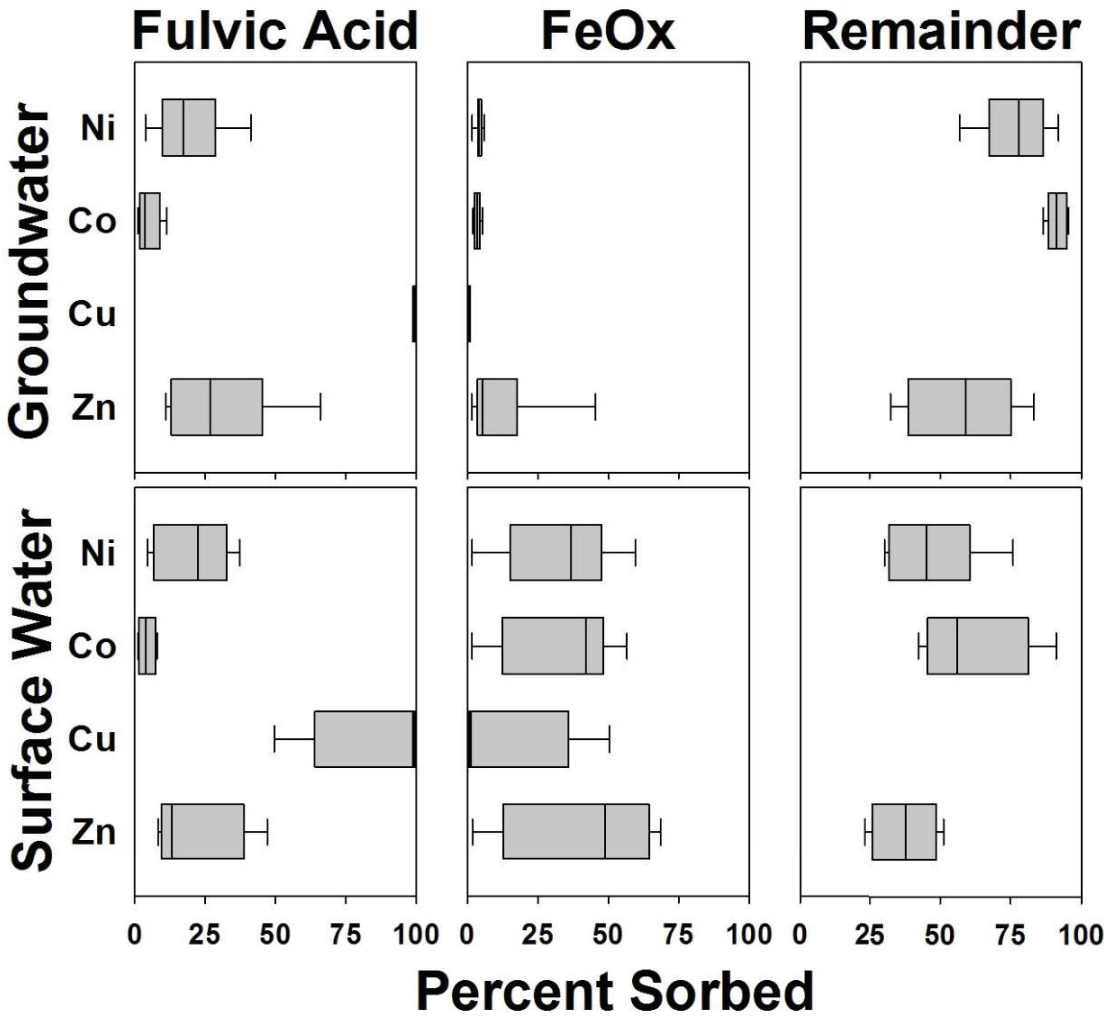

Figure 2- 4: Box and wisker graph of metals that have mixed sorption and variations between groundwater and surface water.

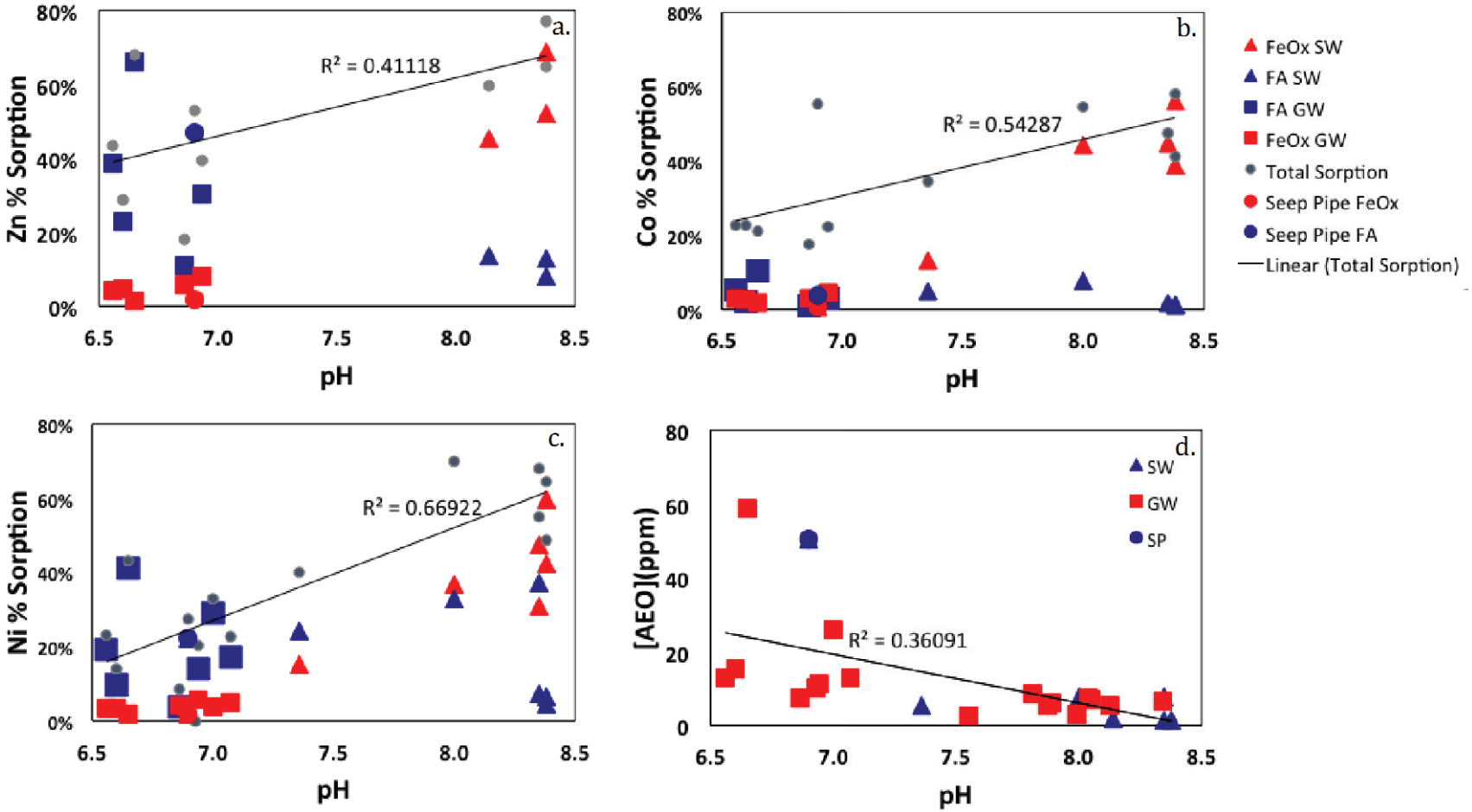

Figure 2- 5: Relationship between pH and sorption for Zn (a); Co (b); Ni (c) and AEOs (d). The solid line represents the total sorption for both phases. In figure 5d, the slope is not steep, indicating that pH impact is relatively small.

4 Discussion

4.1 PHREEQC and Sensitivity Testing

The WHAM7 model is sensitive to uncertainties in input parameters, which can be tested by "sensitivity analysis". A significant uncertainty is the amount and type of colloidal organic and mineral phases (Table 2-2). The method used to calculate Fe and Mn oxyhydroxide colloids generates the potential maximum concentrations. This is likely an overestimation for reduced groundwaters, which had reducing conditions, and should result in the dissolution of both Fe and Mn oxyhydroxide colloids. Javed et al. (2017) demonstrated high amounts of colloidal organic-bound Fe for Athabasca River samples. Organic-bound Fe, as well as clay or carbonate-bound Fe, was reported as part of the total Fe elemental analysis (Javed et al., 2017). This Fe is not part of the solute Fe pool, and thus is a bias in our calculation method that overestimates the actual aqueous Fe^{3+}. The reductive pEs and colloidal Fe-bearing phases together indicate that the calculation method generates a probable Fe^{3+} overestimation. PHREEQC indicates that goethite saturation indices average 5.9 ±0.93 for groundwaters and 5.0 ±0.6 for surface waters; however, conceptually there should be greater goethite saturation in oxidized surface waters than in reduced groundwaters. The sensitivity test for oxyhydroxide overestimation demonstrated that a lack of oxyhydroxide minerals in the subsurface further accentuated the importance of the organic sorption discussed below.

Mn-bearing colloids other than oxyhydroxides may also dominate the groundwater Mn phases, i.e. rhodochrosite which is near equilibrium with an average SI of $^{-}$0.53 ±0.7 in both datasets. PHREEQC indicated groundwaters speciate as Mn^{2+}, and thus Mn oxyhydroxide colloids, which form with Mn^{3+}, were unlikely to be present within the

reduced groundwaters. PHREEQC saturation indices for rhodochrosite were near equilibrium for most of the groundwater samples, which might suggest redox-carbonate buffering of dissolved Mn concentrations. Consequently, a sensitivity test using all dissolved Mn as oxyhydroxides was run to test how such a component would impact the results. Apart from Pb, which changed its preferred sorption to Mn oxyhydroxides, there was no difference in partitioning. The low Mn concentrations in surface waters indicate Mn oxyhydroxide colloids were at most, a minor component for these waters.

4.2 Sorption Sieve

Compared to FAs, HAs are less mobile, have larger molecular weights, and are known to strongly sorb to organic and mineral substrates (Christensen and Christensen, 1999; Weng et al., 2006; Wetzel, 2001). In both datasets examined here, there was a marked and consistent difference between groundwater and surface water Orbitrap mass spectra; groundwater samples were impoverished in higher molecular weight compounds in comparison to surface water samples (Figure 2-1). Given that surface waters are intimately linked to groundwaters, especially for small catchments like the Muskeg River (Figure 2-1c), it is highly unlikely that this difference was simply the result of no higher molecular weight organic molecules being available to groundwaters. This difference is interpreted to reflect the above mentioned sorption preference of HAs, whereby movement of groundwaters through the subsurface generates a strong bias within the pool of dissolved organic substances, such that lower molecular weight FA compounds tend to remain in solution and higher molecular

weight components preferentially sorb to the aquifer matrix. This “sorption sieve” mechanism would generate the differences in AEO mass spectra observed in Figure 2-1.

Groundwaters in Dataset 1 had lower AEO concentrations than those in Dataset 2, which is unexpected given the former is a humic substance-rich peatland, and the latter a minerallic substrate. The degree of sorption of organic components is pH dependent (Anderson and Christensen, 1988; Bradl, 2004), with increased pH leading to higher sorption and lower AEO concentrations (Figure 2-5d). This implies greater sorption of the humic acids in the groundwaters of Dataset 1. The Orbitrap mass spectral mode differs consistently between the two datasets, with those of Dataset 1 shifted to statistically significantly lower masses. This difference could reflect a variation in the complements of organic compounds available to these two different site locations; however, the humic acids for each is derived from the same boreal vegetation, and humous tends to be quite uniform irrespective on environment (Artinger et al., 2000). Therefore, it seems unlikely that there are significant differences in the available humic acids, but rather that this difference is an extension of the reduction of the high molecular mass compounds through the sorption sieve process, likely driven by greater sorptive capacities for organic compounds within the wetland substrate in comparison to the quartz-rich minerallic substrate (Aiken et al., 2011). The combined impacts of pH and substrate sorptive capacity sorption modulate the sorption sieve mechanism, making the mechanism most prevalent in the wetland environment of Dataset 1. The combined result is that organometallic complexes in Dataset 1 would experience a further decrease in their mobility in comparison to Dataset 2, as observed in the chalcophile and siderophile elemental data differences between the two sites.

4.3 Organometallic Complexation – Sorption Sieve Attenuation

Organic compounds sorb metals (Gustafsson and Gschwend, 1997; Weng et al., 2006; Wetzel, 2001) and thus, conceptually at least, the sorption sieve should tend to fix and decrease metal concentrations as those higher molecular weight compounds sorb to the solid-phase organic substrates. This appeared to be the case for Cu, whose affinity for HA over FA (Table 2-2) is consistent with its lower concentrations in groundwaters in comparison to surface waters; demonstrating that the sorption sieve will preferentially attenuate those elements with highest affinity for higher molecular weight organic compounds.

Most other siderophile and chalcophile elements were poorly sorbed to organic phases, except in the no oxyhydroxide sensitivity model, where they mostly transferred their sorption from oxyhydroxides to humic substances (Table 2-3). The probable overestimation of oxyhydroxides in groundwater samples means the no-oxyhydroxide model is probably the most suitable model for assessing the mobility of these elements in reduced groundwaters. Table 2-2 suggests that like Cu, chalcophile and siderophile elements preferred HA over FA. Thus like Cu these elements will be most susceptible to attenuation via the sorption sieve. This is consistent with the analytical data that indicates the wetland site, which is the site with the highest attenuation of higher molecular weight compounds, had the lowest concentrations of these elements (Figure 2-3 & 2-4; Table 2-1). These elemental concentrations strongly contrasted those of the non-metals and generally conservative alkali metals, all of which had higher concentrations in the wetland groundwaters (Table 2-1). Note that these groundwaters

had similar overall water chemistry (Section 3.1, Figure 2-2), suggesting the chalcophile and siderophile element differences were probably not due to dilution, incomparable water chemistries, or a more impoverished metal load. The lower concentrations of siderophile and chalcophile elements are thus interpreted to be the result of enhanced sequestration in the organic-rich peats via the production of organometallic complexes that are removed via the sorption sieve process.

4.4 Organometallic Complexation – Relative Mobility of REE

It is atypical, in a circumneutral pH system, for REEs to occur in their free, ionic form (Luo and Byrne, 2004; Migaszewski and Gałuszka, 2015). In inorganic systems, REEs generally sorb to oxyhydroxides, although studies have repeatedly demonstrated that in competitive reactions between inorganics and humic ligands, they preferentially sorb to humic substances (Cotton, 1997; Davranche et al., 2008; Takahashi et al., 1999; Tan et al., 2010; Zhan et al., 2013). REE concentrations were mostly below detection limits for surface waters, but above detection limits in the groundwater samples of this study (Table 2-1). This is consistent with multiple studies that attributed enhanced mobility of REEs in organic-rich groundwaters to reducing conditions that dissolve oxyhydroxides, increase pH, and promote REE binding to colloidal organic matter (Davranche et al., 2015; Marsac, 2010; Pourret et al., 2010). Sorption of REEs to organic molecules suggests that much of the REE complement could be sequestered to the solid-phase substrate via the sorption sieve. However, REE sorption is probably associated with carboxylic and phenolic groups (Migaszewski and Gałuszka, 2015), which occur across all molecular weight classes of organic molecules, with WHAM7 indicating that REE have a strong preference for lower molecular weight FAs over HA's (Table 2-2).

Thus, a portion of the REEs will be sorbed to lower molecular weight FA organic compounds that remain dissolved in these waters. Thus for REEs, the organometallic binding properties work to counter the sorption sieve and retain a portion of the REE load within the dissolved phase.

Oxidized surface waters had higher proportions of high molecular weight organic molecules within generally substantially lower DOC concentrations than groundwaters; indicating their FA complement is probably small. They also had substantially lower solute concentrations (likely primarily reflecting dilution)(Table 2-1, Figure 2-5d). Given the smaller complement of FAs in surface waters, which is the major organic-phase sorptive carrier of REEs, plus the dilute nature of these samples, it is unsurprising that REE concentrations were lower than those of the groundwaters. It may also reflect the tendency for REEs to sorb to organic and oxyhydroxide phases that are sequestered to the soild-phase organic substrates (Andersson, 2006; Åström et al., 2012; Ingri, 2000).

The REE normalization profile with the North American Shale Constant (NASC) for the groundwaters was slightly enriched in heavy rare earth elements (HREE; Gd, Tb, Dy, Ho, Er, Tm, Yb, Ly, and Y) compared to the light rare earth elements(LREE; La, Ce, Pr, Nd, Pm, Sm, and Eu)(Figure 2-6). This is a REE profile commonly associated with circumneutral, reducing, groundwaters in the wetlands (Davranche, 2011; Pourret et al., 2010). The pattern has been linked to variable organic-metal binding within this type of medium; i.e., each REE has preferred bonding arrangements (chelation; mono- or multi-dentate, ionic) with the various carboxylic or phenolic ligands that generate organometallic REE complexes with diverse environmental chemical behaviours

(Migaszewski and Gałuszka, 2015). WHAM7 does not address such fine-scale differences, as seen by the essentially uniform FA: HA ratios in Table 2-2. Nonetheless, these binding preferences, in concert with the sorption sieve, have the capacity to generate systematic normalised REE patterns (as found for REE profiles from circumneutral, reducing, wetland groundwaters from the diverse localities in the abovementioned studies, including those herein). It seems likely that this repetitive pattern is a fingerprint of these processes in a similar way to the normalised REE patterns that identify microbial-REE interactions (Migaszewski and Gałuszka, 2015; Takahashi et al., 1999, 2007)

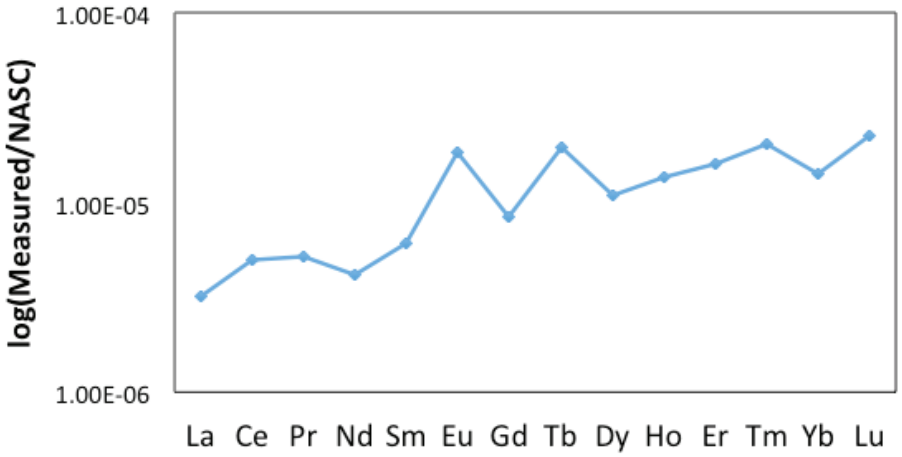

Figure 2- 6: REE normalization with the North American Shale Constant (NASC).

Ce is a redox dependent species and in reducing waters likely occurs as Ce^{3+} (Zhan et al., 2013), which PHREEQC predicted for both groundwater datasets. The lack of a Ce anomaly (either positive or negative) has been observed previously for similar groundwater systems and was attributed to reducing waters and organic colloids that protect from oxidative scavenging (Davranche et al., 2015; Pourret et al., 2010). In

reduced groundwaters, this retains Ce within the system and hence it becomes subject to the sorption sieve mechanism that may play a part in the standard REE profile mentioned above.

There is minimal data on REE concentrations for surface waters in the AOSR, most analyses indicates below detection limit concentrations. Gue (2012) published data for La and Ce from AOSR saline seeps that when normalized to NASC, indicated Ce depletion with respect to La of 1 – 2 orders of magnitude, as might be expected for oxidized surface waters (Gromet et al., 1984; Gue, 2012). However, Athabasca River water analyses for La and Ce (Government of Canada, 2013) indicated NASC-normalized values showed no relative Ce depletion or enrichment. While minimal, this data suggests that REEs may be an important avenue for further exploring element sources and processes in the AOSR surface waters.

4.5 Oxyhydroxide Complexation

Be and Sr are lithophile elements that overall have dissimilar chemistry except for a tendency to have a 2+ valence and form covalent bonds with oxygen (Boschi and Willenbring, 2016). It is likely these characteristics dominate their association with oxyhydroxides.

It is likely that the overestimation of Fe oxyhydroxide in groundwaters exaggerated the amount of Be sorption to this phase. Boschi and Willenbring (2016) demonstrated that Be sorption strongly increases with pH increases from 3 to 6. In the higher pH waters herein (Table 2-2), the Be load was fully sorbed to oxyhydroxides. When oxyhydroxides were removed, Be partitioned primarily to FA (67 ± 16%). Its below detection limit concentrations in surface waters is consistent with its strong

sorption to oxyhydroxides. Its low concentration throughout the groundwaters, with no difference between the two sites, indicated it was likely not strongly partitioned to either HA or FA (Table 2-2).

Some of Dataset 2 surface waters are from Athabasca River sites. The Athabasca River traverses through Sr-rich dolomitic Devonian sediments, while all other surface or groundwater samples do not pass through or over these sediments. This should result in higher, not lower, Sr concentrations in the Athabasca River surface water samples, which is opposite to the analytical data. This implies there was likely sequestration of Sr out of solution in the fully oxidized surface water sites, which the model suggested is likely due to sorption to Fe oxyhydroxide colloids. The sensitivity model run without oxyhydroxides suggested Sr in groundwaters would primarily partition into "Remainder". The probable overestimation of oxyhydroxide colloids for the reduced groundwaters suggested Sr remained dissolved in those samples, which, along with higher loading, might explain the higher Sr concentrations in the groundwater samples (Table 2-2).

Fe^{2+} in groundwater primarily partitioned to Fe oxyhydroxides, with only minor sorption to FAs. This is to be expected given the similar coordination chemistry that would be generated. In a system with no oxyhydroxides, Fe^{2+} remains primarily in solution, as indicated by the sensitivity tests and the Fe^{2+} analytical data.

The siderophile Co, is an element that has overall negligible sorption to FAs with or without oxyhydroxides (Table 2-3). WHAM7 indicated Co primarily resided in the "Remainder" pool or was sorbed to oxyhydroxides, the latter controlled by pH (Figure 2-3 &

2-5b; Anderson and Christensen, 1988). The tendency of oxyhydroxide sorption to remove Co probably controlled the low concentrations of Co in all surface waters.

4.6 Mixed Complexation

Zn sorption was primarily controlled by pH, with a change from primarily FAs to primarily Fe oxyhydroxides as pH increased (Figure 2-5a), an observation consistent with other studies (Anderson and Christensen, 1988; Benjamin, 1981; Bradl, 2004; Christensen and Christensen, 2000). WHAM7 suggested "Remainder" to be the largest Zn pool irrespective of water type. Given that there was Zn even in the relatively dilute surface waters (i.e. the system is not devoid of Zn), the below detection for Dataset 1 groundwaters suggests the Remainder pool is unlikely to be in solution (i.e., it is more likely sequestered into other phases such as carbonates as indicated by PHREEQC). In the reduced groundwaters, Zn sorbed primarily to HAs (Table 2-2), which when subjected to sorption sieving is probably a better explanation for the lowest Zn concentrations being in Dataset 1 groundwaters (Table 2-1). Coincident with the pH increase from groundwaters to surface waters, there is an increase from low oxygen to fully oxygenated conditions. Thus the pH driven ligand switch of Figure 2-5a was probably accompanied by the presence of oxyhydroxide particulates from both detrital and authigenic sources (the data of Javed et al, 2017 indicates oxyhydroxide precipitation is occurring in the Athabasca River system). Filtration will extract the portion of these oxyhydroxide components >0.45 μm in size, but not the dissolved humic substances which are substantially smaller (generally <5 kDa; Javed et al., 2017). The abundance of higher molecular weight organic components in surface waters (Figure 2-1) and Zn's preference for HA over FA (Table 2-2) suggests the organic

complement of surface waters would act to preserve Zn in solution. Thus, in the case of Zn, it seems that oxyhydroxide and sorption sieve processes counteract each other.

WHAM7 predicted the biggest Ni pool was "Remainder", with ~40% split evenly between oxyhydroxides and FAs, which is consistent with other studies indicating this siderophile can form strong bonds to both minerallic and solid-phase organic substrates (Anderson and Christensen, 1988; Benjamin, 1981; Christensen and Christensen, 2000; Ford et al., 1997; Green-Pedersen et al., 1997; Xu et al., 2007). Similar to the Zn discussed above, the Ni concentrations below the detection limit in Dataset 1, suggested the "Remainder" pool did not reside in solution. In reduced groundwaters lacking oxyhydroxides, the Ni component sorbs to FAs as for other siderophile elements (Table 2-2). Thus, the lower Ni concentrations in Dataset 1 versus 2 groundwaters are, like Zn above, interpreted to be at least partly due to the greater impact of the sorption sieve in Dataset 1 groundwaters. Oxyhydroxide Ni sorption is pH dependent, although unlike Zn, Ni sorbed to FA seems pH independent for the pH ranges in this study (Figure 2-5c). Nevertheless, as for Zn it should be expected that in oxidized surface waters, oxyhydroxide sorption will tend to attenuate Ni and sorption sieve processes will tend to accentuate Ni in solution.

It is unlikely that the Zn and Ni, in the "Remainder" category are actually in solution. The cases of Zn and Ni demonstrate how the sorption sieve acts in concert with other sorption processes such-as pH-redox variables and substrate availability. Importantly, the complement of organic molecules, either in solution or sorbed to the solid-phase organic substrate dictates how the sorption sieve can either help the

attenuation or mobility of each element. Essentially the sorption sieve runs in concert with these other mechanisms to generate a complex array of controls.

4.7 Ions Remaining in Solution

Some ions, such-as Na, K, Cl, F, Mg, Ca, SO_4, and B are generally assumed to remain in solution, as found by Holden et al. (2011) for Athabasca sediments. Mg, Ca, Cl, and SO_4, are all conservative elements that would be expected to remain in solution under the conditions represented by these samples (Appelo and Postma, 1994), as also indicated by the WHAM7 model results. The overall higher conservative ion loads and conductivities found in dataset 1 groundwaters compared to those of Dataset 2 suggest the wetland probably receives a higher elemental loading. That these elemental concentrations are the opposite of many transition metals emphasizes the role of sorption for those non-conservative ions, of which the sorption sieve is a major impact.

5 Conclusion

The potential for humic substances to enhance or attenuate metal mobility via formation of organometallic complexes has not been adequately explored for the Athabasca Oil Sands Region. WHAM7 modeling of the geochemical data for surface river waters, organic-rich wetland groundwaters, and minerallic groundwaters indicated pH and redox chemistry produce conditions conducive to organometallic complex formation within the region. Rare earth elements and Cu were almost completely complexed with organic compounds, while Zn, Co and Ni were partitioned between organic matter, iron oxyhydroxides, and solution or alternative minerallic phases. Only Pb, Y, Sr and Be were predominantly sorbed to iron oxyhydroxides. The model

predicted that organometallic complexes dominate the environmental geochemical behavior of much of the trace metal load. There is currently no evaluation of organometallic complexes within the otherwise extensive Athabasca Oil Sands monitoring program.

High-resolution Orbitrap mass spectral data for organic compounds pointed to a "Sorption Sieve" system that strongly depletes, via sorption to the solid-phase organic substrate, the complement of higher molecular weight humic compounds in groundwater samples. This sorption acts to fix metals that sorb preferentially to higher molecular weight organics and thus the organic-rich wetland groundwaters are more depleted for transition metals than those of the minerallic site. Conversely, the preference of REEs to sorb to fulvic acid molecules, which tend to remain in solution, means the sorption sieve acts to retain a portion of the organometallic REE complexes in solution.

By combining sorption sieve processes acting on organometallic complexes with those controlled by pH-redox processes (primarily oxyhydroxide dynamics), much of the environmental chemistry of metals in the Athabasca system becomes clearer for both groundwaters and surface waters. Consequently, organometallic complexation in concert with the sorption sieve should be considered a first-order control over metal mobility and fixation in this system and is integral to adequately predicting the environmental risks associated with this large-scale industry. In particular it is likely important for understanding the distribution of metals around tailings ponds of the Athabasca Oil Sands Region. Organometallic complexes appear to act as in inhibitor to trace metal migration in the occurrence of OSPW infiltration into the surrounding

organic-rich environment. Natural attenuation sequesters the majority of trace metals before they can migrate to the adjacent groundwater and surface water systems.

7 References

Abolfazlzadehdoshanbehbazari, M., Birks, S.J., Moncur, M.C., Ulrich, A.C., 2013. Fate and transport of oil sand process-affected water into the underlying clay till: A field study. J. Contam. Hydrol. 151, 83–92. https://doi.org/10.1016/j.jconhyd.2013.05.002

Aiken, G.R., Hsu-Kim, H., Ryan, J.N., 2011. Influence of Dissolved Organic Matter on the Environmental Fate of Metals, Nanoparticles, and Colloids. Environ. Sci. Technol. 45, 3196–3201. https://doi.org/10.1021/es103992s

Alberta, G. of, 2013. Facts and Statistics [WWW Document]. URL http://www.energy.alberta.ca/OilSands/791.asp#Environment (accessed 10.19.17).

Allen, E.W., 2008. Process water treatment in Canada's oil sands industry: I. Target pollutants and treatment objectives. J. Environ. Eng. Sci. 7, 123–138. https://doi.org/10.1139/S07-038

Allison, J.D., 1991. MINTEQA2/PRODEFA2, a geochemical assessment model for environmental systems :version 3.0 user's manual /. Athens, Ga.

Anderson, P.R., Christensen, T.H., 1988. Distribution coefficients of Cd, Co, Ni, and Zn in soils. J. Soil Sci. 39, 15–22.

Andersson, K., 2006. Colloidal rare earth elements in a boreal river: Changing sources and distributions during the spring flood. Geochim. Cosmochim. Acta 70, 3261–3274.

Andriashek, L.D., 2003. Quaternary Geological Setting of the Athabasca Oil Sands (In Situ) Area, Northeast Alberta (No. 2002-03). Alberta Energy and Utilities Board, EUB/AGS.

Appelo, C.A.J., Postma, D., 1994. Geochemistry, Groundwater, And Pollution, Second. ed. Balkema, Great Britian.

Arbogast, B.F., Geological Survey (U. S.), 1996. Analytical methods manual for the Mineral Resource Surveys Program. U.S. Dept. of the Interior, U.S. Geological Survey, Reston, Va.

Artinger, R., Buckau, G., Geyer, S., Fritz, P., Wolf, M., Kim, J.I., 2000. Characterization of groundwater humic substances: influence of sedimentary organic carbon. Appl. Geochem. 15, 97–116. https://doi.org/10.1016/S0883-2927(99)00021-9

Åström, M.E., Österholm, P., Gustafsson, J.P., Nystrand, M., Peltola, P., Nordmyr, L., Boman, A., 2012. Attenuation of rare earth elements in a boreal estuary. Geochim. Cosmochim. Acta 96, 105–119. https://doi.org/10.1016/j.gca.2012.08.004

Benjamin, M.M., 1981. Multiple-site adsorption of Cd, Cu, Zn, and Pb on amorphous iron oxyhydroxide. J. Colloid Interface Sci. 79, 209–221.

Boschi, V., Willenbring, J.K., 2016. The effect of pH, organic ligand chemistry and mineralogy on the sorption of beryllium over time 711–722.

Bradl, H.B., 2004. Adsorption of heavy metal ions on soils and soils constituents. J. Colloid Interface Sci. 277, 1–18.

Bryan, S.E., Tipping, E., Hamilton-Taylor, J., 2002. Comparison of measured and modelled copper binding by natural organic matter in freshwaters. Comp. Biochem. Physiol. Part C Toxicol. Pharmacol. 133, 37–49. https://doi.org/10.1016/S1532-0456(02)00083-2

Carrigy, M.A., 1962. Effect of texture on the distribution of oil in the Athabasca oil sands, Alberta, Canada. J. Sediment. Res. 32, 312–325. https://doi.org/10.1306/74D70CB3-2B21-11D7-8648000102C1865D

CCME, n.d. CCME Water Quality Guidelines [WWW Document]. URL http://st-ts.ccme.ca/en/index.html (accessed 11.27.17).

Chalaturnyk, R.J., Scott, J.D., Özüm, B., 2002. Management of Oil Sands Tailings. Pet. Sci. Technol. 20, 1025–1046. https://doi.org/10.1081/LFT-120003695

Chen, M., Walshe, G., Chi Fru, E., Ciborowski, J.J.H., Weisener, C.G., 2013. Microcosm assessment of the biogeochemical development of sulfur and oxygen in oil sands fluid fine tailings. Appl. Geochem. 37, 1–11. https://doi.org/10.1016/j.apgeochem.2013.06.007

Christensen, J.B., Christensen, T.H., 2000. The effect of pH on the complexation of Cd, Ni and Zn by dissolved organic carbon from leachate-polluted groundwater. Water Res. 34, 3743–3754. https://doi.org/10.1016/S0043-1354(00)00127-5

Christensen, J.B., Christensen, T.H., 1999. Complexation of Cd, Ni, and Zn by DOC in Polluted Groundwater: A Comparison of Approaches Using Resin Exchange, Aquifer Material Sorption, and Computer Speciation Models (WHAM and MINTEQA2). Environ. Sci. Technol. 33, 3857–3863. https://doi.org/10.1021/es981105t

Cotton, S.A., 1997. Aspects of the lanthanide-carbon σ-bond. Coord. Chem. Rev. 160, 93–127. https://doi.org/10.1016/S0010-8545(96)01340-9

Crabtree, R.H., 2005. The organometallic chemistry of the transition metals. John Wiley.

Davranche, M., 2011. Rare earth element patterns: A tool for identifying trace metal sources during wetland soil reduction. Chem. Geol. 284, 127–137.

Davranche, M., Gruau, G., Dia, A., Marsac, R., Pédrot, M., Pourret, O., 2015. Biogeochemical Factors Affecting Rare Earth Element Distribution in Shallow Wetland Groundwater. Aquat. Geochem. 21, 197–215. https://doi.org/10.1007/s10498-014-9247-6

Davranche, M., Pourret, O., Gruau, G., Dia, A., Jin, D., Gaertner, D., 2008. Competitive binding of REE to humic acid and manganese oxide: Impact of reaction kinetics on development of cerium anomaly and REE adsorption. Chem. Geol. 247, 154–170. https://doi.org/10.1016/j.chemgeo.2007.10.010

Devito, K., Creed, I., Gan, T., Mendoza, C., Petrone, R., Silins, U., Smerdon, B., 2005. A framework for broad- scale classification of hydrologic response units on the Boreal Plain: is topography the last thing to consider? Hydrol. Process. 19, 1705–1714. https://doi.org/10.1002/hyp.5881

Ford, R.G., Bertsch, P.M., Farley, K.J., 1997. Changes in Transition and Heavy Metal Partitioning during Hydrous Iron Oxide Aging. Environ. Sci. Technol. 31, 2028–2033. https://doi.org/10.1021/es960824+

Furguson, G.P., Rudolph, D.L., Baker, J.F., 2009. Hydrodynamics of a large oil sand tailings impoundment and related environmental implications. Canadian Geotech. J. 46, 1446–1460.

Goldschmidt, V.M., 1937. The principles of distribution of chemical elements in minerals and rocks. The seventh Hugo Müller Lecture, delivered before the Chemical Society on March 17th, 1937. J. Chem. Soc. Resumed 655–673.

Government of Alberta, 2007a. About Oil Sands [WWW Document]. Alta. Energy. URL http://www.energy.alberta.ca/OilSands/585.asp (accessed 5.24.16).

Government of Alberta, 2007b. Facts and Statistics [WWW Document]. URL http://www.energy.gov.ab.ca/OilSands/791.asp (accessed 5.24.16).

Government of Canada, E.C., 2013. Canada-Alberta Oil Sands Environmental Monitoring Information Portal - Water [WWW Document]. URL http://jointoilsandsmonitoring.ca/default.asp?lang=En&n=68413213-1 (accessed 6.23.17).

Green-Pedersen, H., Jensen, B.T., Pind, N., 1997. Nickel Adsorption on MnO2, Fe(OH)3, Montmorillonite, Humic Acid and Calcite: A Comparative Study. Environ. Technol. 18, 807–815. https://doi.org/10.1080/09593331808616599

Greenwood, N.N., Earnshaw, A., 1997. Chemistry of the Elements (2nd Edition) - 30. The Lanthanide Elements (Z = 58 - 71) - Knovel. Elservier.

Gromet, L.P., Haskin, L.A., Korotev, R.L., Dymek, R.F., 1984. The "North American shale composite": Its compilation, major and trace element characteristics. Geochim. Cosmochim. Acta 48, 2469–2482.

Gue, A.E., 2012. The geochemistry of saline springs in the Athabasca oil sands region and their impact on the Clearwater and Athabasca rivers (M.Sc.). University of Calgary (Canada), Canada.

Gustafsson, C., Gschwend, P.M., 1997. Aquatic colloids: Concepts, definitions, and current challenges. Limnol. Oceanogr. 42, 519–528. https://doi.org/10.4319/lo.1997.42.3.0519

HACH, 2007. DR 2800 Spectrophotometer Procedures Manual [WWW Document]. Scribd. URL https://www.scribd.com/document/138080069/DR-2800-Spectrophotometer-Procedures-Manual (accessed 3.24.17).

Holden, A.A., Donahue, R.B., Ulrich, A.C., 2011. Geochemical interactions between process-affected water from oil sands tailings ponds and North Alberta surficial sediments. J. Contam. Hydrol. 119, 55–68. https://doi.org/10.1016/j.jconhyd.2010.09.008

Ingri, J., 2000. Temporal variations in the fractionation of the rare earth elements in a boreal river; the role of colloidal particles. Chem. Geol. 166, 23–45.

Johnson, E.A., Miyanishi, K., 2008. Creating New Landscapes and Ecosystems. Ann. N. Y. Acad. Sci. 1134, 120–145. https://doi.org/10.1196/annals.1439.007

Killops, S., Killops, V., 2005. Introduction to Organic Geochemistry, Second. ed. Blackwell Publishing, MA.

Kim, J.I., Buckau, G., Li, G.H., Duschner, H., Psarros, N., 1990. Characterization of humic and fulvic acids from Gorleben groundwater. Fresenius J. Anal. Chem. 338, 245–252. https://doi.org/10.1007/BF00323017

Lamothe, P.J., Meier, A.L., Wilson, S.A., 1999. The determination of forty-four elements in aqueous samples by inductively coupled plasma-mass spectrometry (USGS Numbered Series No. 99–151), Open-File Report. U.S. Geological Survey : Books and Open-File Reports.

Luo, Y.-R., Byrne, R.H., 2004. Carbonate complexation of yttrium and the rare earth elements in natural waters1. Geochim. Cosmochim. Acta 68, 691–699. https://doi.org/10.1016/S0016-7037(03)00495-2

Marsac, R., 2010. Metal loading effect on rare earth element binding to humic acid: Experimental and modelling evidence. Geochim. Cosmochim. Acta 74, 1749–1761.

Masliyah, J., Zhiang, Z. (Joe), Zhenghe, X., Czarnecki, J., Hassan, H., 2004. Understanding Water-Based Bitumen Extraction from Athabasca Oil Sands. Can. J. Chem. Eng. 82, 628–654.

Migaszewski, Z.M., Gałuszka, A., 2015. The Characteristics, Occurrence, and Geochemical Behavior of Rare Earth Elements in the Environment: A Review. Crit. Rev. Environ. Sci. Technol. 45, 429–471. https://doi.org/10.1080/10643389.2013.866622

Oiffer, A.A.L., 2006. Integrated solid phase, aqueous phase and numerical investigation of plume geochemistry at an oil sand mining facility (M.Sc.). University of Waterloo (Canada), Canada.

Pickering, R.J., 1979. Analytical Methods--Recommended procedures for calibrating dissolved oxygen meters [WWW Document]. URL https://water.usgs.gov/admin/memo/QW/qw79.10.html (accessed 3.24.17).

Pourret, O., Gruau, G., Dia, A., Davranche, M., Molénat, J., 2010. Colloidal Control on the Distribution of Rare Earth Elements in Shallow Groundwaters. Aquat. Geochem. 16, 31. https://doi.org/10.1007/s10498-009-9069-0

Savard, M.M., Ahad, J.M.E., Gammon, P., Calderhead, A.I., Rivera, A., Martel, R., Klebek, M., Lefebvre, R., Headley, J.V., Welsh, B., Smirnoff, A., Pakdel, H., Benoit, N., Liao, S., Jautzy, J., Gagnon, C., Vaive, J., Girard, I., Peru, K., 2012. A local test study distinguishes natural from anthropogenic groundwater contaminants near an Athabasca Oil Sands mining operation (No. 7195). Geological Survey of Canada.

Small, C.C., Cho, S., Hashisho, Z., Ulrich, A.C., 2015. Emissions from oil sands tailings ponds: Review of tailings pond parameters and emission estimates. J. Pet. Sci. Eng. 127, 490–501. https://doi.org/10.1016/j.petrol.2014.11.020

Takahashi, Y., Hirata, T., Shimizu, H., Ozaki, T., Fortin, D., 2007. A rare earth element signature of bacteria in natural waters? Chem. Geol. 244, 569–583. https://doi.org/10.1016/j.chemgeo.2007.07.005

Takahashi, Y., Minai, Y., Ambe, S., Makide, Y., Ambe, F., 1999. Comparison of adsorption behavior of multiple inorganic ions on kaolinite and silica in the presence of humic acid using the multitracer technique. Geochim. Cosmochim. Acta 63, 815–836. https://doi.org/10.1016/S0016-7037(99)00065-4

Tan, X., Fang, M., Wang, X., 2010. Sorption Speciation of Lanthanides/Actinides on Minerals by TRLFS, EXAFS and DFT Studies: A Review. Molecules 15, 8431–8468. https://doi.org/10.3390/molecules15118431

Tipping, E., Lofts, S., Sonke, J.E., 2011. Humic Ion-Binding Model VII: a revised parameterisation of cation-binding by humic substances. Environ. Chem. 8, 225–235. https://doi.org/10.1071/EN11016

Tosiani, T., Loubet, M., Viers, J., Valladon, M., Tapia, J., Marrero, S., Yanes, C., Ramirez, A., Dupre, B., 2004. Major and trace elements in river-borne materials from the Cuyuni basin (southern Venezuela): evidence for organo-colloidal control on the dissolved load and element redistribution between the suspended and dissolved load. Chem. Geol. 211, 305–334. https://doi.org/10.1016/j.chemgeo.2004.07.001

US EPA, O., 2014. Toxic and Priority Pollutants Under the Clean Water Act [WWW Document]. URL https://www.epa.gov/eg/toxic-and-priority-pollutants-under-clean-water-act#priority (accessed 7.15.16).

USGS, 2016. PHREEQC Welcome Page [WWW Document]. URL http://wwwbrr.cr.usgs.gov/projects/GWC_coupled/phreeqc/ (accessed 5.26.16).

Warner, B.G., Rubec, C.D.A., Canada Committee on Ecological (Biophysical) Land Classification, National Wetlands Working Group, 1997. The Canadian wetland classification system. Wetlands Research Branch, University of Waterloo, Waterloo, Ont.

Weng, L., Fest, E.P.M.J., Fillius, J., Temminghoff, E.J.M., Van Riemsdijk, W.H., 2002. Transport of Humic and Fulvic Acids in Relation to Metal Mobility in a Copper-Contaminated Acid Sandy Soil. Environ. Sci. Technol. 36, 1699–1704. https://doi.org/10.1021/es010283a

Weng, Van Riemsdijk, W.H., Koopal, L.K., Hiemstra, T., 2006. Adsorption of Humic Substances on Goethite: Comparison between Humic Acids and Fulvic Acids. Environ. Sci. Technol. 40, 7494–7500. https://doi.org/10.1021/es060777d

Wetzel, R.G., 2001. 23 - Detritus: Organic Carbon Cycling and Ecosystem Metabolism, in: Limnology (Third Edition). Academic Press, San Diego, pp. 731–783.

Wood, S.A., 1996. The role of humic substances in the transport and fixation of metals of economic interest (Au, Pt, Pd, U, V). Ore Geol. Rev., Organics and Ore Deposits 11, 1–31. https://doi.org/10.1016/0169-1368(95)00013-5

Xu, Y., Axe, L., Boonfueng, T., Tyson, T.A., Trivedi, P., Pandya, K., 2007. Ni(II) complexation to amorphous hydrous ferric oxide: An X-ray absorption spectroscopy study. J. Colloid Interface Sci. 314, 10–17. https://doi.org/10.1016/j.jcis.2007.05.037

Zhan, Y., Guo, H., Xing, L., 2013. Characteristics of Rare Earth Elements in Groundwaters along the Flow Path in the North China Plain. Procedia Earth Planet. Sci., Proceedings of the Fourteenth International Symposium on Water-Rock Interaction, WRI 14 7, 940–943. https://doi.org/10.1016/j.proeps.2013.03.173

Chapter 3: Metal Transport near a Tailings Facility in the Alberta Oil Sands Region

Stephanie Roussel[1], Paul Gammon[2], Richard Amos[1], Samuel Morton[1,2], Jason Ahad[3], Martine Savard[3], Pierre Pelchat[2], John Sekerka[2], and Isabelle Girard[2]

[1] Department of Earth Sciences, Carleton University, 2115 Herzberg Laboratories 1125 Colonel By, Drive, Ottawa, Ontario, K1S 5B6, Canada
[2] Natural Resources Canada-Geologic Survey of Canada, 601 Booth Street, Ottawa, Ontario, K1A 0E8, Canada
[3] Natural Resources Canada-Geologic Survey of Canada, 490 Rue de la Couronne, Québec, G1K 9A9, Canada

Manuscript to be submitted for publication.

Abstract

The primary concern of the large-scale industrial oil sands operations in the Athabasca Oil Sands Region (AOSR) is the potential for trace metal enriched, oil sands process-affected water (OSPW) to leak from the tailings impoundments into the surrounding environments. As OSPW migrates through the subsurface, many parameters affect the complexation and transportation of trace metals in groundwater, including pH, redox potential (pE), temperature, available organic matter, inorganic water chemistry, and hydrology. The mobility of trace metals can be enhanced or attenuated depending on the complexation state, i.e. in solution, on a mobile surface, or on a stationary surface. To date, there have been no in depth investigations that characterize the geochemical conditions within a field site in the organic-rich, subsurface wetland environments that comprise at least 30% of the AOSR. This investigation characterized groundwaters from a study site north of Fort McMurray, Alberta. The study site was located adjacent to, and down-hydraulic gradient from a large tailings pond where seepage was suspected. The site was also adjacent to the Muskeg River and a sealed road that is salted in winter months. While trace metals were measured in the two monitoring wells between the tailings pond and study site, most trace metals measured below the detection limits in many of the mini-piezometers nests installed in the study site. This suggests that trace metals are complexing and being sequestered from solution onto immobile solid and/or organic phases. Ratios of Na: Cl successfully delineated mini-piezometers that were influenced by OSPW, and which were influenced by road salt. Elevated concentrations of B, Br, F, K, Li, Na, Rb, Sr, Zr and the Na: Cl molar ratios were the primary OSPW indicator elements within the

nests that were interpreted to be impacted by OSPW. This study offers a unique depth discreet characterization of the geochemical conditions as OSPW enters the organic-rich surficial sediments in the AOSR, in an effort to better understand the processes that affect metal transport and complexation, and determine the potential risk of OSPW seepage.

1 Introduction

The increasing demand for fossil fuels has stimulated the development of unconventional hydrocarbon extraction, such as the mining of oil sands in the Athabasca Oil Sands Region (AOSR). By 2024, Alberta Oil Sands production is expected to reach four million barrels of crude oil per day (Government of Alberta, 2007a).

The primary source rock in the AOSR, the McMurray Formation, can contain anywhere from 0-20 wt.% bitumen, but averages about 12 wt.% (Carrigy, 1962; Chalaturnyk et al., 2002). Due to the viscous nature of bitumen, it must be mixed with hot water and chemical diluents (i.e. napthanic acids) in order to be extracted from the other components. Bitumen reserves situated less than 70 meters below the surface are mined using surface mining and processing techniques, while the reserves below that are extracted using *in-situ* methods (Government of Alberta, 2007b). Surface mining and processing recovers more than 90% of bitumen from the source rock (Masliyah et al., 2004), however, given the scale of these operations (millions of barrels/day), there is a substantial amount of waste byproduct created through this process. Surface-mining byproducts include residual bitumen, waste rock, and oil sands process-affected water (OSPW) that must be pumped into large tailings facilities that cover an area of more than 220 square kilometers in Northern Alberta (Government of Alberta, 2007b).

The alkaline OSPW is typically distinguishable by elevated inorganic elements (e.g. Al, As, B, Cd, Cr, Cu, Fe, Pb, Mo, Ni, Ti, V, and Zn), naphthenic acids (NA), and major

ions including sodium, bicarbonate, chloride, sulfate, and ammonia (Allen, 2008; Chen et al., 2013; Frank et al., 2014), although, due to different processing technologies, there are differences in effluent between operations. Of these elements, As, Cd, Cr, Cu, Ni, Pb, and Zn are considered priority pollutants, and of environmental concern if released into the surrounding environments (Allen, 2008; EPA, 2016).

The primary environmental concern of the oil sands industry revolves around the possibility of OSPW leakage from tailings impoundments into the underlying aquifers and surrounding environments (Furguson et al., 2009; Holden et al., 2011; Small et al., 2015). In the AOSR, Quaternary sand deposits often underlie tailings impoundments and create a preferential flow path for OSPW leakage to migrate into the surrounding surface and subsurface (Furguson et al., 2009; Holden et al., 2011).

The AOSR is located within the Northern Boreal Plains Ecozone which is comprised of approximately 30% peatlands within a wetland environment (Warner et al., 1997). A wetland environment is saturated for majority of the year, with a water table at or near ground surface (Warner et al., 1997). These wetlands contain dissolved organic matter (DOM) that is largely composed of humic substances (humic and fulvic acids), which heavily control the geochemistry within a system (Freeze and Cherry, 1979; Weng et al., 2002). Due to the large wetland area in the AOSR, it is highly probable for leaking OSPW to encounter an organic rich environment, however, these interactions are not currently taken into account when monitoring and characterizing the potential impact of mining activities on surrounding environments.

Sorption reactions occur as inorganic elements bind, through a variety of mechanisms, to solid phases (both inorganic and organic). Solid phase colloids can sorb

to larger solid phases and become naturally attenuated, resulting in an overall decrease in dissolved metal concentrations in groundwater, or they can and enhance metal mobility. The most common phases for metal sorption include clays, oxyhydroxides, bicarbonates, phosphates, and colloidal humic substances (Allison and Allison, 2005; Bradl, 2004; Hubard, 2002). These reactions are heavily dependent on pH, redox potential (pE), available organic matter, water chemistry, and temperature (Alloway, 2012). The pE (the relative electron activity of a solution) and pH are the two master variables in environmental geochemistry that play a dominant role in the transport, fixation, and mobilization of dissolved inorganic elements (Freeze and Cherry, 1979). As sorption reactions occur, residual fluids are left behind, creating laterally and vertically variable redox conditions throughout the affected wetland environment (Aiken et al., 2011; Furguson et al., 2009; Holden et al., 2011). The existence of variable redox conditions within plumes has been recognized for nearly 50 years, however, they were not used to describe the evolution of plumes until the early 1990's (Christensen et al., 2000).

To date, most research in the AOSR has focused on the toxicity and transport of naphthenic acids (Abolfazlzadehdoshanbehbazari, 2011; Oiffer, 2006). Holden (2012) studied the potential biogeochemical evolution of an AOSR OSPW plume as it entered a subsurface glacial till aquitard. He characterized the sorption and ion exchange interactions between inorganic species and surficial sediments using batch sorption experiments that aimed to model the effects of adsorption and ion exchange on inorganic species in the clay till aquitard (Holden et al., 2011). He concluded that inflow of OSPW acts as a catalyst for sulfate salt dissolution reactions and calcium-magnesium

carbonate mineral precipitation, and that sodium and chloride primarily remain in solution (Holden et al., 2011). Ferguson et al. (2009) characterized groundwater flow within one of the oldest tailings impoundments in order to establish a base for estimating environmental impact in smaller tailings ponds in the area. Savard et al. (2012) developed a reactive transport model for a small OSPW plume emanating from a large, old tailings pond that entered a sand aquifer. They demonstrated that the oxidized nature of the aquifer generated iron oxyhydroxides that mostly fixed and attenuated heavy metal transport. Much of the past research has focused on surface locations, small-scale field reconstructions, or laboratory based experiments. To the best of our knowledge, Roussel et al (2017), is the first investigation to consider the impact that DOM has on the fate of trace metal transport within a wetland environment in the AOSR. In that investigation, geochemical modeling was used to characterize aqueous species distributions (PHREEQC; USGS, 2016), and sorption onto organic and mineral colloidal phases (WHAM7; Centre For Ecology & Hydrology, 2014) in order to compare the geochemical processes of two datasets in the AOSR. They determined that trace metals are naturally attenuated in organic-rich, wetland environments (Roussel et al., 2017).

Until now, no field investigation has been conducted to determine how lateral and vertical variations in geochemistry and redox potential could affect the processes (i.e. dissolution, precipitation, and complexation) that drive metal migration and attenuation in a predominantly wetland influenced aquifer system in the AOSR. This study characterizes the high-resolution geochemistry of a field site (>14,500 meters squared) located in Northern Alberta within a wetland environment situated between a

large tailings pond and the Muskeg River. Geochemical modeling was used to document how geochemical processes impact trace metal complexation and transport as trace metal-enriched OSPW interacts with microbial oxidative decomposed organic matter. This investigation will help inform the debate on the potential environmental risk an OSPW plume would pose to similar organic-rich environments.

2 Methods

2.1 Field Investigation

2.1.1 Site Description

The study site is located approximately 60 kilometers north of Fort McMurray, Alberta, and is situated between a large tailings pond and the Muskeg River (Figure 3-1), and next to a sealed road that is salted during winter. This site was chosen based on elevated major ions and metal concentrations measured in two monitoring wells (MW1 and MW2) that are located between the tailings pond and the study site (Roussel et al., 2017). The total area of the study site is approximately 14,500 square meters, and is located in a wetland environment with surface water in small depressions, and vegetation dominated by wetland species such-as black spruce, tamarack, and mosses. A small fen (dominated by grasses, bushes, alder, and sedges) occupies an area that looks like a cut-off meander bend (oxbow; Figure 3-4). The primary geologic units within the area include an organic-rich lop layer; overlying a sandy, silty mud; overlaying a Holocene fluvial sand; overlaying the source rock, McMurray Formation.

Figure 3- 1: Study site (in blue) is located adjacent to a tailings pond, between the Muskeg River with an area of approximately 14,500 m^2.

2.1.2 Drive-point Piezometers, Boreholes, and Mini-Piezometer Nests

A grid of 28 Solinst Model 601 Standpipe Piezometers with an internal diameter of ¾“, outer diameter of 1”, and screen length of 12” (labeled DP01- DP28) were installed across the wetland (Figure 3-2). The grid spacing was 20 meters apart parallel to the river, and 40 meters apart perpendicular to the river. The piezometer tips were modified by attaching a 150-µm screen to the outside of each, to prevent clogging by organic material. After installation and development, water levels and field chloride

concentrations were mapped in the standpipe piezometers and used to determine locations to install three contiguous arrays of mini-piezometer nests to get a depth-discrete characterization of both high and low Cl sites. Seven boreholes were dug at DP01, DP04, DP06, DP17, DP24, DP25, and DP27 to characterize the local geology (Figure 3-2).

A total of 45 mini-piezometers were installed at nine nest locations (DP02, DP04, DP10, DP15, DP17, DP22, DP24, DP25, DP27; Figure 3-2). Each nest consists of a surface site (DP##-0) and five mini-piezometers installed at 20 cm vertical intervals (DP##-20, 40, 60, 80, and 100 cm; Figure 3-3). The mini-piezometers were constructed using 3/8" ID HDPE tubing, drilled with ¼" holes, and wrapped with a 20 cm, 100 micron Nitex screen. The screen was melted onto the tubing, and the bottom end of the HDPE tube was heat crimped closed. A 1/8" ID LDPE sampling tube was then melted to the top of the mini-piezometer. The length of the LDPE tube was appropriate for the mini-piezometer depth setting. This metal-free construction ensured that the mini-piezometers had minimal potential to generate metal contamination. This set-up was then soaked for two hours in Milli-Q water to further reduce any potential geochemical contamination from the piezometers.

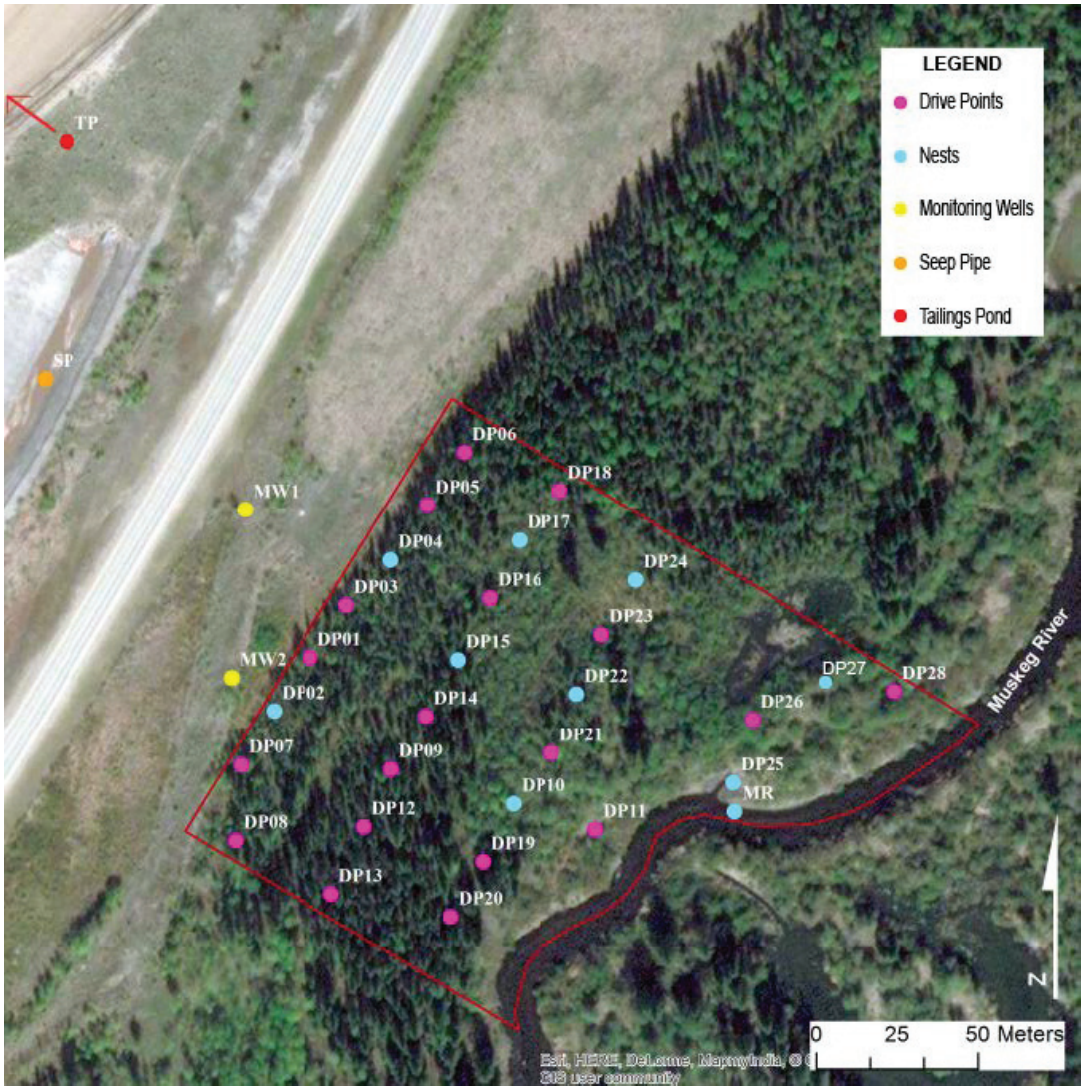

Figure 3- 2: Locations of the drive point piezometers, mini-piezometer nests, two monitoring wells, seep pipe, tailings pond, and Muskeg River sample.

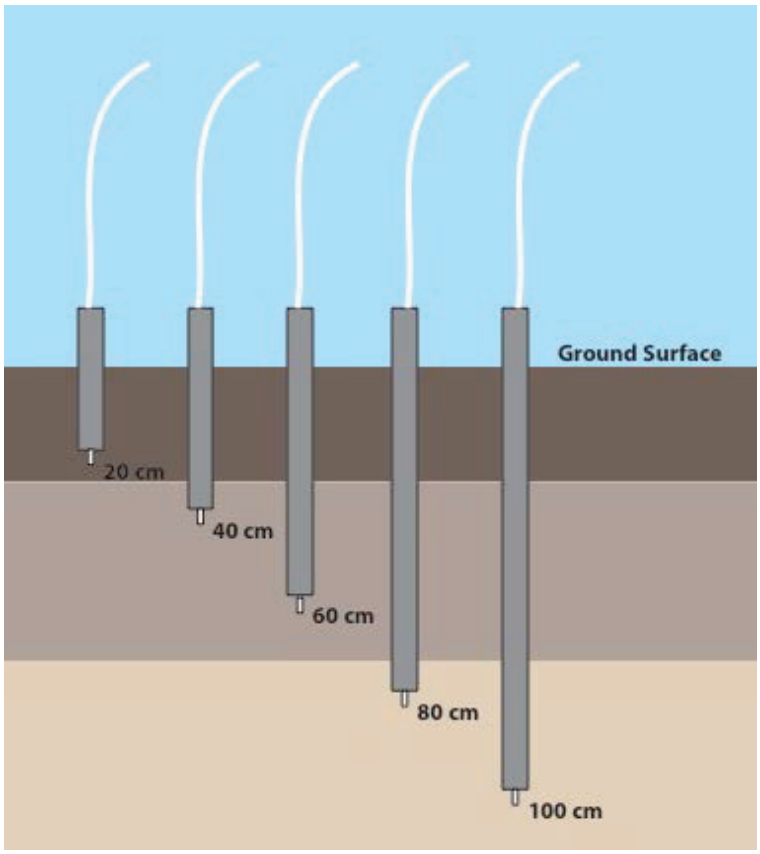

Figure 3- 3: Mini-piezometer nest design schematic.

To insert the piezometers into the ground, a ¾" ID PVC conduit pipe (cleaned by rinsing, scrubbing, and soaking in tap water) was capped with a loose-fitting HDPE cap and pushed, cap first, to the desired depth. The cap ensures the inner portion of the tube remained free of material. The mini-piezometer was then inserted down the inside of the PVC, and then the PVC pipe was retracted 10 cm, a process that detached the loose-fitting cap and directly exposed the mini-piezometer to 10 cm of stratigraphy at the required depth. The top of the mini-piezometer was then capped and taped (with electrical tape) to isolate the mini-piezometer interior from the overlying atmosphere.

2.1.3 Field Sample Collection and Analysis

All samples were collected using a peristaltic pump fitted with 1/8" ID silicon tubing and run at slow flow rates (<0.5 L/min). Prior to collecting surface water samples, and between each groundwater sample, the peristaltic pump was purged with 60 mL of Milli-Q water and then with three pore volumes of well water. After purging, field parameters were measured on unfiltered water using a flow-through cell attached to a YSI ProPlus multiparameter meter, and again after all water samples were taken. The YSI was fitted with probes to measure temperature (T), dissolved oxygen (DO), specific conductivity (SC), pH, and oxidation-reduction potential (ORP). YSI calibration was conducted each morning using standard solutions (Zobells for ORP; pH via buffered solutions of pH 4, 7, and 10; 1413 or 1000 μS/cm solution for SC; and 0 oxygen solution generated via the Na_2SO_3 method for DO (Pickering, 1979)).

To sample, a Millipore Sterivex® 0.45 μm filter was attached to the sample line and purged with ~10 mLs of sample water (the attachment ensures sample water does not come into contact with atmosphere prior to sampling). If a well required more than one filter, each filter was purged after being attached before sampling. Each sample bottle was then triple rinsed with filtered water, and then filled with care to prevent drips (rare given the set-up), atmospheric dust, rain etc. from entering the sample. At all locations where recharge was sufficient, a total of 180 mL of water was taken: 60 mL was collected with no headspace for anion analysis; 60 mL was collected with headspace for lab acidification for cation analysis; 30 mL was collected with head space for humic and fulvic acids analysis; 30 mL was collected with no headspace for deuterium and oxygen analysis. Samples were then refrigerated at 4°C until

transported to the laboratory. In the lab, samples for ICP elemental analysis were acidified to 1% v/v ultrapure HNO_3 (Seaster Chemicals) in a clean hood and left to sit for one month to dissolve any precipitates.

For each surface water and piezometer sample, field measurements for Fe^{2+} and S^{2-} were immediately taken using a battery-powered, field-portable, HACH spectrophotometer (model DR2800), using HACH methods 8146 and 8131, respectively (HACH, 2007). HACH calibration was conducted using the standard methods (HACH, 2007).

Samples were analyzed for inorganic concentrations using standard methods of Inductively Coupled Plasma Optical Emission Spectroscopy (ICP-ES) and Quadrupole Mass Spectroscopy (Q-ICP-MS) at Natural Resources Canada-Geologic Survey of Canada in Ottawa, Ontario (Arbogast and Geological Survey (U. S.), 1996; Lamothe et al., 1999). For anion analysis, a Dionex IC Model ICS2100 was used ("Dionex ICS-2100 Ion Chromatography System Operator's Manual," 2012). Fe^{3+} was calculated by subtracting the HACH measured Fe^{2+} from the ICP-ES measured total Fe concentrations (HACH, 2007).

2.2 Modeling Approach

2.2.1 PHREEQC

PHREEQC was used to calculate the mineral saturation indices for various oxyhydroxide, clay, and sulfide minerals, and the dominant valence states for various redox sensitive elements to ensure input compatibility with WHAM7. For the purpose of this investigation, the database Lawrence Livermore National Laboratory (LLNL; USGS, 2016) was used due to its comprehensive inclusion of elements not included in

other databases. The input parameters Ag, Al, Alkalinity, As, B, Ba, Be, Br, Ca, Cd, Cl, Co, Cr, Cu, F, Fe^{2+}, Fe^{3+}, K, Li, Mg, Mn, Mo, Na, Ni, NO_3, P, Pb, pE, pH, S, Se, Sn, HS^-, SO^4, Sr, Temperature, Tl, U, V, and Zn were used. Speciated Fe^{2+}/Fe^{3+} and S^{2-}/S^{6+} were specified and pE calculated from the YSI ORP calibration was assigned as the redox input parameter. Five surface water samples from the mini-piezometer nests, and five surface water samples calculated pE's that were not reliable due to unreasonably high values, for which, a generic pE of 13 was assigned for modeling purposes.

2.2.2 WHAM7

WHAM7 (Windermere Humic Aqueous Model VII) is a chemical speciation model used to predict metal partitioning in groundwater/soil systems that contains organic ligands (Tipping et al., 2011). It is a combined inorganic speciation model and Humic Ion-Binding Model VII. WHAM7 was used to model the "fraction bound to colloidal phases" within the organic-rich muskeg environment (Appelo and Postma, 1994).

The input parameters included, temperature, pH, inorganic solute concentrations, and colloidal phases (fulvic acids and Fe oxyhydroxides). Colloidal fulvic acid concentrations were estimated as 50% of the ICP measured dissolved organic carbon (DOC) values. Roussel et al. (2017) concluded that approximately 50% of DOC in the AOSR is composed of acid extractable organics (AEO) which is almost entirely made up of fulvic acids. This value agrees with previous research that indicates typical aquifers contain approximately 10-50% of DOC as fulvic acids concentrations with undetectable amounts of humic acids which are likely sorbed to substrates larger than 0.45 microns, and do not pass through the filter (Artinger et al., 2000; Bryan et al., 2002; Christensen et al., 2000).

Calculated Fe^{3+} concentrations were used to estimate molar solution mineral concentration of colloidal goethite (FeO(OH)), which is the default Fe oxyhydroxide mineral in WHAM7 and assumed to be the only Fe oxyhydroxide phase.

The elements modeled within WHAM7 include Ag, Al, Ba, Be, Ca, Cd, Ce, Cl, Co, Cr^{3+}, Cs, Cu, Dy, Er, Eu, F, Fe^{2+}, Fe^{3+}, Gd, Ho, K, La, Lu, Mg, Mn, Na, Nd, Ni, NO^3, Pb, PO^4, Pr, Sm, Sn^{2+}, SO^4, Sr, Tb, Th, Tm, U^4, T, Tb, and Zn. While B, Br, Li, P, Rb, S, and Zr all measure above the detection limits within these waters, WHAM7 does not model them, therefore, they are not included in this section.

The several nests tested positive for S^{2-}, and hence there is the potential for the precipitation of sulfide minerals throughout this system; however, WHAM7 does not model such phases, so they remain unconstrained for this portion of the study.

3 Results

3.1 Site Geology and Geologic History

The site geology was characterized using seven augured boreholes and two core logs from previously drilled monitoring wells. Generally, there are four main units found within the study area that the majority of mini-piezometer nests intersect. Throughout the study area, the McMurray Formation, a bituminous sandstone, was the lowest unit intercepted. It is generally saturated, but cannot transmit any significant water, therefore acts as an aquiclude (Hein and Cotterill, 2006). Overlying the McMurray Formation is a clean to muddy, moderately well sorted, fine to medium grained, grey sand, which is inferred to be a Quaternary fluvial sand deposit with generally permeable aquifer tendencies (Fenton, 1994; Furguson et al., 2009; Holden et

al., 2011). Overlying the sandstone is a variably thick (5-20 cm), sandy, silty mud that rarely yielded sufficient water for sampling, suggesting that it is a less permeable aquitard that is probably slightly leaky. The transverse and longitudinal cross sectional geologic profiles (Figure 3-5 & 3-6) suggest this unit is relatively continuous throughout the area, and linked to the current Muskeg River levee system. Consequently, this unit is inferred to be levee to overbank fluvial mud deposits. Above the mud layer lies an organic-rich layer that varies from incompetent and soupy to a moderately competent peat.

Satellite and air photo imagery suggests a former meandering channel (oxbow) of the Muskeg River that has been cut-off from the present Muskeg River channel (seen traversing through DP24; Figure 3-4). This former channel is filled with the basal sand, that in the area, and further towards the river, is a clean sand with no mud (Figure 3-5 & 3-6). Bounding the present western bank of the Muskeg River are two topographically high levees (about 0.5 m above the wetland surface) comprised of silty to sandy mud. To the west, the wetland system grades out as the land topography rises.

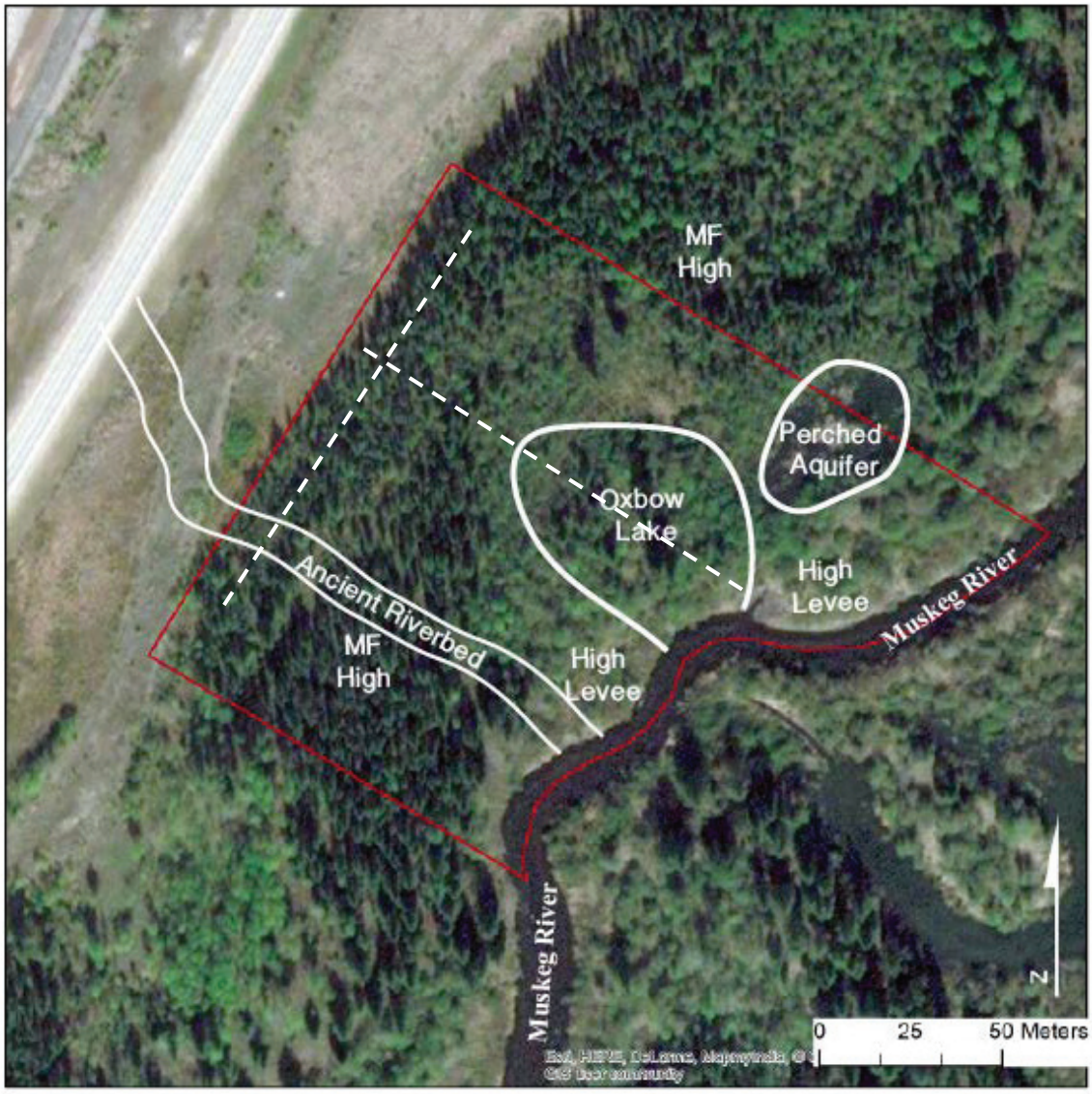

Figure 3- 4: Schematic diagram of the geology in the study site. MF high refers to the unsaturated, higher elevation areas of McMurray Formation. Dashed lines show transverse and longitudinal cross section locations in Figures 3-5 and 3-6.

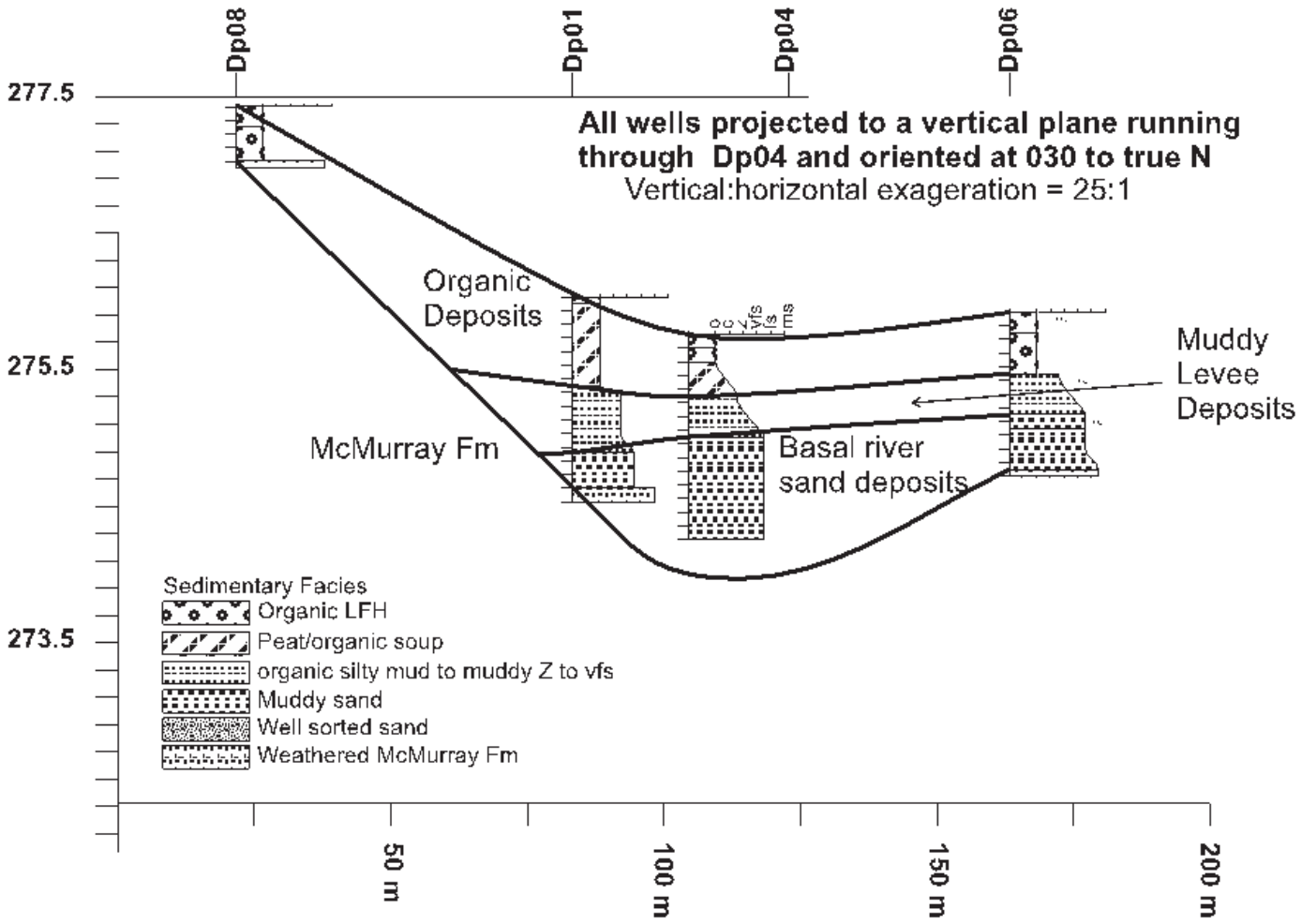

Figure 3- 5: Transverse Cross Section of study area, shows muddy deposit pinching out.

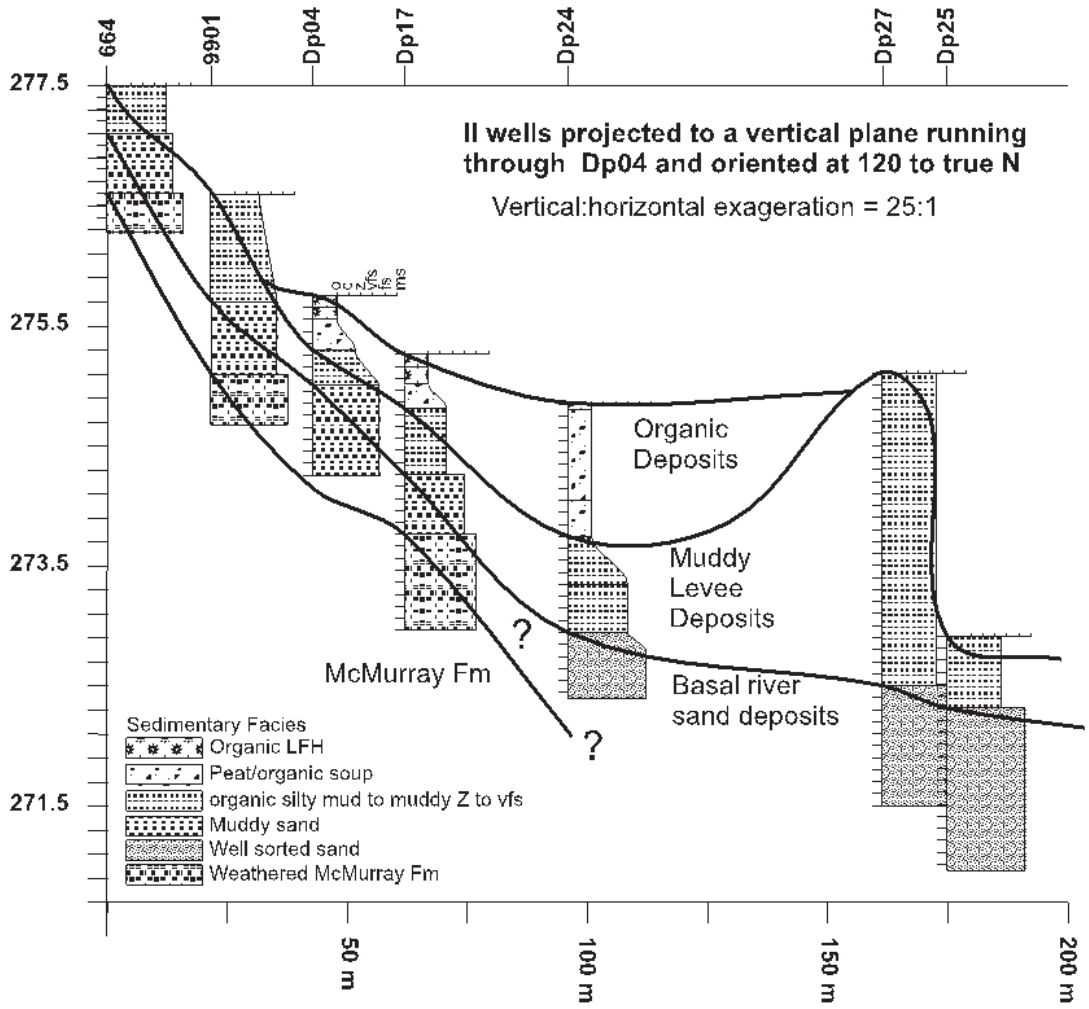

Figure 3- 6: Longitudinal Cross Section. *The boreholes on the longitudinal transect were projected perpendicularly to intersect the transverse transect.

3.2 Water Chemistry

The sample set for this investigation includes nine mini-piezometer nests (each with one surface sample and five groundwater samples installed at 20 cm depth intervals); five surface water samples from the Athabasca and Muskeg Rivers; a background (BG) surface water sample; operation samples from the nearby tailings pond (TP) and its associated drainage conduits (seep pipe (SP) and seep ditch (SD)), and two monitoring wells (MW1 and MW2) located between the tailings pond and study site (Figure 3-2). The BG and TP samples represent the two end members that likely comprise the groundwater samples in the study area. The BG sample (N57.32, W111.12) was taken at the head of the Muskeg River, well away from any possible industry impact; and the TP sample was taken directly from the tailings pond adjacent to the study area. The SP sample is OSPW that has become reduced (anoxic) during transport through the subsurface; while the SD is discharged SP water that has undergone rapid oxidation. Their topographic and geographic positions make it impossible for these samples to be sourced from anything other than the tailings pond, with a potential for dilution via precipitation infiltrating the tailings pond berms.

All groundwater and surface water samples in the nests have generally circumneutral pHs (6.2-7.9; Table 3-1; Figure 3-7). The groundwaters in this investigation are primarily reduced, and the surface waters are all fully oxidized. In surface river waters, the TP sample, and groundwater samples, DO concentrations averaged 8.55 ±1.08 ppm, 4.04 ppm, and 1.73 ±1.37 ppm, respectively (Table 3-1,

Figure 8). The wells in the nest were essentially dysoxic to anoxic, with DO typically decreasing from the surface water sample until around 60-80 cm depth, after which they slightly increased again (Figure 3-8). In both groundwaters and surface waters, Fe^{3+} concentrations were greater than Fe^{2+}, and SO_4 concentrations were greater than S^{2-} (Table 3-1). The DOC in the TP sample was much higher than the groundwater samples (55 ppm and 12-41 ppm respectively; Table 3-1), and the surface water samples generally had less DOC than the groundwater nest samples in the study area (19.2 ±5.6 ppm).

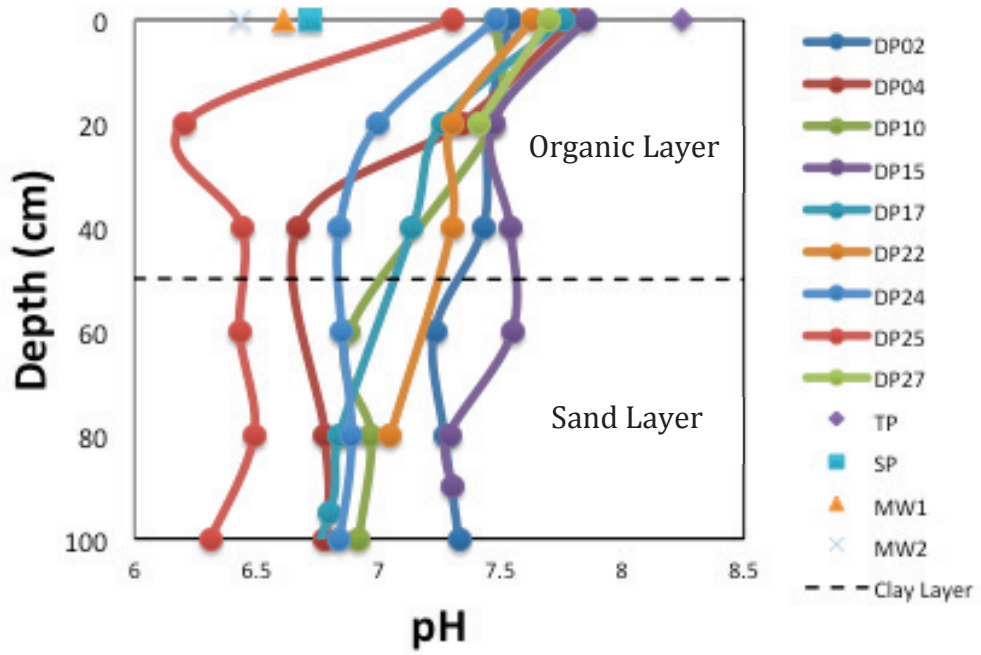

Figure 3- 7: pH vs. depth. The dotted line is the estimated depth where the clay layer is present in each nest and it compares the pH of the top organic layer and lower sand layer.

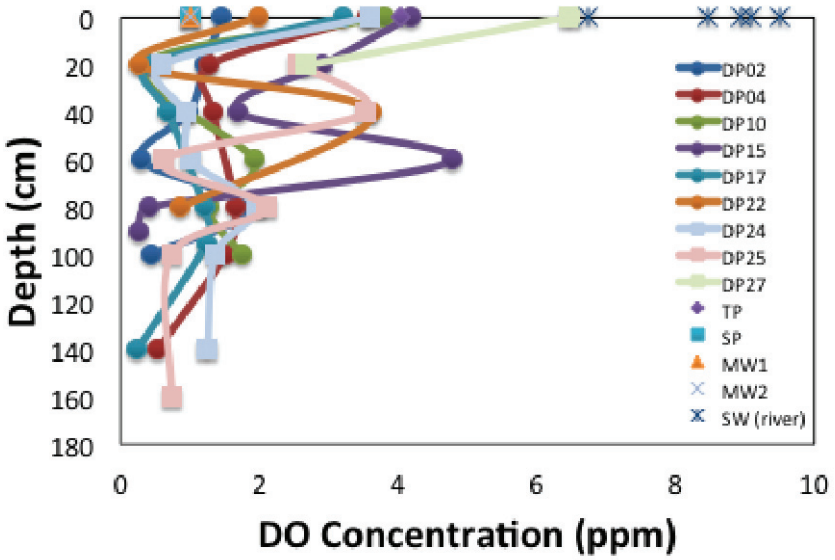

Figure 3- 8: Dissolved oxygen (DO) vs. Depth.

Within each of the nine nests, major ion chemistry was similar irrespective of hydrostratrigraphic unit (i.e. water from the surface sample, organic-rich layer, and sand unit), with slight differences in water composition. Major ion chemistry indicates bicarbonate waters to sulfate waters with varying concentrations of Ca and Na. DP02, DP10, DP15, and DP22 were predominantly bicarbonate waters and DP04, DP17, DP24, and DP25 were a mix of bicarbonate and sulfate waters (Figure 3-9). All surface water river samples were Ca-rich bicarbonate waters. The TP sample is a Na-rich mixture of bicarbonate and sulfate water, the SP and SD are both Na-rich sulfates, and MW1 and MW2 are Ca-rich sulfates (Figure 3-9).

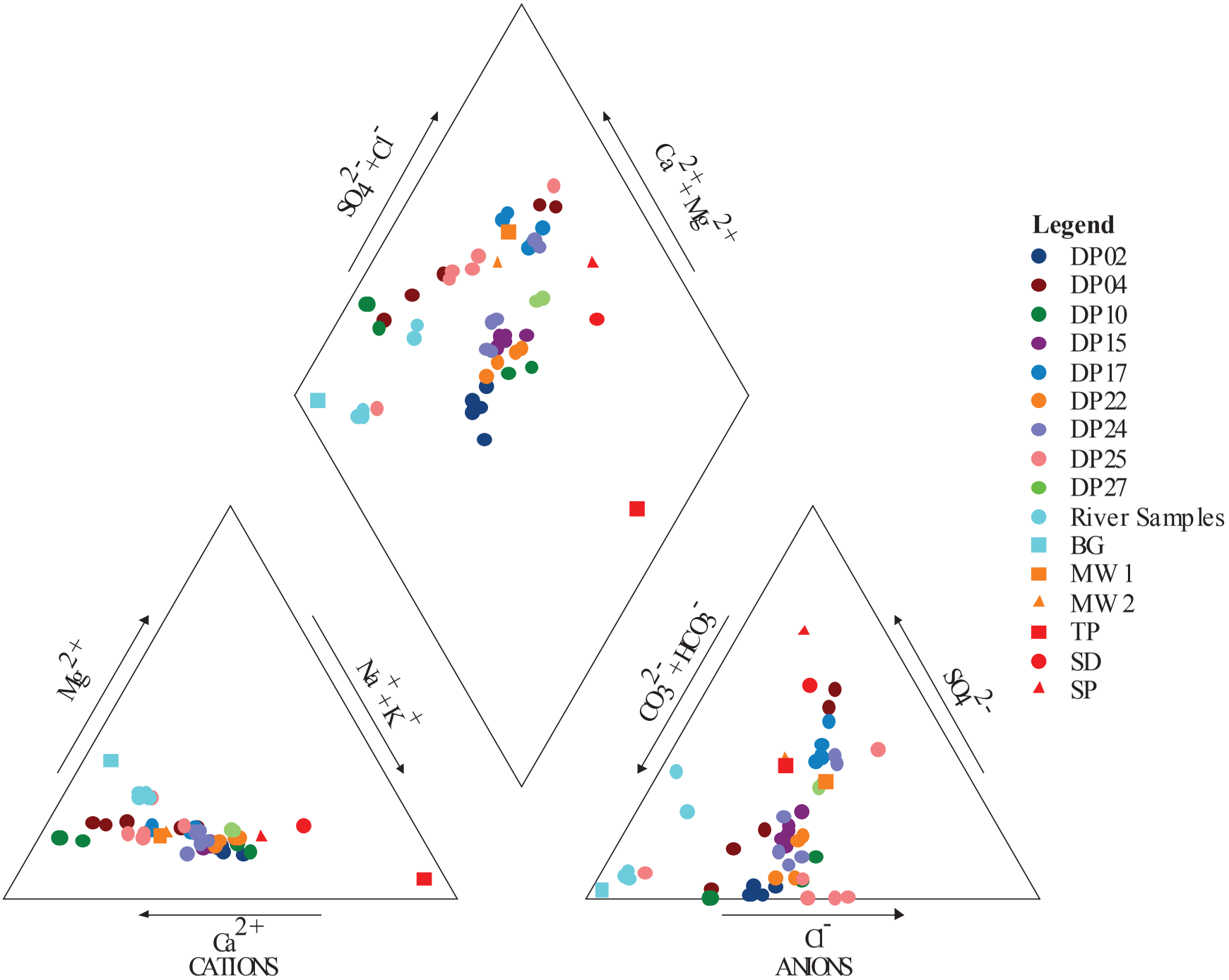

Figure 3-9: Piper diagram showing major ion chemistry of waters.

Within the nests, a significant variation in inorganic chemistry was observed. Alkalinity, As, B, Br, Co, F, K, Li, Mo, Na, Ni, NO_3, Rb, S, Sb, Sr, SO_4, U, V, W and Zr were all elevated in the TP with respect to the nest samples (Table 3-1). However, As, Co, Mo, Ni, Sb, U, V, and W are below detection limits within the nests. Ba, Ca, Ce, Fe, Mg, Mn, Nd, P, Si, and Y were generally elevated in the nest samples with respect to the tailings pond water (Table 3-1). Ag, Al, Be, Bi, Cd, Cr, Cs, Cu, Dy, Er, Eu, Ga, Gd, Ge, Hf, Ho, In, La, Lu, Nb, NO3, Pb, PO_4, Pr, Re, Sc, Se, Sm, Sn, Ta, Tb, Te, Th, Ti, Tl, Tm, Yb, and Zn were below the detection limits in the majority of groundwaters, surface waters, and the tailings pond samples.

DP02 is one of the nests closest to the monitoring wells and generally had the highest concentrations for Alk, B, Li, F, Zr, and K (Figure 10 a, b, c, d, j, and l). In DP25, adjacent to the Muskeg River, Mg, Sr, Na, Ca, and Ba increased slightly with depth, where all other nests had no consistent depth-related trends (Figure 3-10 m, n, and o). The pH was also stable through the vertical characterization, with the exception of DP25, where the surface water that has the highest pH of 7.3 (Figure 3-7).

Table 3- 1: Water Chemistry of background (BG), surface water (SW), Nests, Monitoring Well 1 and 2 (MW1 & MW2), and the tailings pond (TP).

		BG (n=1)	SW (n=5)	Nests (n=49)	MW1 (n=1)	MW2 (n=1)	TP (n=1)
OTHER PARAMETERS							
pH		7.3	8.12 ± 0.29; 7.7-8.5	7.1 ± 0.41; 6.2-7.9	6.6	6.4	8.3
ORP pe		15	15.82 ± 1.19; 14.8-15.8	12.2 ±1.78; 10.3-15.7	13.3	14.2	14.4
DOC	**ppm**	18.1	19.16 ±5.74; 12.6-24	14 ± 3.0; 12.6-41.6	37.6	29	55.4
T	**°C**	2	6.82 ±2.14; 4.1-8.6	5.84 ±1.35; 1.9-8.2	11.5	4.6	12.8
ALK	**ppm**	163	134 ±19.3; 109-155	415 ±104; 82.4-548	623	418	423
DO	**ppm**	6.8	8.55 ± 1.08; 7.7-9.5	1.82 ± 1.38; 0.24-6.5	2.4	2.6	4.0
NO3	**ppm**	<0.02	<0.02	0-0.24; 0.03 ± 0.05	<0.02	<0.02	0.19
ALKALI METALS							
K	**ppm**	1.1	1.12-1.37; 1.2 ± 0.11	0.02-3.67; 1.8 ± 1.0	0.35	2.2	19.3
Li	**ppb**	4.6	7.61-11.27; 9.7 ± 1.4	8.09-34.1; 18.2 ± 6.6	8.3	9.4	187
Na	**ppm**	3.7	11.4-12.9; 12.1 ± 0.62	10.8-201; 102 ± 51.5	161	95.4	349
Rb	**ppb**	1.0	0.83-1.32; 1.1 ± 0.25	0.25-11.1; 1.3 ± 1.6	0.87	1.1	21.7
ALKALINE EARTH METALS							
Ba	**ppb**	18.7	22.4-52.1; 34.3 ± 11.83	27.1-365; 170 ± 71.8	251	215	169
Ca	**ppm**	36.9	31.6-40.7; 35.8 ± 3.7	35.7-256; 1417 ± 44.8	307	168	17
Mg	**ppm**	13.5	9.01-11.1; 10.3 ± 0.90	10.4-57.1; 25.9 ± 9.7	51.1	29.8	10.2
Sr	**ppb**	68.8	94.9-253; 152 ± 65.7	102-773; 386 ± 133	705	602	511
TRANSITION METALS							
Co	**ppb**	<0.5	0.06-0.14; 0.08 ± 0.03	0.03-3.56; 0.40 ± 0.60	8.5	1.5	2.72
Cr	**ppb**	0.19	0.15-0.23; 0.21 ± 0.03	0.22-14.4; 0.76 ± 2.0	<1	<1	<1
Cu	**ppb**	<1	0.13-0.62; 0.37 ± 0.22	<1	<1	<1	<1
Fe (total)	**ppm**	0.10	0.13-0.40; 0.29 ± 0.12	0.01-30.7; 8.3 ± 7.7	0.494	22.5	<0.005
Fe2+	**ppm**	NA	NA	0-5.36; 2.4 ± 1.7	NA	NA	NA
Fe3+	**ppm**	NA	NA	0-27.2; 6.0 ± 6.8	NA	NA	NA
Mn	**ppb**	10.4	8.87-12.6; 11.9 ± 2.6	4.95-2994; 694 ± 639	536	2286	57.7
Mo	**ppb**	0.09	0.06-0.62; 0.25 ± 0.27	<0.05	<0.05	0.9	93.3
Ni	**ppb**	0.41	0.49-1.16; 0.73 ± 0.29	0.10-3.73; 1.1 ± 0.66	11.4	4.2	8.8
Ti	**ppb**	0.69	0.25-0.87; 0.67 ± 0.25	<5	<5	<5	<5
Y	**ppb**	0.03	0.04-0.13; 0.07 ± 0.04	0.04-0.56; 0.15 ± 0.12	0.33	0.5	<0.1
Zr	**ppb**	0.08	0.1400.18; 0.16 ± 0.02	0.14-1.79; 0.47 ± 0.33	5.0	1.1	0.68

Table 3-1 cont.: Water Chemistry of background (BG), surface water (SW), Nests, Monitoring Well 1 and 2 (MW1 & MW2), and the tailings pond (TP).

		BG (n=1)	SW (n=5)	Nests (n=49)	MW1 (n=1)	MW2 (n=1)	TP (n=1)
POST TRANSITION							
Al	**ppb**	2.4	2.70-9.10; 5.0 ± 2.6	4.0-70.1; 14.9 ± 13.6	<20	<20	<20
Pb	**ppb**	<0.01	0.01-0.06; 0.03 ± 0.02	0.01-0.14; 0.05 ± 0.02	<0.1	<0.1	<0.1
V	**ppb**	0.13	0.21-0.30; 0.25 ± 0.03	0.04-0.56; 0.54 ± 0.26	2.5	1.1	5.9
Zn	**ppb**	<0.5	<0.5	0.25-0.62; 3.3 ± 7.9	<5	<5	<5
METALLOIDS							
As	**ppb**	0.25	0.30-0.50; 0.39 ± 0.08	0.21-1.11; 0.51 ± 0.16	<1	3.0	3.4
B	**ppb**	6.8	29.1-42.6; 36.3 ± 5.2	5.34-467; 79.9 ± 90.9	15.9	18.3	2612
Sb	**ppb**	0.02	0.02-0.05; 0.03 ± 0.02	<0.1	<0.1	0.14	1.8
Si	**ppm**	4.5	2.0-4.56; 3.6 ± 1.1	3.47-10.8; 5.1 ± 1.7	3.8	3.9	2.1
NONMETALS							
Br	**ppm**	<0.2	<0.2	0.03-0.37; 0.25 ± 0.07	0.46	0.27	0.3
Cl	**ppm**	1.5	2.30-7.20; 4.2 ± 1.8	9.8-219; 119 ± 44.9	263	99.5	138
F	**ppm**	0.07	0.08-0.11; 0.09 ± 0.01	0.05-0.37; 0.12 ± 0.07	0.09	0.09	3.8
P	**ppm**	<0.05	<0.05	0.03-1.34; 0.14 ± 0.20	<0.05	<0.05	<0.05
S	**ppm**	0.9	1.69-10.8; 4.9 ± 3.9	0.75-196; 33.2 ± 42.6	100	64.5	83.5
S2-	**ppm**	NA	NA	0-0.45; 0.05 ± 0.08	NA	NA	NA
SO4	**ppm**	1.61	3.68-31.2; 13.1 ± 11.8	0-554; 92.6 ± 122	282	184	239
LANTHANIDES							
La	**ppb**	<0.1	0.01-0.04; 0.02 ± 0.01	0.02-0.26; 0.08 ± 0.05	0.3	0.23	<0.1
Ce	**ppb**	0.01	0.02-0.07; 0.04 ± 0.02	0.03-0.47; 0.14 ± 0.12	1.04	0.55	<0.1
Nd	**ppb**	0.01	0.02-0.06; 0.04 ± 0.02	0.02-0.27; 0.08 ± 0.07	0.34	0.25	<0.1
Sm	**ppb**	<0.05	<0.05	<0.05	0.08	0.05	<0.05
ACTINIDES							
U	**ppb**	0.03	0)2-039; 0.15 ± 0.17	0.01-0.38; 0.06 ± 0.07	6.4	1.9	4.1

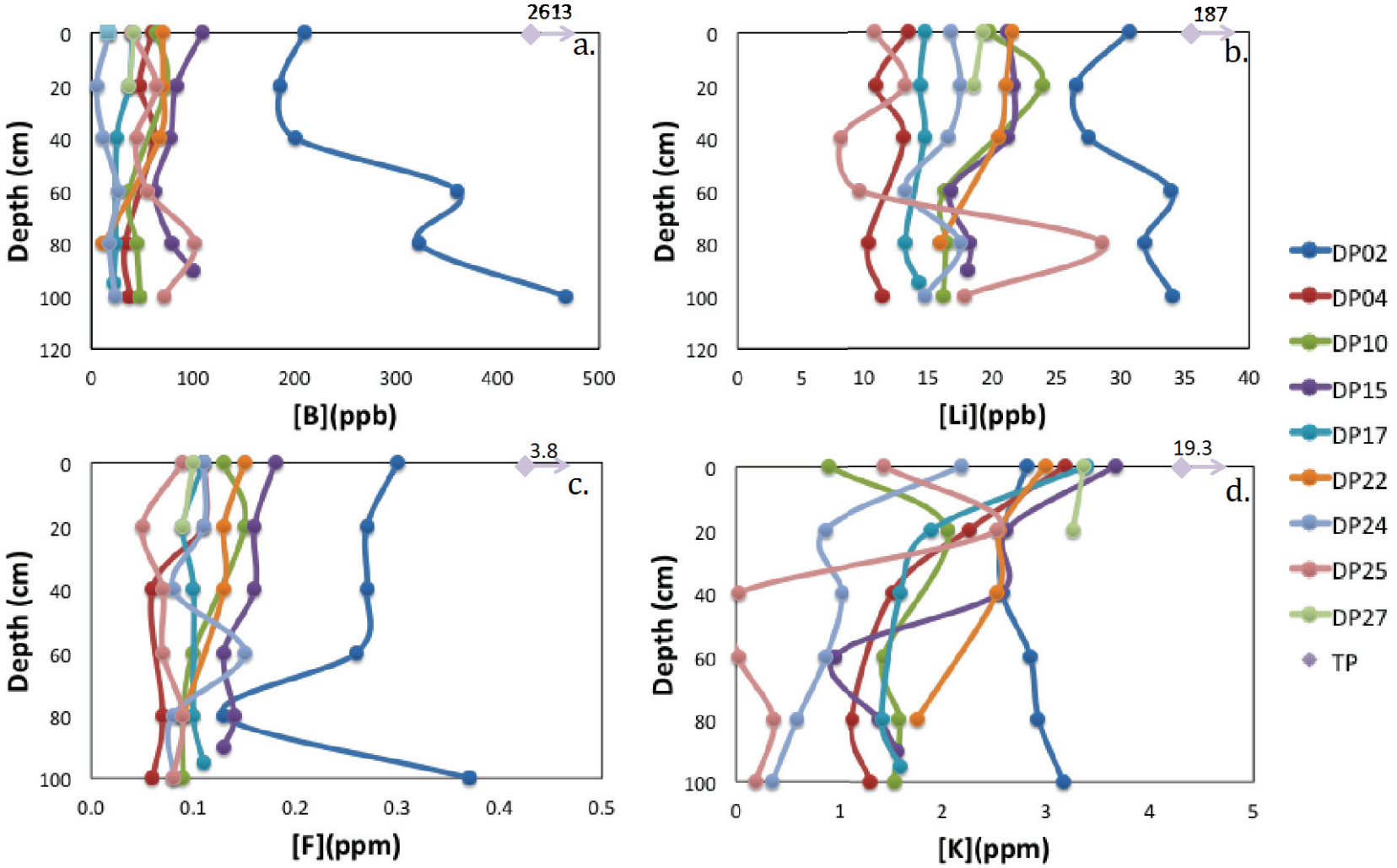

Figure 3- 10: Concentrations of OSPW tracers vs. depth. (a.) B; (b.) Li; (c.) F; (d.) K; (e.) Na; (f.) Cl; (g.) Br; (h.) SO4; (i.) Sr; (j.) Zr; (k.) Rb; (l.) Alkalinity; (m.) Ca; (n.) Mg; (o.) Ba.

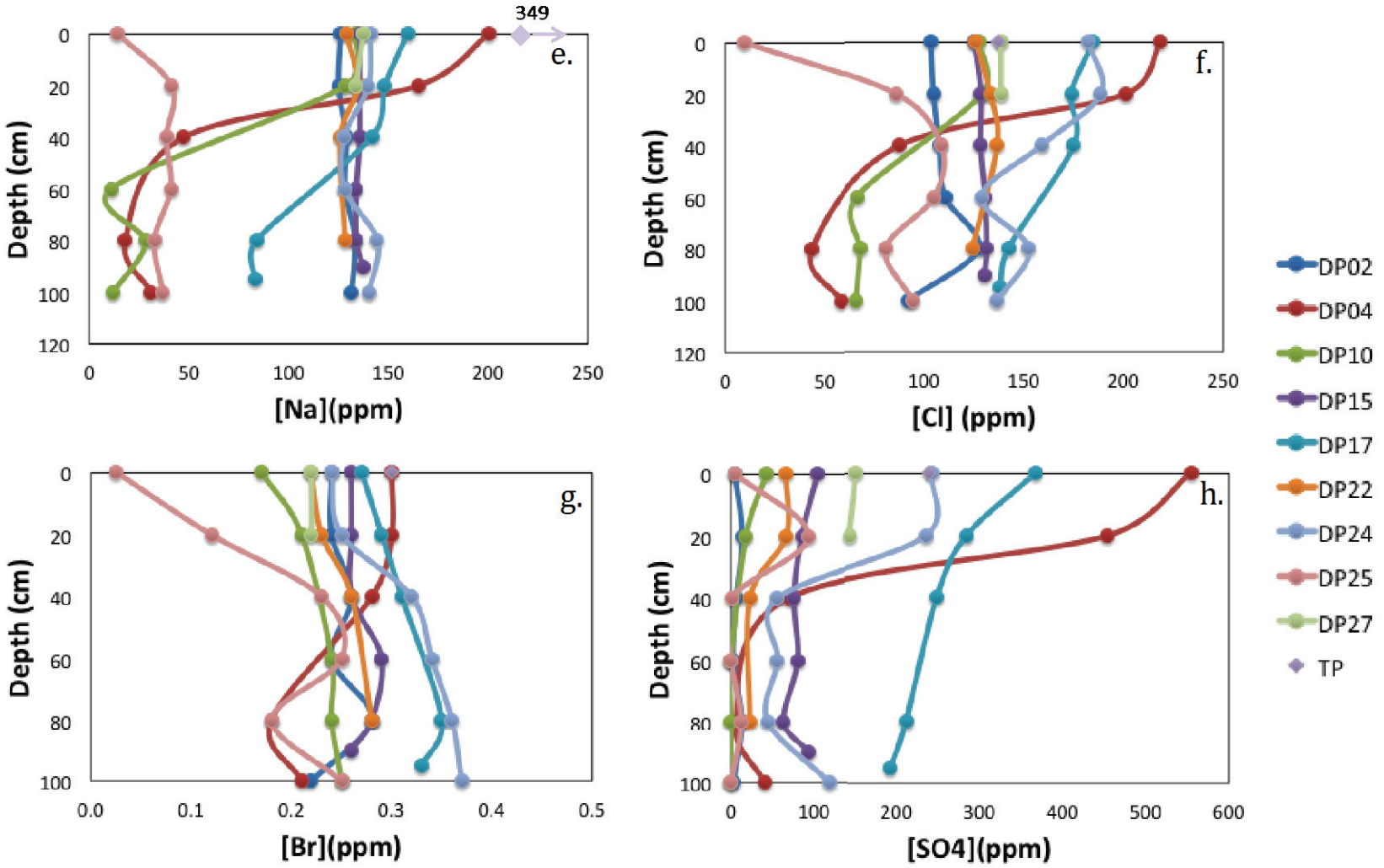

Figure 3- 10 cont.: Concentrations of OSPW tracers vs. depth. (a.) B; (b.) Li; (c.) F; (d.) K; (e.) Na; (f.) Cl; (g.) Br; (h.) SO4; (i.) Sr; (j.) Zr; (k.) Rb; (l.) Alkalinity; (m.) Ca; (n.) Mg; (o.) Ba.

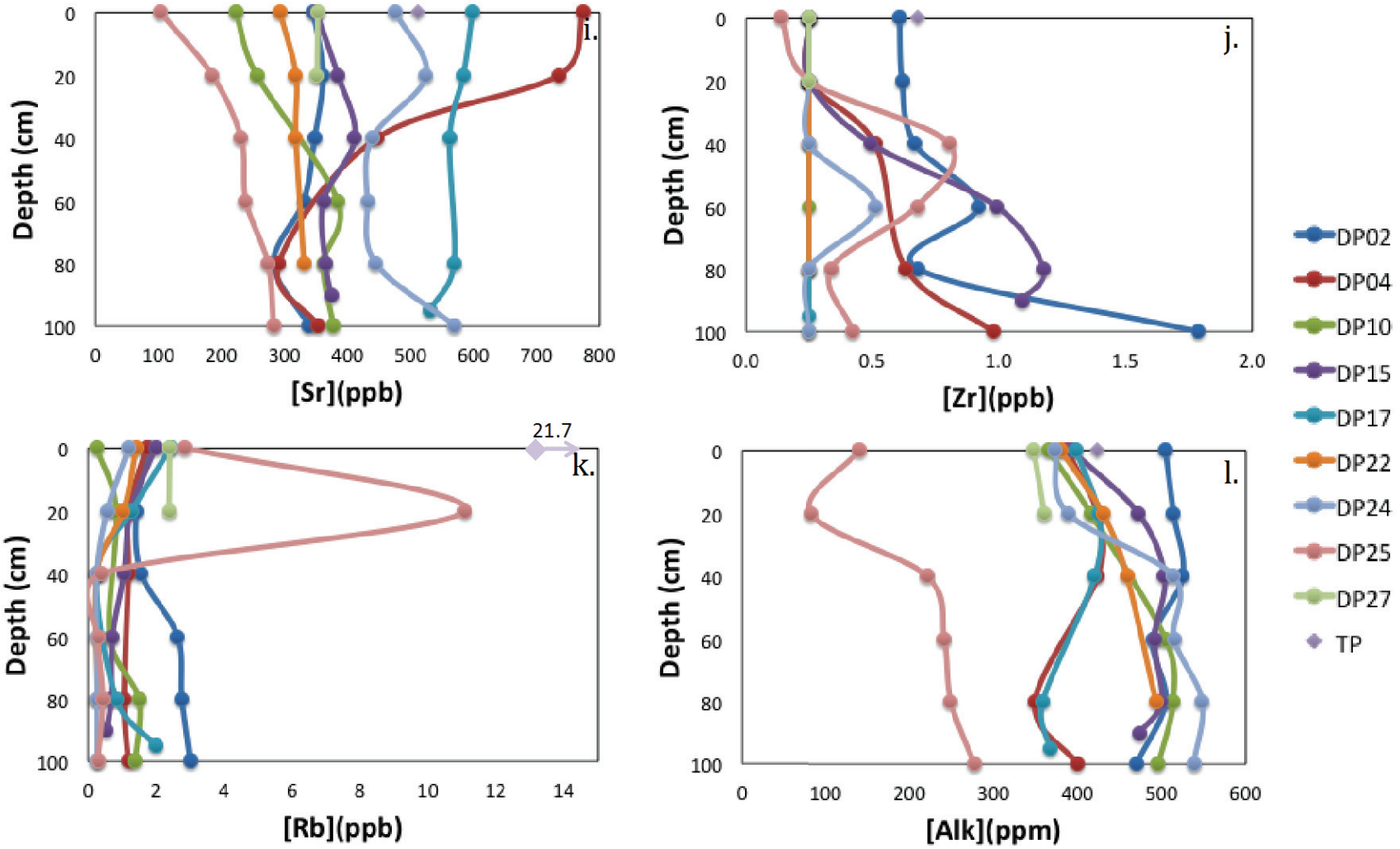

Figure 3- 10 cont.: Concentrations of OSPW tracers vs. depth. (a.) B; (b.) Li; (c.) F; (d.) K; (e.) Na; (f.) Cl; (g.) Br; (h.) SO4; (i.) Sr; (j.) Zr; (k.) Rb; (l.) Alkalinity; (m.) Ca; (n.) Mg; (o.) Ba.

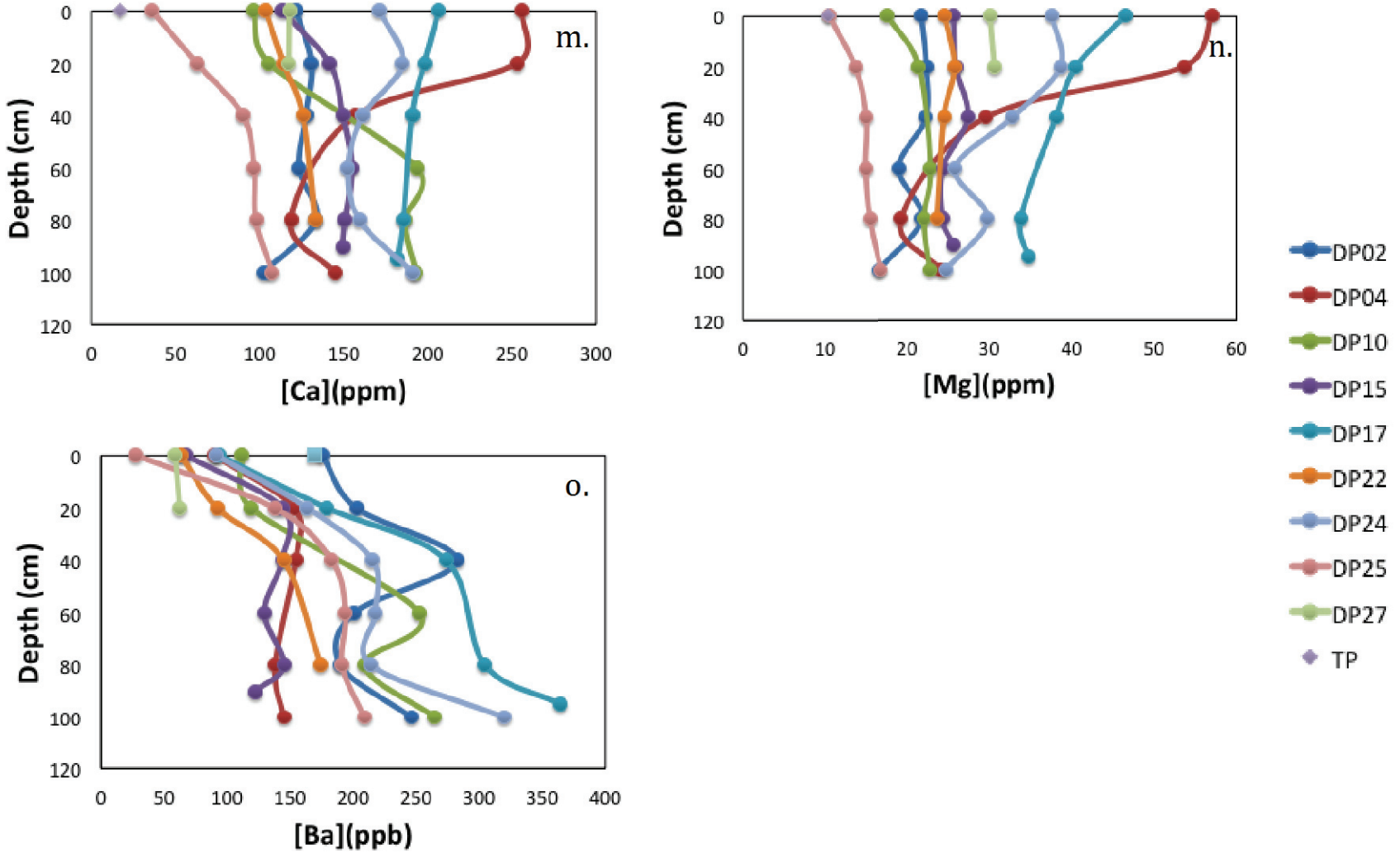

Figure 3- 10 cont.: Concentrations of OSPW tracers vs. depth. (a.) B; (b.) Li; (c.) F; (d.) K; (e.) Na; (f.) Cl; (g.) Br; (h.) SO4; (i.) Sr; (j.) Zr; (k.) Rb; (l.) Alkalinity; (m.) Ca; (n.) Mg; (o.) Ba.

Two distinct aquifers were distinguishable in the study area with the intermediate mud layer as the dividing unit. The waters above the mud layer were in the top organic-rich unit, and the waters below were situated in quartz-rich sand unit (Figure 3-5 & 3-6). Generally, pH decreased from the surface sample to the mud layer, where it increased and stabilized (Figure 3-7).

3.3 OSPW Signature

OSPW from the tailings pond in this investigation is distinguishable by elevated concentrations of Alkalinity, B, Br, F, K, Li, Na, Rb, S, Sr, SO_4, and Zr. For the more conservative ions measured (Cl, B, Li, F, K, Na; and the Na: Cl molar ratio), DP02 displayed the highest concentrations of the aforementioned elements (Figure 3-10 a, b, c, and d; 3-11). For the ratios of B to Na:Cl, Li to Na:Cl, K to Na:Cl, F to Na:Cl, and Rb to Na:Cl both MW1 and MW2 were within the mass with the rest of the nests (Figure 3-14), and the BG samples had low concentrations of B, Li, K, F, and Rb (Figure 3-10 a, b, c, d, & e).

The Na and Cl concentrations in DP02, DP15, DP22, and DP24 were generally consistent throughout all depths, however DP04, DP10, DP17,and DP25 varied substantially with depth (Figure 3-10 e & f). OSPW from the TP had a 4:1 molar ratio of Na: Cl, distinguishing it from groundwater mixing with road salt, which has a Na: Cl of 1:1. MW2, DP02, DP15, the top depths of DP17, DP24, and DP27 all had Na: Cl ratios that were more enriched in Na than Cl (Figure 3-11). The bottom depths of DP04, DP10, the bottom depths of DP17, and DP25 all appeared to have a distinct road salt signature as indicated by their position near to, and below the Na:Cl 1:1 line in Figure 3-11.

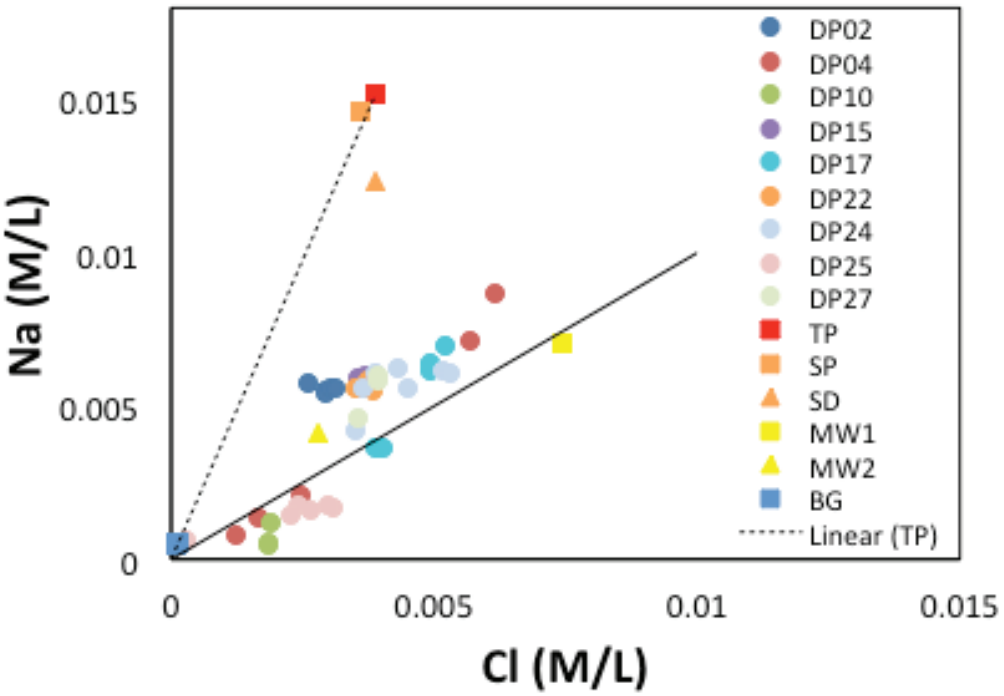

Figure 3- 11: Road salt contribution. The dashed line indicates the Na/Cl in the TP water, and the solid line indicates a 1:1 molar ratio of road salt. Anything above the 1:1 is indicating some kind of OSPW contamination.

3.4 Numerical Modeling

PHREEQC determined a 2+ valence for Mn, and that manganite (MnO(OH)) and rhodochrosite ($MnCO_3$) were the two Mn bearing minerals likely present within the system, with average saturation indicies (SI) of 1.8 ±1.64 and -0.55 ±0.71 respectively. Fe^{3+} was likely precipitating as oxyhydroxides such as goethite, manganite, Mg-rich ferrite, magnetite, and hematite. Goethite was oversaturated (which was likely overestimated and will be discussed later), with an average SI of 6.35 ±0.56. Siderite, on the other hand was near saturation with an average SI of -0.57 ±0.56.

Carbonate minerals including witherite ($BaCO_3$), aragonite ($CaCO_3$), calcite ($CaCO_3$), strontianite ($SrCO_3$), rhodochrosite ($MnCO_3$), siderite ($FeCO_3$), and magnesite ($MgCO_3$) were all near equilibrium, and likely a key component in buffering the system (1.94 ±0.48, -0.03 ±0.53, 0.11 ±0.53, -0.4 ±0.54, -0.55 ±0.71), -0.57 ±0.56, -1.14 ±0.57 respectively).

Most sulfate and sulfide minerals were substantially undersaturated within the system and not likely a primary influential factor driving reactions. Barite and gypsum were the only sulfate minerals near equilibrium, with average SI's of 0.24 ±1.0 and -2.12 ±1.1 respectively.

WHAM7 indicated that Na, K, Mg, Ca, Mg, F, Cl, NO^3, and SO^4 did not preferentially sorb to any of the phases. The rare earth elements (REEs) Ce and Nd preferentially sorb to fulvic acids, nearly 100%. Fe^{2+} and Mn^{2+} preferentially sorb to fulvic acids also (0-10% and, 10-60% respectively). Sr primarily sorbs to Fe oxyhydroxides (0-85%). Yttrium partitioning is heavily dependent on the amount of iron oxyhydroxide present within the system. When iron oxyhydroxides are present, Y preferentially sorbs to it (70-100%), however, when absent, Y preferentially partitions to the FA nearly 100%. There is a linear trend as the iron oxyhydroxides concentration increases so does the sorption percentage (Figure 3-12).

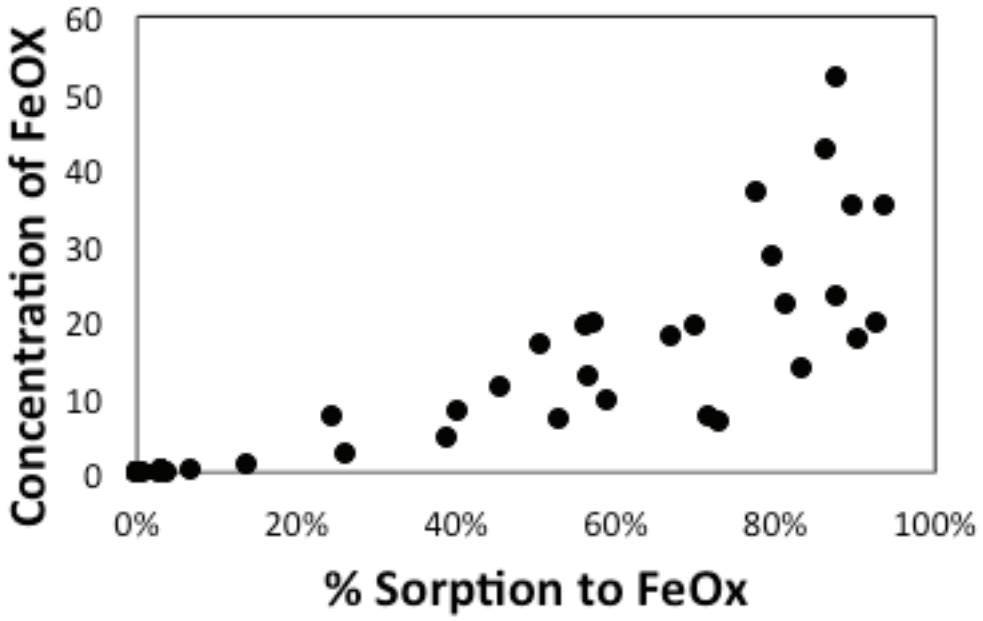

Figure 3- 12: Percent of yttrium sorption vs. iron oxyhydroxide concentration.

4 Discussion

4.1 OSPW Mixing

In this investigation, OSPW contribution cannot be determined by one particular element, or even set of elements. It is distinguishable by elevated B, Br, F, K, Li, Na, Rb, Sr, and Zr, and the Na: Cl molar ratio in the nests with respect to the background water. Holden et al., (2011) measured elevated concentrations, similar to those in this investigation, including elevated levels of B, Li, SO_4, K, Sr, and Na in their tailings pond sample water, as well as similar general water chemistry, and a molar ratio of 2.4 times more Na than Cl (Table 3-2).

Table 3- 2: Compared chemistry of Holden et al. (2011) and Roussel et al. (2017) OSPW sample.

	Holden's OSPW	Roussel's OSPW
pH	8.6	8.25
Sulfate (ppm)	150	239
Alk (ppm)	491	423
TOC/DOC (ppm)	83	55
Cl (ppm)	375	138
Mg (ppm)	4.17	10.2
Ca (ppm)	7.62	17
K (ppm)	10.1	19.3
Na (ppm)	591	349
Li (ppm)	0.16	0.19
B (ppb)	1784	2612
Al (ppb)	6306	b.d.
Si (ppb)	2308	2400
Fe (ppb)	3005	3790
Mn (ppb)	68	57.7
Ni (ppb)	15	8.8
Co (ppb)	6	2.7
Cu (ppb)	b.d.	b.d.
Sr (ppb)	198	511
Pb (ppm)	14	b.d.

Natural boron concentrations are typically low in surface and groundwaters, and can be indicative of waste water contribution (Batayneh, 2012; Butterwick et al., 1989). Boron is never in its elemental form, it typically exists as borate precipitates (i.e. borax, colemanite, and boracite) or most commonly, in aqueous solutions such as boric acids (Butterwick et al., 1989; Dydo and Turek, 2012; Hilal et al., 2011). In this system, borate minerals were all significantly undersaturated. When pH is between 6-9, such as the waters in this investigation, boron is typically present in the form of highly soluble, electrically neutral, polyborates (i.e. $(B_3O_3(OH)_4)$ (Dydo and Turek, 2012; WHO, 1998). While WHAM7 does not include

boron, literature suggests that sorption is strongly pH dependent and prefers phases of organic material when present, followed by clay minerals, and oxyhydroxides (Butterwick et al., 1989; Gu and Lowe, 1989; Lemarchand et al., 2005). As the pH increases over 6.5, sorption to humic acids substantially increases up to a pH of 9.5 where it decreases again. Boron concentrations in fresh water are typically less than 500 ppb, and range significantly in groundwater (300-100,000 ppb) (Dydo and Turek, 2012; WHO, 1998). In this investigation, B concentrations in the TP sample and nests fell between the groundwater range, however, they were still well above the BG levels in the study site (Figure 3-10a.). In the TP, B measured 2613 ppb, which is significantly higher than the concentrations measured in the nests (Figure 3-10a). However, the nest with the highest concentration of B was DP02, ranging from 186-467 ppb.

Due to lithium's aqueous preference, high solubility, reasonable detection limits, low background concentrations, and insensitivity to thermodynamic properties (i.e. pH; Eh), it has the potential to be a good tracer in wetland environments, however, ion exchange reactions with clay minerals can reduce the accuracy (Dierberg and DeBusk, 2005; Négrel et al., 2010; Richards et al., 2015). The concentrations of Li in DP02 compared to the other nests and background indicates that OSPW mixing is in fact occurring (Figure 3-10b).

In solution, F and Br are generally conservative tracers that are not affected by complexation onto minerallic or biological phases (Jha et al., 2013; Keefe et al., 2004). In this investigation, F is elevated in the TP with respect to BG and the nests, and has the highest concentrations in DP02 (Figure 10c). Br concentrations are

similar in the TP and the nests (0.3 and 0.25 ±0.07 ppm respectively), and below the detection limit in the surface river samples.

K and Rb are primarily controlled by cation-exchange with clay minerals (Ceazan et al., 1989; Griffioen, 2001), and Sr and Zr complex with clays, oxyhydroxides, and humic substances (Gulamova, 2010; Langley et al., 2009). In this investigation, K in the TP was higher than the nests (19.3 and 1.77 ±1.01 ppm respectively), with DP02 having the highest concentrations (2.6-3.2 ppm). The TP sample has a Rb concentration of 21.7 ppb, and the nests have significantly less Rb (averaging 1.34 ±1.63 ppb). Sr concentrations are similar in the TP and the nests (511 and 387 ±133 ppb respectively), and average 152 ±66 in the surface river samples. In the majority of the nests, Zr concentrations were below the detection limit, however, the TP sample and DP02 had similar concentrations (0.68 and 0.61-1.8 ppm respectively). While all of these elements collectively help to distinguish OSPW contribution, no single element can be used to characterize OSPW infiltration.

4.2 Road Salt Contribution

Na and Cl are conservative elements that are commonly used as tracers in groundwater (Richards et al., 2015). In 1981, Hackbarth determined the major ion compositions in three groundwater wells unaffected by mining activities in the AOSR. Each well was completed in a glacial sand, reworked oil sands, and glacial till (Hackbarth, 1981). In the glacial reworked oil sands (the unit and depth most similar to the nests in this investigation), the molar ratio of Na: Cl was 1:1. Backstrom et al. concluded that road salt contaminated water has Na and Cl concentrations that range from 10.8-200 ppm and 9.8-218.5 ppm, respectively, with

an average concentration of 101 ±50 ppm and 119 ±44 ppm; this is similar to the concentrations of the groundwater samples in this investigation (Table 3-1). Road salt influenced waters are typically distinguishable by a 1:1 molar ratio of Na: Cl (Bäckström et al., 2004).

MW1 had a distinct correlation with road salt signatures, with minimal OSPW contribution, while TP and SP samples measured four times the amount of Na than Cl. MW2 had a molar ratio of approximately 2:1 Na: Cl, indicating potential mixing of OSPW with local road salt affected groundwater, creating a diluted OSPW signature (Figure 3-11). DP02, DP15, DP17, DP22, DP24, DP27, and DP04-0 and DP04-20 also exhibit this diluted OSPW signature (Figure 3-11). DP10, DP25, and DP04-40, 60, 80, and 100 do not appear to be significantly affected by mixing from OSPW leakage (Figure 3-11).

Historical data from 2001-2013 of MW1 indicates that significant seasonal variation of Na: Cl ratios occur (Figure 3-13). From March to November, the Na: Cl ratio is about 0.64:1 ±0.36. In March, around the time of the snowmelt, the Na: Cl ratio is 1.4:1 ±0.84, indicating that road salt is contributing Na to the system that is being measured in the groundwater well. Historically, in October (when the dataset in this investigation was collected in 2016) the average Na: Cl ratio is 0.67 ± 0.24:1 (Figure 3-13). During the October 2016 sampling event, the Na: Cl molar ratio was just shy of 1:1, however, the majority of nests in this investigation have higher concentrations of Na than Cl, and an average molar ratio of 1.3 ±0.5, with the exception of DP25, which had more Cl than Na (Figure 3-11).

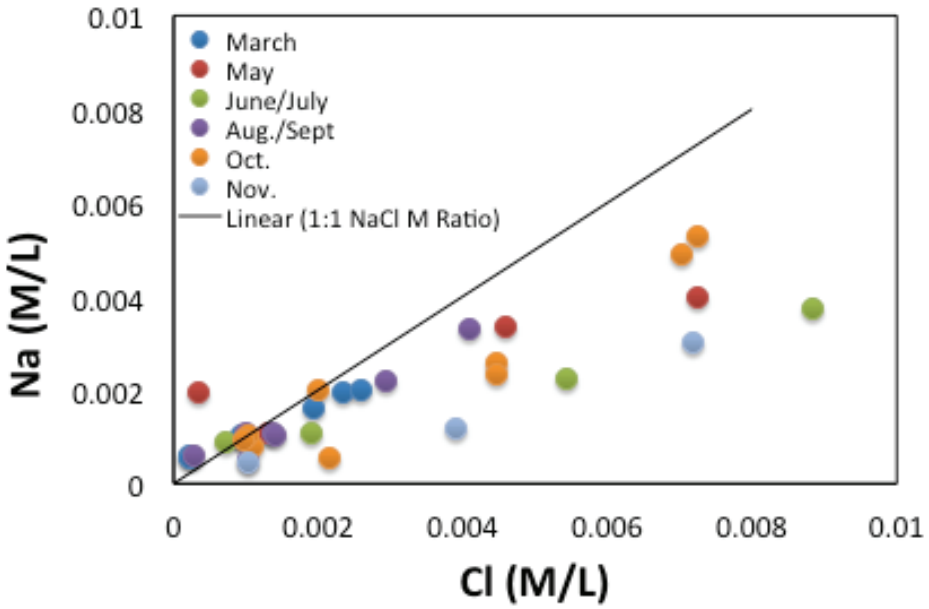

Figure 3- 13: Historical Na/Cl data from MW1. Indicates that there is a 1:1 Na: Cl ratio after the snowmelt.

Together, the B, Li, F, K, and Rb vs. Na:Cl figures indicates the extent of OSPW infiltration into the system (figure 3-14 a, b, c, d, & e). It is assumed that any Na: Cl ratio over 1 indicates OSPW infiltration (as seen in DP02, DP04, DP15, DP17, DP22, DP24, and DP27), and plotting B, Li, F, K, and Rb concentrations show the extent of the infiltration. Based on the Na: Cl ratios, MW2 appears to be a composite of OSPW mixing with the local groundwater, whereas MW1 appears to be primarily local groundwater with road salt contribution, and DP02 is the nest most likely affected by OSPW mixing in terms of B, Li, F, K, and Rb concentrations (Figure 3-14 a, b, c, d, & e)

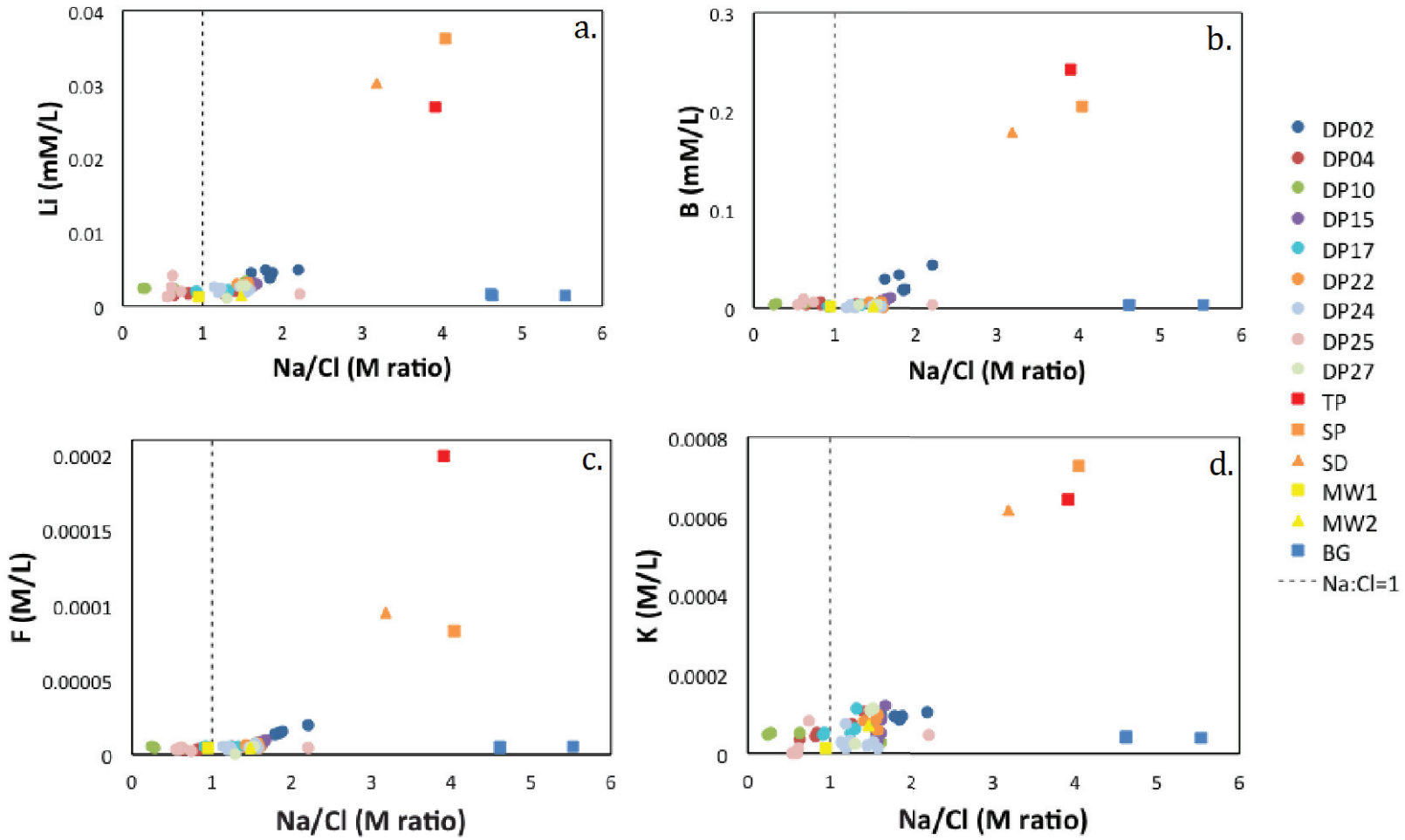

Figure 3- 14: (a.) Li vs. Na: Cl molar ratio; (b.) B vs Na: Cl molar ratio; (c.) Na: Cl ratio; (d.) K vs. Na: Cl; (e.) Rb vs. Na:Cl. The dotted black line is where Na :Cl molar ratio=1, anything <1 indicates OSPW mixing, Li, B, F, K, and Rb concentrations indicate the extent of mixing.

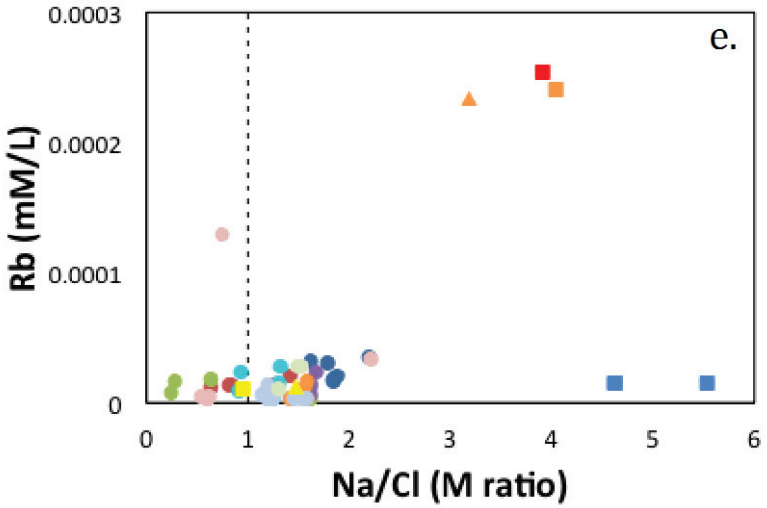

Figure 3- 14 cont.: (a.) Li vs. Na: Cl molar ratio; (b.) B vs Na: Cl molar ratio; (c.) Na: Cl ratio; (d.) K vs. Na: Cl; (e.) Rb vs. Na:Cl. The dotted black line is where Na :Cl molar ratio=1, anything <1 indicates OSPW mixing, Li, B, F, K, and Rb concentrations indicate the extent of mixing.

4.3 Metal Attenuation

It was evident that OSPW was entering the surrounding wetland environment due to the high metal concentrations in MW2, however, there were not equally high metal concentrations measured in the mini-piezometer nests in the study site. This likely indicated metal attenuation via organometallic complexation and, to a lesser extent, mineral precipitation. Roussel et al. (2017) concluded that heavy metals are likely being naturally attenuated from the system via the sorption sieve process. In the presence of humic substances, trace metals (Co, Ni, and Zn) preferentially partition to the humic substances which themselves have high sorption affinity with substrate organic and mineral phases (Anderson and Christensen, 1988; Bradl, 2004; Roussel et al., 2017). As, Mo, Sb, U, V, and W were all elevated in the tailings pond sample, but below the detection limit in the nests. While WHAM7 does not model these elements, literature indicated that they too are likely sequestered by organic molecules (Bowell, 1994; Kautenburger et al., 2017; Larsson et al., 2015; Lu et al., 1998; Maji et al., 2008; Wang et al., 2015; Wichard et al., 2009; Xu et al., 1991). Arsenic and Mo typically prefer oxyhydroxides, such as goethite and hematite, however, in competitive environments with humic substances, they preferentially sorb to organics (Bowell, 1994; Wichard et al., 2009; Xu et al., 1991).

Mineral precipitation could also sequester a smaller portion of the metal load out of solution. High alkalinities caused by microbial activity, create conditions where carbonate minerals (witherite, aragonite, calcite, strontianite, rhodochrosite, siderite, and magnesite) have saturation indicies near equilibrium, which indicates

that carbonate buffering is likely a substantial control with in this system. These minerals likely play an important role in sequestering elements like Mg, Mn, Ba, Sr, Fe, Zn, Ni, and Pb from the system, and likely explain the low Ca concentrations in the nest samples (Appelo and Postma, 1994).

The reduced nature of these groundwaters (oxygen absent and sulphide present in most samples) makes it unlikely that there is substantial Fe^{3+} and consequently iron oxyhydroxides as predicted by PHREEQC analysis. Detailed analysis of AOSR water samples by sector-field ICP-MS indicates that there is substantial iron bound to organic colloids (Jarred et al, 2017). This iron would report in total Fe ICP analysis, but does not represent iron available for oxyhydroxide precipitates. Thus, it seems likely that the method of calculating Fe^{3+} concentrations to estimate the colloidal iron oxyhydroxide mineral concentrations likely results in a large overestimation of the iron oxyhydroxide mineral (Fox, 1988). It is more likely that there is no iron or manganese oxyhydroxide precipitates in these subsurface groundwaters.

4.4 Hydrologic Influences on Solute Transport

While there are four distinct geologic units, the geology in the direct study area can be simplified into two aquifer units: a unit above the mud layer and a unit below. The top organic layer likely has variable aquifer properties, but in general it has full connectivity and effective flow. The abandoned channel indicates that a previous Muskeg River meander transited through the center of the study area, and is inferred to have deposited the basal sands. This meander was eventually abandoned as the river migrated to its present location, building a levee-overbank

system, depositing the muddy aquitard, and leaving an abandoned channel (Figure 3-2). The levee turned the topographic low, behind the levee system, into wetlands accumulating plant debris and organic-rich, swampy deposits, with peat deposits in the oxbow (DP24 has peat to 1.2 meters).

The general basin shape of the study area would promote recharge from the northeastern and southwestern sides of the basin. An intriguing aspect of the depth profiles is that in many nests, there is a general increase in oxygenation below the aquitard layer, which is difficult to explain given the abundant reductive capacity of the overlying wetland organics (Figure 3-8). The basal sands have no visible organic material and thus their capacity to buffer the reduced pE of waters against oxygen penetration is likely dependent upon downward migration of organic matter from above. Oxygenated water infiltration from recharge at the sides of the basin and moving along the sand layer could explain the slight increase in oxygenation in this layer.

5 Conclusions

In the Athabasca Oil Sands Region, the processes that affect metal mobility as oil sands process-affected water enters the organic-rich wetland environments are largely unstudied. Until now, no research has characterized, in detail, the geochemical variations at a field site in a wetland environment in the AOSR. A field investigation and elemental analysis, coupled with geochemical modeling of nine laterally and vertically discrete mini-piezometer nests was conducted. Results indicated that OSPW seepage from the adjacent tailings pond was apparent, as

indicated by the elevated concentrations of B, Br, F, K, Li, Na, Rb, Sr, Zr, and the Na: Cl molar ratios, and that show significant variations in chemistry were present. None of these elements act as a single OSPW indicator element; however, in unison they give a picture of the OSPW infiltration. It is likely that Na and Cl concentrations are influenced by road salt on the adjacent highway during the winter season, and that the water in the nests is likely a composite of OSPW and road salt influenced groundwater. Based on the aforementioned OSPW contribution, you would expect to see elevated metals, such as Co, Ni, and Zn, however, they are below the detection limits in the nests. While OSPW seepage is undeniable, dissimilar concentrations of trace metals in the piezometer nests beyond the monitoring wells indicate that a natural sorption sieve process is likely provoking metal attenuation via formation of organometallic complexes, and to a lesser extent, mineral precipitation. The major ionic chemistry shows trends that would intuitively indicate the extent of OSPW infiltration the further each samples moves away from the TP sample, however, that does not appear to be the case when compared to the other inorganic chemistry. Variable geochemical processes occur even over a relatively small area (>14,500 m^2), and organometallic complexation is likely the dominant process in environments with substantial organic matter present. It is integral to understand these processes in order to properly characterize and understand the impact of mining related activities on surrounding wetland environments.

6 References

Abolfazlzadehdoshanbehbazari, M., 2011. Characterizing the Transport of Process-Affected Water Contained in Oil Sands Tailings Ponds into the underlying Pleistocene clay till in Northern Alberta's Athabasca Oil Sands region: A Field Study (M.S.). University of Alberta (Canada), Canada.

Aiken, G.R., Hsu-Kim, H., Ryan, J.N., 2011. Influence of Dissolved Organic Matter on the Environmental Fate of Metals, Nanoparticles, and Colloids. Environ. Sci. Technol. 45, 3196–3201. https://doi.org/10.1021/es103992s

Allen, E.W., 2008. Process water treatment in Canada's oil sands industry: I. Target pollutants and treatment objectives. J. Environ. Eng. Sci. 7, 123–138. https://doi.org/10.1139/S07-038

Allison, J.D., Allison, T.L., 2005. Partition Coefficients for Metals in Surface Water, Soil, and Waste. US EPA, Athens, GA.

Alloway, B.J., 2012. Heavy metals in soils, 3rd ed, Environmental Pollution. Springer, Dordrecht ; London.

Anderson, P.R., Christensen, T.H., 1988. Distribution coefficients of Cd, Co, Ni, and Zn in soils. J. Soil Sci. 39, 15–22.

Appelo, C.A.J., Postma, D., 1994. Geochemistry, Groundwater, And Pollution, Second. ed. Balkema, Great Britian.

Arbogast, B.F., Geological Survey (U. S.), 1996. Analytical methods manual for the Mineral Resource Surveys Program. U.S. Dept. of the Interior, U.S. Geological Survey, Reston, Va.

Artinger, R., Buckau, G., Geyer, S., Fritz, P., Wolf, M., Kim, J.I., 2000. Characterization of groundwater humic substances: influence of sedimentary organic carbon. Appl. Geochem. 15, 97–116. https://doi.org/10.1016/S0883-2927(99)00021-9

Bäckström, M., Karlsson, S., Bäckman, L., Folkeson, L., Lind, B., 2004. Mobilisation of heavy metals by deicing salts in a roadside environment. Water Res. 38, 720–732. https://doi.org/10.1016/j.watres.2003.11.006

Batayneh, A.T., 2012. Toxic (aluminum, beryllium, boron, chromium and zinc) in groundwater: health risk assessment. Int. J. Environ. Sci. Technol. 9, 153–162. https://doi.org/10.1007/s13762-011-0009-3

Bowell, R.J., 1994. Sorption of arsenic by iron oxides and oxyhydroxides in soils. Appl. Geochem. 9, 279–286.

Bradl, H.B., 2004. Adsorption of heavy metal ions on soils and soils constituents. J. Colloid Interface Sci. 277, 1–18.

Bryan, S.E., Tipping, E., Hamilton-Taylor, J., 2002. Comparison of measured and modelled copper binding by natural organic matter in freshwaters. Comp. Biochem. Physiol. Part C Toxicol. Pharmacol. 133, 37–49. https://doi.org/10.1016/S1532-0456(02)00083-2

Butterwick, L., de Oude, N., Raymond, K., 1989. Safety assessment of boron in aquatic and terrestrial environments. Ecotoxicol. Environ. Saf. 17, 339–371. https://doi.org/10.1016/0147-6513(89)90055-9

Carrigy, M.A., 1962. Effect of texture on the distribution of oil in the Athabasca oil sands, Alberta, Canada. J. Sediment. Res. 32, 312–325. https://doi.org/10.1306/74D70CB3-2B21-11D7-8648000102C1865D

Ceazan, M.L., Thurman, E.M., Smith, R.L., 1989. Retardation of ammonium and potassium transport through a contaminated sand and gravel aquifer: the role of cation exchange. Environ. Sci. Technol. 23, 1402–1408. https://doi.org/10.1021/es00069a012

Centre For Ecology & Hydrology, 2014. Windermere Humic Aqueous Model (WHAM) [WWW Document]. Cent. Ecol. Hydrol. URL http://www.ceh.ac.uk/services/windermere-humic-aqueous-model-wham (accessed 5.26.16).

Chalaturnyk, R.J., Scott, J.D., Özüm, B., 2002. Management of Oil Sands Tailings. Pet. Sci. Technol. 20, 1025–1046. https://doi.org/10.1081/LFT-120003695

Chen, M., Walshe, G., Chi Fru, E., Ciborowski, J.J.H., Weisener, C.G., 2013. Microcosm assessment of the biogeochemical development of sulfur and oxygen in oil sands fluid fine tailings. Appl. Geochem. 37, 1–11. https://doi.org/10.1016/j.apgeochem.2013.06.007

Christensen, T.H., Bjerg, P.L., Banwart, S.A., Jakobsen, R., Heron, G., Albrechtsen, H.-J., 2000. Characterization of redox conditions in groundwater contaminant plumes. J. Contam. Hydrol. 45, 165–241. https://doi.org/10.1016/S0169-7722(00)00109-1

Dierberg, F., DeBusk, T., 2005. An evaluation of two tracers in surface-flow wetlands: Rhodamine-WT and lithium. Wetlands 25, 8–25. https://doi.org/10.1672/0277-5212(2005)025[0008:AEOTTI]2.0.CO;2

Dionex ICS-2100 Ion Chromatography System Operator's Manual, 2012.

Dydo, P., Turek, M., 2012. Boron transport and removal using ion-exchange membranes: A critical review. Desalination 310, 2–8.

EPA, 2016. Priority Pollutant Metals (PP-13) | Curtis & Tompkins Environmental Testing [WWW Document]. URL http://curtisandtompkins.com/major-analytical-categories/trace-metals/priority-pollutant-metals-pp-13/ (accessed 7.3.16).

Fenton, M.., 1994. Chapter 26 - Quaternary Geology of the Western Plains [WWW Document]. URL http://ags.aer.ca/publications/chapter-26-quaternary-geology-of-the-western-plains#Introduction (accessed 5.25.16).

Fox, L.E., 1988. The solubility of colloidal ferric hydroxide and its relevance to iron concentrations in river water. Geochim. Cosmochim. Acta 52, 771–777. https://doi.org/10.1016/0016-7037(88)90337-7

Frank, R.A., Roy, J.W., Bickerton, G., Rowland, S.J., Headley, J.V., Scarlett, A.G., West, C.E., Peru, K.M., Parrott, J.L., Conly, F.M., Hewitt, L.M., 2014. Profiling Oil Sands Mixtures from Industrial Developments and Natural Groundwaters for Source Identification. Environ. Sci. Technol. 48, 2660–2670. https://doi.org/10.1021/es500131k

Freeze, R.A., Cherry, J.A., 1979. Groundwater. Prentice Hall, Inc., Upper Saddle River, NJ.

Furguson, G.P., Rudolph, D.L., Baker, J.F., 2009. Hydrodynamics of a large oil sand tailings impoundment and related environmental implications. Camadian Geotech. J. 46, 1446–1460.

Government of Alberta, 2007a. About Oil Sands [WWW Document]. Alta. Energy. URL http://www.energy.alberta.ca/OilSands/585.asp (accessed 5.24.16).

Government of Alberta, 2007b. Facts and Statistics [WWW Document]. URL http://www.energy.gov.ab.ca/OilSands/791.asp (accessed 5.24.16).

Griffioen, J., 2001. Potassium adsorption ratios as an indicator for the fate of agricultural potassium in groundwater. J. Hydrol. 254, 244–254.

Gu, B., Lowe, L.E., 1989. Studies on the Adsorption of Boron on Humic Acids. Can. J. Soil Sci. 305–311.

Gulamova, N.V., 2010. Sorption of Zirconium Ions by Soils. Russ. J. Phys. Chem. 84, 149–151.

HACH, 2007. DR 2800 Spectrophotometer Procedures Manual [WWW Document]. Scribd. URL https://www.scribd.com/document/138080069/DR-2800-Spectrophotometer-Procedures-Manual (accessed 3.24.17).

Hackbarth, D.A., 1981. Natural temporal variations in the chemistry of shallow groundwater, Athabasca Oil Sands area, Alberta. Can. J. Earth Sci. 10, 1599–1608.

Hein, F.J., Cotterill, D.K., 2006. The Athabasca Oil Sands — A Regional Geological Perspective, Fort McMurray Area, Alberta, Canada. Nat. Resour. Res. 15, 85–102. https://doi.org/10.1007/s11053-006-9015-4

Hilal, N., Kim, G.J., Somerfield, C., 2011. Boron removal from saline water: A comprehensive review. Desalination 273, 23–35. https://doi.org/10.1016/j.desal.2010.05.012

Holden, A.A., Donahue, R.B., Ulrich, A.C., 2011. Geochemical interactions between process-affected water from oil sands tailings ponds and North Alberta surficial sediments. J. Contam. Hydrol. 119, 55–68. https://doi.org/10.1016/j.jconhyd.2010.09.008

Hubard, T., 2002. Encyclopedia of surface and colloid science; Marcel Dekker, Portland, OR.

Jha, S.K., Singh, R.K., Damodaran, T., Mishra, V.K., Sharma, D.K., Rai, D., 2013. Fluoride in Groundwater: Toxicological Exposure and Remedies. J. Toxicol. Environ. Health 16, 52–66.

Kautenburger, R., Sander, J.M., Hein, C., 2017. Europium (III) and Uranium (VI) complexation by natural organic matter (NOM): Effect of source. ELECTROPHORESIS 38, 930–937. https://doi.org/10.1002/elps.201600488

Keefe, S.H., Barber, L.B., Runkel, R.L., Ryan, J.N., McKnight, D.M., Wass, R.D., 2004. Conservative and reactive solute transport in constructed wetlands. Water Resour. Res. 40. https://doi.org/10.1029/2003WR002130

Lamothe, P.J., Meier, A.L., Wilson, S.A., 1999. The determination of forty-four elements in aqueous samples by inductively coupled plasma-mass spectrometry (USGS Numbered Series No. 99–151), Open-File Report. U.S. Geological Survey : Books and Open-File Reports.

Langley, S., Gault, A.G., Ibrahim, A., Takahashi, Y., Renaud, R., Fortin, D., Clark, I.D., Ferris, F.G., 2009. Sorption of Strontium onto Bacteriogenic Iron Oxides - Environmental Science & Technology. Environ. Sci. Technol. 43.

Larsson, M.A., Baken, S., Smolders, E., Cubadda, F., 2015. Vanadium bioavailability in soils amended with blast furnace slag. J. Hazard. Mater. 158–165.

Lemarchand, E., Schott, J., Gaillardet, J., 2005. Boron isotopic fractionation related to boron sorption on humic acid and the structure of surface complexes formed. Geochim. Cosmochim. Acta 69, 3519–3533. https://doi.org/10.1016/j.gca.2005.02.024

Lu, X., Johnson, W.D., Hook, J., 1998. Reaction of Vanadate with Aquatic Humic Substances: An ESR and 51V NMR Study. Environ. Sci. Technol. 32, 2257–2263. https://doi.org/10.1021/es970930r

Maji, P., Wang, W., Greene, A.E., Gimbert, Y., 2008. Studies directed toward the synthesis of chiral tungsten and molybdenum carbonyl complexes. J. Organomet. Chem. 693, 1841–1849. https://doi.org/10.1016/j.jorganchem.2008.02.008

Masliyah, J., Zhiang, Z. (Joe), Zhenghe, X., Czarnecki, J., Hassan, H., 2004. Understanding Water-Based Bitumen Extraction from Athabasca Oil Sands. Can. J. Chem. Eng. 82, 628–654.

Négrel, P., Millot, R., Brenot, A., Bertin, C., 2010. Lithium isotopes as tracers of groundwater circulation in a peat land. Chem. Geol. 276, 119–127. https://doi.org/10.1016/j.chemgeo.2010.06.008

Oiffer, A.A.L., 2006. Integrated solid phase, aqueous phase and numerical investigation of plume geochemistry at an oil sand mining facility (M.Sc.). University of Waterloo (Canada), Canada.

Pickering, R.J., 1979. Analytical Methods--Recommended procedures for calibrating dissolved oxygen meters [WWW Document]. URL https://water.usgs.gov/admin/memo/QW/qw79.10.html (accessed 3.24.17).

Richards, L.A., Magnone, D., van Dongen, B.E., Ballentine, C.J., Polya, D.A., 2015. Use of lithium tracers to quantify drilling fluid contamination for groundwater monitoring in Southeast Asia. Appl. Geochem. 63, 190–202. https://doi.org/10.1016/j.apgeochem.2015.08.013

Roussel, S., Gammon, P., Amos, R., Ahad, J., Hedley, J., Peru, K., Savard, M., 2017. The Sorption Sieve: Organometallic complexes in the Alberta Oil Sands.

Small, C.C., Cho, S., Hashisho, Z., Ulrich, A.C., 2015. Emissions from oil sands tailings ponds: Review of tailings pond parameters and emission estimates. J. Pet. Sci. Eng. 127, 490–501. https://doi.org/10.1016/j.petrol.2014.11.020

Tipping, E., Lofts, S., Sonke, J.E., 2011. Humic Ion-Binding Model VII: a revised parameterisation of cation-binding by humic substances. Environ. Chem. 8, 225–235. https://doi.org/10.1071/EN11016

USGS, 2016. PHREEQC Welcome Page [WWW Document]. URL http://wwwbrr.cr.usgs.gov/projects/GWC_coupled/phreeqc/ (accessed 5.26.16).

Wang, Y., Zhang, D., Shen, Z., Feng, C., Zhang, X., 2015. Investigation of the interaction between As and Sb species and dissolved organic matter in the Yangtze Estuary, China, using excitation–emission matrices with parallel factor analysis | SpringerLink. Environ. Sci. Pollut. Res. 22, 1819–1830.

Warner, B.G., Rubec, C.D.A., Canada Committee on Ecological (Biophysical) Land Classification, National Wetlands Working Group, 1997. The Canadian wetland classification system. Wetlands Research Branch, University of Waterloo, Waterloo, Ont.

Weng, L., Fest, E.P.M.J., Fillius, J., Temminghoff, E.J.M., Van Riemsdijk, W.H., 2002. Transport of Humic and Fulvic Acids in Relation to Metal Mobility in a Copper-Contaminated Acid Sandy Soil. Environ. Sci. Technol. 36, 1699–1704. https://doi.org/10.1021/es010283a

WHO, 1998. Guidelines for drinking-water quality. (No. 2nd ed. Addendum to Vol. 2). Geneva, Health criteria and other supporting information.

Wichard, T., Mishra, B., Myneni, S.C.B., Bellenger, J.-P., Kraepiel, A.M.L., 2009. Storage and bioavailability of molybdenum in soils increased by organic matter complexation. Nat. Geosci. 2, ngeo589. https://doi.org/10.1038/ngeo589

Xu, H., Allard, B., Grimvall, A., 1991. Effects of acidification and natural organic materials on the mobility of arsenic in the environment. Water. Air. Soil Pollut. 57–58, 269–278. https://doi.org/10.1007/BF00282890

Chapter 4: Final Conclusions and Suggested Future Research

1 Final Conclusions

1.1 Summary

As oil sands process-affected water (OSPW) enters humic substance-rich (humic and fulvic acids) wetland environments, organometallic complexes form, creating a "sorption sieve" process that naturally attenuates the trace metals released into the surrounding environments. Geochemical modeling (PHREEQC and WHAM7) indicated that when humic substances are the primary sorption phase within a system, rare earth elements preferentially sorb to them, resulting in enhanced mobility compared to the transition metals. In competitive reactions between humic substances (larger weight humic acids in particular) and oxyhydroxides, transition metals form organometallic complexes that deplete the concentrations in solution. Zinc, Co, Ni, and Cu partitioning is dependent on the concentration of each organic and inorganic phase, when organics are present without Fe oxyhydroxides, they form organometallic complexes. Lead and Y also predominantly partition to iron oxyhydroxides, however, when oxyhydroxides are removed from the system, they partition to humic substances.

A high resolution, depth discrete investigation indicated that geochemistry over a relatively small area (>14,500 square meters) can vary significantly as a result of the underlying geology that creates preferential flow paths for OSPW migration. Boron, Br, F, K, and Li have the potential to be used as OSPW tracers, however, they too likely partition to humic substances and mineral phases to a lesser extent. The Na: Cl ratio is another indicator of OSPW infiltration; a value greater than one indicates OSPW mixing.

The potential sorption of tracer elements excludes them from being used singularly as an OSPW indicator element, however, when used in unison with the Na:Cl ratio, it is possible to get an idea of the extent of OSPW infiltration.

The potential impact that tailings facilities have on local and regional groundwater and surface water supplies is a fundamental concern in the Alberta Oils Sands. The influence organic humic substances have trace metal mobility had not been evaluated until now, even though wetland environments comprise such a large area. A clear understanding of the geochemical processes that control trace metal migration and attenuation in the Athabasca Oil Sands Region is integral to adequately characterize and predict the potential environmental risks associated with the large-scale oil sands mining industry. In the occurrence of OSPW infiltration into the surrounding organic-rich environment, it appears that organometallic complexation attenuates the majority of trace metals before they can migrate to the nearby river systems.

1.2 Proposed Future Research

A more comprehensive and accurate WHAM7 modeling for the sorption to clays would help to determine the partitioning preferences of those metals that typically tend to sorb to clays. Even when clay concentrations were set artificially high, no elements sorbed to any clay minerals.

The overestimation of Fe oxyhydroxides likely skewed the amount of sorption to oxyhydroxide phases. A more precise analysis that could distinguish the real dissolved iron from the colloidal iron would give a more accurate estimation of the real Fe^{3+} concentrations, resulting in a more accurate Fe oxyhydroxide concentration.

Isotopic analysis of Li isotopes for OSPW migration would indicate which species originated from OSPW or minerallic contribution. The two stable isotopes of lithium (6 and 7) have mass difference of approximately 17% (Négrel et al., 2010). The heavy ^{7}Li isotope typically remains in solution and can be used to determine Li sourced from precipitation, groundwater, and anthropogenic origin (Négrel et al., 2010).

2 References

Négrel, P., Millot, R., Brenot, A., Bertin, C., 2010. Lithium isotopes as tracers of groundwater circulation in a peat land. Chem. Geol. 276, 119–127. https://doi.org/10.1016/j.chemgeo.2010.06.008

Appendix A: Aqueous Phase Geochemistry

1 Chapter 2: Aqueous Phase Geochemistry

1.1 Dataset 1

1.1.1 ICP-MS: Dataset 1

Sample	DILUTION	Li	Be	B	Al	Ti	V
		ICP-MS DIRECT	ICP-MS DIRECT	ICP-MS DIRECT	ICP-MS DIRECT	ICP-MS DIRECT	ICP-MS DIRECT
		ppb	ppb	ppb	ppb	ppb	ppb
D.L.	1	0.02	0.005	0.5	2	0.5	0.1
D.L.	10	0.2	0.05	5	20	5	1
GW 1.1	1	76.82	0.022	201.7	8	2.3	1.3
GW 1.2	1	35.22	0.014	272.9	3	1.6	1.0
GW 1.3	1	48.11	0.040	425.4	10	2.7	3.2
GW 1.4	1	64.51	0.018	595.1	4	1.5	1.4
GW 1.5	1	74.81	0.022	819.2	4	1.6	1.4
GW 1.6	1	51.33	0.026	390.5	6	1.7	1.4
GW 1.7	1	54.46	0.014	468.3	3	1.5	1.3
GW 1.8	1	28.44	0.012	121.2	10	1.4	1.3
GW 1.9	1	45.91	0.109	374.1	31	5.5	8.4
SW 1.1	1	8.15	< 0.005	24.6	< 2	< 0.5	< 0.1

Sample	Cr	Mn	Co	Ni	Cu	Zn	Ga
	ICP-MS DIRECT	ICP-MS DIRECT	ICP-MS DIRECT	ICP-MS DIRECT	ICP-MS DIRECT	ICP-MS DIRECT	ICP-MS DIRECT
	ppb	ppb	ppb	ppb	ppb	ppb	ppb
D.L.	0.1	0.1	0.05	0.2	0.1	0.5	0.01
D.L.	1	1	0.5	2	1	5	0.1
GW 1.1	0.3	626.9	< 0.05	< 0.2	< 0.1	< 0.5	< 0.01
GW 1.2	0.3	332.8	< 0.05	< 0.2	< 0.1	< 0.5	< 0.01
GW 1.3	0.6	349.9	< 0.05	< 0.2	< 0.1	< 0.5	< 0.01
GW 1.4	0.3	246.4	< 0.05	< 0.2	< 0.1	< 0.5	< 0.01
GW 1.5	0.3	367.8	< 0.05	< 0.2	< 0.1	< 0.5	< 0.01
GW 1.6	0.4	522.1	< 0.05	< 0.2	< 0.1	< 0.5	< 0.01
GW 1.7	0.3	514.4	< 0.05	< 0.2	< 0.1	< 0.5	< 0.01
GW 1.8	0.3	566.2	< 0.05	< 0.2	< 0.1	< 0.5	< 0.01
GW 1.9	1.4	242.9	< 0.05	< 0.2	< 0.1	< 0.5	< 0.01
SW 1.1	< 0.1	75.4	< 0.05	< 0.2	2.0	0.9	< 0.01

Sample	Ge	As	Se	Rb	Sr	Y	Zr
	ICP-MS	ICP-MS	ICP-MS	ICP-MS	ICP-MS	ICP-MS	ICP-MS
	DIRECT	DIRECT	DIRECT	DIRECT	DIRECT	DIRECT	DIRECT
	ppb	ppb	ppb	ppb	ppb	ppb	ppb
D.L.	0.02	0.1	1	0.05	0.5	0.01	0.05
D.L.	0.2	1	10	0.5	5	0.1	0.5
GW 1.1	0.06	0.3	< 1	1.39	214.2	0.48	0.67
GW 1.2	0.09	0.3	< 1	1.29	239.9	0.12	0.88
GW 1.3	0.10	1.4	< 1	1.74	186.2	0.46	1.23
GW 1.4	0.07	0.5	< 1	2.37	202.4	0.09	0.61
GW 1.5	0.06	0.5	< 1	1.33	221.5	0.11	0.72
GW 1.6	0.07	0.3	< 1	1.07	241.5	0.08	0.69
GW 1.7	0.07	0.2	< 1	1.24	202.0	0.05	0.78
GW 1.8	0.16	1.3	< 1	0.71	279.9	0.51	1.13
GW 1.9	0.06	0.8	< 1	1.39	186.7	1.55	2.08
SW 1.1	< 0.02	< 0.1	< 1	0.64	93.9	< 0.01	< 0.05

Sample	Nb	Mo	Ag	Cd	In	Sn	Sb
	ICP-MS	ICP-MS	ICP-MS	ICP-MS	ICP-MS	ICP-MS	ICP-MS
	DIRECT	DIRECT	DIRECT	DIRECT	DIRECT	DIRECT	DIRECT
	ppb	ppb	ppb	ppb	ppb	ppb	ppb
D.L.	0.01	0.05	0.005	0.02	0.01	0.01	0.01
D.L.	0.1	0.5	0.05	0.2	0.1	0.1	0.1
GW 1.1	0.01	< 0.05	< 0.005	< 0.02	< 0.01	< 0.01	< 0.01
GW 1.2	< 0.01	0.10	< 0.005	< 0.02	< 0.01	< 0.01	< 0.01
GW 1.3	0.02	0.15	< 0.005	< 0.02	< 0.01	< 0.01	< 0.01
GW 1.4	< 0.01	0.29	< 0.005	< 0.02	< 0.01	< 0.01	< 0.01
GW 1.5	< 0.01	0.22	< 0.005	< 0.02	< 0.01	< 0.01	< 0.01
GW 1.6	0.01	0.10	< 0.005	< 0.02	< 0.01	< 0.01	< 0.01
GW 1.7	< 0.01	0.19	< 0.005	< 0.02	< 0.01	< 0.01	< 0.01
GW 1.8	< 0.01	0.12	< 0.005	< 0.02	< 0.01	< 0.01	0.01
GW 1.9	0.03	0.27	< 0.005	< 0.02	< 0.01	0.02	< 0.01
SW 1.1	< 0.01	< 0.05	< 0.005	< 0.02	< 0.01	< 0.01	< 0.01

Sample	Te	Cs	Ba	La	Ce	Pr	Nd
	ICP-MS	ICP-MS	ICP-MS	ICP-MS	ICP-MS	ICP-MS	ICP-MS
	DIRECT	DIRECT	DIRECT	DIRECT	DIRECT	DIRECT	DIRECT
	ppb	ppb	ppb	ppb	ppb	ppb	ppb
D.L.	0.02	0.01	0.2	0.01	0.01	0.005	0.005
D.L.	0.2	0.1	2	0.1	0.1	0.05	0.05
GW 1.1	< 0.02	< 0.01	302.2	0.10	0.16	0.027	0.164
GW 1.2	< 0.02	< 0.01	161.7	0.04	0.08	0.010	0.046
GW 1.3	< 0.02	< 0.01	196.5	0.29	0.65	0.082	0.354
GW 1.4	< 0.02	< 0.01	247.1	0.02	0.04	0.005	0.025
GW 1.5	< 0.02	< 0.01	208.1	0.02	0.04	< 0.005	0.025
GW 1.6	< 0.02	< 0.01	249.3	0.02	0.03	< 0.005	0.026
GW 1.7	< 0.02	< 0.01	195.3	0.01	0.03	< 0.005	0.016
GW 1.8	< 0.02	< 0.01	343.4	0.20	0.41	0.051	0.248
GW 1.9	< 0.02	< 0.01	167.1	0.43	1.00	0.153	0.775
SW 1.1	< 0.02	< 0.01	57.4	< 0.01	< 0.01	< 0.005	< 0.005

Sample	Sm	Eu	Tb	Gd	Dy	Ho	Er
	ICP-MS	ICP-MS	ICP-MS	ICP-MS	ICP-MS	ICP-MS	ICP-MS
	DIRECT	DIRECT	DIRECT	DIRECT	DIRECT	DIRECT	DIRECT
	ppb	ppb	ppb	ppb	ppb	ppb	ppb
D.L.	0.005	0.005	0.005	0.005	0.005	0.005	0.005
D.L.	0.05	0.05	0.05	0.05	0.05	0.05	0.05
GW 1.1	0.041	0.011	0.009	0.061	0.054	0.013	0.037
GW 1.2	0.012	< 0.005	< 0.005	0.016	0.016	< 0.005	0.013
GW 1.3	0.081	0.018	0.012	0.084	0.078	0.016	0.045
GW 1.4	0.006	< 0.005	< 0.005	0.008	0.010	< 0.005	0.008
GW 1.5	0.007	< 0.005	< 0.005	0.011	0.011	< 0.005	0.010
GW 1.6	0.007	< 0.005	< 0.005	0.008	0.009	< 0.005	0.008
GW 1.7	< 0.005	< 0.005	< 0.005	0.006	0.006	< 0.005	0.005
GW 1.8	0.050	0.012	0.008	0.057	0.050	0.012	0.039
GW 1.9	0.179	0.048	0.036	0.237	0.224	0.048	0.141
SW 1.1	< 0.005	< 0.005	< 0.005	< 0.005	< 0.005	< 0.005	< 0.005

Sample	Tm	Yb	Lu	Hf	Ta	W	Re
	ICP-MS	ICP-MS	ICP-MS	ICP-MS	ICP-MS	ICP-MS	ICP-MS
	DIRECT	DIRECT	DIRECT	DIRECT	DIRECT	DIRECT	DIRECT
	ppb	ppb	ppb	ppb	ppb	ppb	ppb
D.L.	0.005	0.005	0.005	0.01	0.01	0.02	0.005
D.L.	0.05	0.05	0.05	0.1	0.1	0.2	0.05
GW 1.1	0.005	0.033	0.005	0.02	< 0.01	< 0.02	0.009
GW 1.2	< 0.005	0.012	< 0.005	0.01	< 0.01	0.05	0.007
GW 1.3	0.006	0.040	0.006	0.03	< 0.01	0.02	0.008
GW 1.4	< 0.005	0.009	< 0.005	0.01	< 0.01	< 0.02	0.010
GW 1.5	< 0.005	0.011	< 0.005	0.01	< 0.01	< 0.02	0.010
GW 1.6	< 0.005	0.009	< 0.005	0.01	< 0.01	< 0.02	0.007
GW 1.7	< 0.005	0.005	< 0.005	0.02	< 0.01	< 0.02	0.009
GW 1.8	0.006	0.036	0.006	0.02	< 0.01	< 0.02	< 0.005
GW 1.9	0.020	0.127	0.020	0.05	< 0.01	< 0.02	0.008
SW 1.1	< 0.005	< 0.005	< 0.005	< 0.01	< 0.01	< 0.02	< 0.005

Sample	Tl	Pb	Bi	Th	U	Br	Ca
	ICP-MS	ICP-MS	ICP-MS	ICP-MS	ICP-MS	ICP-ES	ICP-ES
	DIRECT	DIRECT	DIRECT	DIRECT	DIRECT	DIRECT	DIRECT
	ppb	ppb	ppb	ppb	ppb	ppm	ppm
D.L.	0.005	0.01	0.02	0.02	0.005	0.05	0.02
D.L.	0.05	0.1	0.2	0.2	0.05		
GW 1.1	< 0.005	< 0.01	< 0.02	< 0.02	0.049	0.25	97.32
GW 1.2	< 0.005	< 0.01	< 0.02	< 0.02	0.020	0.19	90.51
GW 1.3	< 0.005	< 0.01	< 0.02	0.04	0.060	0.18	97.75
GW 1.4	< 0.005	< 0.01	< 0.02	< 0.02	0.103	0.21	104.78
GW 1.5	< 0.005	< 0.01	< 0.02	< 0.02	0.110	0.19	81.32
GW 1.6	< 0.005	< 0.01	< 0.02	< 0.02	0.011	0.17	119.18
GW 1.7	< 0.005	< 0.01	< 0.02	< 0.02	0.021	0.17	105.04
GW 1.8	< 0.005	< 0.01	< 0.02	< 0.02	0.079	0.22	164.76
GW 1.9	< 0.005	< 0.01	< 0.02	0.10	0.128	0.18	78.38
SW 1.1	< 0.005	< 0.01	< 0.02	< 0.02	0.013	< 0.05	46.23

Sample	Cl	Fe	K	Mg	Na	P	S
	ICP-ES	ICP-ES	ICP-ES	ICP-ES	ICP-ES	ICP-ES	ICP-ES
	DIRECT	DIRECT	DIRECT	DIRECT	DIRECT	DIRECT	DIRECT
	ppm	ppm	ppm	ppm	ppm	ppm	ppm
D.L.	0.1	0.005	0.05	0.005	0.05	0.05	0.05
D.L.							
GW 1.1	74.0	5.908	2.60	14.774	209.30	0.35	46.65
GW 1.2	56.4	6.904	2.22	13.102	125.80	0.17	39.69
GW 1.3	59.9	7.619	2.46	15.230	163.89	0.18	46.70
GW 1.4	62.5	5.703	2.72	19.258	198.52	0.09	51.63
GW 1.5	66.7	3.127	3.53	20.317	197.79	0.10	47.26
GW 1.6	58.2	8.509	1.98	20.564	143.85	0.18	49.84
GW 1.7	57.5	7.984	2.20	16.268	154.20	0.14	44.34
GW 1.8	57.6	33.462	2.19	22.071	90.17	< 0.05	52.07
GW 1.9	57.5	6.786	3.19	15.827	157.79	0.12	26.42
SW 1.1	0.6	0.203	1.06	11.419	3.13	< 0.05	0.77

Sample	Sc	Si
	ICP-ES	ICP-ES
	DIRECT	DIRECT
	ppm	ppm
D.L.	0.001	0.02
D.L.		
GW 1.1	< 0.001	6.67
GW 1.2	< 0.001	11.38
GW 1.3	< 0.001	7.54
GW 1.4	< 0.001	5.63
GW 1.5	< 0.001	6.12
GW 1.6	< 0.001	7.33
GW 1.7	< 0.001	6.58
GW 1.8	< 0.001	8.51
GW 1.9	< 0.001	5.46
SW 1.1	< 0.001	6.47

1.1.2 ICP-ES: Dataset 1

Sample	Br	Ca	Cl	Fe	K	Mg	Na	P	S	Sc	Si
	ICP-ES DIRECT	ICP-ES DIRECT	ICP-ES DIRECT	ICP-ES DIRECT	ICP-ES DIRECT	ICP-ES DIRECT	ICP-ES DIRECT	ICP-ES DIRECT	ICP-ES DIRECT	ICP-ES DIRECT	ICP-ES DIRECT
	ppm	ppm	ppm	ppm	ppm	ppm	ppm	ppm	ppm	ppm	ppm
D.L.	0.05	0.02	0.1	0.005	0.05	0.005	0.05	0.05	0.05	0.001	0.02
GW 1.1	0.25	97.32	74.0	5.908	2.60	14.774	209.30	0.35	46.65	< 0.001	6.67
GW 1.2	0.19	90.51	56.4	6.904	2.22	13.102	125.80	0.17	39.69	< 0.001	11.38
GW 1.3	0.18	97.75	59.9	7.619	2.46	15.230	163.89	0.18	46.70	< 0.001	7.54
GW 1.4	0.21	104.78	62.5	5.703	2.72	19.258	198.52	0.09	51.63	< 0.001	5.63
GW 1.5	0.19	81.32	66.7	3.127	3.53	20.317	197.79	0.10	47.26	< 0.001	6.12
GW 1.6	0.17	119.18	58.2	8.509	1.98	20.564	143.85	0.18	49.84	< 0.001	7.33
GW 1.7	0.17	105.04	57.5	7.984	2.20	16.268	154.20	0.14	44.34	< 0.001	6.58
GW 1.8	0.22	164.76	57.6	33.462	2.19	22.071	90.17	< 0.05	52.07	< 0.001	8.51
GW 1.9	0.18	78.38	57.5	6.786	3.19	15.827	157.79	0.12	26.42	< 0.001	5.46
SW 1.1	< 0.05	46.23	0.6	0.203	1.06	11.419	3.13	< 0.05	0.77	< 0.001	6.47

1.1.3 Anions: Dataset 1

Sample	F	Cl	SO4	Br	NO3	PO4
	Dionex ICS-2100	Dionex ICS-2100	Dionex ICS-2100	Dionex ICS-2100	Dionex ICS-2100	Dionex ICS-2100
	ppm	ppm	ppm	ppm	ppm	ppm
D.L.	0.01	0.01	0.02	0.02	0.02	0.02
GW 1.1	0.47	77.61	136.25	< 0.02	< 0.02	0.05
GW 1.2	0.21	54.63	112.69	< 0.02	< 0.02	< 0.02
GW 1.3	0.30	57.85	128.65	< 0.02	< 0.02	< 0.02
GW 1.4	0.41	61.30	145.48	< 0.02	< 0.02	< 0.02
GW 1.5	0.68	64.72	132.75	< 0.02	< 0.02	< 0.02
GW 1.6	0.25	55.87	137.67	< 0.02	< 0.02	< 0.02
GW 1.7	0.22	57.94	128.01	< 0.02	< 0.02	< 0.02
GW 1.8	0.06	58.43	150.79	< 0.02	< 0.02	< 0.02
GW 1.9	0.43	55.99	73.06	< 0.02	< 0.02	0.21
SW 1.1	0.15	0.53	1.88	< 0.02	0.14	< 0.02

1.1.4 Other Geochemical Parameters: Dataset 1

Sample	Alkalinity PC-Titrate as CaCO3 ppm	Conductivity meter DIRECT µS/cm	pH meter DIRECT unit	pe ORP Calc.	DOC SHIMADZU DIRECT ppm	Total AEO's ppm	DO ppm	Temp C	Fe2+ HACH ppm	Fe3+ Calc ppm	S2- HACH µg/L
D.L.	1	10	0.1	NA	< 1	NA			NA	NA	NA
GW 1.1	489	1434	8.0	9.9	13	7.2	0.32	6.7	2.11	3.8	73
GW 1.2	346	1034	7.9	10.2	11	6.1	0.69	8.1	2.34	4.6	N/A
GW 1.3	405	1176	8.3	10.5	12	6.5	0.47	9	3.45	4.2	N/A
GW 1.4	516	1378	8.1	10.1	10	5.5	0.03	7	2.16	3.5	63
GW 1.5	469	1303	8.1	10.0	12	7.2	0.97	8.7	2.63	0.5	41
GW 1.6	446	1237	7.9	10.4	10	5.2	0.37	5.6	2.6	5.9	27
GW 1.7	449	1244	8.0	10.8	11	2.8	0.07	6.3	2.5	5.5	26
GW 1.8	460	1278	7.6	10.9	14	2.7	0.84	5	3.67	29.8	0
GW 1.9	422	1113	7.8	10.3	17	8.5	0.04	8	2.78	4.0	47
SW 1.1	167	317	8.1	11.9	5	1.8	6.61	7.4	1.5	0.0	0

1.2 Dataset 2

1.2.1 ICP-MS: Dataset 2

Sample	Li ICP-MS DIRECT ppb	Be ICP-MS DIRECT ppb	B ICP-MS DIRECT ppb	Ti ICP-MS DIRECT ppb	V ICP-MS DIRECT ppb	Cr ICP-MS DIRECT ppb	Mn ICP-MS DIRECT ppb	Co ICP-MS DIRECT ppb	Ni ICP-MS DIRECT ppb
D.L.	**0.02**	**0.005**	**0.5**	**0.5**	**0.1**	**0.1**	**0.1**	**0.05**	**0.2**
GW2.1	28.97	0.009	119.5	0.8	0.3	0.2	370.7	0.41	2.5
GW2.2	16.70	0.017	50.5	0.8	0.4	0.2	218.0	< 0.05	< 0.2
GW2.3	8.37	0.029	20.9	1.4	3.2	0.8	343.9	8.53	7.5
GW2.4	8.65	0.007	60.9	0.8	0.2	< 0.1	760.0	1.96	3.4
GW2.5	116.70	< 0.005	1341.5	1.8	0.3	0.2	225.3	< 0.05	1.1
GW2.6	90.24	0.022	234.8	1.3	0.7	0.3	330.0	< 0.05	0.2
GW2.7	17.10	0.006	261.4	0.6	0.3	0.3	786.0	5.97	11.1
GW2.8	39.54	0.136	619.0	1.4	1.3	0.8	113.8	1.09	6.9
SW2.1	6.64	< 0.005	23.4	< 0.5	0.2	0.1	6.5	0.19	0.7
SW2.2	12.60	< 0.005	47.0	0.6	0.2	< 0.1	12.6	< 0.05	0.5
SW2.3	7.13	< 0.005	27.4	< 0.5	0.2	< 0.1	7.1	0.08	0.6
SW2.4	4.93	< 0.005	7.7	0.9	0.1	< 0.1	118.6	0.17	0.4
SW2.5	5.93	< 0.005	18.3	< 0.5	0.2	< 0.1	7.3	0.08	0.6
SW2.6	12.20	< 0.005	41.6	0.7	0.2	< 0.1	24.9	0.05	0.4
Seep Pipe	211.77	0.017	1981.5	1.2	0.4	0.2	5025.9	49.47	58.1
Seep Ditch	209.44	0.007	1690.6	0.9	< 0.1	0.1	1578.5	28.79	34.7

Sample	Cu	Zn	Ga	Ge	As	Se	Rb	Sr	Y
	ICP-MS DIRECT	ICP-MS DIRECT	ICP-MS DIRECT	ICP-MS DIRECT	ICP-MS DIRECT	ICP-MS DIRECT	ICP-MS DIRECT	ICP-MS DIRECT	ICP-MS DIRECT
	ppb	ppb	ppb	ppb	ppb	ppb	ppb	ppb	ppb
D.L.	0.1	0.5	0.01	0.02	0.1	1	0.05	0.5	0.01
GW2.1	< 0.1	< 0.5	< 0.01	0.11	0.6	< 1	1.63	377.9	0.15
GW2.2	< 0.1	1.0	< 0.01	0.06	0.4	< 1	1.29	320.2	0.24
GW2.3	0.4	4.6	< 0.01	< 0.02	1.3	1	0.85	746.5	0.41
GW2.4	< 0.1	3.1	< 0.01	< 0.02	1.0	< 1	0.75	478.7	0.14
GW2.5	< 0.1	< 0.5	< 0.01	0.11	0.4	< 1	4.68	1054.6	0.12
GW2.6	< 0.1	< 0.5	< 0.01	0.05	0.6	1	0.78	369.9	0.19
GW2.7	0.6	1.5	< 0.01	< 0.02	0.7	< 1	4.68	435.6	0.13
GW2.8	1.9	54.4	0.02	0.46	0.8	< 1	3.14	642.4	1.08
SW2.1	0.5	0.6	< 0.01	< 0.02	0.3	< 1	0.69	338.1	0.06
SW2.2	0.2	< 0.5	< 0.01	< 0.02	0.3	< 1	1.17	132.8	0.04
SW2.3	0.7	< 0.5	< 0.01	< 0.02	0.2	< 1	0.72	280.1	0.05
SW2.4	0.5	< 0.5	< 0.01	< 0.02	0.3	< 1	1.46	90.1	0.02
SW2.5	0.5	0.8	< 0.01	< 0.02	0.3	< 1	0.74	348.8	0.05
SW2.6	0.2	< 0.5	< 0.01	< 0.02	0.3	< 1	1.22	129.7	0.04
Seep Pipe	< 0.1	9.0	0.01	0.07	1.6	< 1	17.69	2351.0	0.14
Seep Ditch	0.2	5.4	< 0.01	0.07	0.8	1	20.85	2387.6	0.05

Sample	Zr	Nb	Mo	Ag	Cd	In	Sn	Sb	Te
	ICP-MS DIRECT	ICP-MS DIRECT	ICP-MS DIRECT	ICP-MS DIRECT	ICP-MS DIRECT	ICP-MS DIRECT	ICP-MS DIRECT	ICP-MS DIRECT	ICP-MS DIRECT
	ppb	ppb	ppb	ppb	ppb	ppb	ppb	ppb	ppb
D.L.	0.05	0.01	0.05	0.005	0.02	0.01	0.01	0.01	0.02
GW2.1	0.87	< 0.01	0.68	< 0.005	< 0.02	< 0.01	< 0.01	< 0.01	< 0.02
GW2.2	0.95	< 0.01	0.17	< 0.005	< 0.02	< 0.01	< 0.01	< 0.01	< 0.02
GW2.3	6.26	0.02	0.30	< 0.005	< 0.02	< 0.01	0.30	0.04	< 0.02
GW2.4	0.29	< 0.01	0.38	< 0.005	< 0.02	< 0.01	< 0.01	0.04	< 0.02
GW2.5	0.71	< 0.01	0.17	< 0.005	< 0.02	< 0.01	< 0.01	< 0.01	< 0.02
GW2.6	1.43	0.02	0.17	< 0.005	< 0.02	< 0.01	< 0.01	0.03	< 0.02
GW2.7	0.53	< 0.01	0.11	< 0.005	0.02	< 0.01	0.01	0.04	< 0.02
GW2.8	3.32	< 0.01	0.68	< 0.005	0.04	< 0.01	0.03	0.22	< 0.02
SW2.1	< 0.05	< 0.01	0.79	< 0.005	< 0.02	< 0.01	< 0.01	0.02	< 0.02
SW2.2	0.21	< 0.01	0.10	< 0.005	< 0.02	< 0.01	< 0.01	0.02	< 0.02
SW2.3	< 0.05	< 0.01	0.66	< 0.005	< 0.02	< 0.01	< 0.01	0.02	< 0.02
SW2.4	0.06	< 0.01	0.05	< 0.005	< 0.02	< 0.01	0.02	0.02	< 0.02
SW2.5	< 0.05	< 0.01	0.84	< 0.005	< 0.02	< 0.01	< 0.01	0.05	< 0.02
SW2.6	0.17	< 0.01	0.06	< 0.005	< 0.02	< 0.01	< 0.01	0.02	< 0.02
Seep Pipe	0.78	< 0.01	4.52	< 0.005	< 0.02	< 0.01	< 0.01	< 0.01	< 0.02
Seep Ditch	0.23	< 0.01	4.47	< 0.005	< 0.02	< 0.01	< 0.01	< 0.01	< 0.02

Sample	Cs	Ba	La	Ce	Pr	Nd	Sm	Eu	Tb
	ICP-MS DIRECT ppb	ICP-MS DIRECT ppb	ICP-MS DIRECT ppb	ICP-MS DIRECT ppb	ICP-MS DIRECT ppb	ICP-MS DIRECT ppb	ICP-MS DIRECT ppb	ICP-MS DIRECT ppb	ICP-MS DIRECT ppb
D.L.	0.01	0.2	0.01	0.01	0.005	0.005	0.005	0.005	0.005
GW2.1	< 0.01	316.5	0.04	0.21	0.012	0.058	0.016	< 0.005	< 0.005
GW2.2	< 0.01	270.6	0.06	0.23	0.017	0.082	0.025	< 0.005	< 0.005
GW2.3	< 0.01	241.1	0.23	0.96	0.068	0.299	0.068	0.013	0.010
GW2.4	< 0.01	129.5	0.05	0.13	0.010	0.047	0.010	< 0.005	< 0.005
GW2.5	0.03	278.3	0.03	0.12	0.008	0.043	0.010	< 0.005	< 0.005
GW2.6	< 0.01	152.6	0.04	0.20	0.011	0.055	0.014	< 0.005	< 0.005
GW2.7	0.01	55.2	0.04	0.28	0.009	0.038	0.008	< 0.005	< 0.005
GW2.8	0.01	118.8	0.59	3.96	0.147	0.625	0.143	0.024	0.024
SW2.1	< 0.01	60.0	0.01	0.02	< 0.005	0.020	0.007	< 0.005	< 0.005
SW2.2	< 0.01	37.8	0.01	0.02	< 0.005	0.016	< 0.005	< 0.005	< 0.005
SW2.3	< 0.01	48.9	0.01	0.02	< 0.005	0.022	< 0.005	< 0.005	< 0.005
SW2.4	< 0.01	26.9	< 0.01	0.02	< 0.005	0.013	< 0.005	< 0.005	< 0.005
SW2.5	< 0.01	62.1	0.01	0.02	< 0.005	0.021	0.006	< 0.005	< 0.005
SW2.6	< 0.01	35.8	0.01	0.02	< 0.005	0.021	< 0.005	< 0.005	< 0.005
Seep Pipe	0.05	76.0	0.02	0.04	0.007	0.037	0.009	< 0.005	< 0.005
Seep Ditch	0.07	183.2	< 0.01	0.01	< 0.005	0.006	< 0.005	< 0.005	< 0.005

Sample	Gd	Dy	Ho	Er	Tm	Yb	Lu	Hf	Ta
	ICP-MS DIRECT ppb	ICP-MS DIRECT ppb	ICP-MS DIRECT ppb	ICP-MS DIRECT ppb	ICP-MS DIRECT ppb	ICP-MS DIRECT ppb	ICP-MS DIRECT ppb	ICP-MS DIRECT ppb	ICP-MS DIRECT ppb
D.L.	0.005	0.005	0.005	0.005	0.005	0.005	0.005	0.01	0.01
GW2.1	0.019	0.019	< 0.005	0.013	< 0.005	0.013	< 0.005	0.02	< 0.01
GW2.2	0.030	0.033	0.007	0.021	< 0.005	0.020	< 0.005	0.02	< 0.01
GW2.3	0.074	0.064	0.014	0.038	< 0.005	0.030	< 0.005	0.13	< 0.01
GW2.4	0.013	0.012	< 0.005	0.009	< 0.005	0.008	< 0.005	0.02	< 0.01
GW2.5	0.016	0.018	< 0.005	0.014	< 0.005	0.012	< 0.005	0.02	< 0.01
GW2.6	0.019	0.023	0.006	0.020	< 0.005	0.023	< 0.005	0.03	< 0.01
GW2.7	0.011	0.010	< 0.005	0.009	< 0.005	0.010	< 0.005	0.01	< 0.01
GW2.8	0.166	0.152	0.033	0.095	0.013	0.088	0.014	0.06	< 0.01
SW2.1	0.008	0.007	< 0.005	< 0.005	< 0.005	< 0.005	< 0.005	< 0.01	< 0.01
SW2.2	< 0.005	0.006	< 0.005	< 0.005	< 0.005	< 0.005	< 0.005	< 0.01	< 0.01
SW2.3	0.006	0.006	< 0.005	< 0.005	< 0.005	< 0.005	< 0.005	< 0.01	< 0.01
SW2.4	< 0.005	< 0.005	< 0.005	< 0.005	< 0.005	< 0.005	< 0.005	< 0.01	< 0.01
SW2.5	0.009	0.007	< 0.005	< 0.005	< 0.005	< 0.005	< 0.005	< 0.01	< 0.01
SW2.6	0.006	0.006	< 0.005	< 0.005	< 0.005	< 0.005	< 0.005	< 0.01	< 0.01
Seep Pipe	0.014	0.019	< 0.005	0.015	< 0.005	0.015	< 0.005	0.06	< 0.01
Seep Ditch	< 0.005	0.007	< 0.005	< 0.005	< 0.005	< 0.005	< 0.005	0.03	< 0.01

Sample	W	Re	Tl	Pb	Bi	U	Al	Br	Ca
	ICP-MS DIRECT ppb	ICP-MS DIRECT ppb	ICP-MS DIRECT ppb	ICP-MS DIRECT ppb	ICP-MS DIRECT ppb	ICP-MS DIRECT ppb	ICP-ES DIRECT ppm	ICP-ES DIRECT ppm	ICP-ES DIRECT ppm
D.L.	0.02	0.005	0.005	0.01	0.02	0.005	0.005	0.05	0.02
GW2.1	0.04	< 0.005	< 0.005	0.02	< 0.02	0.048	< 0.005	0.29	159.58
GW2.2	< 0.02	< 0.005	< 0.005	< 0.01	< 0.02	0.229	< 0.005	0.30	166.60
GW2.3	< 0.02	0.015	0.007	0.04	< 0.02	7.444	< 0.005	0.41	331.87
GW2.4	< 0.02	0.009	0.006	< 0.01	< 0.02	1.549	< 0.005	< 0.05	303.29
GW2.5	< 0.02	0.033	< 0.005	< 0.01	< 0.02	0.009	< 0.005	0.35	101.83
GW2.6	< 0.02	0.032	< 0.005	< 0.01	< 0.02	3.288	< 0.005	0.30	161.35
GW2.7	< 0.02	0.034	0.125	0.01	< 0.02	10.634	< 0.005	0.21	300.07
GW2.8	< 0.02	< 0.005	0.015	0.10	< 0.02	0.082	0.052	0.09	63.21
SW2.1	< 0.02	< 0.005	< 0.005	0.01	< 0.02	0.499	< 0.005	< 0.05	42.10
SW2.2	< 0.02	< 0.005	< 0.005	0.02	< 0.02	0.221	< 0.005	< 0.05	48.80
SW2.3	< 0.02	< 0.005	< 0.005	0.01	< 0.02	0.404	< 0.005	< 0.05	35.85
SW2.4	< 0.02	< 0.005	< 0.005	0.03	< 0.02	0.039	< 0.005	< 0.05	44.84
SW2.5	< 0.02	< 0.005	< 0.005	0.02	< 0.02	0.530	< 0.005	< 0.05	42.60
SW2.6	< 0.02	< 0.005	< 0.005	0.01	< 0.02	0.038	< 0.005	< 0.05	43.83
Seep Pipe	< 0.02	0.042	0.005	0.08	< 0.02	1.943	< 0.005	0.33	202.80
Seep Ditch	0.05	0.020	0.007	< 0.01	< 0.02	0.950	< 0.005	0.55	161.17

Sample	Cl	Fe	K	Mg	Na	P	S	Sc	Si
	ICP-ES DIRECT ppm	ICP-ES DIRECT ppm	ICP-ES DIRECT ppm	ICP-ES DIRECT ppm	ICP-ES DIRECT ppm	ICP-ES DIRECT ppm	ICP-ES DIRECT ppm	ICP-ES DIRECT ppm	ICP-ES DIRECT ppm
D.L.	0.1	0.005	0.05	0.005	0.05	0.05	0.05	0.001	0.02
GW2.1	90.5	1.449	2.01	18.778	66.66	< 0.05	2.20	< 0.001	4.42
GW2.2	99.5	1.204	1.70	18.544	69.87	< 0.05	2.50	< 0.001	4.63
GW2.3	146.7	0.191	0.30	56.543	92.38	< 0.05	124.57	< 0.001	3.73
GW2.4	12.1	4.898	2.77	19.774	15.39	< 0.05	172.69	< 0.001	5.38
GW2.5	189.4	2.353	3.94	17.620	294.51	0.19	89.82	< 0.001	8.51
GW2.6	60.5	0.376	1.77	95.318	115.05	< 0.05	127.55	< 0.001	7.25
GW2.7	94.2	1.689	2.88	26.281	95.41	< 0.05	135.50	< 0.001	3.06
GW2.8	16.9	0.115	3.30	9.266	86.11	< 0.05	42.80	< 0.001	5.31
SW2.1	4.2	0.021	1.12	12.999	13.24	< 0.05	17.08	< 0.001	0.82
SW2.2	7.3	0.336	1.21	12.416	17.93	< 0.05	5.53	< 0.001	3.97
SW2.3	12.1	0.055	1.05	11.092	16.68	< 0.05	12.28	0.002	1.62
SW2.4	0.7	0.340	1.00	17.253	3.61	< 0.05	0.41	0.001	5.90
SW2.5	3.1	0.019	1.19	13.139	12.35	< 0.05	17.63	< 0.001	0.81
SW2.6	4.1	0.386	1.32	12.280	13.97	< 0.05	4.24	< 0.001	4.49
Seep Pipe	151.1	32.350	20.37	66.391	302.93	< 0.05	264.29	0.002	7.86
Seep Ditch	543.3	0.159	17.69	54.228	488.08	< 0.05	158.40	< 0.001	4.33

1.2.2 ICP-ES: Dataset 2

Sample	Al ICP-ES DIRECT ppm	Br ICP-ES DIRECT ppm	Ca ICP-ES DIRECT ppm	Cl ICP-ES DIRECT ppm	Fe ICP-ES DIRECT ppm	K ICP-ES DIRECT ppm	Mg ICP-ES DIRECT ppm	Na ICP-ES DIRECT ppm	P ICP-ES DIRECT ppm	S ICP-ES DIRECT ppm	Sc ICP-ES DIRECT ppm	Si ICP-ES DIRECT ppm
D.L.	0.005	0.05	0.02	0.1	0.005	0.05	0.005	0.05	0.05	0.05	0.001	0.02
GW2.1	< 0.005	0.29	159.58	90.5	1.449	2.01	18.778	66.66	< 0.05	2.20	< 0.001	7.13
GW2.2	< 0.005	0.30	166.60	99.5	1.204	1.70	18.544	69.87	< 0.05	2.50	< 0.001	7.31
GW2.3	< 0.005	0.41	331.87	146.7	0.191	0.30	56.543	92.38	< 0.05	124.57	< 0.001	7.25
GW2.4	< 0.005	< 0.05	303.29	12.1	4.898	2.77	19.774	15.39	< 0.05	172.69	< 0.001	7.28
GW2.5	< 0.005	0.35	101.83	189.4	2.353	3.94	17.620	294.51	0.19	89.82	< 0.001	3.46
GW2.6	< 0.005	0.30	161.35	60.5	0.376	1.77	95.318	115.05	< 0.05	127.55	< 0.001	3.06
GW2.7	< 0.005	0.21	300.07	94.2	1.689	2.88	26.281	95.41	< 0.05	135.50	< 0.001	3.06
GW2.8	0.052	0.09	63.21	16.9	0.115	3.30	9.266	86.11	< 0.05	42.80	< 0.001	3.14
SW2.1	< 0.005	< 0.05	42.10	4.2	0.021	1.12	12.999	13.24	< 0.05	17.08	< 0.001	5.29
SW2.2	< 0.005	< 0.05	48.80	7.3	0.336	1.21	12.416	17.93	< 0.05	5.53	< 0.001	13.51
SW2.3	< 0.005	< 0.05	35.85	12.1	0.055	1.05	11.092	16.68	< 0.05	12.28	0.002	8.67
SW2.4	< 0.005	< 0.05	44.84	0.7	0.340	1.00	17.253	3.61	< 0.05	0.41	0.001	8.62
SW2.5	< 0.005	< 0.05	42.60	3.1	0.019	1.19	13.139	12.35	< 0.05	17.63	< 0.001	5.26
SW2.6	< 0.005	< 0.05	43.83	4.1	0.386	1.32	12.280	13.97	< 0.05	4.24	< 0.001	5.31
Seep Pipe	< 0.005	0.55	161.17	543.3	0.159	17.69	54.228	488.08	< 0.05	158.40	< 0.001	3.67
Seep Ditch	< 0.005	0.33	202.80	151.1	32.350	20.37	66.391	302.93	< 0.05	264.29	0.002	7.60

1.2.3 Anions: Dataset 2

Sample	F Dionex ICS-2100 ppm	Cl Dionex ICS-2100 ppm	SO4 Dionex ICS-2100 ppm	Br Dionex ICS-2100 ppm	NO3 Dionex ICS-2100 ppm	PO4 Dionex ICS-2100 ppm
D.L.	0.01	0.01	0.02	0.02	0.02	0.02
GW2.1	0.17	86.60	3.48	0.26	< 0.02	< 0.02
GW2.2	0.12	95.97	4.14	0.29	< 0.02	< 0.02
GW2.3	0.04	138.53	326.08	< 0.02	0.21	< 0.02
GW2.4	0.05	11.32	503.41	< 0.02	< 0.02	< 0.02
GW2.5	0.15	181.71	251.67	0.07	< 0.02	< 0.02
GW2.6	0.64	56.71	372.75	< 0.02	< 0.02	< 0.02
GW2.7	0.04	87.01	402.06	< 0.02	1.20	< 0.02
GW2.8	0.09	16.05	116.15	< 0.02	0.75	< 0.02
SW2.1	0.09	4.19	48.37	< 0.02	< 0.02	0.06
SW2.2	0.11	6.96	13.68	< 0.02	< 0.02	< 0.02
SW2.3	0.09	11.83	36.04	< 0.02	< 0.02	0.04
SW2.4	0.09	0.75	0.25	< 0.02	< 0.02	< 0.02
SW2.5	0.09	3.32	50.44	< 0.02	0.31	0.07
SW2.6	0.11	4.19	10.30	< 0.02	0.30	< 0.02
Seep Pipe	1.29	509.69	500.50	< 0.02	0.19	< 0.02
Seep Ditch	1.48	141.07	763.32	< 0.02	< 0.02	< 0.02

1.2.4 Other Geochemical Parameters: Dataset 2

Sample	Alkalinity PC-Titrate as CaCO3 ppm	Conductivity meter DIRECT µS/cm	pH meter DIRECT unit	pe ORP Calc.	DOC SHIMADZU DIRECT ppm	Total AEOs ppm	DO ppm	Temp °C	Fe2+ HACH ppm	Fe3+ Calc. ppm	S2- HACH ug/L
GW2.1	496	765	6.940	9.822	20	11.20	3.9	6.100	1.5	-0.051	102
GW2.2	507	838	6.930	11.407	21	10.10	0.4	7.000	1.11	0.094	16
GW2.3	676	1518	6.650	12.457	75	58.90	7.1	8.900	0.05	0.141	3
GW2.4	329	1065	6.860	10.233	13	7.30	0.5	8.900	4.53*	0.368	11
GW2.5	442	1239	7.000	9.747	29	26.00	0.7	5.400	2.1	0.253	68
GW2.6	613	1247	7.070	8.675	21	12.80	0.4	8.100	0.32	0.056	429
GW2.7	539	1300	6.600	11.861	15	15.20	0.9	9.300	1.64	0.049	12
GW2.8	245	915	6.560	11.161	33	12.90	4.3	9.700	0	0.115	N/A
SW2.1	128	246	8.380	13.280	4	1.40	12.6	6.400	0	0.021	N/A
SW2.2	178	246	8.350	13.004	20	7.80	12.3	5.200	0	0.336	N/A
SW2.3	118	237	8.350	13.144	6	1.60	11.8	7.200	0	0.055	N/A
SW2.4	191	235	7.360	13.432	16	5.40	3.9	6.100	0.06	0.280	N/A
SW2.5	125	177	8.380	13.549	4	1.30	11	6.800	0	0.019	N/A
SW2.6	169	226	8.000	12.624	19	7.60	9.7	5.900	0	0.386	N/A
Seep Pipe	459	2065	6.900	10.621	32	50.40	4.1	12.400	5.24	27.110	4
Seep Ditch	471	2489	7.4	10.6	32	NM	8.8	9.3	0	32.4	NA

2 Chapter 3: Aqueous Phase Geochemistry

2.1 ICP-MS

	Dilution	Li ICP-MS DIRECT ppb	Be ICP-MS DIRECT ppb	B ICP-MS DIRECT ppb	Al ICP-MS DIRECT ppb	Ti ICP-MS DIRECT ppb	V ICP-MS DIRECT ppb	Cr ICP-MS DIRECT ppb	Mn ICP-MS DIRECT ppb	Co ICP-MS DIRECT ppb	Ni ICP-MS DIRECT ppb	Cu ICP-MS DIRECT ppb	Zn ICP-MS DIRECT ppb
D.L.	X1	0.02	0.005	0.5	2	0.5	0.1	0.1	0.1	0.05	0.2	0.1	0.5
D.L.	X10	0.2	0.05	5	20	5	1	1	1	0.5	2	1	5
DP02-0 0.45	10	30.7	<0.05	210	<20	<5	<1	<1	851	<0.5	<2	<1	<5
DP02-20 0.45	10	26.5	<0.05	186	<20	<5	<1	<1	1026	<0.5	<2	<1	<5
DP02-40b 0.45	10	27.5	<0.05	201	<20	<5	<1	<1	1202	<0.5	<2	<1	<5
DP02-60 0.45	10	34.0	<0.05	361	66	<5	1	<1	520	<0.5	<2	<1	<5
DP02-80 0.45	10	31.8	<0.05	323	<20	<5	<1	<1	345	<0.5	<2	<1	<5
DP02-100 0.45	10	34.1	<0.05	467	<20	<5	2	<1	690	<0.5	<2	<1	<5
DP04-0 0.45	10	13.4	<0.05	60	<20	<5	<1	<1	51	<0.5	2	<1	<5
DP04-20 0.45	10	10.9	<0.05	48	<20	<5	<1	<1	670	<0.5	<2	<1	<5
DP04-40 0.45	10	13.1	<0.05	61	<20	<5	<1	<1	990	<0.5	<2	<1	<5
DP04-80 0.45	1	10.27	0.008	33.5	5	1.2	0.4	0.4	1278.4	<0.05	<0.2	<0.1	<0.5
DP04-100 0.45	1	11.45	0.015	37.9	10	1.4	0.6	0.3	901.9	<0.05	<0.2	<0.1	<0.5
DP04-140 0.45	1	10.36	0.008	33.6	5	1.1	0.6	0.4	932.7	<0.05	<0.2	<0.1	<0.5
DP10-0 0.45	10	19.7	<0.05	64	<20	<5	<1	<1	52	<0.5	<2	<1	<5
DP10-20 0.45	10	23.8	<0.05	74	<20	<5	<1	<1	361	<0.5	<2	<1	<5
DP10-60 0.45	10	16.3	<0.05	38	<20	<5	<1	<1	380	<0.5	<2	<1	<5
DP10-80 0.45	10	16.4	<0.05	44	<20	<5	<1	<1	197	<0.5	<2	<1	<5
DP10-100 0.45	10	16.2	<0.05	48	<20	<5	<1	<1	316	<0.5	<2	<1	<5
DP15-0 0.45	10	21.2	<0.05	110	<20	<5	<1	<1	6	<0.5	<2	<1	<5
DP15-20 0.45	10	21.7	<0.05	84	<20	<5	<1	<1	1419	<0.5	<2	<1	<5
DP15-40 0.45	10	21.2	<0.05	78	<20	<5	<1	<1	1351	0.9	<2	<1	<5
DP15-60 0.45	10	16.7	<0.05	62	<20	<5	<1	<1	1850	1.5	3	<1	<5
DP15-80 0.45	10	18.2	<0.05	80	<20	<5	<1	<1	2994	2.2	4	<1	<5
DP15-90 0.45	10	18.0	<0.05	100	<20	<5	<1	<1	2216	0.9	2	<1	<5
DP17-0 0.45	10	14.8	<0.05	41	<20	<5	<1	<1	52	<0.5	<2	<1	<5
DP17-20 0.45	10	14.3	<0.05	37	<20	<5	<1	<1	514	<0.5	<2	<1	<5
DP17-40 0.45	10	14.7	<0.05	25	<20	<5	<1	<1	1137	<0.5	<2	<1	<5
DP17-80 0.45	10	13.2	<0.05	24	<20	<5	<1	<1	2189	<0.5	<2	<1	<5
DP17-95 0.45	10	14.3	<0.05	22	<20	<5	<1	<1	1397	<0.5	<2	<1	<5
DP17-W 0.45	1	30.66	0.015	95.3	9	1.0	0.4	0.4	1036.4	0.09	0.4	<0.1	1.1
DP22-0 0.45	10	21.5	<0.05	70	<20	<5	<1	<1	110	<0.5	<2	<1	<5
DP22-20 0.45	10	21.0	<0.05	71	<20	<5	<1	<1	405	<0.5	<2	<1	<5
DP22-40 0.45	10	20.4	<0.05	67	37	<5	<1	<1	518	<0.5	<2	<1	<5
DP22-80 0.45	10	15.9	<0.05	12	<20	<5	<1	<1	234	<0.5	<2	<1	<5
DP24-0 0.45	10	16.7	<0.05	18	<20	<5	<1	<1	158	<0.5	<2	<1	<5
DP24-20 0.45	10	17.5	<0.05	5	<20	<5	<1	<1	638	<0.5	<2	<1	<5
DP24-40 0.45	10	16.5	<0.05	12	<20	<5	<1	<1	374	<0.5	<2	<1	<5
DP24-60 0.45	10	13.2	<0.05	26	40	<5	<1	<1	657	<0.5	<2	<1	<5
DP24-80 0.45	10	17.5	<0.05	18	40	<5	<1	<1	485	<0.5	<2	<1	<5
DP24-100 0.45	10	14.8	<0.05	24	31	<5	<1	<1	608	<0.5	<2	<1	<5
DP24-W 0.45	10	12.8	<0.05	42	23	<5	<1	<1	412	<0.5	<2	<1	<5
DP25-0 0.45	1	10.77	<0.005	39.6	4	0.9	0.2	0.2	8.3	0.07	0.5	<0.1	0.9
DP25-20 0.45	10	13.2	0.08	64	70	<5	<1	14	750	3.6	3	2	57
DP25-40 0.45	1	8.09	0.015	44.0	20	3.3	0.6	0.6	238.7	0.29	0.2	<0.1	0.5
DP25-60 0.45	1	9.61	0.016	55.7	15	5.5	0.5	0.5	164.7	0.09	0.3	<0.1	1.0
DP25-80 0.45	1	28.56	0.009	101.9	10	2.1	0.3	0.4	460.8	0.10	2.0	<0.1	1.2
DP25-100 0.45	1	17.80	0.008	71.6	13	2.7	0.3	0.4	401.5	<0.05	<0.2	<0.1	<0.5
DP25-W 0.45	1	10.93	0.022	48.8	15	2.5	0.5	0.5	345.4	1.17	0.7	0.2	4.1
DP27-0 0.45	10	19.2	<0.05	42	<20	<5	<1	<1	5	<0.5	<2	<1	<5
DP27-20 0.45	10	18.5	<0.05	38	<20	<5	<1	<1	123	<0.5	<2	<1	<5
AR00 0.45	1	9.08	0.006	37.3	9	<0.5	0.2	0.2	8.9	0.14	1.2	0.6	0.5
AR04 0.45	1	7.61	0.010	29.1	6	0.6	0.3	0.2	9.5	0.08	0.9	0.6	<0.5
MR01 0.45	1	11.27	<0.005	42.6	3	0.8	0.3	0.2	13.9	0.07	0.6	0.1	<0.5
MR02 0.45	1	10.47	<0.005	39.0	4	0.9	0.2	0.2	12.8	0.07	0.5	0.4	0.6
MW1	10	8.3	<0.05	16	<20	<5	2	<1	536	8.5	11	<1	<5
MW2	10	9.4	<0.05	18	<20	<5	1	<1	2286	1.5	4	<1	<5
BG	1	4.64	<0.005	6.8	2	0.7	0.1	0.2	10.4	<0.05	0.4	<0.1	<0.5
TP	10	186.6	<0.05	2613	<20	<5	6	<1	58	2.7	9	<1	<5
Seep Ditch	10	210.1	<0.05	1926	<20	<5	<1	<1	1885	41.2	51	<1	10
Seep Pipe	10	251.1	<0.05	2210	<20	<5	<1	<1	3406	65.7	93	<1	16

	Ga ICP-MS DIRECT ppb	Ge ICP-MS DIRECT ppb	As ICP-MS DIRECT ppb	Se ICP-MS DIRECT ppb	Rb ICP-MS DIRECT ppb	Sr ICP-MS DIRECT ppb	Y ICP-MS DIRECT ppb	Zr ICP-MS DIRECT ppb	Nb ICP-MS DIRECT ppb	Mo ICP-MS DIRECT ppb	Ag ICP-MS DIRECT ppb	Cd ICP-MS DIRECT ppb	In ICP-MS DIRECT ppb
D.L.	0.01	0.02	0.1	1	0.05	0.5	0.01	0.05	0.01	0.05	0.005	0.02	0.01
D.L.	0.1	0.2	1	10	0.5	5	0.1	0.5	0.1	0.5	0.05	0.2	0.1
DP02-0 0.45	<0.1	<0.2	<1	<10	1.8	346	0.2	0.6	<0.1	<0.5	<0.05	<0.2	<0.1
DP02-20 0.45	<0.1	<0.2	<1	<10	1.4	361	0.2	0.6	<0.1	<0.5	<0.05	<0.2	<0.1
DP02-40b 0.45	<0.1	<0.2	<1	<10	1.6	348	0.2	0.7	<0.1	<0.5	<0.05	<0.2	<0.1
DP02-60 0.45	<0.1	<0.2	<1	<10	2.6	330	0.4	0.9	<0.1	<0.5	<0.05	<0.2	<0.1
DP02-80 0.45	<0.1	0.3	<1	<10	2.8	283	0.3	0.7	<0.1	<0.5	<0.05	<0.2	<0.1
DP02-100 0.45	<0.1	<0.2	<1	<10	3.0	339	0.6	1.8	<0.1	<0.5	<0.05	<0.2	<0.1
DP04-0 0.45	<0.1	<0.2	<1	<10	1.7	773	<0.1	<0.5	<0.1	<0.5	<0.05	<0.2	<0.1
DP04-20 0.45	<0.1	<0.2	<1	<10	1.2	736	<0.1	<0.5	<0.1	<0.5	<0.05	<0.2	<0.1
DP04-40 0.45	<0.1	<0.2	<1	<10	1.2	447	0.1	0.5	<0.1	<0.5	<0.05	<0.2	<0.1
DP04-80 0.45	0.02	0.07	0.2	<1	1.06	291.1	0.09	0.63	<0.01	<0.05	<0.005	<0.02	<0.01
DP04-100 0.45	0.02	0.05	0.3	<1	1.17	353.4	0.35	0.98	<0.01	<0.05	<0.005	<0.02	<0.01
DP04-140 0.45	0.02	0.03	0.4	<1	0.87	249.1	0.22	0.84	<0.01	<0.05	<0.005	<0.02	<0.01
DP10-0 0.45	<0.1	<0.2	<1	<10	<0.5	223	<0.1	<0.5	<0.1	<0.5	<0.05	<0.2	<0.1
DP10-20 0.45	<0.1	<0.2	<1	<10	0.8	256	<0.1	<0.5	<0.1	<0.5	<0.05	<0.2	<0.1
DP10-60 0.45	<0.1	<0.2	<1	<10	0.6	384	<0.1	<0.5	<0.1	<0.5	<0.05	<0.2	<0.1
DP10-80 0.45	<0.1	<0.2	<1	<10	1.5	362	<0.1	<0.5	<0.1	<0.5	<0.05	<0.2	<0.1
DP10-100 0.45	<0.1	<0.2	<1	<10	1.4	377	<0.1	<0.5	<0.1	<0.5	<0.05	<0.2	<0.1
DP15-0 0.45	<0.1	<0.2	<1	<10	2.0	350	<0.1	<0.5	<0.1	<0.5	<0.05	<0.2	<0.1
DP15-20 0.45	<0.1	<0.2	<1	<10	1.2	385	0.1	<0.5	<0.1	<0.5	<0.05	<0.2	<0.1
DP15-40 0.45	<0.1	<0.2	1	<10	1.0	412	0.1	0.5	<0.1	<0.5	<0.05	<0.2	<0.1
DP15-60 0.45	<0.1	<0.2	<1	<10	0.7	362	0.2	1.0	<0.1	<0.5	<0.05	<0.2	<0.1
DP15-80 0.45	<0.1	<0.2	<1	<10	0.7	365	0.4	1.2	<0.1	<0.5	<0.05	<0.2	<0.1
DP15-90 0.45	<0.1	<0.2	1	<10	0.5	373	0.4	1.1	<0.1	<0.5	<0.05	<0.2	<0.1
DP17-0 0.45	<0.1	<0.2	<1	<10	2.4	599	<0.1	<0.5	<0.1	<0.5	<0.05	<0.2	<0.1
DP17-20 0.45	<0.1	<0.2	1	<10	1.3	584	<0.1	<0.5	<0.1	<0.5	<0.05	<0.2	<0.1
DP17-40 0.45	<0.1	<0.2	<1	<10	<0.5	562	0.1	<0.5	<0.1	<0.5	<0.05	<0.2	<0.1
DP17-80 0.45	<0.1	0.2	<1	<10	0.8	569	0.2	<0.5	<0.1	<0.5	<0.05	<0.2	<0.1
DP17-95 0.45	<0.1	<0.2	<1	<10	2.0	531	0.3	<0.5	<0.1	<0.5	<0.05	<0.2	<0.1
DP17-W 0.45	0.02	0.08	0.3	<1	1.06	512.8	0.08	0.75	<0.01	0.08	<0.005	<0.02	<0.01
DP22-0 0.45	<0.1	<0.2	<1	<10	1.4	293	<0.1	<0.5	<0.1	<0.5	<0.05	<0.2	<0.1
DP22-20 0.45	<0.1	<0.2	<1	<10	1.0	318	<0.1	<0.5	<0.1	<0.5	<0.05	<0.2	<0.1
DP22-40 0.45	<0.1	<0.2	<1	<10	<0.5	318	0.1	<0.5	<0.1	<0.5	<0.05	<0.2	<0.1
DP22-80 0.45	<0.1	<0.2	<1	<10	<0.5	331	0.1	<0.5	<0.1	<0.5	<0.05	<0.2	<0.1
DP24-0 0.45	<0.1	<0.2	<1	<10	1.2	477	<0.1	<0.5	<0.1	<0.5	<0.05	<0.2	<0.1
DP24-20 0.45	<0.1	<0.2	<1	<10	0.6	525	<0.1	<0.5	<0.1	<0.5	<0.05	<0.2	<0.1
DP24-40 0.45	<0.1	<0.2	<1	<10	<0.5	439	<0.1	<0.5	<0.1	<0.5	<0.05	<0.2	<0.1
DP24-60 0.45	<0.1	<0.2	<1	<10	<0.5	431	0.1	0.5	<0.1	<0.5	<0.05	<0.2	<0.1
DP24-80 0.45	<0.1	<0.2	<1	<10	<0.5	445	0.1	<0.5	<0.1	<0.5	<0.05	<0.2	<0.1
DP24-100 0.45	<0.1	<0.2	<1	<10	<0.5	570	0.1	<0.5	<0.1	<0.5	<0.05	<0.2	<0.1
DP24-W 0.45	<0.1	<0.2	<1	<10	<0.5	422	0.1	<0.5	<0.1	<0.5	<0.05	<0.2	<0.1
DP25-0 0.45	<0.01	<0.02	0.3	<1	2.85	102.4	0.04	0.14	<0.01	0.06	<0.005	<0.02	<0.01
DP25-20 0.45	<0.1	<0.2	<1	<10	11.1	185	0.3	<0.5	<0.1	<0.5	<0.05	<0.2	<0.1
DP25-40 0.45	<0.01	0.05	0.5	<1	0.37	231.0	0.22	0.80	0.01	<0.05	<0.005	<0.02	<0.01
DP25-60 0.45	<0.01	0.02	0.4	<1	0.28	238.4	0.19	0.68	<0.01	<0.05	<0.005	<0.02	<0.01
DP25-80 0.45	0.01	<0.02	0.3	<1	0.43	273.6	0.10	0.34	<0.01	<0.05	<0.005	<0.02	<0.01
DP25-100 0.45	<0.01	<0.02	0.4	<1	0.28	282.6	0.13	0.43	<0.01	<0.05	<0.005	<0.02	<0.01
DP25-W 0.45	<0.01	0.03	0.5	<1	0.56	290.2	0.22	0.62	<0.01	0.11	<0.005	<0.02	<0.01
DP27-0 0.45	<0.1	<0.2	<1	<10	2.4	353	<0.1	<0.5	<0.1	<0.5	<0.05	<0.2	<0.1
DP27-20 0.45	<0.1	<0.2	<1	<10	2.4	352	<0.1	<0.5	<0.1	<0.5	<0.05	<0.2	<0.1
AR00 0.45	<0.01	<0.02	0.5	<1	0.84	253.4	0.13	0.18	<0.01	0.62	<0.005	<0.02	<0.01
AR04 0.45	<0.01	<0.02	0.4	<1	0.83	182.9	0.09	0.18	<0.01	0.46	<0.005	<0.02	<0.01
MR01 0.45	<0.01	<0.02	0.3	<1	1.27	119.6	0.04	0.18	<0.01	0.06	<0.005	<0.02	<0.01
MR02 0.45	<0.01	<0.02	0.4	<1	1.26	110.9	0.04	0.14	<0.01	0.06	<0.005	<0.02	<0.01
MW1	<0.1	<0.2	<1	<10	0.9	705	0.3	5.0	<0.1	<0.5	<0.05	<0.2	<0.1
MW2	<0.1	<0.2	3	<10	1.0	602	0.5	1.1	<0.1	0.8	<0.05	<0.2	<0.1
BG	<0.01	<0.02	0.3	<1	1.00	68.8	0.03	0.08	<0.01	0.09	<0.005	<0.02	<0.01
TP	0.1	<0.2	3	<10	21.7	511	<0.1	0.7	<0.1	93.3	<0.05	<0.2	<0.1
Seep Ditch	<0.1	<0.2	<1	<10	20.0	1662	<0.1	<0.5	<0.1	6.3	<0.05	<0.2	<0.1
Seep Pipe	<0.1	<0.2	2	<10	20.6	2315	0.1	<0.5	<0.1	2.6	<0.05	<0.2	<0.1

	Sn ICP-MS DIRECT ppb	Sb ICP-MS DIRECT ppb	Te ICP-MS DIRECT ppb	Cs ICP-MS DIRECT ppb	Ba ICP-MS DIRECT ppb	La ICP-MS DIRECT ppb	Ce ICP-MS DIRECT ppb	Pr ICP-MS DIRECT ppb	Nd ICP-MS DIRECT ppb	Sm ICP-MS DIRECT ppb	Eu ICP-MS DIRECT ppb	Tb ICP-MS DIRECT ppb	Gd ICP-MS DIRECT ppb
D.L.	0.01	0.01	0.02	0.01	0.2	0.01	0.01	0.005	0.005	0.005	0.005	0.005	0.005
D.L.	0.1	0.1	0.2	0.1	2	0.1	0.1	0.05	0.05	0.05	0.05	0.05	0.05
DP02-0 0.45	<0.1	<0.1	<0.2	<0.1	175	<0.1	<0.1	<0.05	0.06	<0.05	<0.05	<0.05	<0.05
DP02-20 0.45	<0.1	<0.1	<0.2	<0.1	202	<0.1	<0.1	<0.05	0.07	<0.05	<0.05	<0.05	<0.05
DP02-40b 0.45	<0.1	<0.1	<0.2	<0.1	282	<0.1	<0.1	<0.05	0.07	<0.05	<0.05	<0.05	<0.05
DP02-60 0.45	<0.1	<0.1	<0.2	<0.1	201	0.2	0.4	0.05	0.23	<0.05	<0.05	<0.05	0.05
DP02-80 0.45	<0.1	<0.1	<0.2	<0.1	190	<0.1	0.1	<0.05	0.09	<0.05	<0.05	<0.05	<0.05
DP02-100 0.45	<0.1	<0.1	<0.2	<0.1	246	<0.1	0.2	<0.05	0.17	<0.05	<0.05	<0.05	0.05
DP04-0 0.45	<0.1	<0.1	<0.2	<0.1	90	<0.1	<0.1	<0.05	<0.05	<0.05	<0.05	<0.05	<0.05
DP04-20 0.45	<0.1	<0.1	<0.2	<0.1	153	<0.1	<0.1	<0.05	<0.05	<0.05	<0.05	<0.05	<0.05
DP04-40 0.45	<0.1	<0.1	<0.2	<0.1	154	0.1	0.3	<0.05	0.11	<0.05	<0.05	<0.05	<0.05
DP04-80 0.45	0.03	<0.01	<0.02	<0.01	138.2	0.06	0.12	0.016	0.071	0.016	<0.005	<0.005	0.014
DP04-100 0.45	<0.01	<0.01	<0.02	<0.01	144.8	0.19	0.36	0.046	0.208	0.045	0.009	0.007	0.052
DP04-140 0.45	<0.01	0.02	<0.02	<0.01	109.6	0.10	0.23	0.029	0.133	0.028	0.005	<0.005	0.033
DP10-0 0.45	<0.1	<0.1	<0.2	<0.1	111	<0.1	<0.1	<0.05	<0.05	<0.05	<0.05	<0.05	<0.05
DP10-20 0.45	<0.1	<0.1	<0.2	<0.1	119	<0.1	<0.1	<0.05	<0.05	<0.05	<0.05	<0.05	<0.05
DP10-60 0.45	<0.1	<0.1	<0.2	<0.1	252	<0.1	<0.1	<0.05	<0.05	<0.05	<0.05	<0.05	<0.05
DP10-80 0.45	<0.1	<0.1	<0.2	<0.1	209	<0.1	<0.1	<0.05	<0.05	<0.05	<0.05	<0.05	<0.05
DP10-100 0.45	<0.1	<0.1	<0.2	<0.1	265	<0.1	<0.1	<0.05	<0.05	<0.05	<0.05	<0.05	<0.05
DP15-0 0.45	<0.1	<0.1	<0.2	<0.1	67	<0.1	<0.1	<0.05	<0.05	<0.05	<0.05	<0.05	<0.05
DP15-20 0.45	<0.1	<0.1	<0.2	<0.1	144	<0.1	<0.1	<0.05	<0.05	<0.05	<0.05	<0.05	<0.05
DP15-40 0.45	<0.1	<0.1	<0.2	<0.1	143	<0.1	<0.1	<0.05	<0.05	<0.05	<0.05	<0.05	<0.05
DP15-60 0.45	<0.1	<0.1	<0.2	<0.1	130	0.1	0.2	<0.05	0.11	<0.05	<0.05	<0.05	<0.05
DP15-80 0.45	<0.1	<0.1	<0.2	<0.1	145	0.2	0.4	<0.05	0.18	<0.05	<0.05	<0.05	<0.05
DP15-90 0.45	<0.1	<0.1	<0.2	<0.1	122	0.3	0.5	0.06	0.27	<0.05	<0.05	<0.05	0.07
DP17-0 0.45	<0.1	<0.1	<0.2	<0.1	93	<0.1	<0.1	<0.05	<0.05	<0.05	<0.05	<0.05	<0.05
DP17-20 0.45	<0.1	<0.1	<0.2	<0.1	179	<0.1	<0.1	<0.05	<0.05	<0.05	<0.05	<0.05	<0.05
DP17-40 0.45	<0.1	<0.1	<0.2	<0.1	274	<0.1	0.1	<0.05	0.08	<0.05	<0.05	<0.05	<0.05
DP17-80 0.45	<0.1	<0.1	<0.2	<0.1	305	0.1	0.2	<0.05	0.13	<0.05	<0.05	<0.05	<0.05
DP17-95 0.45	<0.1	<0.1	<0.2	<0.1	365	0.2	0.3	<0.05	0.19	<0.05	<0.05	<0.05	<0.05
DP17-W 0.45	0.04	0.02	<0.02	<0.01	158.4	0.03	0.05	0.008	0.040	0.008	<0.005	<0.005	0.012
DP22-0 0.45	<0.1	<0.1	<0.2	<0.1	63	<0.1	<0.1	<0.05	<0.05	<0.05	<0.05	<0.05	<0.05
DP22-20 0.45	<0.1	<0.1	<0.2	<0.1	92	<0.1	<0.1	<0.05	<0.05	<0.05	<0.05	<0.05	<0.05
DP22-40 0.45	<0.1	<0.1	<0.2	<0.1	145	<0.1	0.2	<0.05	0.08	<0.05	<0.05	<0.05	<0.05
DP22-80 0.45	<0.1	<0.1	<0.2	<0.1	174	<0.1	0.1	<0.05	0.06	<0.05	<0.05	<0.05	<0.05
DP24-0 0.45	<0.1	<0.1	<0.2	<0.1	92	<0.1	<0.1	<0.05	<0.05	<0.05	<0.05	<0.05	<0.05
DP24-20 0.45	<0.1	<0.1	<0.2	<0.1	164	<0.1	<0.1	<0.05	<0.05	<0.05	<0.05	<0.05	<0.05
DP24-40 0.45	<0.1	<0.1	<0.2	<0.1	215	<0.1	0.1	<0.05	0.06	<0.05	<0.05	<0.05	<0.05
DP24-60 0.45	<0.1	<0.1	<0.2	<0.1	217	<0.1	0.2	<0.05	0.10	<0.05	<0.05	<0.05	<0.05
DP24-80 0.45	<0.1	<0.1	<0.2	<0.1	214	<0.1	0.2	<0.05	0.08	<0.05	<0.05	<0.05	<0.05
DP24-100 0.45	<0.1	<0.1	<0.2	<0.1	320	<0.1	0.2	<0.05	0.10	<0.05	<0.05	<0.05	<0.05
DP24-W 0.45	<0.1	<0.1	<0.2	<0.1	193	<0.1	0.1	<0.05	0.08	<0.05	<0.05	<0.05	<0.05
DP25-0 0.45	<0.01	0.02	<0.02	<0.01	27.1	0.02	0.03	<0.005	0.024	0.005	<0.005	<0.005	<0.005
DP25-20 0.45	<0.1	<0.1	<0.2	<0.1	138	0.2	0.4	<0.05	0.19	<0.05	<0.05	<0.05	0.05
DP25-40 0.45	0.03	0.03	<0.02	<0.01	182.9	0.14	0.32	0.040	0.173	0.037	0.005	0.006	0.040
DP25-60 0.45	0.01	0.02	<0.02	<0.01	193.9	0.11	0.27	0.033	0.157	0.033	0.006	0.005	0.034
DP25-80 0.45	0.02	0.03	<0.02	<0.01	191.2	0.05	0.11	0.014	0.070	0.016	<0.005	<0.005	0.017
DP25-100 0.45	0.01	0.02	<0.02	<0.01	208.7	0.08	0.19	0.023	0.106	0.024	<0.005	<0.005	0.023
DP25-W 0.45	0.02	0.04	<0.02	<0.01	193.6	0.13	0.30	0.037	0.168	0.039	0.005	0.006	0.040
DP27-0 0.45	<0.1	<0.1	<0.2	<0.1	59	<0.1	<0.1	<0.05	<0.05	<0.05	<0.05	<0.05	<0.05
DP27-20 0.45	<0.1	<0.1	<0.2	<0.1	62	<0.1	<0.1	<0.05	<0.05	<0.05	<0.05	<0.05	<0.05
AR00 0.45	<0.01	0.05	<0.02	<0.01	52.2	0.04	0.07	0.014	0.061	0.016	<0.005	<0.005	0.020
AR04 0.45	<0.01	0.04	<0.02	<0.01	39.8	0.04	0.07	0.012	0.054	0.012	<0.005	<0.005	0.016
MR01 0.45	<0.01	0.02	<0.02	<0.01	28.9	0.02	0.03	<0.005	0.021	<0.005	<0.005	<0.005	0.007
MR02 0.45	<0.01	0.02	<0.02	<0.01	28.1	0.02	0.03	<0.005	0.024	<0.005	<0.005	<0.005	0.006
MW1	<0.1	<0.1	<0.2	<0.1	251	0.3	1.0	0.07	0.34	0.08	<0.05	<0.05	0.06
MW2	<0.1	0	<0.2	<0.1	215	0.2	0.5	0.05	0.25	0.05	<0.05	<0.05	0.07
BG	<0.01	0.02	<0.02	<0.01	18.7	<0.01	0.01	<0.005	0.014	<0.005	<0.005	<0.005	<0.005
TP	<0.1	2	<0.2	<0.1	169	<0.1	<0.1	<0.05	<0.05	<0.05	<0.05	<0.05	<0.05
Seep Ditch	<0.1	<0.1	<0.2	<0.1	168	<0.1	<0.1	<0.05	<0.05	<0.05	<0.05	<0.05	<0.05
Seep Pipe	<0.1	<0.1	<0.2	<0.1	41	<0.1	0.1	<0.05	0.06	<0.05	<0.05	<0.05	<0.05

	Dy ICP-MS DIRECT ppb	Ho ICP-MS DIRECT ppb	Er ICP-MS DIRECT ppb	Tm ICP-MS DIRECT ppb	Yb ICP-MS DIRECT ppb	Lu ICP-MS DIRECT ppb	Hf ICP-MS DIRECT ppb	Ta ICP-MS DIRECT ppb	W ICP-MS DIRECT ppb	Re ICP-MS DIRECT ppb	Tl ICP-MS DIRECT ppb	Pb ICP-MS DIRECT ppb	Bi ICP-MS DIRECT ppb
D.L.	0.005	0.005	0.005	0.005	0.005	0.005	0.01	0.01	0.02	0.005	0.005	0.01	0.02
D.L.	0.05	0.05	0.05	0.05	0.05	0.05	0.1	0.1	0.2	0.05	0.05	0.1	0.2
DP02-0 0.45	<0.05	<0.05	<0.05	<0.05	<0.05	<0.05	<0.1	<0.1	<0.2	<0.05	<0.05	<0.1	<0.2
DP02-20 0.45	<0.05	<0.05	<0.05	<0.05	<0.05	<0.05	<0.1	<0.1	<0.2	<0.05	<0.05	<0.1	<0.2
DP02-40b 0.45	<0.05	<0.05	<0.05	<0.05	<0.05	<0.05	<0.1	<0.1	0.3	<0.05	<0.05	<0.1	<0.2
DP02-60 0.45	0.06	<0.05	<0.05	<0.05	<0.05	<0.05	<0.1	<0.1	<0.2	<0.05	<0.05	0.1	<0.2
DP02-80 0.45	<0.05	<0.05	<0.05	<0.05	<0.05	<0.05	<0.1	<0.1	<0.2	<0.05	<0.05	<0.1	<0.2
DP02-100 0.45	0.07	<0.05	0.05	<0.05	0.06	<0.05	<0.1	<0.1	<0.2	<0.05	<0.05	<0.1	<0.2
DP04-0 0.45	<0.05	<0.05	<0.05	<0.05	<0.05	<0.05	<0.1	<0.1	<0.2	<0.05	<0.05	<0.1	<0.2
DP04-20 0.45	<0.05	<0.05	<0.05	<0.05	<0.05	<0.05	<0.1	<0.1	<0.2	<0.05	<0.05	0.1	<0.2
DP04-40 0.45	<0.05	<0.05	<0.05	<0.05	<0.05	<0.05	<0.1	<0.1	<0.2	<0.05	<0.05	<0.1	<0.2
DP04-80 0.45	0.015	<0.005	0.009	<0.005	0.009	<0.005	0.01	<0.01	<0.02	<0.005	<0.005	0.01	<0.02
DP04-100 0.45	0.042	0.010	0.030	<0.005	0.025	<0.005	0.02	<0.01	0.04	<0.005	<0.005	0.02	<0.02
DP04-140 0.45	0.030	0.007	0.019	<0.005	0.019	<0.005	0.02	<0.01	<0.02	<0.005	<0.005	0.03	<0.02
DP10-0 0.45	<0.05	<0.05	<0.05	<0.05	<0.05	<0.05	<0.1	<0.1	<0.2	<0.05	<0.05	<0.1	<0.2
DP10-20 0.45	<0.05	<0.05	<0.05	<0.05	<0.05	<0.05	<0.1	<0.1	<0.2	<0.05	<0.05	<0.1	<0.2
DP10-60 0.45	<0.05	<0.05	<0.05	<0.05	<0.05	<0.05	<0.1	<0.1	<0.2	<0.05	<0.05	<0.1	<0.2
DP10-80 0.45	<0.05	<0.05	<0.05	<0.05	<0.05	<0.05	<0.1	<0.1	<0.2	<0.05	<0.05	<0.1	<0.2
DP10-100 0.45	<0.05	<0.05	<0.05	<0.05	<0.05	<0.05	<0.1	<0.1	<0.2	<0.05	<0.05	<0.1	<0.2
DP15-0 0.45	<0.05	<0.05	<0.05	<0.05	<0.05	<0.05	<0.1	<0.1	<0.2	<0.05	<0.05	<0.1	<0.2
DP15-20 0.45	<0.05	<0.05	<0.05	<0.05	<0.05	<0.05	<0.1	<0.1	<0.2	<0.05	<0.05	<0.1	<0.2
DP15-40 0.45	<0.05	<0.05	<0.05	<0.05	<0.05	<0.05	<0.1	<0.1	<0.2	<0.05	<0.05	<0.1	<0.2
DP15-60 0.45	<0.05	<0.05	<0.05	<0.05	<0.05	<0.05	<0.1	<0.1	<0.2	<0.05	<0.05	<0.1	<0.2
DP15-80 0.45	<0.05	<0.05	<0.05	<0.05	<0.05	<0.05	<0.1	<0.1	<0.2	<0.05	<0.05	<0.1	<0.2
DP15-90 0.45	0.05	<0.05	<0.05	<0.05	<0.05	<0.05	<0.1	<0.1	<0.2	<0.05	<0.05	<0.1	<0.2
DP17-0 0.45	<0.05	<0.05	<0.05	<0.05	<0.05	<0.05	<0.1	<0.1	0.2	<0.05	<0.05	<0.1	<0.2
DP17-20 0.45	<0.05	<0.05	<0.05	<0.05	<0.05	<0.05	<0.1	<0.1	<0.2	<0.05	<0.05	0.1	<0.2
DP17-40 0.45	<0.05	<0.05	<0.05	<0.05	<0.05	<0.05	<0.1	<0.1	<0.2	<0.05	<0.05	<0.1	<0.2
DP17-80 0.45	<0.05	<0.05	<0.05	<0.05	<0.05	<0.05	<0.1	<0.1	<0.2	<0.05	<0.05	<0.1	<0.2
DP17-95 0.45	<0.05	<0.05	<0.05	<0.05	<0.05	<0.05	<0.1	<0.1	<0.2	<0.05	<0.05	<0.1	<0.2
DP17-W 0.45	0.013	<0.005	0.009	<0.005	0.009	<0.005	0.02	<0.01	0.03	<0.005	<0.005	0.01	<0.02
DP22-0 0.45	<0.05	<0.05	<0.05	<0.05	<0.05	<0.05	<0.1	<0.1	<0.2	<0.05	<0.05	<0.1	<0.2
DP22-20 0.45	<0.05	<0.05	<0.05	<0.05	<0.05	<0.05	<0.1	<0.1	<0.2	<0.05	<0.05	<0.1	<0.2
DP22-40 0.45	<0.05	<0.05	<0.05	<0.05	<0.05	<0.05	<0.1	<0.1	<0.2	<0.05	<0.05	<0.1	<0.2
DP22-80 0.45	<0.05	<0.05	<0.05	<0.05	<0.05	<0.05	<0.1	<0.1	0.2	<0.05	<0.05	<0.1	<0.2
DP24-0 0.45	<0.05	<0.05	<0.05	<0.05	<0.05	<0.05	<0.1	<0.1	<0.2	<0.05	<0.05	<0.1	<0.2
DP24-20 0.45	<0.05	<0.05	<0.05	<0.05	<0.05	<0.05	<0.1	<0.1	0.3	<0.05	<0.05	<0.1	<0.2
DP24-40 0.45	<0.05	<0.05	<0.05	<0.05	<0.05	<0.05	<0.1	<0.1	<0.2	<0.05	<0.05	<0.1	<0.2
DP24-60 0.45	<0.05	<0.05	<0.05	<0.05	<0.05	<0.05	<0.1	<0.1	<0.2	<0.05	<0.05	<0.1	<0.2
DP24-80 0.45	<0.05	<0.05	<0.05	<0.05	<0.05	<0.05	<0.1	<0.1	<0.2	<0.05	<0.05	<0.1	<0.2
DP24-100 0.45	<0.05	<0.05	<0.05	<0.05	<0.05	<0.05	<0.1	<0.1	<0.2	<0.05	<0.05	<0.1	<0.2
DP24-W 0.45	<0.05	<0.05	<0.05	<0.05	<0.05	<0.05	<0.1	<0.1	<0.2	<0.05	<0.05	<0.1	<0.2
DP25-0 0.45	0.006	<0.005	<0.005	<0.005	<0.005	<0.005	<0.01	<0.01	<0.02	<0.005	<0.005	0.01	<0.02
DP25-20 0.45	<0.05	<0.05	<0.05	<0.05	<0.05	<0.05	<0.1	<0.1	<0.2	<0.05	<0.05	0.1	<0.2
DP25-40 0.45	0.034	0.007	0.020	<0.005	0.021	<0.005	0.02	<0.01	<0.02	<0.005	<0.005	0.05	<0.02
DP25-60 0.45	0.031	0.007	0.019	<0.005	0.018	<0.005	0.02	<0.01	<0.02	<0.005	<0.005	0.03	<0.02
DP25-80 0.45	0.015	<0.005	0.011	<0.005	0.011	<0.005	<0.01	<0.01	0.02	<0.005	<0.005	0.03	<0.02
DP25-100 0.45	0.021	<0.005	0.012	<0.005	0.012	<0.005	0.01	<0.01	<0.02	<0.005	<0.005	0.02	0.08
DP25-W 0.45	0.032	0.007	0.022	<0.005	0.021	<0.005	0.01	<0.01	0.10	<0.005	<0.005	0.03	<0.02
DP27-0 0.45	<0.05	<0.05	<0.05	<0.05	<0.05	<0.05	<0.1	<0.1	<0.2	<0.05	<0.05	<0.1	<0.2
DP27-20 0.45	<0.05	<0.05	<0.05	<0.05	<0.05	<0.05	<0.1	<0.1	<0.2	<0.05	<0.05	<0.1	<0.2
AR00 0.45	0.017	<0.005	0.009	<0.005	0.009	<0.005	<0.01	<0.01	<0.02	<0.005	<0.005	0.04	<0.02
AR04 0.45	0.014	<0.005	0.008	<0.005	0.007	<0.005	<0.01	<0.01	<0.02	<0.005	<0.005	0.06	<0.02
MR01 0.45	0.006	<0.005	<0.005	<0.005	<0.005	<0.005	<0.01	<0.01	<0.02	<0.005	<0.005	0.02	<0.02
MR02 0.45	0.006	<0.005	<0.005	<0.005	<0.005	<0.005	<0.01	<0.01	<0.02	<0.005	<0.005	0.02	<0.02
MW1	0.05	<0.05	<0.05	<0.05	<0.05	<0.05	0.1	<0.1	<0.2	<0.05	<0.05	<0.1	<0.2
MW2	0.05	<0.05	<0.05	<0.05	<0.05	<0.05	<0.1	<0.1	<0.2	<0.05	<0.05	<0.1	<0.2
BG	<0.005	<0.005	<0.005	<0.005	<0.005	<0.005	<0.01	<0.01	<0.02	<0.005	<0.005	<0.01	<0.02
TP	<0.05	<0.05	<0.05	<0.05	<0.05	<0.05	<0.1	<0.1	7.0	0.07	<0.05	<0.1	<0.2
Seep Ditch	<0.05	<0.05	<0.05	<0.05	<0.05	<0.05	<0.1	<0.1	<0.2	<0.05	<0.05	<0.1	<0.2
Seep Pipe	<0.05	<0.05	<0.05	<0.05	<0.05	<0.05	<0.1	<0.1	<0.2	0.05	<0.05	<0.1	<0.2

	Th ICP-MS DIRECT ppb	U ICP-MS DIRECT ppb
D.L.	0.02	0.005
D.L.	0.2	0.05
DP02-0 0.45	<0.2	<0.05
DP02-20 0.45	<0.2	<0.05
DP02-40b 0.45	<0.2	<0.05
DP02-60 0.45	<0.2	0.10
DP02-80 0.45	<0.2	0.09
DP02-100 0.45	<0.2	0.19
DP04-0 0.45	<0.2	0.13
DP04-20 0.45	<0.2	<0.05
DP04-40 0.45	<0.2	<0.05
DP04-80 0.45	<0.02	0.011
DP04-100 0.45	<0.02	0.014
DP04-140 0.45	<0.02	0.019
DP10-0 0.45	<0.2	0.20
DP10-20 0.45	<0.2	<0.05
DP10-60 0.45	<0.2	<0.05
DP10-80 0.45	<0.2	<0.05
DP10-100 0.45	<0.2	<0.05
DP15-0 0.45	<0.2	0.05
DP15-20 0.45	<0.2	<0.05
DP15-40 0.45	<0.2	0.13
DP15-60 0.45	<0.2	0.23
DP15-80 0.45	<0.2	0.38
DP15-90 0.45	<0.2	0.16
DP17-0 0.45	<0.2	0.10
DP17-20 0.45	<0.2	<0.05
DP17-40 0.45	<0.2	0.09
DP17-80 0.45	<0.2	<0.05
DP17-95 0.45	<0.2	<0.05
DP17-W 0.45	<0.02	0.028
DP22-0 0.45	<0.2	<0.05
DP22-20 0.45	<0.2	<0.05
DP22-40 0.45	<0.2	<0.05
DP22-80 0.45	<0.2	<0.05
DP24-0 0.45	<0.2	0.07
DP24-20 0.45	<0.2	0.06
DP24-40 0.45	<0.2	<0.05
DP24-60 0.45	<0.2	<0.05
DP24-80 0.45	<0.2	<0.05
DP24-100 0.45	<0.2	<0.05
DP24-W 0.45	<0.2	<0.05
DP25-0 0.45	<0.02	0.023
DP25-20 0.45	<0.2	<0.05
DP25-40 0.45	0.03	0.015
DP25-60 0.45	0.03	0.010
DP25-80 0.45	<0.02	0.007

2.2 ICP-ES

Sample	Br ICP-ES DIRECT ppm 0.05	Ca ICP-ES DIRECT ppm 0.02	Cl ICP-ES DIRECT ppm 0.1	Fe ICP-ES DIRECT ppm 0.005	K ICP-ES DIRECT ppm 0.05	Mg ICP-ES DIRECT ppm 0.005	Na ICP-ES DIRECT ppm 0.05	P ICP-ES DIRECT ppm 0.05	S ICP-ES DIRECT ppm 0.05	Sc ICP-ES DIRECT ppm 0.001	Si ICP-ES DIRECT ppm 0.02
DP02-0 0.45	0.24	121.84	103.4	4.724	2.82	21.795	125.91	< 0.05	3.11	< 0.001	4.67
DP02-20 0.45	0.24	130.78	104.8	10.925	2.59	22.366	125.00	0.05	6.21	< 0.001	4.98
DP02-40b 0.45	0.26	127.42	107.7	23.357	2.58	22.311	128.68	0.10	3.71	< 0.001	5.09
DP02-60 0.45	0.24	123.37	110.7	3.923	2.85	18.989	128.24	< 0.05	2.24	< 0.001	4.65
DP02-80 0.45	0.28	133.29	127.2	2.981	2.93	21.776	133.26	0.10	6.23	< 0.001	4.73
DP02-100 0.45	0.22	102.29	92.1	4.206	3.17	16.576	131.52	< 0.05	2.27	< 0.001	4.83
DP04-0 0.45	0.30	255.52	218.5	0.185	3.19	57.056	200.52	< 0.05	196.05	< 0.001	4.02
DP04-20 0.45	0.30	253.23	201.2	5.069	2.26	53.594	164.74	0.08	161.08	< 0.001	4.09
DP04-40 0.45	0.28	156.93	87.8	12.630	1.52	29.579	47.25	0.21	26.40	< 0.001	4.64
DP04-80 0.45	0.18	118.52	43.6	15.613	1.13	19.307	18.12	0.11	2.95	< 0.001	4.05
DP04-100 0.45	0.21	144.56	58.2	13.333	1.31	24.028	30.88	0.11	14.21	< 0.001	4.40
DP04-140 0.45	0.11	104.48	26.0	11.127	1.10	17.189	12.10	< 0.05	0.89	< 0.001	4.18
DP10-0 0.45	0.17	96.54	127.6	0.379	0.89	17.617	133.85	< 0.05	16.17	< 0.001	3.51
DP10-20 0.45	0.21	105.63	128.9	6.604	2.05	21.442	128.31	0.22	7.34	< 0.001	4.01
DP10-60 0.45	0.24	193.63	66.3	5.433	1.44	22.859	10.80	< 0.05	0.76	< 0.001	3.47
DP10-80 0.45	0.24	186.40	67.9	1.845	1.59	22.066	27.98	< 0.05	0.75	< 0.001	3.48
DP10-100 0.45	0.25	193.00	66.0	5.251	1.54	22.751	12.10	< 0.05	0.76	< 0.001	3.50
DP15-0 0.45	0.26	113.41	125.5	0.008	3.67	25.686	136.03	< 0.05	36.68	< 0.001	4.05
DP15-20 0.45	0.26	141.39	128.6	12.887	2.62	25.938	135.63	0.16	29.29	< 0.001	4.66
DP15-40 0.45	0.26	149.40	128.4	12.488	2.56	27.372	135.61	0.08	27.37	< 0.001	4.90
DP15-60 0.45	0.29	154.80	130.7	0.198	0.95	24.362	133.91	< 0.05	28.98	< 0.001	4.33
DP15-80 0.45	0.28	150.75	131.5	0.073	1.39	24.315	133.91	< 0.05	23.01	< 0.001	4.31
DP15-90 0.45	0.26	149.08	130.5	0.436	1.57	25.608	137.39	< 0.05	33.10	< 0.001	4.65
DP17-0 0.45	0.27	206.67	185.0	0.127	3.40	46.532	159.50	< 0.05	128.06	< 0.001	4.05
DP17-20 0.45	0.29	197.88	173.9	8.153	1.90	40.534	148.13	0.25	99.04	< 0.001	4.36
DP17-40 0.45	0.31	190.55	175.1	15.608	1.60	38.073	141.44	0.25	85.78	< 0.001	4.58
DP17-80 0.45	0.35	185.27	142.3	21.478	1.42	33.803	83.72	0.14	73.66	< 0.001	4.37
DP17-95 0.45	0.33	181.86	138.2	17.917	1.60	34.737	83.10	0.13	68.99	< 0.001	4.58
DP17-W 0.45	0.08	74.50	18.5	8.416	1.47	17.049	20.80	0.07	8.87	< 0.001	3.93
DP22-0 0.45	0.22	103.59	126.0	0.464	2.99	24.597	128.70	< 0.05	23.61	< 0.001	4.15
DP22-20 0.45	0.23	114.04	133.3	0.789	2.56	25.778	134.63	0.10	23.46	< 0.001	4.41
DP22-40 0.45	0.26	125.65	136.7	4.742	2.53	24.495	125.91	0.18	9.36	< 0.001	4.83
DP22-80 0.45	0.28	133.03	124.3	8.806	1.76	23.610	128.19	0.13	9.31	< 0.001	4.93
DP24-0 0.45	0.24	171.19	182.6	0.154	2.19	37.605	141.16	< 0.05	83.66	< 0.001	4.04
DP24-20 0.45	0.25	184.93	188.6	8.296	0.86	38.613	139.89	0.07	82.26	< 0.001	4.34
DP24-40 0.45	0.32	161.32	158.9	12.433	1.02	32.789	127.86	0.39	21.69	< 0.001	5.18
DP24-60 0.45	0.34	152.55	128.8	30.706	0.87	25.892	128.09	0.34	20.63	< 0.001	6.10

Sample	Br	Ca	Cl	Fe	K	Mg	Na	P	S	Sc	Si
	ICP-ES DIRECT	ICP-ES DIRECT	ICP-ES DIRECT	ICP-ES DIRECT	ICP-ES DIRECT	ICP-ES DIRECT	ICP-ES DIRECT	ICP-ES DIRECT	ICP-ES DIRECT	ICP-ES DIRECT	ICP-ES DIRECT
	ppm	ppm	ppm	ppm	ppm	ppm	ppm	ppm	ppm	ppm	ppm
	0.05	0.02	0.1	0.005	0.05	0.005	0.05	0.05	0.05	0.001	0.02
DP24-80 0.45	0.36	159.30	152.6	22.807	0.59	29.794	144.43	0.42	16.76	< 0.001	5.99
DP24-100 0.45	0.37	191.14	136.9	24.316	0.35	24.753	140.35	0.19	42.47	< 0.001	5.46
DP24-W 0.45	0.33	146.10	124.6	14.797	0.37	21.192	96.66	0.15	21.66	< 0.001	5.48
DP25-0 0.45	< 0.05	35.77	9.8	0.357	1.44	10.393	14.06	< 0.05	3.10	< 0.001	4.37
DP25-20 0.45	0.12	62.74	86.1	1.160	2.53	13.628	41.21	0.06	35.21	< 0.001	6.84
DP25-40 0.45	0.23	89.99	108.7	13.461	< 0.05	14.941	38.69	0.30	0.91	< 0.001	10.25
DP25-60 0.45	0.25	96.62	105.1	12.030	< 0.05	14.870	40.78	1.34	0.81	< 0.001	9.94
DP25-80 0.45	0.18	97.61	80.9	8.698	0.36	15.436	32.59	0.17	4.66	< 0.001	9.42
DP25-100 0.45	0.25	107.49	94.4	8.762	0.19	16.809	36.88	0.19	0.75	< 0.001	10.77
DP25-W 0.45	0.22	101.37	133.4	10.182	0.14	18.708	77.42	0.31	27.42	< 0.001	7.75
DP27-0 0.45	0.22	117.72	138.6	0.016	3.37	30.079	137.43	< 0.05	52.98	< 0.001	4.26
DP27-20 0.45	0.22	117.38	138.6	0.387	3.26	30.625	133.58	< 0.05	49.51	< 0.001	4.59
AR00 0.45	< 0.05	36.22	2.3	0.125	1.37	10.603	12.68	< 0.05	10.81	< 0.001	2.00
AR04 0.45	< 0.05	31.60	7.2	0.209	1.12	9.009	11.89	< 0.05	6.82	< 0.001	3.00
MR01 0.45	< 0.05	40.73	4.3	0.385	1.16	11.122	12.87	< 0.05	2.90	< 0.001	4.26
MR02 0.45	< 0.05	37.63	3.3	0.402	1.15	10.923	11.84	< 0.05	2.09	< 0.001	4.56
MR1023 0.45	< 0.05	32.90	3.8	0.346	1.29	9.657	11.38	< 0.05	1.69	< 0.001	4.00
MW1	0.46	307.14	263.3	0.494	0.35	51.066	161.43	< 0.05	100.36	< 0.001	3.79
MW2	0.27	167.96	99.5	22.456	2.15	29.795	95.37	< 0.05	64.52	< 0.001	3.92
BG	< 0.05	36.85	1.5	0.098	1.08	13.521	3.69	< 0.05	0.90	< 0.001	4.45
TP	0.30	16.95	137.6	< 0.005	19.25	10.216	348.61	< 0.05	83.51	< 0.001	2.14
Seep Ditch	0.30	110.44	137.7	1.721	18.45	50.470	284.11	< 0.05	168.04	< 0.001	5.48
Seep Pipe	0.29	218.30	128.1	42.712	21.79	57.810	336.04	< 0.05	300.92	< 0.001	7.49

2.3 Anions

	F Dionex ICS-2100 ppm	Cl Dionex ICS-2100 ppm	SO4 Dionex ICS-2100 ppm	Br Dionex ICS-2100 ppm	NO3 Dionex ICS-2100 ppm	PO4 Dionex ICS-2100 ppm
D.L.	0.01	0.01	0.02	0.02	0.02	0.02
DP02-0	0.30	103.50	5.06	0.03	0.01	0.01
DP02-20	0.27	105.69	13.56	0.02	0.01	0.01
DP02-40b	0.27	108.80	6.64	0.03	0.01	0.01
DP02-60	0.26	111.24	2.60	0.01	0.01	0.01
DP02-80	0.13	128.64	13.25	0.01	0.01	0.01
DP02-100	0.37	92.92	2.84	0.01	0.01	0.01
DP04-0	0.11	220.03	554.12	0.01	0.01	0.01
DP04-20	0.11	202.48	454.77	0.01	0.01	0.01
DP04-40	0.06	87.53	69.11	0.01	0.01	0.01
DP04-80	0.07	46.34	6.19	0.01	0.01	0.01
DP04-100	0.06	61.23	40.31	0.01	0.01	0.01
DP04-140	0.06	29.00	0.89	0.01	0.01	0.01
DP10-0	0.13	132.68	42.92	0.01	0.01	0.01
DP10-20	0.15	133.47	18.13	0.01	0.01	0.01
DP10-60	0.10	67.03	0.08	0.01	0.24	0.01
DP10-80	0.09	68.39	0.01	0.01	0.21	0.01
DP10-100	0.09	67.30	0.13	0.01	0.03	0.01
DP15-0	0.18	126.11	104.31	0.01	0.01	0.01
DP15-20	0.16	129.52	85.18	0.01	0.01	0.01
DP15-40	0.16	129.91	75.92	0.01	0.01	0.01
DP15-60	0.13	134.24	80.38	0.01	0.01	0.01
DP15-80	0.14	134.47	63.53	0.01	0.01	0.01
DP15-90	0.13	131.36	93.02	0.01	0.01	0.01
DP17-0	0.11	186.01	367.63	0.01	0.01	0.01
DP17-20	0.09	174.81	284.74	0.01	0.01	0.01
DP17-40	0.10	174.02	248.64	0.01	0.01	0.01
DP17-80	0.10	142.45	211.62	0.01	0.01	0.01
DP17-95	0.11	137.25	193.09	0.01	0.01	0.01
DP17-W	0.18	21.23	22.98	0.01	0.01	0.01
DP22-0	0.15	122.92	66.01	0.01	0.01	0.01
DP22-20	0.13	131.66	66.38	0.01	0.01	0.01
DP22-40	0.13	138.41	23.05	0.01	0.01	0.01
DP22-80	0.09	123.45	22.47	0.01	0.08	0.01
DP24-0	0.11	180.65	242.17	0.01	0.01	0.01
DP24-20	0.11	192.29	235.55	0.01	0.01	0.01
DP24-40	0.08	163.35	55.66	0.01	0.01	0.01
DP24-60	0.15	130.65	56.22	0.01	0.15	0.01
DP24-80	0.08	155.86	44.12	0.01	0.00	0.01
DP24-100	0.08	138.03	118.96	0.01	0.12	0.01
DP24-W	0.07	124.45	62.33	0.01	0.01	0.01
DP25-0	0.09	5.79	5.30	0.01	0.01	0.01
DP25-20	0.05	82.34	93.33	0.01	0.01	0.01
DP25-40	0.07	107.84	0.69	0.01	0.01	0.09
DP25-60	0.07	104.66	0.25	0.01	0.01	0.20
DP25-80	0.09	81.77	12.21	0.01	0.01	0.08
DP25-100	0.08	94.40	0.14	0.01	0.01	0.01
DP25-W	0.06	134.59	77.75	0.01	0.01	0.08
DP27-0	0.10	141.76	151.79	0.01	0.01	0.01
DP27-20	0.09	138.62	143.01	0.01	0.01	0.01
AR00	0.08	2.47	31.18	0.01	0.01	0.01
AR04	0.08	7.22	19.09	0.01	0.01	0.01
MR01	0.10	4.40	6.96	0.01	0.01	0.01
MR02	0.11	3.39	4.79	0.01	0.01	0.01
BG	0.07	1.54	1.61	0.01	0.01	0.01
TP	3.79	140.50	238.99	0.01	0.19	0.01
MW1	0.09	261.78	282.27	0.07	0.01	0.01
MW2	0.09	99.55	184.39	0.01	0.01	0.01
Seep Ditch	1.80	144.69	490.13	0.01	0.02	0.01
Seep Pipe	1.57	131.64	843.92	0.01	0.01	0.01

2.4 Other Geochemical Parameters

Sample	Alkalinity	Conductivity	pH	pe	DOC	T (°C)	DO	Fe2+	Fe3+	S2-
	PC-Titrate	meter	meter	ORP Calc.	SHIMADZU					
	as CaCO3	DIRECT	DIRECT		DIRECT			HACH		HACH
	ppm	uS/cm	unit		ppm		ppm	ppm	ppm	ppb
DP02-0 0.45	505	1187	7.54	13.1	32	6.4	1.46	0.60	1.28	10
DP02-20 0.45	514	1234	7.45	11.4	32	6.3	1.21	1.85	-1.42	0
DP02-40b 0.45	525	1257	7.43	10.8	31	6.4	0.98	2.50	1.07	7
DP02-60 0.45	490	1191	7.23	10.9	35	6.3	0.3	2.60	-1.32	51
DP02-80 0.45	505	1261	7.27	11.1	35	6.3	1.88	2.70	-1.37	61
DP02-100 0.45	470	1099	7.33	10.8	33	6.1	0.43	2.10	-0.45	356
DP04-0 0.45	387	2267	7.8	14.5	34	5.2	3.57	0.11	1.39	0.6
DP04-20 0.45	423	2079	7.34	11.3	37	6.4	1.28	1.85	-1.32	122
DP04-40 0.45	424	1134	6.67	11.6	23	6.8	1.33	1.21	2.59	103
DP04-80 0.45	350	767	6.78	11.4	13	6.3	1.65	1.71	-1.36	78
DP04-100 0.45	400	963	6.78	11.6	27	7.1	1.5	1.98	-0.07	59
DP04-140 0.45	320	689	6.62	12.0	25	6.4	0.53	0.26	1.01	46
DP10-0 0.45	365	1159	7.48	13.0	25	4.8	3.8	0.14	1.61	3
DP10-20 0.45	416	1216	7.47	10.6	20	4.5	0.35	1.40	2.78	28
DP10-60 0.45	505	1092	6.88	11.5	19	5.7	1.91	0.83	2.07	24
DP10-80 0.45	514	1101	6.97	12.1	20	6	1.27	0.58	1.12	12
DP10-100 0.45	496	1078	6.92	11.9	19	6.3	1.75	1.46	3.33	32
DP15-0 0.45	393	1238	7.85	13.5	25	6.1	4.18	0.00	0.40	0
DP15-20 0.45	472	1271	7.47	11.3	29	5.8	2.9	1.25	-0.99	15
DP15-40 0.45	503	1374	7.54	10.3	35	6.4	1.7	1.63	1.57	12
DP15-60 0.45	492	1362	7.55	13.5	33	5.6	4.79	0.38	0.04	0
DP15-80 0.45	500	1352	7.29	11.3	32	7.7	0.4	0.07	0.62	3
DP15-90 0.45	474	1359	7.3	12.5	33	7.2	0.26	0.40	0.80	0
DP17-0 0.45	398	1812	7.76	13.0	38	6.8	3.2	0.01	1.22	2
DP17-20 0.45	425	1713	7.26	10.6	33	7	0.42	1.60	-1.36	53
DP17-40 0.45	421	1672	7.14	10.4	33	7	0.69	2.05	-0.08	26
DP17-80 0.45	359	1455	6.84	11.2	27	7.2	1.2	1.53	-1.27	30
DP17-95 0.45	367	1383	6.8	11.3	33	7	1.23	1.49	2.14	49
DP17-W 0.45	249	582	6.43	13.0	19	5.6	0.24	2.47	-1.61	9
DP22-0 0.45	380	1223	7.63	13.9	26	2.8	1.97	0.28	3.32	19
DP22-20 0.45	430	1273	7.3	10.9	29	4.6	0.26	0.54	0.05	450
DP22-40 0.45	459	1301	7.3	11.1	30	4.4	3.63	2.23	-1.30	59
DP22-80 0.45	493	1325	7.05	10.6	33	5.3	0.86	1.04	0.90	61
DP24-0 0.45	372	1666	7.48	13.0	33	4.8	3.6	0.00	1.36	0
DP24-20 0.45	388	1743	7	10.8	38	5.7	0.59	1.99	-0.74	150
DP24-40 0.45	514	1544	6.84	10.8	42	6	0.93	1.03	-1.03	124
DP24-60 0.45	515	1490	6.85	10.6	31	5.7	1	1.76	0.80	50
DP24-80 0.45	548	1579	6.89	10.9	35	6.1	1.94	0.28	3.25	44
DP24-100 0.45	538	1657	6.84	10.9	36	4.6	1.36	2.52	-1.91	61

Sample	Alkalinity	Conductivity	pH	pe	DOC	T (°C)	DO	Fe2+	Fe3+	S2-
	PC-Titrate as CaCO3	meter DIRECT	meter DIRECT	ORP Calc.	SHIMADZU DIRECT			HACH		HACH
	ppm	uS/cm	unit		ppm		ppm	ppm	ppm	ppb
DP24-W 0.45	432	1327	6.67		29	5.1	1.25	1.24	0.86	8
DP25-0 0.45	140	284	7.3	15.5	23	3		0.04	0.69	4
DP25-20 0.45	82	647	6.2	15.7	17	5	2.56	0.60	0.13	3
DP25-40 0.45	221	765	6.44	12.7	18	6.2	3.53	1.65	4.82	86
DP25-60 0.45	241	809	6.43	11.3	18	7.7	0.61	1.60	1.08	72
DP25-80 0.45	249	735	6.49	11.7	17	7.8	2.1	1.40	8.10	115
DP25-100 0.45	277	836	6.31	11.7	20	8.2	0.73	2.47	5.98	68
DP25-W 0.45	226	1043	6.36	12.1	21	6.8	0.73	2.26	6.68	38
DP27-0 0.45	348	1362	7.7	13.0	28	1.9	6.47	0.03	6.71	0
DP27-20 0.45	360	1361	7.41	13.9	29	3.1	2.68	0.36	6.46	29
AR00 0.45	123	301.6	8.27	13.0	13	4.9	9.5	NA	0.13	NA
AR04 0.45	109	256.9	8.2	13.0	13	8.3	8.45	NA	0.21	NA
MR01 0.45	155	300.9	8.46	13.0	23	8.6	8.94	NA	0.39	NA
MR02 0.45	151	284.8	7.72	13.0	24	8.2	6.74	NA	0.37	NA
BG	163	274	7.33	13.0	18	2	6.82	NA	0.35	NA
TP	423	1699	8.25	14.4	55	12.8	4.04	NA	0.00	NA
MW1	623	2217	6.61	13.3	38	11.5	2.4	NA	0.49	NA
MW2	418	1406	6.43	14.2	29	4.6	2.55	1.13	21.33	4
Seep Ditch	425	2731	7.46	11.7	28	10.7	7.11	NA	1.71	NA
Seep Pipe	446	1406	6.72	11.0	38	10.3	0.33	NA	42.71	NA

Appendix B: PHREEQC Input Files

1 Chapter 2 PHREEQC Input File

SOLUTION_SPREAD -units ppm Ag ppb	Al ppm	Alkalinity ppm	As ppb	B ppb	Ba ppb	Be ppb	Br ppm	Ca ppm	Cd ppb	Ce ppb
0.0025	0.0079	488.7	0.29	201.65	302.22	0.0216	0.245	97.315	0.01	0.16
0.0025	0.0034	346.1	0.31	272.92	161.74	0.0139	0.191	90.511	0.01	0.083
0.0025	0.0096	405.3	1.43	425.37	196.49	0.04	0.183	97.752	0.01	0.646
0.0025	0.0037	516.3	0.5	595.14	247.07	0.018	0.205	104.777	0.01	0.038
0.0025	0.0039	468.9	0.48	819.19	208.06	0.0221	0.193	81.322	0.01	0.037
0.0025	0.0055	446	0.28	390.51	249.34	0.0261	0.167	119.177	0.01	0.034
0.0025	0.0032	448.6	0.21	468.26	195.32	0.0137	0.166	105.036	0.01	0.027
0.0025	0.01	459.9	1.3	121.19	343.42	0.0123	0.218	164.755	0.01	0.407
0.0025	0.0312	422.3	0.82	374.05	167.06	0.1089	0.183	78.384	0.01	0.995
0.0025	0.001	167.4	0.05	24.58	57.41	0.0025	0.025	46.233	0.01	0.005
0.0025	0.0025	128	0.26	23.43	59.96	0.0025	0.025	42.098	0.01	0.024
0.0025	0.0025	178.2	0.29	47.04	37.76	0.0025	0.025	48.798	0.01	0.02
0.0025	0.0025	117.5	0.23	27.43	48.87	0.0025	0.025	35.853	0.01	0.024
0.0025	0.0025	190.7	0.26	7.71	26.92	0.0025	0.025	44.841	0.01	0.015
0.0025	0.0025	496.2	0.57	119.54	316.49	0.0089	0.293	159.584	0.01	0.213
0.0025	0.0025	507.1	0.42	50.5	270.57	0.0174	0.303	166.604	0.01	0.233
0.0025	0.0025	676	1.29	20.91	241.11	0.0285	0.414	331.874	0.01	0.96
0.0025	0.0025	329.3	1	60.87	129.45	0.0065	0.025	303.29	0.01	0.132
0.0025	0.0025	441.8	0.4	1341.48	278.25	0.0025	0.348	101.834	0.01	0.118
0.0025	0.0025	612.6	0.62	234.79	152.63	0.0222	0.297	161.353	0.01	0.197
0.0025	0.0025	538.5	0.72	261.36	55.17	0.0062	0.213	300.069	0.02	0.277
0.0025	0.0519	245	0.76	619	118.84	0.1362	0.087	63.214	0.036	3.96
0.0025	0.0025	459.1	1.55	1981.46	76.02	0.0172	0.331	202.801	0.01	0.042
0.0025	0.0025	125	0.27	18.31	62.08	0.0025	0.025	42.599	0.01	0.023
0.0025	0.0025	168.8	0.33	41.61	35.79	0.0025	0.025	43.832	0.01	0.024

Cl ppm	Co ppb	Cr ppb	Cs ppb	Cu ppb	Dy ppb	Er ppb	Eu ppb	F ppm	Fe(2) ppm	Fe(3) ppm	Ga ppb
74.01	0.025	0.3	0.005	0.05	0.0541	0.0369	0.0112	0.47	2.11	3.7983	0.005
56.35	0.025	0.28	0.005	0.05	0.016	0.0125	0.0025	0.21	2.34	4.5642	0.005
59.92	0.025	0.64	0.005	0.05	0.0779	0.0445	0.0179	0.301	3.45	4.1692	0.005
62.49	0.025	0.25	0.005	0.05	0.0096	0.0079	0.0025	0.408	2.16	3.5432	0.005
66.68	0.025	0.26	0.005	0.05	0.0113	0.0099	0.0025	0.675	2.63	0.4969	0.005
58.16	0.025	0.35	0.005	0.05	0.009	0.0082	0.0025	0.248	2.6	5.9085	0.005
57.53	0.025	0.27	0.005	0.05	0.0064	0.0052	0.0025	0.22	2.5	5.4841	0.005
57.6	0.025	0.27	0.005	0.05	0.05	0.0388	0.0121	0.057	3.67	29.7924	0.005
57.46	0.025	1.42	0.005	0.05	0.2241	0.141	0.0482	0.43	2.78	4.0062	0.005
0.62	0.025	0.05	0.005	2	0.0025	0.0025	0.0025	0.151	0.00001	0.2025	0.005
4.17	0.191	0.11	0.005	0.49	0.0074	0.0025	0.0025	0.088	0.00001	0.0209	0.005
7.34	0.025	0.05	0.005	0.16	0.0055	0.0025	0.0025	0.108	0.00001	0.3357	0.005
12.06	0.079	0.05	0.005	0.7	0.0064	0.0025	0.0025	0.09	0.00001	0.0546	0.005
0.72	0.167	0.05	0.005	0.52	0.0025	0.0025	0.0025	0.09	0.06	0.2795	0.005
90.45	0.411	0.15	0.005	0.05	0.0193	0.0127	0.0025	0.174	1.5	-0.0508	0.005
99.46	0.025	0.24	0.005	0.05	0.0326	0.0214	0.0025	0.117	1.11	0.0943	0.005
146.73	8.534	0.77	0.005	0.41	0.0637	0.0377	0.0132	0.039	0.05	0.1414	0.005
12.11	1.957	0.05	0.005	0.05	0.0119	0.0091	0.0025	0.045	4.53	0.3678	0.005
189.44	0.025	0.21	0.027	0.05	0.0184	0.0139	0.0025	0.146	2.1	0.2528	0.005
60.45	0.025	0.28	0.005	0.05	0.0232	0.0197	0.0025	0.639	0.32	0.0555	0.005
94.17	5.965	0.26	0.011	0.64	0.0104	0.0091	0.0025	0.036	1.64	0.0485	0.005
16.88	1.091	0.77	0.012	1.88	0.1517	0.0949	0.0244	0.088	0.00001	0.1152	0.017
151.12	49.466	0.21	0.045	0.05	0.0189	0.0149	0.0025	1.482	5.24	27.1096	0.012
3.11	0.081	0.05	0.005	0.5	0.0067	0.0025	0.0025	0.089	0.00001	0.0186	0.005
4.07	0.054	0.05	0.005	0.24	0.0059	0.0025	0.0025	0.113	0.00001	0.3855	0.005

Gd ppb	Hf ppb	Ho ppb	In ppb	K ppm	La ppb	Li ppb	Lu ppb	Mg ppm	Mn ppb	Mo ppb	Na ppm
0.0605	0.015	0.0131	0.005	2.595	0.099	76.821	0.0052	14.7738	626.92	0.025	209.297
0.0155	0.013	0.0025	0.005	2.215	0.04	35.217	0.0025	13.1015	332.77	0.098	125.797
0.0842	0.025	0.0156	0.005	2.459	0.288	48.114	0.0062	15.2298	349.9	0.151	163.892
0.0081	0.012	0.0025	0.005	2.721	0.02	64.508	0.0025	19.2582	246.44	0.29	198.517
0.0108	0.014	0.0025	0.005	3.532	0.018	74.809	0.0025	20.3169	367.81	0.218	197.79
0.0082	0.014	0.0025	0.005	1.98	0.016	51.333	0.0025	20.5635	522.08	0.102	143.853
0.0055	0.015	0.0025	0.005	2.203	0.01	54.457	0.0025	16.2677	514.41	0.185	154.198
0.0565	0.016	0.0121	0.005	2.191	0.202	28.435	0.0063	22.0706	566.17	0.122	90.174
0.2366	0.046	0.048	0.005	3.194	0.43	45.906	0.0196	15.8265	242.92	0.268	157.791
0.0025	0.005	0.0025	0.005	1.061	0.005	8.151	0.0025	11.4194	75.37	0.025	3.132
0.0078	0.005	0.0025	0.005	1.117	0.011	6.64	0.0025	12.9994	6.52	0.792	13.239
0.0025	0.005	0.0025	0.005	1.205	0.01	12.604	0.0025	12.4159	12.56	0.099	17.926
0.0059	0.005	0.0025	0.005	1.054	0.012	7.125	0.0025	11.0918	7.08	0.662	16.676
0.0025	0.005	0.0025	0.005	1.004	0.005	4.932	0.0025	17.2534	118.61	0.054	3.613
0.0189	0.017	0.0025	0.005	2.01	0.04	28.968	0.0025	18.7779	370.68	0.676	66.66
0.0298	0.02	0.0074	0.005	1.696	0.055	16.696	0.0025	18.5435	217.97	0.169	69.874
0.0739	0.125	0.0136	0.005	0.304	0.231	8.368	0.0025	56.5433	343.91	0.296	92.376
0.0125	0.018	0.0025	0.005	2.769	0.052	8.651	0.0025	19.7738	760.02	0.375	15.391
0.0157	0.02	0.0025	0.005	3.94	0.03	116.697	0.0025	17.6202	225.3	0.171	294.511
0.0192	0.032	0.0055	0.005	1.767	0.036	90.239	0.0025	95.3178	330	0.168	115.052
0.0109	0.011	0.0025	0.005	2.877	0.043	17.096	0.0025	26.2811	786.02	0.111	95.408
0.1657	0.057	0.0333	0.005	3.296	0.586	39.535	0.014	9.266	113.82	0.682	86.109
0.0135	0.057	0.0025	0.005	20.373	0.015	211.772	0.0025	66.3912	5025.9	4.515	302.93
0.0086	0.005	0.0025	0.005	1.19	0.013	5.933	0.0025	13.1389	7.33	0.837	12.347
0.0057	0.005	0.0025	0.005	1.323	0.014	12.201	0.0025	12.2801	24.9	0.06	13.97

Nd ppb	Ni ppb	N(5) ppm	P ppm	Pb ppb	pe	pH	Pr ppb	Rb ppb	Re ppb	S(-2) ppm
0.1644	0.1	0.01	0.346	0.005	9.942311286	8.04	0.027	1.387	0.009	0.136252
0.0459	0.1	0.01	0.167	0.005	10.24028887	7.89	0.0103	1.285	0.0066	0
0.3539	0.1	0.01	0.177	0.005	10.46046043	8.34	0.0815	1.735	0.008	0
0.0247	0.1	0.01	0.09	0.005	10.13476367	8.13	0.0051	2.367	0.0096	0.145482
0.0248	0.1	0.01	0.101	0.005	10.02068549	8.05	0.0025	1.334	0.0103	0.132746
0.0258	0.1	0.01	0.176	0.005	10.44925403	7.87	0.0025	1.073	0.007	0.137673
0.0161	0.1	0.01	0.137	0.005	10.77773385	7.99	0.0025	1.236	0.0085	0.12801
0.2482	0.1	0.01	0.025	0.005	10.85884348	7.55	0.0509	0.706	0.0025	0.150792
0.7748	0.1	0.01	0.116	0.005	10.33404037	7.81	0.1529	1.39	0.008	0.073064
0.0025	0.1	0.01	0.025	0.005	11.88641628	8.14	0.0025	0.643	0.0025	0.001884
0.02	0.65	0.01	0.025	0.014	13.27979927	8.38	0.0025	0.69	0.0025	0
0.016	0.47	0.01	0.025	0.022	13.00351472	8.35	0.0025	1.167	0.0025	0
0.0224	0.59	0.01	0.025	0.014	13.14443737	8.35	0.0025	0.715	0.0025	0
0.0127	0.37	0.01	0.025	0.026	13.43153295	7.36	0.0025	1.457	0.0025	0
0.0584	2.53	0.01	0.025	0.016	9.821683353	6.94	0.0121	1.633	0.0025	0.003477
0.0816	0.1	0.01	0.025	0.005	11.40677087	6.93	0.017	1.292	0.0025	0.004135
0.299	7.5	0.209	0.025	0.042	12.45742154	6.65	0.0681	0.85	0.0149	0.326082
0.0468	3.39	0.01	0.025	0.005	10.23308794	6.86	0.0098	0.754	0.0094	0.50341
0.0427	1.14	0.01	0.192	0.005	9.746544269	7	0.0079	4.682	0.0332	0.251673
0.0547	0.2	0.01	0.025	0.005	8.675261622	7.07	0.0106	0.783	0.0322	0.37275
0.0383	11.14	1.197	0.025	0.013	11.86094597	6.6	0.0089	4.683	0.0337	0.40206
0.6248	6.91	0.751	0.025	0.097	11.16075362	6.56	0.1466	3.138	0.0025	0
0.0373	58.06	0.01	0.025	0.083	10.62087364	6.9	0.0072	17.686	0.0419	0.76332
0.0206	0.64	0.311	0.025	0.018	13.54933769	8.38	0.0025	0.739	0.0025	0
0.0212	0.39	0.299	0.025	0.011	12.62392555	8	0.0025	1.224	0.0025	0

Sb ppb	Sc ppm	Se ppb	Si ppm	Sm ppb	Sn ppb	Sr ppb	Tb ppb	Temperature	Ti ppb	Tl ppb	Tm ppb
0.005	0.0005	0.5	6.671	0.0412	0.005	214.2	0.0086	6.7	2.3	0.0025	0.005
0.005	0.0005	0.5	11.38	0.0117	0.005	239.92	0.0025	8.1	1.6	0.0025	0.0025
0.005	0.0005	0.5	7.535	0.0814	0.005	186.19	0.0124	9	2.68	0.0025	0.0061
0.005	0.0005	0.5	5.63	0.006	0.005	202.4	0.0025	7	1.5	0.0025	0.0025
0.005	0.0005	0.5	6.121	0.0071	0.005	221.45	0.0025	8.7	1.55	0.0025	0.0025
0.005	0.0005	0.5	7.325	0.0068	0.005	241.51	0.0025	5.6	1.68	0.0025	0.0025
0.005	0.0005	0.5	6.578	0.0025	0.005	201.98	0.0025	6.3	1.53	0.0025	0.0025
0.005	0.0005	0.5	8.51	0.0496	0.005	279.9	0.0076	5	1.39	0.0025	0.0056
0.005	0.0005	0.5	5.455	0.179	0.019	186.66	0.0364	8	5.54	0.0025	0.0204
0.005	0.0005	0.5	6.468	0.0025	0.005	93.9	0.0025	7.4	0.25	0.0025	0.0025
0.02	0.0005	0.5	0.818	0.0066	0.005	338.12	0.0025	6.4	0.25	0.0025	0.0025
0.021	0.0005	0.5	3.965	0.0025	0.005	132.75	0.0025	5.2	0.61	0.0025	0.0025
0.018	0.0024	0.5	1.616	0.0025	0.005	280.1	0.0025	7.2	0.25	0.0025	0.0025
0.022	0.001	0.5	5.896	0.0025	0.023	90.06	0.0025	6.1	0.88	0.0025	0.0025
0.005	0.0005	0.5	4.418	0.0155	0.005	377.94	0.0025	6.1	0.81	0.0025	0.0025
0.005	0.0005	0.5	4.629	0.0249	0.005	320.22	0.0025	7	0.75	0.0025	0.0025
0.04	0.0005	1.2	3.728	0.0683	0.303	746.52	0.0102	8.9	1.43	0.0065	0.0025
0.04	0.0005	0.5	5.379	0.0096	0.005	478.67	0.0025	8.9	0.78	0.0057	0.0025
0.005	0.0005	0.5	8.513	0.0097	0.005	1054.59	0.0025	5.4	1.79	0.0025	0.0025
0.029	0.0005	1	7.25	0.0143	0.005	369.91	0.0025	8.1	1.32	0.0025	0.0025
0.041	0.0005	0.5	3.056	0.008	0.013	435.62	0.0025	9.3	0.59	0.1251	0.0025
0.216	0.0005	0.5	5.309	0.143	0.026	642.42	0.024	9.7	1.36	0.0145	0.0133
0.005	0.0018	0.5	7.856	0.0094	0.005	2350.95	0.0025	12.4	1.17	0.0054	0.0025
0.053	0.0005	0.5	0.807	0.0058	0.005	348.78	0.0025	6.8	0.25	0.0025	0.0025
0.017	0.0005	0.5	4.493	0.0025	0.005	129.68	0.0025	5.9	0.68	0.0025	0.0025

U ppb	V ppb	W ppb	Y ppb	Yb ppb	Zn ppb	Zr ppb	S(6) ppm
0.0493	1.34	0.01	0.484	0.033	0.25	0.674	136.252
0.0196	0.96	0.046	0.122	0.0119	0.25	0.882	112.686
0.0595	3.21	0.022	0.461	0.0401	0.25	1.23	128.645
0.1029	1.37	0.01	0.093	0.0088	0.25	0.608	145.482
0.1102	1.41	0.01	0.107	0.0112	0.25	0.723	132.746
0.011	1.43	0.01	0.081	0.0089	0.25	0.685	137.673
0.021	1.27	0.01	0.05	0.0054	0.25	0.784	128.01
0.0787	1.34	0.01	0.508	0.0355	0.25	1.126	150.792
0.1282	8.35	0.01	1.547	0.1265	0.25	2.084	73.064
0.0131	0.05	0.01	0.005	0.0025	0.94	0.025	1.884
0.4993	0.15	0.01	0.057	0.0025	0.55	0.025	48.374
0.2207	0.21	0.01	0.036	0.0025	0.25	0.21	13.678
0.4038	0.16	0.01	0.051	0.0025	0.25	0.025	36.038
0.0387	0.11	0.01	0.024	0.0025	0.25	0.062	0.251
0.0482	0.34	0.043	0.147	0.0128	0.25	0.865	3.477
0.2288	0.44	0.01	0.237	0.0201	0.95	0.954	4.135
7.4442	3.16	0.01	0.408	0.0297	4.6	6.264	326.082
1.5494	0.21	0.01	0.135	0.0079	3.1	0.285	503.41
0.0085	0.28	0.01	0.117	0.0122	0.25	0.712	251.673
3.2875	0.66	0.01	0.19	0.0227	0.25	1.434	372.75
10.6335	0.29	0.01	0.134	0.0103	1.52	0.528	402.06
0.0822	1.28	0.01	1.081	0.0875	54.44	3.323	116.145
1.9432	0.41	0.01	0.14	0.0154	9.04	0.783	763.32
0.5297	0.15	0.01	0.054	0.0025	0.78	0.025	50.441
0.0384	0.22	0.01	0.036	0.0025	0.25	0.168	763.32

2 Chapter 3 PHREEQC Input File

SOLUTION_SPREAD																
-units	ppm															
Ag	Al	Alkalinity	As	B	Ba	Be	Br	Ca	Cd	Ce	Cl	Co	Cr	Cs	Cu	Dy
ppb	ppb	ppm	ppb	ppb	ppb	ppb	ppm	ppm	ppb	ppb	ppm	ppb	ppb	ppb	ppb	ppb
0.03	10	505	0.5	209.69	175.31	0.03	0.24	121.84	0.1	0.05	103.4	0.25	0.5	0.05	0.5	0.03
0.03	10	514	0.5	185.84	202.48	0.03	0.24	130.78	0.1	0.05	104.8	0.25	0.5	0.05	0.5	0.03
0.03	10	525	0.5	201.28	281.97	0.03	0.26	127.42	0.1	0.05	107.7	0.25	0.5	0.05	0.5	0.03
0.03	65.8	490	0.5	360.92	200.74	0.03	0.24	123.37	0.1	0.36	110.7	0.25	0.5	0.05	0.5	0.06
0.03	10	505	0.5	322.99	189.96	0.03	0.28	133.29	0.1	0.11	127.2	0.25	0.5	0.05	0.5	0.03
0.03	10	470	0.5	466.89	246	0.03	0.22	102.29	0.1	0.22	92.1	0.25	0.5	0.05	0.5	0.07
0.03	10	387	0.5	59.56	90.16	0.03	0.3	255.52	0.1	0.05	218.5	0.25	0.5	0.05	0.5	0.03
0.03	10	423	0.5	47.71	153.08	0.03	0.3	253.23	0.1	0.05	201.2	0.25	0.5	0.05	0.5	0.03
0.03	10	424	0.5	61.14	154.42	0.03	0.28	156.93	0.1	0.28	87.8	0.25	0.5	0.05	0.5	0.03
0	4.8	350	0.21	33.49	138.16	0.01	0.18	118.52	0.01	0.12	43.6	0.03	0.37	0.01	0.05	0.02
0	10.2	400	0.32	37.89	144.8	0.01	0.21	144.56	0.01	0.36	58.2	0.03	0.34	0.01	0.05	0.04
0.03	10	365	0.5	64.03	111.04	0.03	0.17	96.54	0.1	0.05	127.6	0.25	0.5	0.05	0.5	0.03
0.03	10	416	0.5	73.68	119.01	0.03	0.21	105.63	0.1	0.05	128.9	0.25	0.5	0.05	0.5	0.03
0.03	10	505	0.5	37.55	252.23	0.03	0.24	193.63	0.1	0.05	66.3	0.25	0.5	0.05	0.5	0.03
0.03	10	514	0.5	44.46	208.88	0.03	0.24	186.4	0.1	0.05	67.9	0.25	0.5	0.05	0.5	0.03
0.03	10	496	0.5	48.1	264.89	0.03	0.25	193	0.1	0.05	66	0.25	0.5	0.05	0.5	0.03
0.03	10	393	0.5	109.62	67.3	0.03	0.26	113.41	0.1	0.05	125.5	0.25	0.5	0.05	0.5	0.03
0.03	10	472	0.5	83.7	144.21	0.03	0.26	141.39	0.1	0.05	128.6	0.25	0.5	0.05	0.5	0.03
0.03	10	503	1.11	77.86	143.46	0.03	0.26	149.4	0.1	0.05	128.4	0.94	0.5	0.05	0.5	0.03
0.03	10	492	0.5	62.32	129.61	0.03	0.29	154.8	0.1	0.2	130.7	1.45	0.5	0.05	0.5	0.03
0.03	10	500	0.5	79.93	144.92	0.03	0.28	150.75	0.1	0.36	131.5	2.21	0.5	0.05	0.5	0.03
0.03	10	474	1.08	100.43	122.15	0.03	0.26	149.08	0.1	0.47	130.5	0.86	0.5	0.05	0.5	0.05
0.03	10	398	0.5	40.56	93.24	0.03	0.27	206.67	0.1	0.05	185	0.25	0.5	0.05	0.5	0.03
0.03	10	425	0.98	37.27	179.35	0.03	0.29	197.88	0.1	0.05	173.9	0.25	0.5	0.05	0.5	0.03
0.03	10	421	0.5	25.11	273.81	0.03	0.31	190.55	0.1	0.13	175.1	0.25	0.5	0.05	0.5	0.03
0.03	10	359	0.5	23.76	304.52	0.03	0.35	185.27	0.1	0.23	142.3	0.25	0.5	0.05	0.5	0.03
0.03	10	367	0.5	21.61	364.65	0.03	0.33	181.86	0.1	0.33	138.2	0.25	0.5	0.05	0.5	0.03
0.03	10	380	0.5	70.42	63.28	0.03	0.22	103.59	0.1	0.05	126	0.25	0.5	0.05	0.5	0.03
0.03	10	430	0.5	70.65	92.14	0.03	0.23	114.04	0.1	0.05	133.3	0.25	0.5	0.05	0.5	0.03
0.03	36.6	459	0.5	67.27	144.68	0.03	0.26	125.65	0.1	0.17	136.7	0.25	0.5	0.05	0.5	0.03
0.03	10	493	0.5	12.25	174.47	0.03	0.28	133.03	0.1	0.11	124.3	0.25	0.5	0.05	0.5	0.03
0.03	10	372	0.5	17.63	91.65	0.03	0.24	171.19	0.1	0.05	182.6	0.25	0.5	0.05	0.5	0.03
0.03	10	388	0.5	5.34	163.87	0.03	0.25	184.93	0.1	0.05	188.6	0.25	0.5	0.05	0.5	0.03
0.03	10	514	0.5	12.15	215.29	0.03	0.32	161.32	0.1	0.11	158.9	0.25	0.5	0.05	0.5	0.03
0.03	39.9	515	0.5	26.1	217.49	0.03	0.34	152.55	0.1	0.18	128.8	0.25	0.5	0.05	0.5	0.03
0.03	40	548	0.5	17.59	214.13	0.03	0.36	159.3	0.1	0.17	152.6	0.25	0.5	0.05	0.5	0.03
0.03	31.2	538	0.5	23.59	319.85	0.03	0.37	191.14	0.1	0.16	136.9	0.25	0.5	0.05	0.5	0.03
0	4	140	0.33	39.62	27.12	0	0.03	35.77	0.01	0.03	9.8	0.07	0.22	0.01	0.05	0.01
0.03	70.1	82	0.5	63.67	137.62	0.08	0.12	62.74	0.1	0.36	86.1	3.56	14.35	0.05	1.67	0.03
0	19.8	221	0.51	44.04	182.92	0.01	0.23	89.99	0.01	0.32	108.7	0.29	0.55	0.05	0.05	0.03
0	14.9	241	0.44	55.72	193.87	0.02	0.25	96.62	0.01	0.27	105.1	0.09	0.53	0.05	0.05	0.03
0	9.5	249	0.33	101.85	191.16	0.01	0.18	97.61	0.01	0.11	80.9	0.1	0.39	0.05	0.05	0.01
0	13	277	0.38	71.59	208.65	0.01	0.25	107.49	0.01	0.19	94.4	0.03	0.39	0.05	0.05	0.02
0.03	10	348	0.5	42.33	59.13	0.03	0.22	117.72	0.1	0.05	138.6	0.25	0.5	0.05	0.5	0.03
0.03	10	360	0.5	37.74	62.27	0.03	0.22	117.38	0.1	0.05	138.6	0.25	0.5	0.05	0.5	0.03
0	9.1	123	0.5	37.29	52.16	0.01	0.03	36.22	0.01	0.07	2.3	0.14	0.15	0.01	0.62	0.02
0	5.7	109	0.43	29.13	39.76	0.01	0.03	31.6	0.01	0.07	7.2	0.08	0.23	0.01	0.55	0.01
0	2.7	155	0.34	42.59	28.88	0	0.03	40.73	0.01	0.03	4.3	0.07	0.21	0.01	0.13	0.01
0	3.9	151	0.38	38.95	28.07	0	0.03	37.63	0.01	0.03	3.3	0.07	0.23	0.01	0.35	0.01
0	3.4	132	0.3	33.45	22.36	0	0.03	32.9	0.01	0.02	3.8	0.06	0.22	0.01	0.19	0
0.03	10	446	0.5	1413	275.17	0.03	0.36	99.16	0.1	0.05	173.8	0.25	0.5	0.05	0.5	0.03
0.03	10	623	0.5	15.88	251.14	0.03	0.46	307.14	0.1	1.04	263.3	8.5	0.5	0.05	0.5	0.05
0	2.4	163	0.25	6.79	18.68	0	0.03	36.85	0.01	0.01	1.5	0.03	0.19	0.01	0.05	0
0.03	10	423	3.4	2612.87	169.25	0.03	0.3	16.95	0.1	0.05	137.6	2.72	0.5	0.05	0.5	0.03
0.03	10	425	0.5	1925.67	168.3	0.03	0.3	110.44	0.1	0.05	137.7	41.17	0.5	0.05	0.5	0.03
0.03	10	446	2.13	2210.41	40.88	0.03	0.29	218.3	0.1	0.14	128.1	65.74	0.5	0.05	0.5	0.03
0.03	10	418	3.03	18.34	215.15	0.03	0.27	167.96	0.1	0.55	99.5	1.47	0.5	0.05	0.5	0.05
0	4.7	110	0.45	37.08	15.32	0.01	0.03	26.8	0.01	0.03	2.4	0.07	0.19	0.01	0.32	0.01

Er ppb	Eu ppb	F ppm	Ga ppb	Gd ppb	Hf ppb	Ho ppb	In ppb	K ppm	La ppb	Li ppb	Lu ppb	Mg ppm	Mn ppb	Mo ppb	N(5) ppm	Na ppm	Nd ppb
0.03	0.03	0.3	0.05	0.03	0.05	0.03	0.05	2.82	0.05	30.69	0.03	21.8	851.1	0.25	0.01	125.91	0.06
0.03	0.03	0.27	0.05	0.03	0.05	0.03	0.05	2.59	0.05	26.5	0.03	22.37	1026.49	0.25	0.01	125	0.07
0.03	0.03	0.27	0.05	0.03	0.05	0.03	0.05	2.58	0.05	27.52	0.03	22.31	1201.54	0.25	0.01	128.68	0.07
0.03	0.03	0.26	0.05	0.05	0.05	0.03	0.05	2.85	0.16	33.95	0.03	18.99	520.08	0.25	0.01	128.24	0.23
0.03	0.03	0.13	0.05	0.03	0.05	0.03	0.05	2.93	0.05	31.83	0.03	21.78	345.08	0.25	0.01	133.26	0.09
0.05	0.03	0.37	0.05	0.05	0.05	0.03	0.05	3.17	0.05	34.07	0.03	16.58	690.34	0.25	0.01	131.52	0.17
0.03	0.03	0.11	0.05	0.03	0.05	0.03	0.05	3.19	0.05	13.44	0.03	57.06	51.2	0.25	0.01	200.52	0.03
0.03	0.03	0.11	0.05	0.03	0.05	0.03	0.05	2.26	0.05	10.94	0.03	53.59	670.07	0.25	0.01	164.74	0.03
0.03	0.03	0.06	0.05	0.03	0.05	0.03	0.05	1.52	0.11	13.1	0.03	29.58	989.71	0.25	0.01	47.25	0.11
0.01	0	0.07	0.02	0.01	0.01	0	0.01	1.13	0.06	10.27	0	19.31	1278.42	0.03	0.01	18.12	0.07
0.03	0.01	0.06	0.02	0.05	0.02	0.01	0.01	1.31	0.19	11.45	0	24.03	901.9	0.03	0.01	30.88	0.21
0.03	0.03	0.13	0.05	0.03	0.05	0.03	0.05	0.89	0.05	19.74	0.03	17.62	52.45	0.25	0.01	133.85	0.03
0.03	0.03	0.15	0.05	0.03	0.05	0.03	0.05	2.05	0.05	23.83	0.03	21.44	360.51	0.25	0.01	128.31	0.03
0.03	0.03	0.1	0.05	0.03	0.05	0.03	0.05	1.44	0.05	16.33	0.03	22.86	380.01	0.25	0.24	10.8	0.03
0.03	0.03	0.09	0.05	0.03	0.05	0.03	0.05	1.59	0.05	16.37	0.03	22.07	196.88	0.25	0.21	27.98	0.03
0.03	0.03	0.09	0.05	0.03	0.05	0.03	0.05	1.54	0.05	16.16	0.03	22.75	316.27	0.25	0.03	12.1	0.03
0.03	0.03	0.18	0.05	0.03	0.05	0.03	0.05	3.67	0.05	21.18	0.03	25.69	5.68	0.25	0.01	136.03	0.03
0.03	0.03	0.16	0.05	0.03	0.05	0.03	0.05	2.62	0.05	21.67	0.03	25.94	1419.44	0.25	0.01	135.63	0.03
0.03	0.03	0.16	0.05	0.03	0.05	0.03	0.05	2.56	0.05	21.21	0.03	27.37	1351.11	0.25	0.01	135.61	0.03
0.03	0.03	0.13	0.05	0.03	0.05	0.03	0.05	0.95	0.1	16.69	0.03	24.36	1849.67	0.25	0.01	133.91	0.11
0.03	0.03	0.14	0.05	0.03	0.05	0.03	0.05	1.39	0.19	18.22	0.03	24.32	2993.97	0.25	0.01	133.91	0.18
0.03	0.03	0.13	0.05	0.07	0.05	0.03	0.05	1.57	0.26	18.03	0.03	25.61	2216.43	0.25	0.01	137.39	0.27
0.03	0.03	0.11	0.05	0.03	0.05	0.03	0.05	3.4	0.05	14.78	0.03	46.53	51.76	0.25	0.01	159.5	0.03
0.03	0.03	0.09	0.05	0.03	0.05	0.03	0.05	1.9	0.05	14.32	0.03	40.53	514.44	0.25	0.01	148.13	0.03
0.03	0.03	0.1	0.05	0.03	0.05	0.03	0.05	1.6	0.05	14.68	0.03	38.07	1136.53	0.25	0.01	141.44	0.08
0.03	0.03	0.1	0.05	0.03	0.05	0.03	0.05	1.42	0.13	13.2	0.03	33.8	2188.73	0.25	0.01	83.72	0.13
0.03	0.03	0.11	0.05	0.03	0.05	0.03	0.05	1.6	0.16	14.26	0.03	34.74	1397.37	0.25	0.01	83.1	0.19
0.03	0.03	0.15	0.05	0.03	0.05	0.03	0.05	2.99	0.05	21.5	0.03	24.6	110.3	0.25	0.01	128.7	0.03
0.03	0.03	0.13	0.05	0.03	0.05	0.03	0.05	2.56	0.05	21.01	0.03	25.78	405.02	0.25	0.01	134.63	0.03
0.03	0.03	0.13	0.05	0.03	0.05	0.03	0.05	2.53	0.05	20.4	0.03	24.5	518.15	0.25	0.01	125.91	0.08
0.03	0.03	0.09	0.05	0.03	0.05	0.03	0.05	1.76	0.05	15.9	0.03	23.61	233.55	0.25	0.08	128.19	0.06
0.03	0.03	0.11	0.05	0.03	0.05	0.03	0.05	2.19	0.05	16.73	0.03	37.61	157.77	0.25	0.01	141.16	0.03
0.03	0.03	0.11	0.05	0.03	0.05	0.03	0.05	0.86	0.05	17.51	0.03	38.61	637.88	0.25	0.01	139.89	0.03
0.03	0.03	0.08	0.05	0.03	0.05	0.03	0.05	1.02	0.05	16.5	0.03	32.79	373.58	0.25	0.01	127.86	0.06
0.03	0.03	0.15	0.05	0.03	0.05	0.03	0.05	0.87	0.05	13.16	0.03	25.89	657.26	0.25	0.15	128.09	0.1
0.03	0.03	0.08	0.05	0.03	0.05	0.03	0.05	0.59	0.05	17.5	0.03	29.79	485.33	0.25	0	144.43	0.08
0.03	0.03	0.08	0.05	0.03	0.05	0.03	0.05	0.35	0.05	14.75	0.03	24.75	608.26	0.25	0.12	140.35	0.1
0	0	0.09	0.01	0.03	0.01	0	0.01	1.44	0.02	10.77	0	10.39	8.33	0.06	0.01	14.06	0.02
0.03	0.03	0.05	0.05	0.05	0.05	0.03	0.05	2.53	0.15	13.18	0.03	13.63	749.68	0.25	0.01	41.21	0.19
0.02	0.01	0.07	0.01	0.04	0.02	0.01	0.01	0.03	0.14	8.09	0	14.94	238.7	0.03	0.01	38.69	0.17
0.02	0.01	0.07	0.01	0.03	0.02	0.01	0.01	0.03	0.11	9.61	0	14.87	164.65	0.03	0.01	40.78	0.16
0.01	0	0.09	0.01	0.02	0.01	0	0.01	0.36	0.05	28.56	0	15.44	460.79	0.03	0.01	32.59	0.07
0.01	0	0.08	0.01	0.02	0.01	0	0.01	0.19	0.08	17.8	0	16.81	401.51	0.03	0.01	36.88	0.11
0.03	0.03	0.1	0.05	0.03	0.05	0.03	0.05	3.37	0.05	19.22	0.03	30.08	4.95	0.25	0.01	137.43	0.03
0.03	0.03	0.09	0.05	0.03	0.05	0.03	0.05	3.26	0.05	18.54	0.03	30.63	123.28	0.25	0.01	133.58	0.03
0.01	0	0.08	0.01	0.02	0.01	0	0.01	1.37	0.04	9.08	0	10.6	8.87	0.62	0.01	12.68	0.06
0.01	0	0.08	0.01	0.02	0.01	0	0.01	1.12	0.04	7.61	0	9.01	9.54	0.46	0.01	11.89	0.05
0	0	0.1	0.01	0.01	0.01	0	0.01	1.16	0.02	11.27	0	11.12	13.94	0.06	0.01	12.87	0.02
0	0	0.11	0.01	0.01	0.01	0	0.01	1.15	0.02	10.47	0	10.92	12.8	0.06	0.01	11.84	0.02
0	0	0.09	0.01	0	0.01	0	0.01	1.29	0.01	10.04	0	9.66	14.56	0.06	0.01	11.38	0.02
0.03	0.03	0.69	0.05	0.03	0.05	0.03	0.05	5.09	0.05	132.01	0.03	18	200.59	0.25	0.01	289.62	0.04
0.03	0.03	0.09	0.05	0.06	0.1	0.03	0.05	0.35	0.3	8.27	0.03	51.07	535.89	0.25	0.01	161.43	0.34
0	0	0.07	0.01	0	0.01	0	0.01	1.08	0.01	4.64	0	13.52	10.36	0.09	0.01	3.69	0.01
0.03	0.03	3.79	0.11	0.03	0.05	0.03	0.05	19.25	0.05	186.56	0.03	10.22	57.67	93.32	0.19	348.61	0.03
0.03	0.03	1.8	0.05	0.03	0.05	0.03	0.05	18.45	0.05	210.11	0.03	50.47	1885.2	6.3	0.02	284.11	0.03
0.03	0.03	1.57	0.05	0.03	0.05	0.03	0.05	21.79	0.05	251.14	0.03	57.81	3405.87	2.59	0.01	336.04	0.06
0.03	0.03	0.09	0.05	0.07	0.05	0.03	0.05	2.15	0.23	9.41	0.03	29.8	2285.97	0.81	0.01	95.37	0.25
0	0	0.09	0.01	0	0.01	0	0.01	0.95	0.02	11.15	0	7.92	15.67	0.05	0.01	12.62	0.02

Ni ppb	P ppm	Pb ppb	pe	pH	Pr ppb	Rb ppb	Re ppb	Sb ppb	Se ppb	Si ppm	Sm ppb	Sn ppb	Sr ppb	Tb ppb	Temperature
1	0.03	0.05	13.10148078	7.54	0.03	1.76	0.03	0.05	5	4.67	0.03	0.05	346.07	0.03	6.4
1	0.05	0.05	11.39346737	7.45	0.03	1.42	0.03	0.05	5	4.98	0.03	0.05	360.94	0.03	6.3
1	0.1	0.05	10.80042992	7.43	0.03	1.56	0.03	0.05	5	5.09	0.03	0.05	347.71	0.03	6.4
1	0.03	0.05	10.94049062	7.23	0.05	2.63	0.03	0.05	5	4.65	0.03	0.05	330.4	0.03	6.3
1	0.1	0.05	11.0729762	7.27	0.03	2.76	0.03	0.05	5	4.73	0.03	0.05	282.65	0.03	6.3
1	0.03	0.05	10.80577472	7.33	0.03	3	0.03	0.05	5	4.83	0.03	0.05	339.38	0.03	6.1
2.03	0.03	0.05	14.47515963	7.8	0.03	1.72	0.03	0.05	5	4.02	0.03	0.05	772.94	0.03	5.2
1	0.08	0.14	11.28124619	7.34	0.03	1.18	0.03	0.05	5	4.09	0.03	0.05	735.64	0.03	6.4
1	0.21	0.05	11.58359763	6.67	0.03	1.18	0.03	0.05	5	4.64	0.03	0.05	446.96	0.03	6.8
0.1	0.11	0.01	11.39397412	6.78	0.02	1.06	0	0.01	0.5	4.05	0.02	0.03	291.06	0	6.3
0.1	0.11	0.02	11.60389961	6.78	0.05	1.17	0	0.01	0.5	4.4	0.04	0.01	353.39	0.01	7.1
1	0.03	0.05	13	7.48	0.03	0.25	0.03	0.05	5	3.51	0.03	0.05	222.59	0.03	4.8
1	0.22	0.05	10.57281291	7.47	0.03	0.82	0.03	0.05	5	4.01	0.03	0.05	255.95	0.03	4.5
1	0.03	0.05	11.53890394	6.88	0.03	0.64	0.03	0.05	5	3.47	0.03	0.05	384.22	0.03	5.7
1	0.03	0.05	12.14244493	6.97	0.03	1.48	0.03	0.05	5	3.48	0.03	0.05	361.86	0.03	6
1	0.03	0.05	11.93858857	6.92	0.03	1.39	0.03	0.05	5	3.5	0.03	0.05	377.38	0.03	6.3
1	0.03	0.05	13.50372748	7.85	0.03	1.97	0.03	0.05	5	4.05	0.03	0.05	349.75	0.03	6.1
1	0.16	0.05	11.28858063	7.47	0.03	1.25	0.03	0.05	5	4.66	0.03	0.05	384.67	0.03	5.8
1	0.08	0.05	10.30237248	7.54	0.03	1.05	0.03	0.05	5	4.9	0.03	0.05	411.66	0.03	6.4
2.64	0.03	0.05	13.52317117	7.55	0.03	0.71	0.03	0.05	5	4.33	0.03	0.05	361.84	0.03	5.6
3.73	0.03	0.05	11.31600382	7.29	0.03	0.68	0.03	0.05	5	4.31	0.03	0.05	364.93	0.03	7.7
2.11	0.03	0.05	12.521426	7.3	0.06	0.54	0.03	0.05	5	4.65	0.03	0.05	373.43	0.03	7.2
1	0.03	0.05	13	7.76	0.03	2.42	0.03	0.05	5	4.05	0.03	0.05	598.9	0.03	6.8
1	0.25	0.13	10.55979848	7.26	0.03	1.28	0.03	0.05	5	4.36	0.03	0.05	583.73	0.03	7
1	0.25	0.05	10.41229252	7.14	0.03	0.25	0.03	0.05	5	4.58	0.03	0.05	562.16	0.03	7
1	0.14	0.05	11.16066563	6.84	0.03	0.83	0.03	0.05	5	4.37	0.03	0.05	568.95	0.03	7.2
1	0.13	0.05	11.28653514	6.8	0.03	1.97	0.03	0.05	5	4.58	0.03	0.05	530.64	0.03	7
1	0.03	0.05	13.88610842	7.63	0.03	1.42	0.03	0.05	5	4.15	0.03	0.05	292.78	0.03	2.8
1	0.1	0.05	10.93502203	7.3	0.03	1.03	0.03	0.05	5	4.41	0.03	0.05	317.98	0.03	4.6
1	0.18	0.05	11.0836965	7.3	0.03	0.25	0.03	0.05	5	4.83	0.03	0.05	317.96	0.03	4.4
1	0.13	0.05	10.62718914	7.05	0.03	0.25	0.03	0.05	5	4.93	0.03	0.05	330.75	0.03	5.3
1	0.03	0.05	13	7.48	0.03	1.2	0.03	0.05	5	4.04	0.03	0.05	476.7	0.03	4.8
1	0.07	0.05	10.84311677	7	0.03	0.56	0.03	0.05	5	4.34	0.03	0.05	524.76	0.03	5.7
1	0.39	0.05	10.7668085	6.84	0.03	0.25	0.03	0.05	5	5.18	0.03	0.05	438.89	0.03	6
1	0.34	0.05	10.5919105	6.85	0.03	0.25	0.03	0.05	5	6.1	0.03	0.05	431.15	0.03	5.7
1	0.42	0.05	10.93931887	6.89	0.03	0.25	0.03	0.05	5	5.99	0.03	0.05	444.61	0.03	6.1
1	0.19	0.05	10.94590841	6.84	0.03	0.25	0.03	0.05	5	5.46	0.03	0.05	570.39	0.03	4.6
0.5	0.03	0.01	15.52477893	7.3	0	2.85	0	0.02	0.5	4.37	0.01	0.01	102.38	0	3
2.54	0.06	0.11	15.66058955	6.2	0.03	11.08	0.03	0.05	5	6.84	0.03	0.05	185.18	0.03	5
0.22	0.3	0.05	12.65954173	6.44	0.04	0.37	0	0.03	0.5	10.25	0.04	0.03	230.99	0.01	6.2
0.28	1.34	0.03	11.341125	6.43	0.03	0.28	0	0.02	0.5	9.94	0.03	0.01	238.44	0.01	7.7
2.02	0.17	0.03	11.67382289	6.49	0.01	0.43	0	0.03	0.5	9.42	0.02	0.02	273.59	0	7.8
0.1	0.19	0.02	11.70185221	6.31	0.02	0.28	0	0.02	0.5	10.77	0.02	0.01	282.63	0	8.2
1	0.03	0.05	13	7.7	0.03	2.4	0.03	0.05	5	4.26	0.03	0.05	352.67	0.03	1.9
1	0.03	0.05	13.92244639	7.41	0.03	2.38	0.03	0.05	5	4.59	0.03	0.05	351.59	0.03	3.1
1.16	0.03	0.04	13	8.27	0.01	0.84	0	0.05	0.5	2	0.02	0.01	253.35	0	4.9
0.91	0.03	0.06	13	8.2	0.01	0.83	0	0.04	0.5	3	0.01	0.01	182.93	0	8.3
0.57	0.03	0.02	13	8.46	0	1.27	0	0.02	0.5	4.26	0	0.01	119.59	0	8.6
0.53	0.03	0.02	13	7.72	0	1.26	0	0.02	0.5	4.56	0	0.01	110.85	0	8.2
0.49	0.03	0.01	14.83247921	7.96	0	1.32	0	0.02	0.5	4	0	0.01	94.85	0	4.1
2.15	0.14	0.05	10.50789266	7.09	0.03	4.99	0.03	0.05	5	8.07	0.03	0.05	1008.26	0.03	6.6
11.41	0.03	0.05	13.26536918	6.61	0.07	0.87	0.03	0.05	5	3.79	0.08	0.05	705.27	0.03	11.5
0.41	0.03	0.01	13	7.33	0	1	0	0.02	0.5	4.45	0	0.01	68.75	0	2
8.84	0.03	0.05	14.4118469	8.25	0.03	21.72	0.07	1.77	5	2.14	0.03	0.05	510.65	0.03	12.8
50.5	0.03	0.05	11.73765181	7.46	0.03	19.97	0.03	0.05	5	5.48	0.03	0.05	1661.59	0.03	10.7
93.21	0.03	0.05	10.94897457	6.72	0.03	20.62	0.05	0.05	5	7.49	0.03	0.05	2315.09	0.03	10.3
4.17	0.03	0.05	14.20949835	6.43	0.05	1.05	0.03	0.14	5	3.92	0.05	0.05	602.4	0.03	4.6
0.48	0.03	0.02	13	7.69	0	1.31	0	0.02	0.5	3.78	0	0.01	95.88	0	7.7

Th ppb	Ti ppb	Tl ppb	Tm ppb	U ppb	V ppb	W ppb	Y ppb	Yb ppb	Zn ppb	Zr ppb	Fe(2) ppm	Fe(3) ppm	S(-2) ppm	S(6) ppm
0.1	2.5	0.03	0.03	0.03	0.5	0.1	0.19	0.03	2.5	0.61	1.19	3.53	0.010314352	5.06
0.1	2.5	0.03	0.03	0.03	0.5	0.1	0.23	0.03	2.5	0.62	3.67	7.25	0	13.56
0.1	2.5	0.03	0.03	0.03	0.5	0.28	0.25	0.03	2.5	0.67	4.97	18.39	0.007220046	6.64
0.1	2.5	0.03	0.03	0.1	1.39	0.1	0.42	0.03	2.5	0.92	5.16	0	0.052603193	2.6
0.1	2.5	0.03	0.03	0.09	0.5	0.1	0.27	0.03	2.5	0.68	5.36	0	0.062917545	13.25
0.1	2.5	0.03	0.03	0.19	1.99	0.1	0.56	0.06	2.5	1.79	4.17	0.04	0.367190919	2.84
0.1	2.5	0.03	0.03	0.13	0.5	0.1	0.05	0.03	2.5	0.25	0.22	0	0.000618861	554.12
0.1	2.5	0.03	0.03	0.03	0.5	0.1	0.05	0.03	2.5	0.25	3.67	1.39	0.12583509	454.77
0.1	2.5	0.03	0.03	0.03	0.5	0.1	0.13	0.03	2.5	0.51	2.4	10.23	0.106237822	69.11
0.01	1.16	0	0	0.01	0.44	0.01	0.09	0.01	0.25	0.63	3.4	12.22	0.080451943	6.19
0.01	1.38	0	0	0.01	0.59	0.04	0.35	0.03	0.25	0.98	3.93	9.4	0.060854675	40.31
0.1	2.5	0.03	0.03	0.2	0.5	0.1	0.05	0.03	2.5	0.25	0.28	0.1	0.003094305	42.92
0.1	2.5	0.03	0.03	0.03	0.5	0.1	0.05	0.03	2.5	0.25	2.78	3.82	0.028880185	18.13
0.1	2.5	0.03	0.03	0.03	0.5	0.1	0.05	0.03	2.5	0.25	1.65	3.78	0.024754444	0.08
0.1	2.5	0.03	0.03	0.03	0.5	0.1	0.05	0.03	2.5	0.25	1.15	0.69	0.012377222	0.01
0.1	2.5	0.03	0.03	0.03	0.5	0.1	0.05	0.03	2.5	0.25	2.9	2.35	0.033005925	0.13
0.1	2.5	0.03	0.03	0.05	0.5	0.1	0.05	0.03	2.5	0.25	0	0.01	0	104.31
0.1	2.5	0.03	0.03	0.03	0.5	0.1	0.12	0.03	2.5	0.25	2.48	10.4	0.015471527	85.18
0.1	2.5	0.03	0.03	0.13	0.5	0.1	0.12	0.03	2.5	0.5	3.24	9.25	0.012377222	75.92
0.1	2.5	0.03	0.03	0.23	0.5	0.1	0.23	0.03	2.5	0.99	0.75	0	0	80.38
0.1	2.5	0.03	0.03	0.38	0.5	0.1	0.35	0.03	2.5	1.17	0.14	0	0.003094305	63.53
0.1	2.5	0.03	0.03	0.16	0.5	0.1	0.36	0.03	2.5	1.09	0.79	0	0	93.02
0.1	2.5	0.03	0.03	0.1	0.5	0.24	0.05	0.03	2.5	0.25	0.02	0.11	0.00206287	367.63
0.1	2.5	0.03	0.03	0.03	0.5	0.1	0.05	0.03	2.5	0.25	3.18	4.98	0.054666064	284.74
0.1	2.5	0.03	0.03	0.09	0.5	0.1	0.12	0.03	2.5	0.25	4.07	11.54	0.026817314	248.64
0.1	2.5	0.03	0.03	0.03	0.5	0.1	0.2	0.03	2.5	0.25	3.04	18.44	0.030943055	211.62
0.1	2.5	0.03	0.03	0.03	0.5	0.1	0.31	0.03	2.5	0.25	2.96	14.96	0.050540323	193.09
0.1	2.5	0.03	0	0.03	0.5	0.1	0.05	0.03	2.5	0.25	0.56	0	0.019597268	66.01
0.1	2.5	0.03	0	0.03	0.5	0.1	0.05	0.03	2.5	0.25	1.07	0	0.464145824	66.38
0.1	2.5	0.03	0	0.03	0.5	0.1	0.12	0.03	2.5	0.25	4.43	0.31	0.060854675	23.05
0.1	2.5	0.03	0	0.03	0.5	0.2	0.12	0.03	2.5	0.25	2.07	6.74	0.062917545	22.47
0.1	2.5	0.03	0	0.07	0.5	0.1	0.05	0.03	2.5	0.25	0	0.15	0	242.17
0.1	2.5	0.03	0	0.06	0.5	0.29	0.05	0.03	2.5	0.25	3.95	4.34	0.154715275	235.55
0.1	2.5	0.03	0	0.03	0.5	0.1	0.05	0.03	2.5	0.25	2.05	10.39	0.12789796	55.66
0.1	2.5	0.03	0	0.03	0.5	0.1	0.14	0.03	2.5	0.51	3.5	27.21	0.051571758	56.22
0.1	2.5	0.03	0	0.03	0.5	0.1	0.14	0.03	2.5	0.25	0.56	22.25	0.045383147	44.12
0.1	2.5	0.03	0	0.03	0.5	0.1	0.15	0.03	2.5	0.25	5	19.31	0.062917545	118.96
0.01	0.86	0	0	0.02	0.2	0.01	0.04	0	0.85	0.14	0.08	0.28	0.004125741	5.3
0.1	2.5	0.03	0.03	0.03	0.5	0.1	0.28	0.03	57.34	0.25	1.19	0	0.003094305	93.33
0.03	3.28	0	0	0.01	0.62	0.01	0.22	0.02	0.54	0.8	3.28	10.18	0.088703424	0.69
0.03	5.48	0	0	0.01	0.47	0.01	0.19	0.02	1	0.68	3.18	8.85	0.074263332	0.25
0.01	2.07	0	0	0.01	0.31	0.02	0.1	0.01	1.21	0.34	2.78	5.92	0.118615044	12.21
0.02	2.7	0	0	0.01	0.3	0.01	0.13	0.01	0.25	0.43	4.91	3.86	0.070137591	0.14
0.1	2.5	0.03	0.03	0.09	0.5	0.1	0.05	0.03	2.5	0.25	0.06	0	0	151.79
0.1	2.5	0.03	0.03	0.09	0.5	0.1	0.05	0.03	2.5	0.25	0.71	0	0.02991162	143.01
0.01	0.25	0	0	0.39	0.24	0.01	0.13	0.01	0.51	0.18		0.13		32.43
0.01	0.63	0	0	0.25	0.3	0.01	0.09	0.01	0.25	0.18		0.21		20.46
0.01	0.82	0	0	0.05	0.25	0.01	0.04	0	0.25	0.18		0.39		8.7
0.01	0.87	0	0	0.03	0.24	0.01	0.04	0	0.62	0.14		0.4		6.27
0.01	0.79	0	0	0.02	0.21	0.03	0.04	0	0.25	0.14		0.35		5.07
0.1	2.5	0.03	0.03	0.03	0.5	0.1	0.1	0.03	2.5	0.56		2.21		272.43
0.1	2.5	0.03	0.03	6.35	2.49	0.1	0.33	0.03	2.5	4.98		0.49		301.08
0.01	0.69	0	0	0.03	0.13	0.01	0.03	0	0.25	0.08		0.1		2.7
0.1	2.5	0.03	0.03	4.11	5.86	7	0.05	0.03	2.5	0.68		0		250.53
0.1	2.5	0.03	0.03	0.94	0.5	0.1	0.05	0.03	10.46	0.25		1.72		504.12
0.1	2.5	0.03	0.03	1.49	0.5	0.1	0.12	0.03	16.28	0.25		42.71		902.76
0.1	2.5	0.03	0.03	1.92	1.08	0.1	0.47	0.03	2.5	1.1		22.46		193.56
0.01	0.63	0	0	0.01	0.19	0.01	0.03	0	0.25	0.1		0.3		3.72

Appendix C: WHAM7 Input Files

1 Chapter 2 WHAM7 Input File

Description	SPM	Temperature	pCO2	pH	Colloidal Fulvic Acid	Colloidal Iron oxide	Be	Na	Mg
Units	g/l	deg C	atm		mg/l	mg/l	µg/l	mg/l	mg/l
GW1.1	0.00E+00	6.7	999	8.04	7.2	7.267	0.022	209.297	14.774
GW1.2	0.00E+00	8.1	999	7.89	6.05	9.18	0.014	125.797	13.102
GW1.3	0.00E+00	9	999	8.34	6.5	11.093	0.04	163.892	15.23
GW1.4	0.00E+00	7	999	8.13	5.48	13.006	0.018	198.517	19.258
GW1.5	0.00E+00	8.7	999	8.05	7.16	14.919	0.022	197.79	20.317
GW1.6	0.00E+00	5.6	999	7.87	5.23	16.833	0.026	143.853	20.564
GW1.7	0.00E+00	6.3	999	7.99	2.85	18.746	0.014	154.198	16.268
GW1.8	0.00E+00	5	999	7.55	2.65	20.659	0.012	90.174	22.071
GW1.9	0.00E+00	8	999	7.81	8.53	22.572	0.109	157.791	15.827
SW1.1	0.00E+00	7.4	999	8.14	1.78	24.485	3.00E-03	3.132	11.419
GW2.1	0.00E+00	6.1	999	6.94	11.2	35.964	9.00E-03	66.66	18.778
GW2.2	0.00E+00	7	999	6.93	10.1	37.877	0.017	69.874	18.544
GW2.3	0.00E+00	8.9	999	6.65	58.9	39.79	0.029	92.376	56.543
GW2.4	0.00E+00	8.9	999	6.86	7.3	41.704	7.00E-03	15.391	19.774
GW2.5	0.00E+00	5.4	999	7	26	43.617	3.00E-03	294.511	17.62
GW2.6	0.00E+00	8.1	999	7.07	12.8	45.53	0.022	115.052	95.318
GW2.7	0.00E+00	9.3	999	6.6	15.2	47.443	6.00E-03	95.408	26.281
GW2.8	0.00E+00	9.7	999	6.56	12.9	49.356	0.136	86.109	9.266
SW2.1	0.00E+00	6.4	999	8.38	1.4	28.312	3.00E-03	13.239	12.999
SW2.2	0.00E+00	5.2	999	8.35	7.8	30.225	3.00E-03	17.926	12.416
SW2.3	0.00E+00	7.2	999	8.35	1.6	32.138	3.00E-03	16.676	11.092
SW2.4	0.00E+00	6.1	999	7.36	5.4	34.051	3.00E-03	3.613	17.253
SW2.5	0.00E+00	6.8	999	8.38	1.3	53.183	3.00E-03	12.347	13.139
SW2.6	0.00E+00	5.9	999	8	7.6	55.096	3.00E-03	13.97	12.28
Seep Pipe	0.00E+00	12.4	999	6.9	50.4	51.269	0.017	302.93	66.391

Description	Al	K	Ca	Sc	Cr(III)	Fe(II)	Co	Ni	Cu	Zn
Units	µg/l	mg/l	mg/l	mg/l	µg/l	mg/l	µg/l	µg/l	µg/l	µg/l
GW1.1	7.9	2.595	97.315	1.00E-03	0.3	2.11	0.025	0.1	0.05	0.25
GW1.2	3.4	2.215	90.511	1.00E-03	0.28	2.34	0.025	0.1	0.05	0.25
GW1.3	9.6	2.459	97.752	1.00E-03	0.64	3.45	0.025	0.1	0.05	0.25
GW1.4	3.7	2.721	104.777	1.00E-03	0.25	2.16	0.025	0.1	0.05	0.25
GW1.5	3.9	3.532	81.322	1.00E-03	0.26	2.63	0.025	0.1	0.05	0.25
GW1.6	5.5	1.98	119.177	1.00E-03	0.35	2.6	0.025	0.1	0.05	0.25
GW1.7	3.2	2.203	105.036	1.00E-03	0.27	2.5	0.025	0.1	0.05	0.25
GW1.8	10	2.191	164.755	1.00E-03	0.27	3.67	0.025	0.1	0.05	0.25
GW1.9	31.2	3.194	78.384	1.00E-03	1.42	2.78	0.025	0.1	0.05	0.25
SW1.1	1	1.061	46.233	1.00E-03	0.05	0.00E+00	0.025	0.1	2	0.94
GW2.1	2.5	2.01	159.584	1.00E-03	0.15	1.5	0.411	2.53	0.05	0.25
GW2.2	2.5	1.696	166.604	1.00E-03	0.24	1.11	0.025	0.1	0.05	0.95
GW2.3	2.5	0.304	331.874	1.00E-03	0.77	0.05	8.534	7.5	0.41	4.6
GW2.4	2.5	2.769	303.29	1.00E-03	0.05	4.53	1.957	3.39	0.05	3.1
GW2.5	2.5	3.94	101.834	1.00E-03	0.21	2.1	0.025	1.14	0.05	0.25
GW2.6	2.5	1.767	161.353	1.00E-03	0.28	0.32	0.025	0.2	0.05	0.25
GW2.7	2.5	2.877	300.069	1.00E-03	0.26	1.64	5.965	11.14	0.64	1.52
GW2.8	51.9	3.296	63.214	1.00E-03	0.77	0.00E+00	1.091	6.91	1.88	54.44
SW2.1	2.5	1.117	42.098	1.00E-03	0.11	0.00E+00	0.191	0.65	0.49	0.55
SW2.2	2.5	1.205	48.798	1.00E-03	0.05	0.00E+00	0.025	0.47	0.16	0.25
SW2.3	2.5	1.054	35.853	2.00E-03	0.05	0.00E+00	0.079	0.59	0.7	0.25
SW2.4	2.5	1.004	44.841	1.00E-03	0.05	0.06	0.167	0.37	0.52	0.25
SW2.5	2.5	1.19	42.599	1.00E-03	0.05	0.00E+00	0.081	0.64	0.5	0.78
SW2.6	2.5	1.323	43.832	1.00E-03	0.05	0.00E+00	0.054	0.39	0.24	0.25
Seep Pipe	2.5	20.373	202.801	2.00E-03	0.21	5.24	49.466	58.06	0.05	9.04

Description	Sr	Y	Ag	Cd	Sn(II)	Cs	Ba	La	Ce
Units	µg/l	µg/l	µg/l	µg/l	µg/l	µg/l	µg/l	µg/l	µg/l
GW1.1	214.2	0.484	3.00E-03	0.01	5.00E-03	5.00E-03	302.22	0.099	0.16
GW1.2	239.92	0.122	3.00E-03	0.01	5.00E-03	5.00E-03	161.74	0.04	0.083
GW1.3	186.19	0.461	3.00E-03	0.01	5.00E-03	5.00E-03	196.49	0.288	0.646
GW1.4	202.4	0.093	3.00E-03	0.01	5.00E-03	5.00E-03	247.07	0.02	0.038
GW1.5	221.45	0.107	3.00E-03	0.01	5.00E-03	5.00E-03	208.06	0.018	0.037
GW1.6	241.51	0.081	3.00E-03	0.01	5.00E-03	5.00E-03	249.34	0.016	0.034
GW1.7	201.98	0.05	3.00E-03	0.01	5.00E-03	5.00E-03	195.32	0.01	0.027
GW1.8	279.9	0.508	3.00E-03	0.01	5.00E-03	5.00E-03	343.42	0.202	0.407
GW1.9	186.66	1.547	3.00E-03	0.01	0.019	5.00E-03	167.06	0.43	0.995
SW1.1	93.9	5.00E-03	3.00E-03	0.01	5.00E-03	5.00E-03	57.41	5.00E-03	5.00E-03
GW2.1	377.94	0.147	3.00E-03	0.01	5.00E-03	5.00E-03	316.49	0.04	0.213
GW2.2	320.22	0.237	3.00E-03	0.01	5.00E-03	5.00E-03	270.57	0.055	0.233
GW2.3	746.52	0.408	3.00E-03	0.01	0.303	5.00E-03	241.11	0.231	0.96
GW2.4	478.67	0.135	3.00E-03	0.01	5.00E-03	5.00E-03	129.45	0.052	0.132
GW2.5	1054.59	0.117	3.00E-03	0.01	5.00E-03	0.027	278.25	0.03	0.118
GW2.6	369.91	0.19	3.00E-03	0.01	5.00E-03	5.00E-03	152.63	0.036	0.197
GW2.7	435.62	0.134	3.00E-03	0.02	0.013	0.011	55.17	0.043	0.277
GW2.8	642.42	1.081	3.00E-03	0.036	0.026	0.012	118.84	0.586	3.96
SW2.1	338.12	0.057	3.00E-03	0.01	5.00E-03	5.00E-03	59.96	0.011	0.024
SW2.2	132.75	0.036	3.00E-03	0.01	5.00E-03	5.00E-03	37.76	0.01	0.02
SW2.3	280.1	0.051	3.00E-03	0.01	5.00E-03	5.00E-03	48.87	0.012	0.024
SW2.4	90.06	0.024	3.00E-03	0.01	0.023	5.00E-03	26.92	5.00E-03	0.015
SW2.5	348.78	0.054	3.00E-03	0.01	5.00E-03	5.00E-03	62.08	0.013	0.023
SW2.6	129.68	0.036	3.00E-03	0.01	5.00E-03	5.00E-03	35.79	0.014	0.024
Seep Pipe	2350.95	0.14	3.00E-03	0.01	5.00E-03	0.045	76.02	0.015	0.042

Description	Pr	Nd	Sm	Eu	Gd	Tb	Dy	Ho	Er
Units	µg/l	µg/l	µg/l	µg/l	µg/l	µg/l	µg/l	µg/l	µg/l
GW1.1	0.027	0.164	0.041	0.011	0.061	9.00E-03	0.054	0.013	0.037
GW1.2	0.01	0.046	0.012	3.00E-03	0.016	3.00E-03	0.016	3.00E-03	0.013
GW1.3	0.082	0.354	0.081	0.018	0.084	0.012	0.078	0.016	0.045
GW1.4	5.00E-03	0.025	6.00E-03	3.00E-03	8.00E-03	3.00E-03	0.01	3.00E-03	8.00E-03
GW1.5	3.00E-03	0.025	7.00E-03	3.00E-03	0.011	3.00E-03	0.011	3.00E-03	0.01
GW1.6	3.00E-03	0.026	7.00E-03	3.00E-03	8.00E-03	3.00E-03	9.00E-03	3.00E-03	8.00E-03
GW1.7	3.00E-03	0.016	3.00E-03	3.00E-03	6.00E-03	3.00E-03	6.00E-03	3.00E-03	5.00E-03
GW1.8	0.051	0.248	0.05	0.012	0.057	8.00E-03	0.05	0.012	0.039
GW1.9	0.153	0.775	0.179	0.048	0.237	0.036	0.224	0.048	0.141
SW1.1	3.00E-03	3.00E-03	3.00E-03	3.00E-03	3.00E-03	3.00E-03	3.00E-03	3.00E-03	3.00E-03
GW2.1	0.012	0.058	0.016	3.00E-03	0.019	3.00E-03	0.019	3.00E-03	0.013
GW2.2	0.017	0.082	0.025	3.00E-03	0.03	3.00E-03	0.033	7.00E-03	0.021
GW2.3	0.068	0.299	0.068	0.013	0.074	0.01	0.064	0.014	0.038
GW2.4	0.01	0.047	0.01	3.00E-03	0.013	3.00E-03	0.012	3.00E-03	9.00E-03
GW2.5	8.00E-03	0.043	0.01	3.00E-03	0.016	3.00E-03	0.018	3.00E-03	0.014
GW2.6	0.011	0.055	0.014	3.00E-03	0.019	3.00E-03	0.023	6.00E-03	0.02
GW2.7	9.00E-03	0.038	8.00E-03	3.00E-03	0.011	3.00E-03	0.01	3.00E-03	9.00E-03
GW2.8	0.147	0.625	0.143	0.024	0.166	0.024	0.152	0.033	0.095
SW2.1	3.00E-03	0.02	7.00E-03	3.00E-03	8.00E-03	3.00E-03	7.00E-03	3.00E-03	3.00E-03
SW2.2	3.00E-03	0.016	3.00E-03	3.00E-03	3.00E-03	3.00E-03	6.00E-03	3.00E-03	3.00E-03
SW2.3	3.00E-03	0.022	3.00E-03	3.00E-03	6.00E-03	3.00E-03	6.00E-03	3.00E-03	3.00E-03
SW2.4	3.00E-03	0.013	3.00E-03	3.00E-03	3.00E-03	3.00E-03	3.00E-03	3.00E-03	3.00E-03
SW2.5	3.00E-03	0.021	6.00E-03	3.00E-03	9.00E-03	3.00E-03	7.00E-03	3.00E-03	3.00E-03
SW2.6	3.00E-03	0.021	3.00E-03	3.00E-03	6.00E-03	3.00E-03	6.00E-03	3.00E-03	3.00E-03
Seep Pipe	7.00E-03	0.037	9.00E-03	3.00E-03	0.014	3.00E-03	0.019	3.00E-03	0.015

Description	Tm	Yb	Lu	Pb	U(IV)	NO3	SO4	F	PO4
Units	µg/l	µg/l	µg/l	µg/l	µg/l	mg/l	mg/l	mg/l	mg/l
GW1.1	5.00E-03	0.033	5.00E-03	5.00E-03	0.049	0.01	136.252	0.47	0.047
GW1.2	3.00E-03	0.012	3.00E-03	5.00E-03	0.02	0.01	112.686	0.21	0.01
GW1.3	6.00E-03	0.04	6.00E-03	5.00E-03	0.06	0.01	128.645	0.301	0.01
GW1.4	3.00E-03	9.00E-03	3.00E-03	5.00E-03	0.103	0.01	145.482	0.408	0.01
GW1.5	3.00E-03	0.011	3.00E-03	5.00E-03	0.11	0.01	132.746	0.675	0.01
GW1.6	3.00E-03	9.00E-03	3.00E-03	5.00E-03	0.011	0.01	137.673	0.248	0.01
GW1.7	3.00E-03	5.00E-03	3.00E-03	5.00E-03	0.021	0.01	128.01	0.22	0.01
GW1.8	6.00E-03	0.036	6.00E-03	5.00E-03	0.079	0.01	150.792	0.057	0.01
GW1.9	0.02	0.127	0.02	5.00E-03	0.128	0.01	73.064	0.43	0.209
SW1.1	3.00E-03	3.00E-03	3.00E-03	5.00E-03	0.013	0.01	1.884	0.151	0.01
GW2.1	3.00E-03	0.013	3.00E-03	0.016	0.048	0.01	3.477	0.174	0.01
GW2.2	3.00E-03	0.02	3.00E-03	5.00E-03	0.229	0.01	4.135	0.117	0.01
GW2.3	3.00E-03	0.03	3.00E-03	0.042	7.444	0.209	326.082	0.039	0.01
GW2.4	3.00E-03	8.00E-03	3.00E-03	5.00E-03	1.549	0.01	503.41	0.045	0.01
GW2.5	3.00E-03	0.012	3.00E-03	5.00E-03	9.00E-03	0.01	251.673	0.146	0.01
GW2.6	3.00E-03	0.023	3.00E-03	5.00E-03	3.288	0.01	372.75	0.639	0.01
GW2.7	3.00E-03	0.01	3.00E-03	0.013	10.634	1.197	402.06	0.036	0.01
GW2.8	0.013	0.088	0.014	0.097	0.082	0.751	116.145	0.088	0.01
SW2.1	3.00E-03	3.00E-03	3.00E-03	0.014	0.499	0.01	48.374	0.088	0.061
SW2.2	3.00E-03	3.00E-03	3.00E-03	0.022	0.221	0.01	13.678	0.108	0.01
SW2.3	3.00E-03	3.00E-03	3.00E-03	0.014	0.404	0.01	36.038	0.09	0.041
SW2.4	3.00E-03	3.00E-03	3.00E-03	0.026	0.039	0.01	0.251	0.09	0.01
SW2.5	3.00E-03	3.00E-03	3.00E-03	0.018	0.53	0.311	50.441	0.089	0.068
SW2.6	3.00E-03	3.00E-03	3.00E-03	0.011	0.038	0.299	10.298	0.113	0.01
Seep Pipe	3.00E-03	0.015	3.00E-03	0.083	1.943	0.01	763.32	1.482	0.01

2 Chapter 3 WHAM7 Input File

Description	SPM	Temperature	pCO2	pH	Colloidal Fulvic acid	Colloidal Iron oxide	Be
	g/l	deg C	atm		mg/l	mg/l	µg/l
DP02-0	0.00E+00	6.4	999	7.54	15.75	6.7580473	0.03
DP02-20	0.00E+00	6.3	999	7.45	15.85	13.872134	0.03
DP02-40	0.00E+00	6.4	999	7.43	15.65	35.186843	0.03
DP02-60	0.00E+00	6.3	999	7.23	17.25	0.00E+00	0.03
DP02-80	0.00E+00	6.3	999	7.27	17.35	0.00E+00	0.03
DP02-100	0.00E+00	6.1	999	7.33	16.7	0.0677259	0.03
DP04-0	0.00E+00	5.2	999	7.8	17.15	0.00E+00	0.03
DP04-20	0.00E+00	6.4	999	7.34	18.7	2.6686672	0.03
DP04-40	0.00E+00	6.8	999	6.67	11.65	19.565775	0.03
DP04-80	0.00E+00	6.3	999	6.78	6.3	23.372964	0.01
DP04-100	0.00E+00	7.1	999	6.78	13.45	17.985084	0.01
DP10-0	0.00E+00	4.8	999	7.48	12.5	0.1931527	0.03
DP10-20	0.00E+00	4.5	999	7.47	9.8	7.3151595	0.03
DP10-60	0.00E+00	5.7	999	6.88	9.5	7.2405845	0.03
DP10-80	0.00E+00	6	999	6.97	10.05	1.3260496	0.03
DP10-100	0.00E+00	6.3	999	6.92	9.35	4.4986815	0.03
DP15-0	0.00E+00	6.1	999	7.85	12.55	0.0153053	0.03
DP15-20	0.00E+00	5.8	999	7.47	14.35	19.905476	0.03
DP15-40	0.00E+00	6.4	999	7.54	17.25	17.698301	0.03
DP15-60	0.00E+00	5.6	999	7.55	16.5	0.00E+00	0.03
DP15-80	0.00E+00	7.7	999	7.29	16.1	0.00E+00	0.03
DP15-90	0.00E+00	7.2	999	7.3	16.55	0.00E+00	0.03
DP17-0	0.00E+00	6.8	999	7.76	19	0.204976	0.03
DP17-20	0.00E+00	7	999	7.26	16.35	9.5187375	0.03
DP17-40	0.00E+00	7	999	7.14	16.65	22.071556	0.03
DP17-80	0.00E+00	7.2	999	6.84	13.5	35.277565	0.03
DP17-95	0.00E+00	7	999	6.8	16.25	28.616783	0.03
DP22-0	0.00E+00	2.8	999	7.63	12.75	0.00E+00	0.03
DP22-20	0.00E+00	4.6	999	7.3	14.45	0.00E+00	0.03
DP22-40	0.00E+00	4.4	999	7.3	15.2	0.5992401	0.03
DP22-80	0.00E+00	5.3	999	7.05	16.25	12.8947	0.03
DP24-0	0.00E+00	4.8	999	7.48	16.65	0.286974	0.03
DP24-20	0.00E+00	5.7	999	7	18.95	8.3031155	0.03
DP24-40	0.00E+00	6	999	6.84	20.8	19.877735	0.03
DP24-60	0.00E+00	5.7	999	6.85	15.3	52.05709	0.03
DP24-80	0.00E+00	6.1	999	6.89	17.7	42.567816	0.03
DP24-100	0.00E+00	4.6	999	6.84	17.8	36.943124	0.03
DP25-0	0.00E+00	3	999	7.3	11.35	0.5356849	0.00E+00
DP25-20	0.00E+00	5	999	6.2	8.7	0.00E+00	0.08
DP25-40	0.00E+00	6.2	999	6.44	8.95	19.475971	0.01
DP25-60	0.00E+00	7.7	999	6.43	8.95	16.931468	0.02
DP25-80	0.00E+00	7.8	999	6.49	8.5	11.325909	0.01
DP25-100	0.00E+00	8.2	999	6.31	9.8	7.3847986	0.01
DP27-0	0.00E+00	1.9	999	7.7	14.2	0.00E+00	0.03
DP27-20	0.00E+00	3.1	999	7.41	14.5	0.00E+00	0.03

Description	Na	mg/l	Al	K	Ca	Cr(III)	Mn
	mg/l	mg/l	µg/l	mg/l	mg/l	µg/l	µg/l
DP02-0	125.91	21.8	10	2.82	121.84	0.5	851.1
DP02-20	125	22.37	10	2.59	130.78	0.5	1026.49
DP02-40	128.68	22.31	10	2.58	127.42	0.5	1201.54
DP02-60	128.24	18.99	65.8	2.85	123.37	0.5	520.08
DP02-80	133.26	21.78	10	2.93	133.29	0.5	345.08
DP02-100	131.52	16.58	10	3.17	102.29	0.5	690.34
DP04-0	200.52	57.06	10	3.19	255.52	0.5	51.2
DP04-20	164.74	53.59	10	2.26	253.23	0.5	670.07
DP04-40	47.25	29.58	10	1.52	156.93	0.5	989.71
DP04-80	18.12	19.31	4.8	1.13	118.52	0.37	1278.42
DP04-100	30.88	24.03	10.2	1.31	144.56	0.34	901.9
DP10-0	133.85	17.62	10	0.89	96.54	0.5	52.45
DP10-20	128.31	21.44	10	2.05	105.63	0.5	360.51
DP10-60	10.8	22.86	10	1.44	193.63	0.5	380.01
DP10-80	27.98	22.07	10	1.59	186.4	0.5	196.88
DP10-100	12.1	22.75	10	1.54	193	0.5	316.27
DP15-0	136.03	25.69	10	3.67	113.41	0.5	5.68
DP15-20	135.63	25.94	10	2.62	141.39	0.5	1419.44
DP15-40	135.61	27.37	10	2.56	149.4	0.5	1351.11
DP15-60	133.91	24.36	10	0.95	154.8	0.5	1849.67
DP15-80	133.91	24.32	10	1.39	150.75	0.5	2993.97
DP15-90	137.39	25.61	10	1.57	149.08	0.5	2216.43
DP17-0	159.5	46.53	10	3.4	206.67	0.5	51.76
DP17-20	148.13	40.53	10	1.9	197.88	0.5	514.44
DP17-40	141.44	38.07	10	1.6	190.55	0.5	1136.53
DP17-80	83.72	33.8	10	1.42	185.27	0.5	2188.73
DP17-95	83.1	34.74	10	1.6	181.86	0.5	1397.37
DP22-0	128.7	24.6	10	2.99	103.59	0.5	110.3
DP22-20	134.63	25.78	10	2.56	114.04	0.5	405.02
DP22-40	125.91	24.5	36.6	2.53	125.65	0.5	518.15
DP22-80	128.19	23.61	10	1.76	133.03	0.5	233.55
DP24-0	141.16	37.61	10	2.19	171.19	0.5	157.77
DP24-20	139.89	38.61	10	0.86	184.93	0.5	637.88
DP24-40	127.86	32.79	10	1.02	161.32	0.5	373.58
DP24-60	128.09	25.89	39.9	0.87	152.55	0.5	657.26
DP24-80	144.43	29.79	40	0.59	159.3	0.5	485.33
DP24-100	140.35	24.75	31.2	0.35	191.14	0.5	608.26
DP25-0	14.06	10.39	4	1.44	35.77	0.22	8.33
DP25-20	41.21	13.63	70.1	2.53	62.74	14.35	749.68
DP25-40	38.69	14.94	19.8	0.03	89.99	0.55	238.7
DP25-60	40.78	14.87	14.9	0.03	96.62	0.53	164.65
DP25-80	32.59	15.44	9.5	0.36	97.61	0.39	460.79
DP25-100	36.88	16.81	13	0.19	107.49	0.39	401.51
DP27-0	137.43	30.08	10	3.37	117.72	0.5	4.95
DP27-20	133.58	30.63	10	3.26	117.38	0.5	123.28

Description	Fe(II)	Fe(III)	Co	Ni	Cu	Zn	Sr
	mg/l	mg/l	µg/l	µg/l	µg/l	µg/l	µg/l
DP02-0	1.19	3.53	0.25	1	0.5	2.5	346.07
DP02-20	3.67	7.25	0.25	1	0.5	2.5	360.94
DP02-40	4.97	18.39	0.25	1	0.5	2.5	347.71
DP02-60	5.16	0.00E+00	0.25	1	0.5	2.5	330.4
DP02-80	5.36	0.00E+00	0.25	1	0.5	2.5	282.65
DP02-100	4.17	0.04	0.25	1	0.5	2.5	339.38
DP04-0	0.22	0.00E+00	0.25	2.03	0.5	2.5	772.94
DP04-20	3.67	1.39	0.25	1	0.5	2.5	735.64
DP04-40	2.4	10.23	0.25	1	0.5	2.5	446.96
DP04-80	3.4	12.22	0.03	0.1	0.05	0.25	291.06
DP04-100	3.93	9.4	0.03	0.1	0.05	0.25	353.39
DP10-0	0.28	0.1	0.25	1	0.5	2.5	222.59
DP10-20	2.78	3.82	0.25	1	0.5	2.5	255.95
DP10-60	1.65	3.78	0.25	1	0.5	2.5	384.22
DP10-80	1.15	0.69	0.25	1	0.5	2.5	361.86
DP10-100	2.9	2.35	0.25	1	0.5	2.5	377.38
DP15-0	0.00E+00	0.01	0.25	1	0.5	2.5	349.75
DP15-20	2.48	10.4	0.25	1	0.5	2.5	384.67
DP15-40	3.24	9.25	0.94	1	0.5	2.5	411.66
DP15-60	0.75	0.00E+00	1.45	2.64	0.5	2.5	361.84
DP15-80	0.14	0.00E+00	2.21	3.73	0.5	2.5	364.93
DP15-90	0.79	0.00E+00	0.86	2.11	0.5	2.5	373.43
DP17-0	0.02	0.11	0.25	1	0.5	2.5	598.9
DP17-20	3.18	4.98	0.25	1	0.5	2.5	583.73
DP17-40	4.07	11.54	0.25	1	0.5	2.5	562.16
DP17-80	3.04	18.44	0.25	1	0.5	2.5	568.95
DP17-95	2.96	14.96	0.25	1	0.5	2.5	530.64
DP22-0	0.56	0.00E+00	0.25	1	0.5	2.5	292.78
DP22-20	1.07	0.00E+00	0.25	1	0.5	2.5	317.98
DP22-40	4.43	0.31	0.25	1	0.5	2.5	317.96
DP22-80	2.07	6.74	0.25	1	0.5	2.5	330.75
DP24-0	0.00E+00	0.15	0.25	1	0.5	2.5	476.7
DP24-20	3.95	4.34	0.25	1	0.5	2.5	524.76
DP24-40	2.05	10.39	0.25	1	0.5	2.5	438.89
DP24-60	3.5	27.21	0.25	1	0.5	2.5	431.15
DP24-80	0.56	22.25	0.25	1	0.5	2.5	444.61
DP24-100	5	19.31	0.25	1	0.5	2.5	570.39
DP25-0	0.08	0.28	0.07	0.5	0.05	0.85	102.38
DP25-20	1.19	0.00E+00	3.56	2.54	1.67	57.34	185.18
DP25-40	3.28	10.18	0.29	0.22	0.05	0.54	230.99
DP25-60	3.18	8.85	0.09	0.28	0.05	1	238.44
DP25-80	2.78	5.92	0.1	2.02	0.05	1.21	273.59
DP25-100	4.91	3.86	0.03	0.1	0.05	0.25	282.63
DP27-0	0.06	0.00E+00	0.25	1	0.5	2.5	352.67
DP27-20	0.71	0.00E+00	0.25	1	0.5	2.5	351.59

Description	Y	Ag	Cd	Sn(II)	Cs	Ba	La
	µg/l	µg/l	µg/l	µg/l	µg/l	µg/l	µg/l
DP02-0	0.19	0.03	0.1	0.05	0.05	175.31	0.05
DP02-20	0.23	0.03	0.1	0.05	0.05	202.48	0.05
DP02-40	0.25	0.03	0.1	0.05	0.05	281.97	0.05
DP02-60	0.42	0.03	0.1	0.05	0.05	200.74	0.16
DP02-80	0.27	0.03	0.1	0.05	0.05	189.96	0.05
DP02-100	0.56	0.03	0.1	0.05	0.05	246	0.05
DP04-0	0.05	0.03	0.1	0.05	0.05	90.16	0.05
DP04-20	0.05	0.03	0.1	0.05	0.05	153.08	0.05
DP04-40	0.13	0.03	0.1	0.05	0.05	154.42	0.11
DP04-80	0.09	0.00E+00	0.01	0.03	0.01	138.16	0.06
DP04-100	0.35	0.00E+00	0.01	0.01	0.01	144.8	0.19
DP10-0	0.05	0.03	0.1	0.05	0.05	111.04	0.05
DP10-20	0.05	0.03	0.1	0.05	0.05	119.01	0.05
DP10-60	0.05	0.03	0.1	0.05	0.05	252.23	0.05
DP10-80	0.05	0.03	0.1	0.05	0.05	208.88	0.05
DP10-100	0.05	0.03	0.1	0.05	0.05	264.89	0.05
DP15-0	0.05	0.03	0.1	0.05	0.05	67.3	0.05
DP15-20	0.12	0.03	0.1	0.05	0.05	144.21	0.05
DP15-40	0.12	0.03	0.1	0.05	0.05	143.46	0.05
DP15-60	0.23	0.03	0.1	0.05	0.05	129.61	0.1
DP15-80	0.35	0.03	0.1	0.05	0.05	144.92	0.19
DP15-90	0.36	0.03	0.1	0.05	0.05	122.15	0.26
DP17-0	0.05	0.03	0.1	0.05	0.05	93.24	0.05
DP17-20	0.05	0.03	0.1	0.05	0.05	179.35	0.05
DP17-40	0.12	0.03	0.1	0.05	0.05	273.81	0.05
DP17-80	0.2	0.03	0.1	0.05	0.05	304.52	0.13
DP17-95	0.31	0.03	0.1	0.05	0.05	364.65	0.16
DP22-0	0.05	0.03	0.1	0.05	0.05	63.28	0.05
DP22-20	0.05	0.03	0.1	0.05	0.05	92.14	0.05
DP22-40	0.12	0.03	0.1	0.05	0.05	144.68	0.05
DP22-80	0.12	0.03	0.1	0.05	0.05	174.47	0.05
DP24-0	0.05	0.03	0.1	0.05	0.05	91.65	0.05
DP24-20	0.05	0.03	0.1	0.05	0.05	163.87	0.05
DP24-40	0.05	0.03	0.1	0.05	0.05	215.29	0.05
DP24-60	0.14	0.03	0.1	0.05	0.05	217.49	0.05
DP24-80	0.14	0.03	0.1	0.05	0.05	214.13	0.05
DP24-100	0.15	0.03	0.1	0.05	0.05	319.85	0.05
DP25-0	0.04	0.00E+00	0.01	0.01	0.01	27.12	0.02
DP25-20	0.28	0.03	0.1	0.05	0.05	137.62	0.15
DP25-40	0.22	0.00E+00	0.01	0.03	0.05	182.92	0.14
DP25-60	0.19	0.00E+00	0.01	0.01	0.05	193.87	0.11
DP25-80	0.1	0.00E+00	0.01	0.02	0.05	191.16	0.05
DP25-100	0.13	0.00E+00	0.01	0.01	0.05	208.65	0.08
DP27-0	0.05	0.03	0.1	0.05	0.05	59.13	0.05
DP27-20	0.05	0.03	0.1	0.05	0.05	62.27	0.05

Description	Ce	Pr	Nd	Sm	Eu	Gd	Tb
	µg/l	µg/l	µg/l	µg/l	µg/l	µg/l	µg/l
DP02-0	0.05	0.03	0.06	0.03	0.03	0.03	0.03
DP02-20	0.05	0.03	0.07	0.03	0.03	0.03	0.03
DP02-40	0.05	0.03	0.07	0.03	0.03	0.03	0.03
DP02-60	0.36	0.05	0.23	0.03	0.03	0.05	0.03
DP02-80	0.11	0.03	0.09	0.03	0.03	0.03	0.03
DP02-100	0.22	0.03	0.17	0.03	0.03	0.05	0.03
DP04-0	0.05	0.03	0.03	0.03	0.03	0.03	0.03
DP04-20	0.05	0.03	0.03	0.03	0.03	0.03	0.03
DP04-40	0.28	0.03	0.11	0.03	0.03	0.03	0.03
DP04-80	0.12	0.02	0.07	0.02	0.00E+00	0.01	0.00E+00
DP04-100	0.36	0.05	0.21	0.04	0.01	0.05	0.01
DP10-0	0.05	0.03	0.03	0.03	0.03	0.03	0.03
DP10-20	0.05	0.03	0.03	0.03	0.03	0.03	0.03
DP10-60	0.05	0.03	0.03	0.03	0.03	0.03	0.03
DP10-80	0.05	0.03	0.03	0.03	0.03	0.03	0.03
DP10-100	0.05	0.03	0.03	0.03	0.03	0.03	0.03
DP15-0	0.05	0.03	0.03	0.03	0.03	0.03	0.03
DP15-20	0.05	0.03	0.03	0.03	0.03	0.03	0.03
DP15-40	0.05	0.03	0.03	0.03	0.03	0.03	0.03
DP15-60	0.2	0.03	0.11	0.03	0.03	0.03	0.03
DP15-80	0.36	0.03	0.18	0.03	0.03	0.03	0.03
DP15-90	0.47	0.06	0.27	0.03	0.03	0.07	0.03
DP17-0	0.05	0.03	0.03	0.03	0.03	0.03	0.03
DP17-20	0.05	0.03	0.03	0.03	0.03	0.03	0.03
DP17-40	0.13	0.03	0.08	0.03	0.03	0.03	0.03
DP17-80	0.23	0.03	0.13	0.03	0.03	0.03	0.03
DP17-95	0.33	0.03	0.19	0.03	0.03	0.03	0.03
DP22-0	0.05	0.03	0.03	0.03	0.03	0.03	0.03
DP22-20	0.05	0.03	0.03	0.03	0.03	0.03	0.03
DP22-40	0.17	0.03	0.08	0.03	0.03	0.03	0.03
DP22-80	0.11	0.03	0.06	0.03	0.03	0.03	0.03
DP24-0	0.05	0.03	0.03	0.03	0.03	0.03	0.03
DP24-20	0.05	0.03	0.03	0.03	0.03	0.03	0.03
DP24-40	0.11	0.03	0.06	0.03	0.03	0.03	0.03
DP24-60	0.18	0.03	0.1	0.03	0.03	0.03	0.03
DP24-80	0.17	0.03	0.08	0.03	0.03	0.03	0.03
DP24-100	0.16	0.03	0.1	0.03	0.03	0.03	0.03
DP25-0	0.03	0.00E+00	0.02	0.01	0.00E+00	0.03	0.00E+00
DP25-20	0.36	0.03	0.19	0.03	0.03	0.05	0.03
DP25-40	0.32	0.04	0.17	0.04	0.01	0.04	0.01
DP25-60	0.27	0.03	0.16	0.03	0.01	0.03	0.01
DP25-80	0.11	0.01	0.07	0.02	0.00E+00	0.02	0.00E+00
DP25-100	0.19	0.02	0.11	0.02	0.00E+00	0.02	0.00E+00
DP27-0	0.05	0.03	0.03	0.03	0.03	0.03	0.03
DP27-20	0.05	0.03	0.03	0.03	0.03	0.03	0.03

Description	Dy	Ho	Er	Tm	Yb	Lu	Pb
	µg/l	µg/l	µg/l	µg/l	µg/l	µg/l	µg/l
DP02-0	0.03	0.03	0.03	0.03	0.03	0.03	0.05
DP02-20	0.03	0.03	0.03	0.03	0.03	0.03	0.05
DP02-40	0.03	0.03	0.03	0.03	0.03	0.03	0.05
DP02-60	0.06	0.03	0.03	0.03	0.03	0.03	0.05
DP02-80	0.03	0.03	0.03	0.03	0.03	0.03	0.05
DP02-100	0.07	0.03	0.05	0.03	0.06	0.03	0.05
DP04-0	0.03	0.03	0.03	0.03	0.03	0.03	0.05
DP04-20	0.03	0.03	0.03	0.03	0.03	0.03	0.14
DP04-40	0.03	0.03	0.03	0.03	0.03	0.03	0.05
DP04-80	0.02	0.00E+00	0.01	0.00E+00	0.01	0.00E+00	0.01
DP04-100	0.04	0.01	0.03	0.00E+00	0.03	0.00E+00	0.02
DP10-0	0.03	0.03	0.03	0.03	0.03	0.03	0.05
DP10-20	0.03	0.03	0.03	0.03	0.03	0.03	0.05
DP10-60	0.03	0.03	0.03	0.03	0.03	0.03	0.05
DP10-80	0.03	0.03	0.03	0.03	0.03	0.03	0.05
DP10-100	0.03	0.03	0.03	0.03	0.03	0.03	0.05
DP15-0	0.03	0.03	0.03	0.03	0.03	0.03	0.05
DP15-20	0.03	0.03	0.03	0.03	0.03	0.03	0.05
DP15-40	0.03	0.03	0.03	0.03	0.03	0.03	0.05
DP15-60	0.03	0.03	0.03	0.03	0.03	0.03	0.05
DP15-80	0.03	0.03	0.03	0.03	0.03	0.03	0.05
DP15-90	0.05	0.03	0.03	0.03	0.03	0.03	0.05
DP17-0	0.03	0.03	0.03	0.03	0.03	0.03	0.05
DP17-20	0.03	0.03	0.03	0.03	0.03	0.03	0.13
DP17-40	0.03	0.03	0.03	0.03	0.03	0.03	0.05
DP17-80	0.03	0.03	0.03	0.03	0.03	0.03	0.05
DP17-95	0.03	0.03	0.03	0.03	0.03	0.03	0.05
DP22-0	0.03	0.03	0.03	0.00E+00	0.03	0.03	0.05
DP22-20	0.03	0.03	0.03	0.00E+00	0.03	0.03	0.05
DP22-40	0.03	0.03	0.03	0.00E+00	0.03	0.03	0.05
DP22-80	0.03	0.03	0.03	0.00E+00	0.03	0.03	0.05
DP24-0	0.03	0.03	0.03	0.00E+00	0.03	0.03	0.05
DP24-20	0.03	0.03	0.03	0.00E+00	0.03	0.03	0.05
DP24-40	0.03	0.03	0.03	0.00E+00	0.03	0.03	0.05
DP24-60	0.03	0.03	0.03	0.00E+00	0.03	0.03	0.05
DP24-80	0.03	0.03	0.03	0.00E+00	0.03	0.03	0.05
DP24-100	0.03	0.03	0.03	0.00E+00	0.03	0.03	0.05
DP25-0	0.01	0.00E+00	0.00E+00	0.00E+00	0.00E+00	0.00E+00	0.01
DP25-20	0.03	0.03	0.03	0.03	0.03	0.03	0.11
DP25-40	0.03	0.01	0.02	0.00E+00	0.02	0.00E+00	0.05
DP25-60	0.03	0.01	0.02	0.00E+00	0.02	0.00E+00	0.03
DP25-80	0.01	0.00E+00	0.01	0.00E+00	0.01	0.00E+00	0.03
DP25-100	0.02	0.00E+00	0.01	0.00E+00	0.01	0.00E+00	0.02
DP27-0	0.03	0.03	0.03	0.03	0.03	0.03	0.05
DP27-20	0.03	0.03	0.03	0.03	0.03	0.03	0.05

Description	Th	U(IV)	Cl	NO3	SO4	F	PO4
	µg/l	µg/l	mg/l	mg/l	mg/l	mg/l	mg/l
DP02-0	0.1	0.03	103.4	0.01	5.06	0.3	0.01
DP02-20	0.1	0.03	104.8	0.01	13.56	0.27	0.01
DP02-40	0.1	0.03	107.7	0.01	6.64	0.27	0.01
DP02-60	0.1	0.1	110.7	0.01	2.6	0.26	0.01
DP02-80	0.1	0.09	127.2	0.01	13.25	0.13	0.01
DP02-100	0.1	0.19	92.1	0.01	2.84	0.37	0.01
DP04-0	0.1	0.13	218.5	0.01	554.12	0.11	0.01
DP04-20	0.1	0.03	201.2	0.01	454.77	0.11	0.01
DP04-40	0.1	0.03	87.8	0.01	69.11	0.06	0.01
DP04-80	0.01	0.01	43.6	0.01	6.19	0.07	0.01
DP04-100	0.01	0.01	58.2	0.01	40.31	0.06	0.01
DP10-0	0.1	0.2	127.6	0.01	42.92	0.13	0.01
DP10-20	0.1	0.03	128.9	0.01	18.13	0.15	0.01
DP10-60	0.1	0.03	66.3	0.24	0.08	0.1	0.01
DP10-80	0.1	0.03	67.9	0.21	0.01	0.09	0.01
DP10-100	0.1	0.03	66	0.03	0.13	0.09	0.01
DP15-0	0.1	0.05	125.5	0.01	104.31	0.18	0.01
DP15-20	0.1	0.03	128.6	0.01	85.18	0.16	0.01
DP15-40	0.1	0.13	128.4	0.01	75.92	0.16	0.01
DP15-60	0.1	0.23	130.7	0.01	80.38	0.13	0.01
DP15-80	0.1	0.38	131.5	0.01	63.53	0.14	0.01
DP15-90	0.1	0.16	130.5	0.01	93.02	0.13	0.01
DP17-0	0.1	0.1	185	0.01	367.63	0.11	0.01
DP17-20	0.1	0.03	173.9	0.01	284.74	0.09	0.01
DP17-40	0.1	0.09	175.1	0.01	248.64	0.1	0.01
DP17-80	0.1	0.03	142.3	0.01	211.62	0.1	0.01
DP17-95	0.1	0.03	138.2	0.01	193.09	0.11	0.01
DP22-0	0.1	0.03	126	0.01	66.01	0.15	0.01
DP22-20	0.1	0.03	133.3	0.01	66.38	0.13	0.01
DP22-40	0.1	0.03	136.7	0.01	23.05	0.13	0.01
DP22-80	0.1	0.03	124.3	0.08	22.47	0.09	0.01
DP24-0	0.1	0.07	182.6	0.01	242.17	0.11	0.01
DP24-20	0.1	0.06	188.6	0.01	235.55	0.11	0.01
DP24-40	0.1	0.03	158.9	0.01	55.66	0.08	0.01
DP24-60	0.1	0.03	128.8	0.15	56.22	0.15	0.01
DP24-80	0.1	0.03	152.6	0.00E+00	44.12	0.08	0.01
DP24-100	0.1	0.03	136.9	0.12	118.96	0.08	0.01
DP25-0	0.01	0.02	9.8	0.01	5.3	0.09	0.01
DP25-20	0.1	0.03	86.1	0.01	93.33	0.05	0.01
DP25-40	0.03	0.01	108.7	0.01	0.69	0.07	0.09
DP25-60	0.03	0.01	105.1	0.01	0.25	0.07	0.2
DP25-80	0.01	0.01	80.9	0.01	12.21	0.09	0.08
DP25-100	0.02	0.01	94.4	0.01	0.14	0.08	0.01
DP27-0	0.1	0.09	138.6	0.01	151.79	0.1	0.01
DP27-20	0.1	0.09	138.6	0.01	143.01	0.09	0.01